รายงานวิจัยฉบับสมบูรณ์

โครงการ

การศึกษาจลนพลศาสตร์ของการอบแห้งและคุณภาพของกล้วยแผ่นกรอบ

โดย

รศ.ดร. สมเกียรติ ปรัชญาวรากร

พฤษภาคม พ.ศ. 2554

รายงานวิจัยฉบับสมบูรณ์

โครงการ การศึกษาจลนพลศาสตร์ของการอบแห้งและ
คุณภาพของกล้วยแผ่นกรอบ

มหาวิทยาลัยเทคโนโลยีพระจอมเกล้าธนบุรี

สนับสนุนโดยสำนักงานกองทุนสนับสนุนการวิจัย
และมหาวิทยาลัยเทคโนโลยีพระจอมเกล้าธนบุรี

Project Code: RSA 5180014

Project Title: Study of drying kinetics and quality attributes of crisp bananas

Investigator: Somkiat Prachayawarakorn King Mongkut's University of Technology Thonburi

E-mail Address: somkiat.pra@kmutt.ac.th

Project period: 3 years

บทคัดย่อ

กล้วยอบกรอบที่มาจากการทอดมักมีอายุในการเก็บรักษาสั้นเนื่องจากมีกลิ่นหืนซึ่งเกิดจากปฏิกิริยาออกซิเดชันของไขมัน เพื่อเลี่ยงปัญหาดังกล่าววิธีการผลิตกล้วยกรอบด้วยวิธีการให้ความร้อนสูงในระยะเวลาสั้นหรือการพัฟฟิง และ วิธีการทำโฟมเป็นทางเลือกหนึ่ง ข้อดีของวิธีหลังนี้คือไม่ต้องใช้อุณหภูมิสูงในการอบแห้ง นอกจากนี้ในโครงงานวิจัยนี้ยังมีการศึกษาแบบจำลองทางคณิตศาสตร์เพื่ออธิบายการแพร่ในกล้วยกรอบ

ด้วยวิธีการพัฟฟิง กล้วยแผ่นซึ่งมีความหนา 3.5 mm มาลวกด้วยน้ำร้อนและผ่านการออสโมติกด้วยสารละลายน้ำตาลซูโครส นำตัวอย่างที่ผ่านการออสโมติกมาอบแห้งด้วยอากาศร้อนที่ 90°C จนกระทั่งได้ความชื้นในระดับหนึ่งและนำตัวอย่างไปพัฟด้วยไอน้ำร้อนยวดยิ่งเป็นระยะเวลาสั้น ๆ จากนั้นนำมาอบแห้งด้วยอากาศร้อนต่อจนได้ความชื้นต่ำกว่าร้อยละ 4 ฐานแห้ง จากผลการทดลองที่ได้แสดงให้เห็นว่าการออสโมติกกล้วยก่อนผ่านกระบวนการอบแห้งต่างๆ สามารถปรับปรุงสีของผลิตภัณฑ์ สีของกล้วยที่ได้เป็นสีน้ำตาลอ่อนกว่ากล้วยที่ไม่ได้ผ่านการออสโมติกดังสังเกตได้จากค่า L- and a-values ซึ่งมีค่าต่ำกว่าและ b-value สูงกว่ากล้วยที่ไม่ได้ผ่านการออสโมติก อุณหภูมิพัฟฟิงที่สูงขึ้นและความเข้มข้นของสารละลายน้ำตาลกลูโครสที่สูงขึ้นไม่ส่งผลให้กล้วยมีสีน้ำตาลเข้มขึ้นแต่ส่งผลต่อระยะเวลาในการอบแห้งและสมบัติทางด้านเนื้อสัมผัส และการหดตัว ระยะเวลาอบแห้งและการหดตัวของกล้วยออสโมติกสูงกว่าในกรณีกล้วยที่ไม่ผ่านการออสโมติก การหดตัวของกล้วยออสโมติกสูงนี้เป็นผลจากการเกิดพันธะของไฮโดรเจนระหว่างกลุ่มไฮดรอกซิล (OH-) ของกลูโคส และผนังเซลของกล้วย ส่งผลให้ผนังเซลมีความแข็งแรงและยากต่อการขยายตัวของวัสดุ นอกจากนี้ผลดังกล่าวส่งผลให้เนื้อสัมผัสแข็งและมีความกรอบน้อย

สำหรับวิธีผลิตกล้วยกรอบโดยวิธีโฟมนั้น ผลของความหนาแน่นโฟมและชนิดของสารก่อโฟมมีผลต่อค่าสัมประสิทธิ์การแพร่ประสิทธิผลและคุณภาพทางกายภาพของโฟมกล้วยหลังการอบแห้ง โฟมกล้วยที่ใช้โปรตีนเวย์ในการก่อโฟมมีความสเถียรของฟองอากาศและมีความเป็นรูพรุนของผลิตภัณฑ์สูงกว่าโฟมกล้วยที่ใช้โปรตีนถั่วเหลืองและไข่ขาว ผลดังกล่าวนี้ส่งผลให้มีการหดตัวน้อยและค่าสัมประสิทธิ์การแพร่สูงสำหรับโฟมกล้วยโปรตีนเวย์ สำหรับคุณสมบัติของเนื้อสัมผัสพบว่าโฟมกล้วยจากโปรตีนเวย์และไข่ขาวค่อนข้างนุ่มและไม่กรอบเมื่อเทียบกับโปรตีนถั่วเหลือง กล้วยโฟมที่มีความหนาแน่นต่ำกว่าจะมีค่าสัมประสิทธิ์การแพร่สูงกว่าและแข็งน้อยกว่า องค์ประกอบของสารระเหยง่ายที่มีในกล้วยมีการสูญเสียเกิดขึ้นทั้งในขั้นตอนของการตีโฟมกล้วยและการอบแห้ง การสูญเสียกลิ่นส่วนใหญ่เกิดขึ้นในขั้นตอนของการตีโฟม

จากการศึกษาการดูดความชื้นของโฟมกล้วยพบว่าความเป็นรูพรุนของโฟมกล้วยสูงทำให้มีการดูดความชื้นในอากาศเร็วส่งผลให้โฟมกล้วยสูญเสียความกรอบ เพื่อชะลอการดูดความชื้นกลับ โฟมกล้วยสองชั้นเป็นแนวทางหนึ่งในการแก้ปัญหานี้ จากผลการทดลองพบว่าเมื่อใช้โฟมกล้วยที่มีความหนาแน่น 0.31 g/cm^{3}วางอยู่บนโฟมกล้วยที่มีความหนาแน่น 0.26 g/cm^3 สามารถชะลอการดูดซับความชื้นได้ และ ผลิตภัณฑ์ที่ได้มีความกรอบดีกว่าในกรณีโฟมกล้วยชั้นเดียวที่ความหนาแน่น 0.26 g/cm^3

จากผลงานวิจัยที่กล่าวมาทั้งหมดข้างต้นสามารถผลิตบัณฑิตในระดับดุษฎีบัณฑิตเป็นจำนวน 1 ท่าน และระดับบัณฑิตศึกษา 9 ท่าน พร้อมกับมีผลงานวิจัยที่ตีพิมพ์ในวารสารระดับนานาชาติเป็นจำนวน 4 เรื่อง ในวารสารระดับชาติ 1 เรื่อง การประชุมวิชาการระดับนานาชาติ 5 เรื่อง 1 บทใน edited book และกำลังดำเนินการแก้ไขบทความตามคำแนะนำของผู้ทรงคุณวุฒิ 1 เรื่อง

คำหลัก: ขนมขบเคี้ยว, พัฟฟิง, เนื้อสัมผัส, สัมประสิทธิ์การแพร่

ABSTRACT

Crispy bananas produced by frying method have a short shelf life due to lipid oxidation leading to ran acidity. To alleviate the remaining vegetable oil inside the product, drying will be used instead. In this project, the high temperature short time or puffing method and foaming method were proposed to produce crispy bananas. The mathematical model has been developed to describe the moisture transfer in the porous banana.

In the puffing method, the banana slices were blanched and osmotic with sucrose solution. The samples were then dried with hot air at 90°C until their moisture content reached a certain level. After that, they were puffed with superheated steam for a very short period and dried again with hot air to 4% dry basis or lower. The experimental results have shown that the osmotic dehydration before processing could improve the color of banana. The puffed osmotic banana color was less brown than the puffed non osmotic banana as indicated by the lower values of L and a, and higher value of b. The puffing temperature and osmotic concentrations did not enhance the browning rate. The impregnation for banana with sucrose caused longer drying time than r the non osmotic one and also limited the banana cell wall expansion, due to hydrogen bonding between hydroxyl group in sucrose and that in cell wall. This bonding resulted further in the less porous structure of the osmotic sample than those of the non osmotic. The texture of the osmotic sample was less crisp and harder as compared to that of the non osmotic sample.

For foaming method, the influences of foam densities and types of foaming agent on the moisture diffusivity and the qualities of the final products in terms of shrinkage, texture, microstructure and volatile loss were investigated. Three foaming agents, i.e., fresh egg albumen (EA), soy protein isolate (SPI) and whey protein concentrate (WPC) were used. The experimental results showed that the WPC banana foam after drying could retain more open structure, indicating high foam stability. This encouraged the lower shrinkage and higher value of effective diffusivity than that of dried SPI and EA banana foams. For the textural properties of banana foam mats, the WPC and EA banana foams were spongy and less crisp than SPI banana foam. The samples with lower foam densities for all foaming agents had higher effective diffusivity and smaller hardness than those with higher foam densities. However, the crispness was lower. The volatile substances lost during the foaming and drying steps, the main loss occurring during foaming.

Due to very high porosity of dry banana foam, it could rapidly adsorb water vapor, leading to the loss of crisp texture. The prevention of water vapor adsorption can be made by bi-layer banana foam where the high-density banana foam was laid down on the top of the low-density banana foam. The experimental results have been shown that the banana foam density of 0.31 g/cm^3 laid down on the top of banana foam density of 0.26 g/cm^3 can delay the water vapor adsorption as compared to the single-layer banana foam density of 0.26 g/cm^3. The textural property of this bi-layer banana foam regarding to the number of peaks was higher than that the single density, but the initial slope was insignificantly different.

One PhD student and 9 undergraduate students were the output of this project, along with 4 papers published in the international journal, one paper in local journal, 5 papers in the international conferences one chapter in edited book and one article which is being revised according to reviewer's comment.

Keywords: snack, puffing, texture, diffusion coefficient

Rational and Motivation

Bananas are a favourite fruit widely grown in the areas of tropical and subtropical climates. After harvesting, the quality of bananas deteriorates rapidly. To reduce their losses and add value to them, the fresh bananas are processed to produce several products such as candy, banana starch and banana chips. Banana chips, one of the most favourite products, can be consumed as a snack or used as an ingredient in breakfast cereal. To produce banana chips, thin-sliced bananas are normally fried with vegetable oil. The product characteristics obtained from frying are crispy and puffed in particular when bananas are fried undergoing vacuum pressure. However, the obtained product generally contains high oil content, approximately 10-20%, and cannot be kept for an extended period of time due to possible lipid oxidation leading to rancidity. To alleviate this problem, drying can be employed instead to produce banana chips with desired texture (crispness). The crisp texture can be achieved when the moisture content of banana is lower than 4% dry basis (d.b.).

The crispiness is also related to voids or pores that are produced inside product. The material containing a larger number of pores will be crispier. Creation of pores can be made by vacuum drying, high-temperature drying and foaming technique. The latter two techniques will be studied in this project since the vacuum drying has a high operating cost and also the vacuum pump cost is very high in particular when the very low pressure is required.

High-temperature drying results in moisture inside the product to be vaporized, yielding an increase of volume of water vapor and product to be puffed. From our previous work, however, it was found that the high-temperature drying at the early drying period resulted in banana slices to be puffed but the puffing was not stable; it collapsed or broke because the vapor pressure generated inside the material was very high and the skeleton of banana was very soft. These will subsequently affect the

product quality such as less crispiness, less rehydration capacity and slow rehydration rate. Improvement of the weaken structure of banana can be made by several methods. The first method involves making the existing banana starch to be gelatinized before contacting high-temperature drying. The gelatinized starch will connect among them in the network and this may result in the strong banana structure. Another method involves making the banana surface to be rigid before subjecting to high-temperature drying. To create the surface rigidity, the banana must be dried to a certain moisture content. The surface rigidity also limits the capability of moisture movement and this will cause a build up of vapor pressure when the high-temperature drying is used. Hence, a porous structure of banana can be produced and its volume increases as a consequent result. The increase of material volume also depends upon the heat transfer; high heat transfer rate will promote material volume to be largely expanded.

In addition to the high-temperature drying method, the formation of pores inside material is made by foaming technique. In foaming technique, the semi solid foods will be whipped to form foams by adding the food foaming and stabilizing agents. While the food foams are being dried, gas bubbles produced during whipping become porous. Such porous food foams provide the advantage to drying in that the drying time is shorter, compared to drying of non food foam, and hence the energy consumption is lesser. In addition, the temperature used for drying is remarkably lower when compared to the porous food produced by high-temperature drying. Drying temperature is important to the final food foam quality because the collapse of gas bubbles will occur if the drying temperature used is not suitable. This may result in longer drying time, less crispness and darkening of food. The crispness of food foams also depends on the foaming agent since different agents provide different foaming ability and different stabilities of foams.

The porous bananas obtained from the above-mentioned methods contain low moisture and when they expose to high relative humidity, they will adsorb water rapidly, leading to obtain undesirable texture. The study of moisture adsorption kinetics of products needs to see the effect of environmental conditions on the product quality.

This project will therefore be studied the drying kinetics and quality of crispy banana obtained by high-temperature drying and foaming technique. Also, the moisture adsorption kinetics of porous banana is subject to be investigated.

Objectives

1. Development of banana crisp using puffing and foaming techniques.
2. Study the effect of heating media and dryer types on quality of crispy bananas.
3. Study the effects of foaming agents and drying temperature on qualities of banana foam.

4. Study of the effect of osmotic pretreatments on the drying characteristics and quality attributes of puffed bananas.
5. Study of moisture adsorption of porous banana.
6. Development of mathematical models to describe the moisture inside porous banana.

Methodology

Osmotic Treatment

Fresh bananas were obtained from local market and their soluble solid contents were given in the range of 20-23°Brix. Before processing, the banana was sliced into 3.5 mm thickness and blanched by hot water at 95°C for 1 min. Osmotic solution was prepared by using commercial sucrose with concentrations of 30, 35 and 40°Brixes. The banana slices were immersed into various sucrose solution concentrations and the mass ratio of osmotic media to the sample was about 30:1 to avoid the dilution effect. The samples were immersed into the osmotic solution until the banana moisture content was not changed.

Process for producing crispy banana used in this study was consisted of 3 main steps. In the first step, the banana was dried by a hot air tray dryer to certain level, puffed by a superheated steam tray dryer and dried by the hot air tray dryer again. From the preliminary study, it was found that the banana moisture content before puffing and the puffing time were less affected on the volume expansion than the puffing temperature. In addition, the intermediate moisture content of sample of 30% dry basis (d.b.) and puffing time for 150 s were suitable for puffing banana. Before puffing, the banana was dried at 90^{O}C to the recommended moisture content. Drying banana at this temperature did not form the brown color (Thuwapanichayanan et al. (**2011 see Annex A**)). After reducing moisture content to 30% d.b., the osmotic banana was puffed at temperatures of 180, 200 and 220°°C for 150 s and dried by hot air again at the same temperature as the first stage drying. The final moisture content required at 4% d.b. At the end of each experiment, the moisture content of samples was determined by drying them in the oven at 103°C for 3 h. The moisture content determined by this method was closed to the vacuum oven method 934.06 (AOAC, 1995). The color and textural property of finished product were determined (**See Annex B**).

Drying of banana foam

Gros Michel bananas at a mature stage of 5, which contained total soluble solids of approximately 23-25ºBrix, were used. Soy protein isolate (SPI) and whey protein concentrate (WPC) were used as foaming agents in this study. SPI (90.2% protein, dry basis) was supplied by Shandong Sinoglory Health Food CO., LTD (Qingdao, China). WPC (80% protein, dry basis) was obtained from

Agri-Mark, Inc. (Lawrence, MA). Bananas were cut into slices with a slicing machine. To prevent discoloration during foaming, the sliced bananas were pretreated by immersing them in 1% (w/w) sodium metabisulphite solution for 2 min and then rinsed with distilled water for 30 s. The pretreated banana slices were chopped into small pieces and then blended with a blender (Waring, model no. 8011 BU, Torrington, CT) for 1 min. About 800 g of the banana puree was then poured into a mixing bowl and then added with different foaming agents. SPI and WPC were added as a dry solid form at a concentration of 5%. The concentration of SPI and WPC used in this study was the same of fresh egg albumen (EA) used in the previous work. The protein content of the egg white was approximately 10% (w/w). The banana puree with a foaming agent was whipped by a Kitchen Aid Mixer (model no. 5K5SS, Strombeek-Bever, Belgium) at a maximum speed (220 rpm) to foam densities of 0.3, 0.5 and 0.7 g/cm^3. Foam density was determined by measuring the mass of a fixed volume of the foam. The experiments were done in duplicate.

Banana foam mats with a thickness of 5 mm were placed on a mesh tray, which was covered with aluminum foil, and then placed in the drying chamber. The samples were dried to about 0.03 kg/kg db using the drying air temperature of 80°C and a superficial air velocity of 0.5 m/s. Moisture loss from the samples was determined by weighing the sample tray outside the drying chamber using an electronic balance with an accuracy of ±0.01 g.

Adsorption

Gros Michel bananas (*Musa sapientum* L.) with a maturity stage of 5 were purchased from a local market. The banana contained total soluble solid content of 23-25° Brix. To prepare banana foam, the bananas were sliced and pretreated by immersing them in 1% (w/w) sodium metabisulphite solution for 2 min and rinsing them with distilled water for 30 s, in order to prevent discoloration during foaming process. The banana puree with 5% of fresh egg albumen, used as foaming agent, were foamed to densities of 0.3, 0.5 and 0.7 g/cm^3. The banana foam density was determined by measuring the mass of a fixed volume of the foam. The banana foam was poured slowly into a steel block and then placed on a mesh tray, which was covered with aluminium foil. After that, it was dried to about 3% kg/kg d.b. using tray dryer which was operated at 80°C and a 0.5 m/s superficial air velocity. The banana foam prepared from the initial foam densities of 0.3, 0.5 and 0.7 g/cm^3 could produce the dried banana densities of 0.21 ± 0.02, 0.26 ± 0.02 and 0.30 ± 0.02 g/cm^3, respectively. The product thicknesses after drying were 2.8, 3.2 and 3.4 mm for the banana foam densities of 0.21, 0.26 and 0.30 g/cm^3, respectively.

Moisture adsorption experiments were carried out using the static method. The dry samples prepared from the above drying method were placed into the glass jars contained the saturated salt solutions ($MgCl_2 \cdot 6H_2O$, $Mg(NO_3)_2 \cdot 6H_2O$, KI, NaCl and KCl) which provided the relative humidity (RH) in

range of 32-82% at the corresponding temperatures of 35, 40 and 45^{o}C. All the jars were placed in the temperature-controlled oven with a precision of ±1^{O}C (UFE500, Memmert, Germany). Samples were weighed at different exposure times ranging from 1 to 120 h. At RH > 74%, a small amount of toluene was held in a vial and fixed in the glass jars in order to prevent the sample spoilage by microbial.[11] Moisture content of each sample after reaching the equilibrium condition was determined by drying it with the hot air oven at a temperature of 103°C for 3 h. At this temperature, the percentage error was approximately 0.4% when compared to the result obtained by the standard vacuum method. The experiment at each adsorption condition was repeated three times and the mean value was reported. The sample was taken out from the jars to examine quality of product.

Results and Discussions

Effect of osmotic treatment on Drying characteristics and quality of puffed banana slices

When the banana sample was immersed into the higher sucrose concentration, the osmotic pressure difference increased, resulting in the larger loss of moisture content. Although the larger amount of moisture lost, the solid gain also increased. The increase of solid gain is caused by the diffusion of sucrose from the solution into the sample. From the experimental results, it was found that the ratios of water loss to solid gain increased with the increased sucrose solution concentrations, implying higher loss of moisture content than the solid gain. This is because the size of sucrose molecule is larger than that of water molecules. Hence, the water molecule can move with a rate faster than the sucrose molecule.

Osmotic treatment of banana slices with sucrose solution concentration, given in the range of 30 to 40^{O}Brix, can retard the browning reactions and the subsequent product color was less brown than that of product without osmotic treatment. This is because the monosaccharide, i.e. glucose and fructose, serving as a main active component for non-enzymatic browning reactions leaches out during the osmotic dehydration (**details see Annex B**). Consequently the browning rate is retarded during high temperature puffing, resulting in less brown for the osmotic samples than the non osmotic sample. The osmotic agent concentrations seemed to be not affect the osmotic product color, as indicated by L-, a- and b- values and hue angle, whether it was puffed at 180 or 220^{O}C. The product color had brownish-yellow. In addition, the impregnation of banana with sucrose allowed more difficulty of moisture travelling to the exterior surface, hence lengthening the drying time as compared to that of the non osmotic banana. Also, the sucrose containing OH interact with OH in the banana tissue by hydrogen bonding and the resulting tissue may relatively rigid. Their interaction leaded to more difficulty of expansion of banana during puffing as indicated by shrinkage property which showed a larger shrinkage for the osmotic banana slices than the non-osmotic ones. Microstructure of the osmotic banana after puffing

exhibited small pores or less porous structure whilst it showed very porous for the non osmotic sample. The low porous structure of the osmotic sample made poor texture, very hard and less crisp. The range of puffing temperature used in this study could not improve the aforementioned qualities. The details of osmotic treatment can be seen in **Annex B.**

Effect of foaming agents on drying characteristics and quality of dried banana foam

EA and WPC at 5% by weight were found to be efficient foam inducer, decreasing banana foam density to 0.3 g/cm^3, whilst the addition of SPI at this percent weight or higher could not produce at this foam density. The minimum density of the SPI banana foam produced was at 0.5 g/cm^3. Banana foams produced using WPC had more stability during whipping than another two foaming agents and this, in turn, provided less shrinkage during drying. The shrinkage of EA, WPC and SPI banana foam mats at the density of 0.5 g/cm^3, as for example, were 50, 36 and 66%, respectively. Due to good foam stability, the gas bubbles dispersed in the WPC banana could withstand the stresses occurring during drying and less collapsed, thereby providing the higher void area fraction or, in other word, higher porosity than the other two foaming agents. Furthermore, the value of effective moisture diffusivity was also higher for the WPC banana foam (details see **Annex C)**.

From the highest void area fraction, the WPC banana foam after drying provided correspondingly the highest number of peak and it should have crisp texture. However, its texture was not crisp since the initial slope of the first peak force from the force deformation curve was relatively lower than that of the SPI banana foam. For example, the initial slopes for the banana foam density of 0.5 g/cm^3 were 30, 12 and 16 N/mm for SPI, EA and WPC, respectively. From the texture results, it indicated that using only number of peak was not a good indicator for characterizing the crisp food foam. The initial slope of the first peak should be taken into account as well.

The volatile components present in the banana foam were also determined, besides textural properties. The most significant volatile compounds in fresh banana were the isoamyl acetate, isobutyl butanoate, butyl butyrate, isoamyl butyrate and isoamyl isovalerate. Among these five esters, only isoamyl acetate, isoamyl butyrate and isoamyl isovalerate, are the key components of the banana's fruity odor. The volatile components in the banana foam samples before and after drying were analyzed using GC-MS. It found the substantial loss of volatile substances during the foaming process (> 60%) although the foaming was performed at room temperature. The isoamyl acetate, which is the lowest molecular weight, exhibited the highest loss during the foaming process. At the drying end, the total loss of volatile components was over 90% for all foaming agents used in this study.

Effect of adsorption conditions on diffusivity and textural property of dry banana foam mat

Diffusion coefficient of moisture during adsorption were determined by two approaches, continuum and pore network. The moisture diffusion coefficient determined by the pore network referred to pore diffusivity and the diffusion coefficient determined by the continuum referred to effective diffusivity. The details can be seen in **Annex D**. The effective diffusivity, assuming the diffusivity independent on the moisture content, was significantly higher than the pore diffusivity (see Annex C), and the value of effective diffusivity was higher at lower density of banana foam mat. On the other hand, the change of pore diffusivity with banana foam density was less sensitive to foam density. This indicated that the determined pore diffusivity is rather universal and could possibly be applied to other porous foods.

Since the banana foam mat is very porous, it can adsorb water vapor rapidly, which leads subsequently to poor texture in particular crispiness. As measured from the experiments, the number of peaks and initial slope for all foam densities significantly decreased with increasing moisture content (See **Annex E**). In contrast to the number of peaks or the initial slope, the maximum forces for samples with foam densities, except at foam density below 0.26 g/cm^3, increased with increasing moisture content. At the lower foam density of 0.26 g/cm^3, the insignificant change in the maximum force is observed in the moisture range of 0.039-0.078 kg/kg d.b. From this study, it indicated that the number of peaks were almost absent at the moisture content of 0.078 kg/kg d.b., and it may be expected that the banana foam samples loss their crispy texture. This moisture content for the banana foam is given in same range of other crisp products such as crispy breads, cereals, popcorn and puffed corns, and it may be concluded that the moisture content of crisp products should not be higher than 0.07-0.08 kg/kg d.b. in order to preserve their textures.

Designing porous structure of banana foam to resist moisture adsorption using a 2-D stochastic pore network

Because of rapid moisture adsorption of the finished banana foam mat when exposed to atmosphere, the restriction on water vapor diffusing into the product is important in order to preserve the crisp characteristic of the product. The pore network was therefore used to design the porous structure configurations of banana foam mat and the experiment were carried out in order to validate the results. Two configurations of porous banana foam were proposed in this study. For each configuration, the banana foam mat was divided into two layers. The lower layer of the network was assigned from a fixed pore size distribution of the dried banana foam density of 0.26 g/cm^3. This is because the texture at this density was rather crispy and not very hard. For the upper layer, where it was exposed to environment, the pore size distribution from the banana foam density of 0.21 g/cm^3 or from the density of 0.31 g/cm^3

were assigned (see details in **Annex F**). The simulation results at the adsorption temperature of 35^{o}C and 67% relative humidity showed that the slowest adsorption rate was evident in the two-layer network of which the pore sizes obtained from the foam density of 0.31 g/cm^{3} was laid at the upper half. On the other hand, the fastest adsorption rate was found in the case that the pore sizes from the foam density of 0.21 g/cm^{3} was laid on the upper half layer. This is because the dry banana foam at density 0.21 g/cm^{3} had a higher porosity as compared to that at 0.31 g/cm^{3}. The simulation results agreed well with the experiments.

For the textural property, it was found that it is not crispy for the two-layer banana foam with density of 0.21 g/cm^{3} laid on the upper layer. In contrast, the two-layer banana foam with high density of 0.31 g/cm^{3} laid on the upper layer was crisp and more crispness than the single density of banana foam (0.26 g/cm^{3}) as indicated by the number of peaks which showed higher than 20 for the two-layer banana foam while it was 12 for the single density. In contrast,. However, from the sensory test using trained panelists, the textural properties i.e. hardness and crispness and overall acceptability between such both samples were not different.

LWT - Food Science and Technology 44 (2011) 1502–1510

Contents lists available at ScienceDirect

LWT - Food Science and Technology

journal homepage: www.elsevier.com/locate/lwt

Determination of effective moisture diffusivity and assessment of quality attributes of banana slices during drying

Ratiya Thuwapanichayanan [a], Somkiat Prachayawarakorn [b,*], Jaruwan Kunwisawa [b], Somchart Soponronnarit [c]

[a] Department of Farm Mechanics, Faculty of Agriculture, Kasetsart University, 50 Phaholyothin Road, Bangkok 10900, Thailand
[b] Department of Chemical Engineering, Faculty of Engineering, King Mongkut's University of Technology Thonburi, 126 Pracha u-tid Road, Bangkok 10140, Thailand
[c] School of Energy, Environment and Materials, King Mongkut's University of Technology Thonburi, 126 Pracha u-tid Road, Bangkok 10140, Thailand

ARTICLE INFO

Article history:
Received 21 January 2010
Received in revised form
26 December 2010
Accepted 9 January 2011

Keywords:
Banana
Drying
Effective moisture diffusivity
Volatile compounds
Texture

ABSTRACT

The influence of drying temperatures on the moisture diffusivity and quality attributes of the dried banana slices in terms of volatile compound, shrinkage, color, texture and microstructure were studied. Bananas with peel color index of 5 corresponding to yellow color with green tip were sliced into 3 mm thickness, dipped into ascorbic acid solution and dried at four temperatures of 70, 80, 90 and 100 °C. Drying rate of banana slices can be divided into two sub-drying periods, first and second falling rate periods. The effective diffusivity estimated by the optimization technique was found to decrease sharply with moisture content in the first falling rate period and changed slightly in the second falling rate period. High-temperature drying seems to provide lower loss of volatile compounds in the dried sample. Moreover, the dried banana was very porous, resulting in remarkably lower hardness value than that obtained from the low-temperature drying whilst the crispiness was not significantly different amongst the samples obtained at various drying temperatures. Although the textural property could be improved at high temperature, the product color was brown as manifested by the low L- and hue values in particular at the drying temperature of 100 °C.

1. Introduction

Banana, one of the most favorite fruits, is widely grown in many countries. It is normally consumed as fresh, however, the qualities of fresh banana deteriorate rapidly after harvesting. Drying is an alternative method to preserve the food quality and to reduce losses. During drying, moisture present in a food diffuses from the internal to the food surface and evaporates into the air stream and at the same time, the heat is transferred from the air to the food. When moisture is removed, the volume of food decreases. Moisture gradient occurring inside the food during drying generates stresses in the cellular structure of the food resulting in the structure collapse which responds to the physical changes of shape and dimension or the volume change of material (Mayor & Sereno, 2004; Pan, Shih, McHugh, & Hirschberg, 2008). Such cell wall disruption subsequently affects the diffusing distance of moisture which moves from inside to the outside. This factor must be included into the mathematical model in order to predict accurately the sample moisture content during drying or to determine the correct effective diffusion coefficient (Katekawa & Silva, 2006; Thuwapanichayanan, Prachayawarakorn, & Soponronnarit, 2008). In drying of bananas, empirical models and diffusion models have frequently been used to describe the drying kinetics of bananas (Dandamrongrak, Young, & Mason, 2002; Demirel & Turhan, 2003; Jannot, Talla, Nganhou, & Puiggali, 2004). The shrinkage effect was not included into the previously proposed models for drying of banana. Ignorance of shrinkage may lead to inaccurate prediction of moisture content when the industrial scale dryer is designed based on these data.

Drying temperature is an important parameter required for dryer operation. High temperature is practically used in order to accelerate the drying rate. However, the use of high-temperature drying may cause degradation of banana quality regarding to the changes in color, texture and size and the loss of volatiles (Baini & Langrish, 2009; Boudhrioua, Giampaoli, & Bonazzi, 2003; Hofsetz, Lopes, Hubinger, Mayor, & Sereno, 2007; Prachayawarakorn, Tia, Plyto, & Soponronnarit, 2008). The evaluation of the quality degradations at drying temperatures can help the selection of drying temperature that optimizes the quality of dried banana.

* Corresponding author. Tel.: +662 470 9221 30; fax: +662 428 3534.
E-mail address: somkiat.pra@kmutt.ac.th (S. Prachayawarakorn).

0023-6438/$ – see front matter © 2011 Elsevier Ltd. All rights reserved.
doi:10.1016/j.lwt.2011.01.003

As mentioned above, the objectives of this work were therefore to determine the moisture diffusivity and evaluate the qualities of the dried banana in terms of volatile compound, shrinkage, color and textual property.

2. Materials and methods

2.1. Experimental set-up

A thin-layer dryer as shown in Fig. 1 was used in this study; it consists of a backward curved blade centrifugal fan (driven by a 0.37 kW motor), an electrical heater and a drying chamber. Ambient air heated by the electrical heater under Proportional-Integral-Derivative (PID) control was passed through the samples that were placed on a perforated tray within the drying chamber. The air velocity was fixed at 1.3 m/s by setting a frequency inverter, which controls the rotation speed of the motor.

2.2. Material preparation

Gros Michel bananas with peel color index of 5 corresponding to yellow color with green tip, which contained total soluble solids of approximately 23–25°Brix, were peeled and sliced into 3 mm thickness with a slicing machine. The sliced bananas were pretreated by dipping them in 0.1g/100 ml ascorbic acid solution for 1 min to prevent enzymatic browning reaction (Krokida, Kiranoudis, Maroulis, & Marinos, 2000).

2.3. Drying procedure

Banana slices were placed on a perforated tray, with a size of square hole of 2 × 2 cm, and then put into the drying chamber. Drying was performed in duplicate at the drying air temperatures of 70, 80, 90 and 100 °C and at the superficial air velocity of 1.3 m/s. As observed from the experiments, the deviation of moisture content from the two experiments was very small. The samples were dried to about 0.04 kg/kg db. In order to follow moisture evolution, moisture loss from the samples was determined throughout the drying period by weighing them every 5 min using an electronic balance (±0.01 g). At the end of drying, the moisture content of the samples was determined by drying them at 103 °C for 3 h in a hot air oven. Normally, the moisture content of banana was determined by the vacuum oven method 934.06 (AOAC, 1995). However, drying of banana in a hot air oven at 103 °C for 3 h was used instead of AOAC method (AOAC, 1995). The moisture content determined by the hot air oven was closed to that obtained by the vacuum oven method, the percentage error from two methods approximately 0.4%.

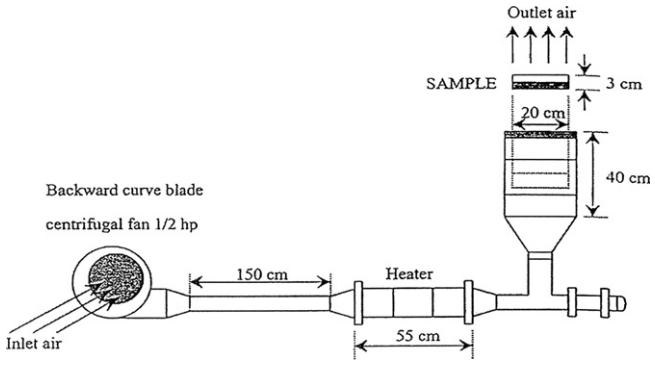

Fig. 1. A schematic diagram of thin-layer dryer.

2.4. Determination of effective moisture diffusivity

A diffusion model based on the Fick's second law of diffusion was used to describe the transport of moisture inside a banana slice (Crank, 1975):

$$\frac{\partial M}{\partial t} = \frac{\partial}{\partial x}\left(D\frac{\partial M}{\partial x}\right) \tag{1}$$

where D is the effective moisture diffusivity (m^2/s), M is the local moisture content (kg/kg d.b.), x is the coordinate along the diffusion path and t is the drying time (s).

The assumptions used in this model were that the product shape was an infinite slab and the moisture distribution inside a banana slice was uniform at the beginning of drying. In addition, the moisture transfer occurred only in the thickness direction and the external resistance to moisture transfer was negligible. The shrinkage effect should be taken into account for determining the effective moisture diffusivity, particularly when the material shrinkage is high. This is because the mean diffusion path of moisture which travels from the inside to outside is shorter. If this effect is not included into the diffusion model, it subsequently results in the overestimation of the effective coefficient (Ruiz-López & García-Alvarado, 2007; Mulet, 1994).

The diffusion model including shrinkage can be solved by the moving or immobilizing boundary methods. However, the use of latter method is rather limited with some applications. Thuwapanichayanan et al. (2008) reported that the immobilizing boundary can predict the average moisture content accurately when applied to the high density foods of which their shrinkage equals to the volume of evaporated water. On the other hand, the moving boundary method can be used in a broader case, and this method is therefore used in this study.

Several works have been reported about the drying rate of banana and found that the drying rate, when plotted against the moisture content, is mainly in the falling rate with two sub periods (Mowlah, Takano, Kamoi, & Obara, 1983; Prachayawarakorn et al., 2008). Furthermore, Jannot et al. (2004) found the third falling rate period, characterized by the convexity of the drying rate curve, when the sample was dried to moisture ratio lower than 0.2. The development of such events inside the banana while being dried indicated that the molecular mobility of moisture changes as the moisture content inside the banana is altered. Such change can be described by the relationship between the effective moisture diffusivity and the moisture content of material.

To obtain moisture dependent diffusivity, Eq. (1) was first transformed into differential elements using the variable grid central finite difference method in its explicit and its expression is shown below:

$$\frac{M_i^{j+1}-M_i^j}{\Delta t} = D_i^j \frac{\dfrac{M_{i+1}^j-M_i^j}{\Delta x_{i+1}^j} - \dfrac{M_i^j-M_{i-1}^j}{\Delta x_i^j}}{\dfrac{\Delta x_{i+1}^j}{2}+\dfrac{\Delta x_i^j}{2}} + \frac{M_{i+1}^j-M_{i-1}^j}{\Delta x_{i+1}^j+\Delta x_i^j}\cdot\frac{D_{i+1}^j-D_{i-1}^j}{\Delta x_{i+1}^j+\Delta x_i^j} \tag{2}$$

where the subscript i and j represent node and time indexes, respectively. The Eq. (2) describes the moisture content inside the banana slice. For the moistures at the center and both surfaces, they can be described by the following equations:

At the center:

$$\frac{M_0^{j+1} - M_0^j}{\Delta t} = 2D_0^j \left(\frac{M_1^j - M_0^j}{\left(\Delta x_1^j\right)^2} \right) \quad (3)$$

At the top and bottom surfaces:

$$M|_{x=\pm\frac{L}{2}} = M_{eq} \quad (4)$$

Before calculating the moisture contents inside the banana sample, it is necessary to identify the diffusivity equation that can suitably describe the variation of effective diffusivity with moisture content. An empirical form of Eq. (5) in which the effective diffusivity decreases exponentially with decreasing moisture content was tested and the calculated results showed this form adequately describe the moisture diffusion in banana slice.

$$D(M) = A\exp(BM) \quad (5)$$

where A and B are the constant parameters, which can be estimated by the optimization technique using a modified Nelder-Mead simplex method. If the initial guess values of A and B is not appropriate, the solution can be diverged or the computation time rather takes a long time. To alleviate such problems, the initial guess of the above-mentioned constant parameters was determined by the method of slopes, where the values of effective moisture diffusivity was estimated at moisture contents, and the regression technique was then used to obtain the values of A and B at a drying temperature.

After the moisture contents at inner side were determined, the spacing between each grid points was then adjusted according to the average moisture content of each section. The relationship between spacing of each section and average moisture content in that section was assume to be a linear function. It can be calculated by the following equation:

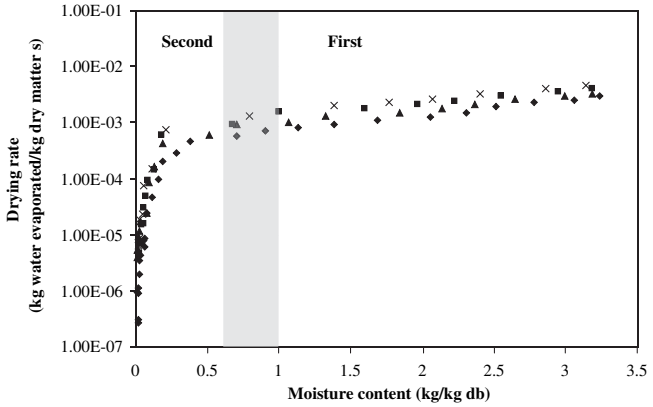

Fig. 3. Changes of drying rate of banana slice at different drying temperatures (3.5 mm thickness): 70 °C (◆), 80 °C (▲), 90 °C (■), 100 °C (×). Values are means ($n = 2$).

$$\Delta x_i/\Delta x_0 = c + d(M_{av}/M_0) \quad (6)$$

where c and d are the constant parameters that were obtained by linear regression analysis of the experimental shrinkage data (both values are shown in the shrinkage section), M_{av} is the average moisture content of each section (kg/kg d.b.), M_0 is the initial moisture content (kg/kg d.b.), Δx_i is the spacing between each grid point (m), Δx_0 is the spacing between grid point at the beginning (m).

After the moisture contents at positions inside the sample was known, the average moisture content was then calculated by integrating the moisture contents at all grid points, and then compared to the experimental values. If the root mean square error (RMSE) was not minimized, a new guess of the constant parameters in Eq. (5) was searched and the same calculation procedure as mentioned before was used.

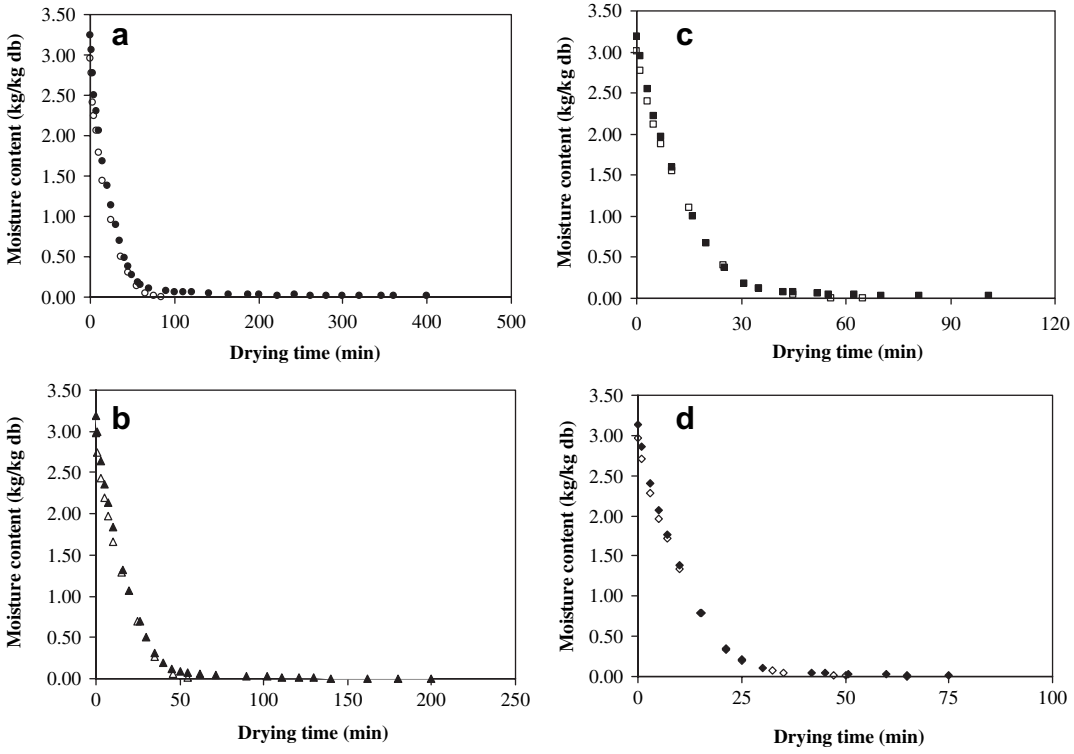

Fig. 2. Drying curves of banana slices at different diameters and drying temperatures (3.5 mm thickness): (a) 70 °C (○ $D = 25$ mm; ● $D = 35$ mm), (b) 80 °C (△ $D = 25$ mm; ▲ $D = 35$ mm), (c) 90 °C (□ $D = 25$ mm; ■ $D = 35$ mm), (d) 100 °C (◇ $D = 25$ mm; ◆ $D = 35$ mm). Values are means ($n = 2$).

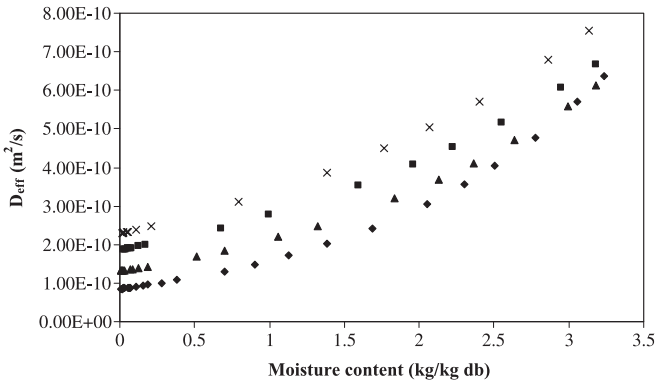

Fig. 4. Variation of effective diffusivity with moisture content at different drying temperatures: 70 °C (◆), 80 °C (▲), 90 °C (■), 100 °C (×).

2.5. Analysis of volatiles

2.5.1. Sample preconcentration (SPME)

The volatile components of fresh and dried banana slices were isolated by solid phase micro-extraction (SPME). Each sample was done in duplicate. Each sample was homogenized, placed in a 20 ml vial and then weighed by a balance with precision of ± 0.01 g; 4 g for fresh banana (including moisture) and 1 g for dried banana slice. The sample with a mass of 4 g was filled up with 6 ml of distilled water and the sample with a mass of 1 g was filled up with 9 ml of distilled water. The internal standard, which consists of 0.2 μl of caproic acid ethyl ester in 1 ml/l methanol solution, was added to those samples. The vial was then covered with a silicone Teflon-lined septum. A stainless steel needle covered with an 85 μm length carboxane/polydimethyl siloxane fiber penetrated the septum. The fiber was then pushed into the headspace above the sample for absorption at 30 °C for 30 min.

2.5.2. Gas chromatography-mass spectrometry analysis (GC-MS)

Sample analysis was carried out with a Hewlett–Packard 6890 gas chromatography (GC). An HP5 column, with a 30 m length, 0.25 mm diameter, 0.25 μm thickness was used. Helium used as the carrier gas flowed at a rate of 1 ml/min. Thermal desorption of the volatile components from the fiber was carried out in the GC split injector (1:10) at 200 °C for 5 min. The oven temperature was programmed by starting at 40 °C and holding at that temperature for a 1 min. After that, the temperature was increased to 120 °C with a rate of 3 °C/min. The volatile compounds were analyzed by mass spectrometry with electronic impact (EI) 70 eV quadripolar filter and identified by comparison with spectra stored in a data bank.

2.6. Shrinkage measurement

Three banana slices were taken at different drying times to measure their dimensions (diameter and thickness). The diameter was measured using a vernier and the thickness was measured by caliper. The mean values were reported. Diameter and thickness shrinkage were defined as:

$$\text{Diameter Shrinkage} = D/D_0 \quad (7)$$

$$\text{Thickness Shrinkage} = L/L_0 \quad (8)$$

where D is the sample diameter of dried sample (mm), D_0 is the sample diameter before drying (mm), L is the dried sample thickness (mm), L_0 is the sample thickness before drying (mm).

Table 1
Estimated values of constant parameters for moisture dependent diffusivities (A and B in Eq. (5)) of banana slices dried at different drying temperatures.

Drying conditions	Moisture dependent diffusivity (m^2/s)		
	A	B	RMSE
70	8.500E-11	0.622	0.036
80	1.310E-10	0.484	0.037
90	1.853E-10	0.402	0.045
100	2.290E-10	0.381	0.043

2.7. Color measurement

The surface color of dried banana slices was measured using a colorimeter (ColorFlex, HunterLab, USA). The colors were expressed as L-value (lightness), a-value (redness/greenness) and b-value (yellowness/blueness). The overall color of dried banana slices was presented using hue angle (^{o}h), which was calculated by $^o h = \tan^{-1}(b/a)$. The colorimeter was calibrated with a standard white plate ($L^* = 96.98$, $a^* = 0.03$ and $b^* = 1.84$) before each color measurement. The measurements were performed at different positions for each sample. Ten samples were tested and the average value was reported.

2.8. Texture analysis

Dried banana slices at moisture content of 0.04 kg/kg db were taken to examine their textural properties. The texture of dried banana slices was measured using a texture analyzer model TA.XT.plus (Stable Micro Systems, Surrey, UK). A cutting probe was used to apply a direct force to the sample at a constant rate of 2 mm/s. The maximum force of the force-deformation curve is defined as hardness and the initial slope of the first peak is represented as crispiness. Eight samples for each treatment were tested and the average values of hardness and initial slope were reported.

2.9. Microstructure evaluation

A scanning electron microscope (JEOL JSM-5800LV, Tokyo, Japan) was used to characterize the microstructure of dried banana slices. Before scanning, the dried banana slices were dipped into liquid N_2 for 5 s to prevent the morphology change during specimen preparation. The samples were then placed on two-side adhesive tape attached to metal stub and were coated with gold.

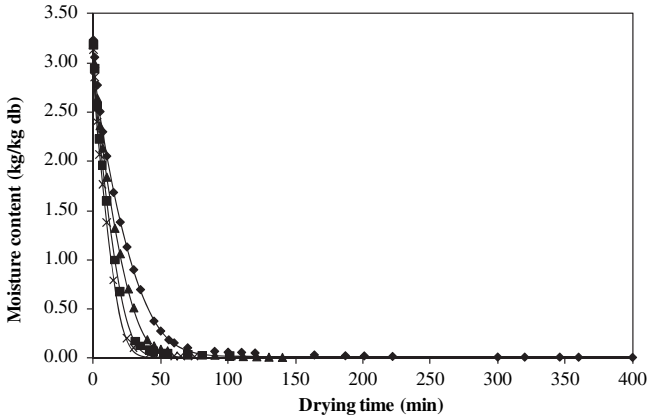

Fig. 5. Predictions of moisture content of banana slices dried at different drying temperatures: 70 °C (exp.) (◆), 80 °C (exp.) (▲), 90 °C (exp.) (■), 100 °C (exp.) (×), prediction (—).

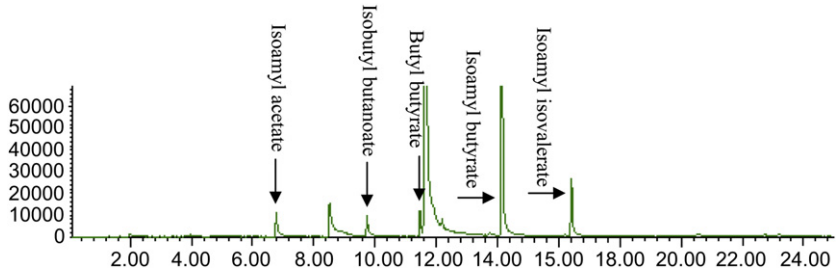

Fig. 6. Chromatograms profiles of fresh banana at ripeness stage of 5.

SEM micrographs were taken at an accelerating voltage of 15 kV and a magnification of 200×.

2.10. Image analysis

Image analysis software (ImagePro + 5.0, MediaCybernetic, MD, USA) was used to characterize the pore size. Each pixel of SEM micrograph was assigned a gray-level value (0–255). The pores were distinguished from the solid phase using threshold-based segmentation method, and a binary image was obtained. The pixels with gray-level values lower than the specified threshold were assigned as pore, which appeared as black color in a binary image whereas the pixels with gray-level values above the specified threshold were set as solid phase, which appeared as white color in a binary image. With an assumption of spherical shape, a pore diameter was estimated from the known pore area.

2.11. Statistical analysis

The analysis of variance (ANOVA) was used to perform the effect of drying temperatures on the quality attributes. Duncan's test was used to establish the multiple comparisons of mean values. Mean values were considered at 95% significance level ($p < 0.05$).

3. Results and discussion

3.1. Drying characteristics of banana slices

Fig. 2 shows the influence of diameter of banana samples with a 3 mm thickness dried at 70, 80, 90 and 100 °C. The banana slices were prepared at two diameter sizes, 25 and 35 mm, and the corresponding $\frac{L}{D}$ ratios of sample were 0.12 and 0.09. It was found that the changes of moisture content with time were not different amongst two diameter sizes. These results justify the mobility of moisture during drying taking place in direction of thickness, and Eq.(1) describing the diffusion of moisture in one dimension was reasonable to explain the moisture diffusion inside the banana slice during drying.

Fig. 3 shows the variation of drying rate at different temperatures (semi-log scale plot), indicating the falling rate being a main drying mechanism in controlling the water evaporation rate. This drying rate curve is a typical drying behavior for agricultural materials that possess porous structures or cellular structures i.e. paddy, carrot, apple and potato (Pakowski & Adamski, 2007; Poomsa-ad, Soponronnarit, Prachayawarakorn, & Terdyothin, 2002; Simal, Deyá, Frau, & Rossello, 1997; Srikiatden & Roberts, 2006). From the drying rate change of banana as shown in Fig. 3, it can be divided into two sub-drying periods; first and second falling rate periods. In the first falling rate period, the drying rate changed linearly with moisture content for all drying temperatures. As the moisture content of banana was lower than the critical value which was in the range of 0.75–1.0 d.b., the second falling rate period started and its change was in a non-linear fashion. Some of early works involved with the banana drying have also found two

Table 2
Volatile compounds identified in fresh bananas at ripeness stage of 5.

Retention time (min)	Compounds	Fraction[a,b] (%)
1.96	Ethyl acetate	0.68
3.95	Isobutyl acetate	0.48
6.74	Isoamyl acetate	5.89
9.72	Isobutyl butanoate	5.27
11.46	Butyl butyrate	3.82
12.18	n-Amyl isobutyrate	7.14
13.72	n-Butyl isovalerate	0.63
14.17	Isoamyl butyrate	61.42
16.41	Isoamyl isovalerate	11.76
20.47	Hexyl butanoate	1.04
21	E-3-hexenyl butanoate	0.31
22.7	Hexyl valerate	0.67
23.19	trans-3-Hexen-1-ol	0.8

[a] Fraction is calculated by the peak area of the volatile compound divided by the total area of volatile compounds.
[b] Values are means ($n = 2$).

Table 3
Peak areas of five major volatile compounds in fresh and dried bananas.

Lot	Drying temperature	Volatile compound	Peak area[a] (×10^6/g dry weight)		% loss
			Fresh	Dried	
1	70	Isoamyl acetate	69.44	6.13	91.17
		Isobutyl butanoate	68.48	19.17	72.01
		Butyl butyrate	44.90	14.18	68.42
		Isoamyl butyrate	666.78	278.80	58.19
		Isoamyl isovalerate	235.18	91.61	61.05
		Total of 13 compounds	1314.65	496.99	62.20
	80	Isoamyl acetate	41.40	15.86	61.69
		Isobutyl butanoate	36.68	16.99	53.68
		Butyl butyrate	39.73	22.27	43.95
		Isoamyl butyrate	514.73	308.69	40.03
		Isoamyl isovalerate	102.98	54.40	47.17
		Total of 13 compounds	835.29	484.84	41.96
2	90	Isoamyl acetate	12.01	3.56	70.36
		Isobutyl butanoate	9.58	1.79	81.32
		Butyl butyrate	12.29	3.65	70.30
		Isoamyl butyrate	111.24	35.66	67.94
		Isoamyl isovalerate	9.62	1.92	80.04
		Total of 13 compounds	183.13	47.21	74.22
	100	Isoamyl acetate	18.77	9.61	48.80
		Isobutyl butanoate	15.48	8.38	45.87
		Butyl butyrate	17.54	12.58	28.28
		Isoamyl butyrate	177.27	132.45	25.28
		Isoamyl isovalerate	7.00	6.23	11.00
		Total of 13 compounds	292.33	182.79	37.47

[a] Values are means ($n = 2$).

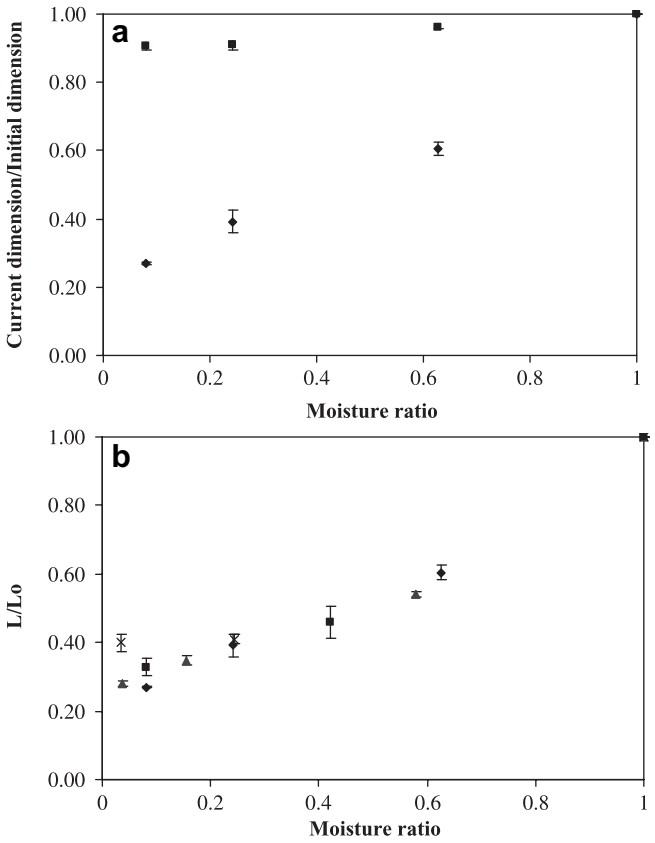

Fig. 7. (a) Diameter and thickness changes (D/D_0 and L/L_0) of banana slices dried at temperature of 70 °C: D/D_0 (■), L/L_0 (◆). Values are means ± SD ($n = 3$). (b) Thickness changes of banana slices dried at different temperatures ($L_0 = 3$ mm, $D_0 = 35$ mm); 70 °C (◆), 80 °C (▲), 90 °C (■), 100 °C (×). Values are means ± SD ($n = 3$).

falling rate periods (Mowlah et al., 1983; Prachayawarakorn et al., 2008; Sankat, Castaigne, & Maharaj, 1996). In the first falling rate period, the moisture evaporation takes place near the banana surface. When the drying continues, the dry patch surface occurs whilst the internal area is still wet. This results in moisture taking a longer time to reach surface and hence provides a rapid drop in the drying rate, implying that the drying enters into the second falling rate period. For banana slice drying, the critical moisture content found in this study was close to that reported by several workers who studied the drying of osmotic or non osmotic bananas (Prachayawarakorn et al., 2008; Sankat et al., 1996) although the operating conditions in their studies were different from the present investigation.

3.2. Effective diffusivity

Fig. 4 shows the changes of effective diffusion coefficients with moisture contents and temperatures. The higher drying temperature can accelerate the water molecules present in the banana to evaporate faster, thus providing a faster decrease of the material moisture content and the corresponding higher value of effective moisture diffusivity. During isothermal drying, the value of effective moisture diffusivity decreased with moisture content. As shown in Fig. 4, the effective diffusivity declined sharply with moisture content in the first falling rate period and when the drying entered into the second period, the diffusivity changed slightly with moisture content. From these results, it suggested that the constant diffusivity can be assumed in the second falling rate period.

The constant parameters of A and B in Eq. (5) for the drying temperatures are shown in Table 1, along with the values of RMSE. The values of RMSE ranged between 0.037 and 0.045. These values were rather small, indicating that Eq. (5) was reasonable to explain the relationship of moisture diffusivity with the banana moisture content. The prediction of moisture contents as shown in Fig. 5 agreed well with the experimental results. The values of moisture diffusivity found in this study was in the order of 10^{-11}–10^{-9} m^2/s which is typical value for drying of agricultural products (Dissa, Desmorieux, Bathiebo, & Koulidiati, 2008; Ruiz-López, I.I. and García-Alvarado (2007); Ramesh, 2003), and these values also indicated that the moisture movement inside the banana at the drying temperatures was in the liquid form.

3.3. Volatile compounds

Fig. 6 shows the typical chromatogram profiles of fresh banana at ripeness stage of 5; the stage of ripeness can be divided by the color of the peel. The banana with a peel color index of 5, representing yellow with green tip, was used in this study. There were 13 volatile compounds found in banana at this ripeness stage and the fraction of each volatile compound, determined by dividing an area of the peak of a component by total areas of all volatile components, is shown in Table 2. The major volatile compounds were isobutyl butanoate, butyl butyrate, isoamyl acetate, isoamyl butyrate and isoamyl isovalerat, three latter volatile compounds presenting the banana odor (Salmon, Martin, Remaud, & Fourel, 1996). These 5 representative volatile compounds were determined quantitatively for the final product obtained from drying temperatures.

Table 3 presents the remaining volatile compounds of banana after drying. The banana used in the experiments came from a different lot. The amounts of volatile compounds present in the fresh banana had a remarkable difference between lot 1 and lot 2 although the ripeness stage of banana used in this study was identical. The differences in volatile contents were not clear. However, one of the possible reasons is that the banana in each lot used in the experiments might come from different cultivation areas. Brat et al. (2004) showed that the banana at the ripeness stage of 5 had a different volatile composition if it was cultivated in different areas; the cultivation at the hills exhibited higher concentrations of ketones, alcohols and esters than that at the plain.

When the banana was subject to be dried at different temperatures, the total amount of 13 volatile compounds present in the dried banana decreased from that of the fresh banana and the remaining volatile compositions in the dried sample seem to be dependent on the drying temperature. Drying at high temperature may lose the total amounts of the volatile compounds in the dried sample lower than the low-temperature drying. These results can possibly be described by the exposure time that contacts the drying air. The drying times were 400, 140, 100 and 75 min for the drying temperatures of 70, 80, 90 and 100 °C, respectively. Several works have been reported that the loss of volatile compounds depended on the drying time and temperature (Boudhrioua et al., 2003; Krokida & Philippoulos, 2006). Yousif, Scaman, Durance, and Girard (1999)

Table 4
Color of dried banana slices dried at different temperatures.

Temperature (°C)	L-value	a-value	b-value	Hue angle (°h)
70	64.34 ± 1.49^a	4.55 ± 0.73^a	24.11 ± 0.58^a	79.35 ± 1.56^a
80	63.16 ± 0.72^a	4.59 ± 0.45^a	24.81 ± 0.58^a	79.53 ± 0.80^a
90	63.11 ± 1.44^a	4.39 ± 0.48^a	21.78 ± 0.97^b	78.59 ± 1.27^a
100	59.27 ± 1.70^b	7.06 ± 0.95^b	23.30 ± 0.45^c	73.16 ± 2.19^b

$^{a, b, c}$ means ± SD ($n = 10$) with different superscripts in the same column are significantly different at $p < 0.05$.

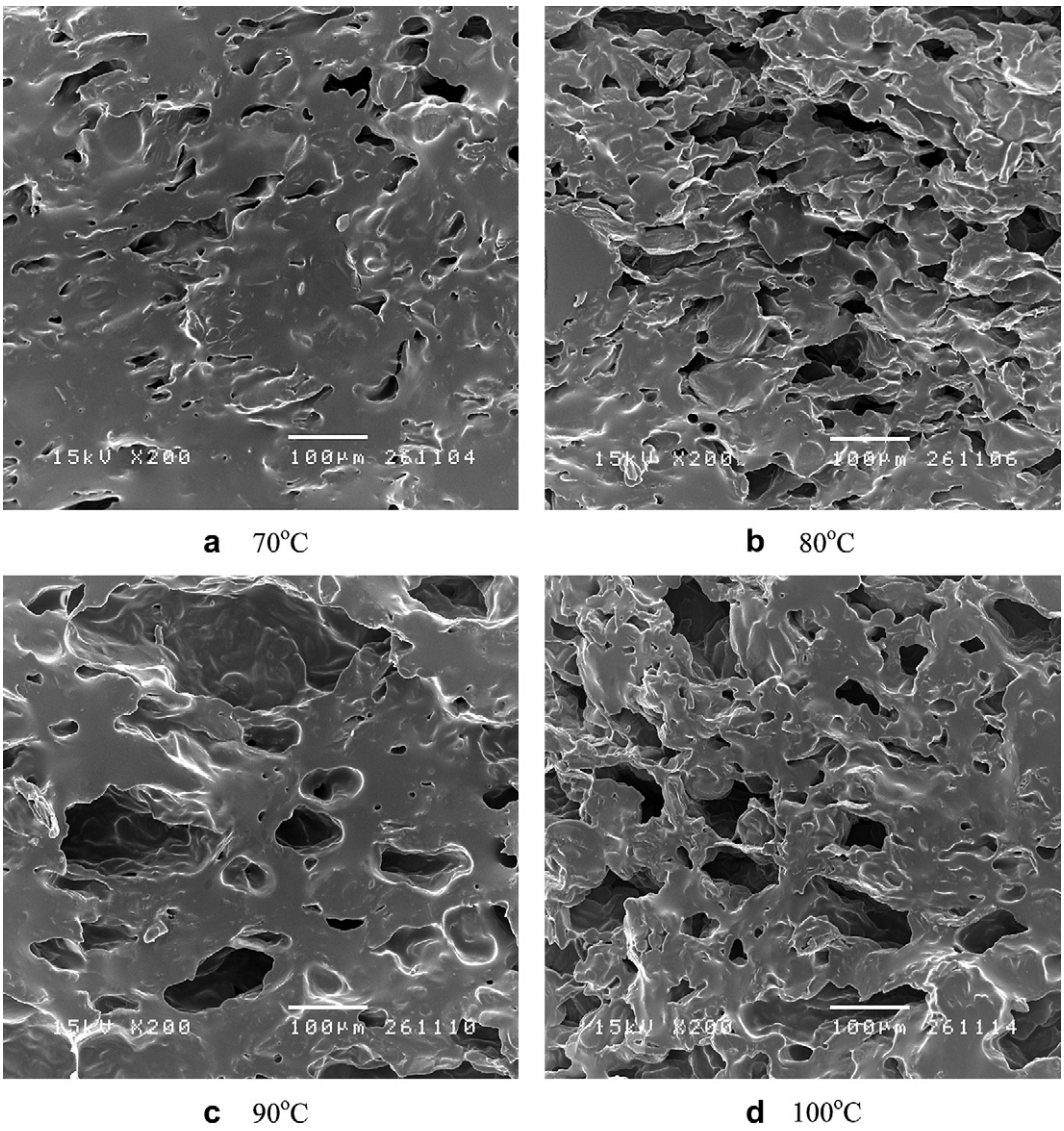

Fig. 8. Morphologies of banana slices dried at different temperatures.

performed the drying of sweet basil using the vacuum microwave at temperature of 45 °C and the hot air at temperature of 48 °C and found that the shorter drying time in the vacuum microwave could retain more volatile compounds than in the hot air drying.

Some interesting observations could be made concerning the changes of individual volatile compounds. The reduction in volatile compounds at a given drying temperature is different, depending on the characteristics of the compound. The isoamyl acetate and isobutyl butanoate exhibited the higher losses than the other volatile compounds. Factors such as boiling point, relative volatility and molecular weight may play an important role to volatile retention (Mui, Durance, & Scaman, 2002). The volatile with low molecular weight would be expected to have high diffusion coefficient and high loss as a result. The molecular weights of isoamyl acetate and isobutyl butanoate are relatively lower than the other volatile compounds.

3.4. Dimension

Fig. 7 (a) illustrates the changes of sample diameter and its thickness at the drying temperature of 70 °C. During drying, the sample dimensions changed linearly with the moisture content and the main change took place along the thickness. From this experimental result, the diameter of banana changed only 10% whilst the thickness change was approximately 60–70% at the drying end. Such dimension change can be attributed to the removed moisture and developing stresses during drying (Ketelaars, Jomaa, Puigalli, & Coumans, 1992). From the dimension change results, it is reasonable to assume that the shrinkage in the thickness direction was taken into account when calculating the transfer of moisture inside the banana sample during drying.

The effect of drying temperatures on the thickness change is shown in Fig. 7 (b). It seemed insignificant difference of banana shrinkage when the sample was dried within the temperature range studied. The shrinkage of banana at drying temperatures was described by Eq. (9).

$$L/L_0 = a + bM/M_0 \quad (9)$$

The values of parameters a and b in Eq. (9) were constant and obtained by linear regression analysis of the experimental data. The constant parameters of a and b were 0.2543 and 0.6384, respectively.

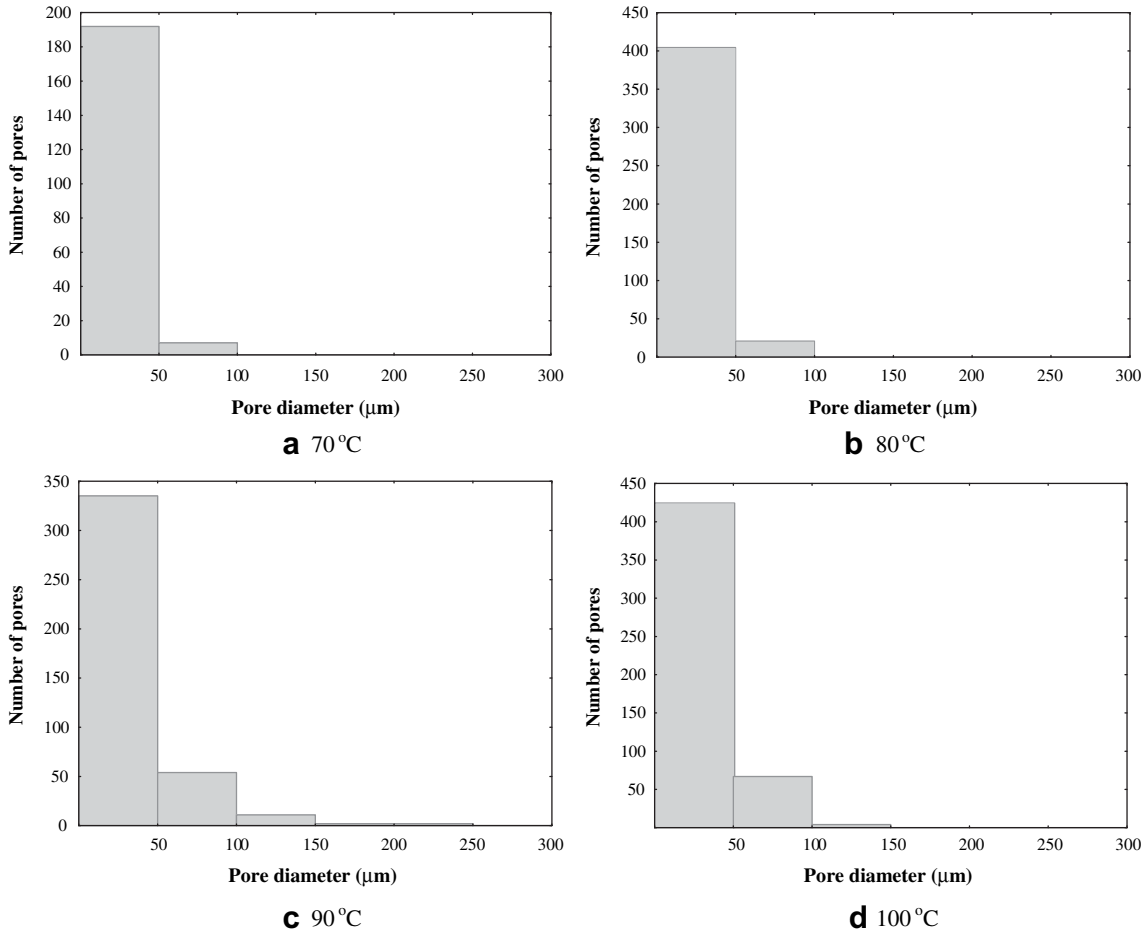

Fig. 9. Pore diameter distribution of banana slices dried at different temperatures.

3.5. Color

Table 4 shows the color of dried banana slices in terms of L-, a- and b-values. In addition, the overall color of dried banana slices was also presented using hue angle. A larger value of hue angle indicates a more shift from red to yellow. Color of banana slices was slightly yellow before drying and became brownish after drying. The discoloration decreased with decreasing drying temperature. Drying at the temperature of 100 °C provided the browner product color than the other drying temperatures as manifested by the lowest L- and hue values. From statistical analysis using ANOVA, the dried banana color obtained from the drying temperatures of 70–90 °C was not different, indicating the insignificant effect of these drying temperatures on the browning rate. This result corresponded to the experimental result reported by Baini and Langrish (2009); they found that the drying temperatures ranging from 50 to 80 °C did not affect the browning rate in banana, but it was significant at the drying temperature of 100 °C.

3.6. Microstructure and image analysis

Dried banana morphologies obtained at temperatures are shown in Fig. 8 (a–d). The drying temperature strongly affected the dried banana morphology. The shrinkage stresses occurring during drying caused numerous breaks of banana tissue. The microstructure of dried banana was characterized by the small or large pores depending on the drying temperature. As shown in Fig. 9, drying at a temperature of 70 °C could create the pores with diameters smaller than 100 μm. Moreover, the number of these pores was also small. Smalls in number of pores and sizes led to the dense structure. The pore sizes and the number of pores increased with increasing drying temperature. The banana tissue dried at the drying temperatures of 90 and 100 °C were extensive structural damage as characterized by larger number of pores and large pore size. It can clearly be seen from the Fig. 9 (c) and (d) that the pores with diameters larger than 100 μm was produced. Such a different morphology of dried banana slices would be affected on the textural property of finished product.

3.7. Texture

The texture property of dried banana slices was reported in terms of hardness, which was defined as the maximum force in the force-deformation curve. Table 5 shows the effect of drying

Table 5
Effect of drying temperatures on maximum force and initial slope of dried banana slices.

Temperature (°C)	Maximum force (N)	Initial slope (N/mm)
70	N/A	N/A
80	74.03 ± 26.84^{b}	9.24 ± 4.57^{a}
90	41.31 ± 22.49^{c}	9.39 ± 9.87^{a}
100	24.49 ± 4.09^{c}	9.23 ± 5.35^{a}

Note: N/A is not available since the moisture content of banana can not be dried to the desired value.
^{a,b,c} means $\pm$ SD ($n = 8$) with different superscripts in the same column are significantly different($p < 0.05$).

temperatures on hardness of dried banana slices. Banana slice dried at 70 °C were not tested its textural property because its moisture content could not be reduced to the desired value as compared to the other cases. From Table 5, it was found that the structural morphology strongly affected the maximum force. The samples dried at temperature of 100 °C which possesses large porous structure provided the lowest maximum force, and the sample, with less porous structure, exhibited the highest maximum force. The values of initial slope for samples were not significantly different amongst the samples dried at temperatures.

4. Conclusions

This study has shown the effect of drying temperature on the drying kinetics and quality attributes of banana. The falling rate period was obviously evident from the drying characteristic curve and it could be divided into two sub periods, implying the different mass transfer mechanisms occurring during drying of banana. The effective diffusion coefficient of moisture related to the moisture content was proposed and used to describe such drying events. The shrinkage of banana slice was also included into the diffusion model for determining the effective diffusion coefficient. The shrinkage mainly occurred in the axial direction of banana slices. Drying temperatures slightly affected the degree of shrinkage but affected the amount of volatile compounds. The loss of total volatile compounds seems to be lower at high-temperature drying than at low temperature. In addition, high-temperature drying produced high porous structure of dried banana slices and, in turn, the value of hardness decreased whilst the crispiness was not different for samples dried at temperature range studied. Although the textural properties of dried banana were improved at high-temperature drying, the dried banana color became browner. To preserve the color, it recommended to dry banana at lower temperature of 100 °C.

Acknowledgments

The authors express their appreciation to the Thailand Research Fund (TRF), King Mongkut's University of Technology Thonburi, the National Science and Technology Development Agency (NSTDA) and the Commission on Higher Education for the financial supports.

References

AOAC. (1995). *Official methods of analysis* (16th ed.). Washington, D.C.: Association of Official Agricultural Chemists.

Baini, R., & Langrish, T. A. G. (2009). Assessment of colour development in dried bananas – measurements and implications for modelling. *Journal of Food Engineering, 93*, 177–182.

Boudhrioua, N., Giampaoli, P., & Bonazzi, C. (2003). Changes in aromatic components of banana during ripening and air-drying. *Lebensmittel-Wissenschaft und-Technologie, 36*, 633–642.

Brat, P., Yahia, A., Chillet, M., Bugaud, C., Bakry, F., Reynes, M., et al. (2004). Influence of cultivar, growth altitude and maturity stage on banana volatile compound composition. *Fruits, 59*, 75–82.

Crank, J. (1975). *The Mathematics of diffusion*. Oxford: Clarendon Press.

Dandamrongrak, R., Young, G., & Mason, R. (2002). Evaluation of various pretreatments for the dehydration of banana and selection of suitable drying models. *Journal of Food Engineering, 55*, 139–146.

Demirel, D., & Turhan, M. (2003). Air-drying behavior of Dwarf Cavendish and Gros Michel banana slices. *Journal of Food Engineering, 59*, 1–11.

Dissa, A. O., Desmorieux, H., Bathiebo, J., & Koulidiati, J. (2008). Convective drying characteristics of Amelie mango (Mangifera Indica L. cv. 'Amelie') with correction for shrinkage. *Journal of Food Engineering, 88*, 429–437.

Hofsetz, K., Lopes, C. C., Hubinger, M. D., Mayor, L., & Sereno, A. M. (2007). Changes in the physical properties of bananas on applying HTST pulse during air-drying. *Journal of Food Engineering, 83*, 531–540.

Jannot, Y., Talla, A., Nganhou, J., & Puiggali, J.-R. (2004). Modeling of banana convective drying by the drying characteristic curve (DCC) method. *Drying Technology, 22*, 1949–1968.

Katekawa, M. E., & Silva, M. A. (2006). A Review of drying models including shrinkage effects. *Drying Technology, 24*, 5–20.

Ketelaars, A. A. J., Jomaa, W., Puigalli, J. R., & Coumans, W. J. (1992). Drying shrinkage and stress. In A. S. Mujumdar (Ed.), *Drying_92, Part A* (pp. 293–303). Amsterdam, The Netherlands: Elsevier.

Krokida, M. K., Kiranoudis, C. T., Maroulis, Z. B., & Marinos, D. (2000). Effect of pretreatment on color of dehydrated products. *Drying Technology, 18*, 1239–1250.

Krokida, M. K., & Philippoulos, C. (2006). Volatility of apples during air and freeze drying. *Journal of Food Engineering, 73*, 135–141.

Mayor, L., & Sereno, A. M. (2004). Modelling shrinkage during convective drying of food materials: a review. *Journal of Food Engineering, 61*, 373–386.

Mowlah, G., Takano, K., Kamoi, I., & Obara, T. (1983). Water transport mechanism and some aspects of quality changes during air dehydration of bananas. *Lebensmittel-Wissenschaft und-Technologie, 16*, 103–107.

Mui, W. W. Y., Durance, T. D., & Scaman, C. H. (2002). Flavor and texture of banana chips dried by combinations of hot air, vacuum and microwave processing. *Journal of Agricultural and Food Chemistry, 50*, 1883–1889.

Mulet, A. (1994). Drying modelling and water diffusivity in carrots and potatoes. *Journal of Food Engineering, 22*, 329–348.

Pakowski, Z., & Adamski, A. (2007). The comparison of two models of convective drying of shrinking materials using apple tissue as an example. *Drying Technology, 25*, 1139–1147.

Pan, Z., Shih, C., McHugh, T. H., & Hirschberg, E. (2008). Study of banana dehydration using sequential radiation heating and freeze-drying. *LWT-Food Science and Technology, 41*, 1944–1951.

Poomsa-ad, N., Soponronnarit, S., Prachayawarakorn, S., & Terdyothin, A. (2002). Effect of tempering on subsequent drying of paddy using fluidisation technique. *Drying Technology, 20*, 195–210.

Prachayawarakorn, S., Tia, W., Plyto, N., & Soponronnarit, S. (2008). Drying kinetics and quality attributes of low-fat banana slices dried at high temperature. *Journal of Food Engineering, 85*, 509–517.

Ramesh, M. N. (2003). Moisture transfer properties of cooked rice during drying. *Lebensmittel-Wissenschaft und-Technologie, 36*, 245–255.

Ruiz-López, I. I., & García-Alvarado, M. A. (2007). Analytical solution for food-drying kinetics considering shrinkage and variable diffusivity. *Journal of Food Engineering, 79*, 208–216.

Salmon, B., Martin, G. J., Remaud, G., & Fourel, F. (1996). Compositional and isotopic studies of fruit flavours. Part I. The banana aroma. *Flavour and Fragrance Journal, 11*, 353–359.

Sankat, C. K., Castaigne, F., & Maharaj, R. (1996). The air drying behaviour of fresh and osmotically dehydrated banana slices. *International Journal of Food Science and Technology, 31*, 123–135.

Simal, S., Deyá, E., Frau, M., & Rossello, C. (1997). Simple modelling of air drying curves of fresh and osmotically pre-dehydrated apples cubes. *Journal of Food Engineering, 33*, 139–150.

Srikiatden, J., & Roberts, J. S. (2006). Measuring moisture diffusivity of potato and carrot (core and cortex) during convective hot air and isothermal drying. *Journal of Food Engineering, 74*, 143–152.

Thuwapanichayanan, R., Prachayawarakorn, S., & Soponronnarit, S. (2008). Modeling of diffusion with shrinkage and quality investigation of banana Foam Mat drying. *Drying Technology, 26*, 1326–1333.

Yousif, A. N., Scaman, C. H., Durance, T. D., & Girard, B. (1999). Flavor volatiles and physical properties of vacuum-microwave and air-dried sweet basil (*Ocimum basilicum* L.). *Journal of Agricultural and Food Chemistry, 47*, 4777–4781.

Accepted to be published in Drying Technology

Effect of Adsorption Conditions on Effective Diffusivity and Textural Property of Dry Banana Foam Mat

Preeda Prakotmak,[1] Somchart Soponronnarit,[1]

Somkiat Prachayawarakorn[2]

[1]*School of Energy, Environment and Materials, King Mongkut's University of Technology Thonburi126 Pracha u-tid Road, Bangkok 10140, Thailand*

[2]*Faculty of Engineering, Department of Chemical Engineering King Mongkut's University of Technology Thonburi126 Pracha u-tid Road, Bangkok 10140, Thailand*

ABSTRACT

Foamed banana product serving as a crispy snack could quickly adsorb the moisture from the moist air, leading to loss of textural property. The main purpose of this research was therefore to study moisture adsorption kinetics of dry banana foam mat and its texture quality change. The adsorption isotherm experiments were carried out with standard static method using saturated salt solutions over a wide range of relative humidities from 32 to 82%, and temperatures of 35, 40 and 45^{o}C. Three dry banana foam densities of 0.21, 0.26 and 0.30 g/cm^{3} were adsorbed water vapour under the controlled conditions. A Fick's second law couple with the optimization technique was used to estimate the effective moisture diffusivity at sorption conditions. Empirical equations

[1] Correspondence: P. Prakotmak, School of Energy, Environment and Materials, King Mongkut's University of Technology Thonburi126 Pracha u-tid Road, Bangkok 10140, Thailand; E-mail: preeda_list@hotmail.com

with two and three constant parameters for describing the dependence of the effective moisture diffusivity on moisture content were tested. The two constant parameters could suitably describe the variation of the effective moisture diffusivity with moisture content. The initial foam density, relative humidity and temperature significantly affected the effective moisture diffusivity. The banana foam mats for all densities lost their crispy texture at moisture content of 0.078 kg/kg d.b.

Keywords adsorption kinetics; capillary condensation; crispness; food foam; snack

INTRODUCTION

Foam mat drying is a process in which a semi liquid food is whipped to form stable foams by incorporating large volume of air in the presence of a foaming agent, which acts as a foam inducer. It is then spread as a thin mat and exposed to drying air until the moisture content of product reduces to certain level.[1,2] The drying time required for food foam is significantly shorter than that for the non foam because the development of porous structure in the food foam reduces the mass transfer resistance.[1,3] Foaming has successfully been applied to some fruits such as apple juice[4] mango[5] star fruit[6] blackcurrant pulp [7,8] and banana[1,9]. To produce the crispy banana snack, the banana foam is usually dried to the moisture content below 0.04 kg/kg d.b. At this moisture content, the partial pressure of water vapor inside the product is lower than that in the environment. Hence, the prolonged exposure of the product to ambient storage condition can lead to the adsorption of moisture from the atmosphere into the product matrix. The uptake of moisture is commonly associated with deleterious changes in quality. For

crispy foods such as breakfast cereals, crispy breads and popcorn, their textures became unacceptable at the moisture content of 0.042-0.07 kg/kg d.b.[10] Ready-to-eat snacks and white bread loss their crispness at the moisture content about 0.1 kg/kg d.b.[11,12]

Food products can adsorb moisture rapidly or slowly depending on a partial pressure of water vapor in the exposed environment. The rate of flow of adsorbable gases is known to be dependent on the adsorption condition. In a single capillary tube, the amount of adsorption varies in a wide range starting from negligible adsorption at very low relative humidity to complete liquid filling at 100% relative humidity. Between these two extreme points, it can divided into three regimes i.e. monolayer, multilayer and capillary condensation. In the whole range of relative humidity, it corresponds to each regime which depends on the size and shape of pore. In real porous materials, however, they contain distribution of pore sizes and may experience different types of adsorption. At low relative humidity, monolayer adsorption is dominant. When the relative humidity increases, the material surface becomes increasingly covered with adsorbed molecules and, simultaneously, the filling of liquid into smaller pores. The amount of pores that are filled with liquid increases with increasing relative humidity and eventually the entire pore volume is covered with liquid. Hence, in the wide range of relative humidity, the phases of both liquid and gas are present inside the porous materials.

As mentioned above, the coexistence of these two phases may affect the movements of liquid and gas inside the porous material and subsequent transport property. The gas relative permeability decreases and the liquid relative permeability increases as number of liquid-filled pores in porous material increase.[13] Upon a certain number of liquid-filled pores, the gas relative permeability becomes zero but the liquid

68 relative permeability still increases continually. To describe the transport of water vapor
69 inside the banana foam during adsorption, it is convenient to include the transport
70 mechanism for each phase into a single transport property, namely effective diffusivity.
71 The effective moisture diffusivity of food is known to be either independent or
72 dependent moisture content.[14-18] In case of independence of moisture content, Arrhenius
73 relation is often used to represent its variation with temperature. However, the
74 dependence of diffusion coefficient on moisture content is not clearly demonstrated. Up
75 until now, there is no general model for describing the relationship between effective
76 diffusivity and moisture content.[19] Many empirical forms such as power-law,
77 polynomial and exponential forms have frequently been used to describe their
78 relationships.[15-17] Nevertheless, the model for relating the effective diffusivity to
79 moisture content of porous banana foam has not existed and literature data concerning the
80 effect of relative humidity on moisture diffusivity have been limited. The objectives of
81 this study were therefore to select a suitable empirical equation of diffusivity, to
82 investigate the influences of relative humidity, temperature and foam density on the
83 effective moisture diffusivity, and also to explore the change of textural properties of the
84 banana foam mat during adsorption.

85

86 **MATERIALS AND METHODS**

87

88 **Dried Banana Foam Preparation**

89 Gros Michel bananas (*Musa sapientum* L.) with a maturity stage of 5 corresponding to
90 yellow peel and green tip were purchased from a local market. The total soluble solid of

the banana was measured using an ATC-1E hand-held refractometer (ATAGO, Japan) at a temperature of 23°C. The banana used in the experiments contained total soluble solid content of 23-25^{o}Brix. To prepare banana foam, the bananas were sliced and pretreated by immersing them in 1 g/100 g sodium metabisulphite solution for 2 min and rinsing them with distilled water for 30 s[1], in order to prevent discoloration during foaming process. 100 g banana puree with 5 g fresh egg albumen, used as foaming agent, was whipped with a kitchen aid mixer (model no. 5K5SS, Strombeek-Bever, Belgium) at the maximum speed to produce the foam densities of 0.3, 0.5 and 0.7 g/cm^3. The banana foam density was determined by measuring the mass of a fixed volume of the foam. The banana foam was poured slowly into a steel block with dimensions of $45 \times 45 \times 42$ mm ($W \times L \times H$) and then placed on a mesh tray, which was covered with aluminium foil. After that, it was dried to about 0.03 kg/kg d.b. using tray dryer which was operated at 80^{o}C and an air velocity of 0.5 m/s. The banana foam prepared from the initial foam densities of 0.3, 0.5 and 0.7 g/cm^3 could produce the dried banana foam densities of 0.21 ± 0.02, 0.26 ± 0.02 and 0.30 ± 0.02 g/cm^3, respectively. The product thicknesses after drying were 2.8 ± 0.15, 3.2 ± 0.1 and 3.4 ± 0.1 mm for the banana foam densities of 0.21, 0.26 and 0.30 g/cm^3, respectively. Five replications were performed for each banana foam density.

Adsorption Experiment

Moisture adsorption experiments were carried out using the static method. Samples were placed into the glass jars contained the saturated salt solutions ($MgCl_2 \cdot 6H_2O$, $Mg(NO_3)_2 \cdot 6H_2O$, KI, NaCl and KCl) which provided the relative humidity (*RH*)

114 in range of 32-82% at the corresponding temperatures of 35, 40 and 45^{o}C. All the jars
115 were placed in the temperature-controlled oven with a precision of ±1°C (UFE500,
116 Memmert, Germany). Samples were weighed at different exposure times ranging from 1
117 to 120 h. At $RH > 74\%$, 1 mL of toluene was held in a vial and fixed in the glass jars in
118 order to prevent the sample spoilage by microbial.[20] Moisture content of each sample
119 after reaching the equilibrium condition was determined by drying it with the hot air oven
120 at a temperature of 103°C for 3 h.[21] At this temperature, the percentage error of moisture
121 content determination was approximately 0.4% when compared to the result obtained by
122 the standard vacuum method.[1] The experiment at each adsorption condition was
123 repeated three times and the mean value was reported.
124
125 **SEM Photograph**
126 The morphologies of dried banana foam mats were characterized using scanning
127 electron microscope (JSM-5600LV, JEOL Ltd., Tokyo, Japan) with an accelerating
128 voltage of 10 kV. Before photographing, the specimens were cut into a dimension of 5×5
129 mm and then glued on the metal stub. The samples were coated with gold, scanned, and
130 photographed at $15 \times$ magnification
131 Image J software was used to quantify the porous banana foam characteristics
132 such as pore diameter and pore area. SEM image is composed of 8-bit grayscale pixels.
133 Each pixel of the SEM micrograph was assigned a value of gray intensity between 0 and
134 255. The SEM images were then segmented into binary images based on a manual
135 threshold setting using their grey level histogram. The threshold setting consisted of
136 finding the grey level of the histogram which suitably separates the classes associated

with solids and pores. From this threshold setting, it could create binary black and white images. The pixels with gray levels lower than the selected threshold were assigned as space, which appeared as black colour, and the pixels with gray levels above the selected threshold were set as solid, which appeared as white colour in binary image. The pore diameter was estimated from the known pore area by counting the number of pixels filled in the specified space.

Texture Analysis

The effects of moisture content and storage temperature on product textures were studied by a compressive test using a texture analyzer model TA.XT.plus (Stable Micro System, Surrey, UK). The banana foam with moisture content of 0.038 kg/kg d.b. was used to adsorb water vapour at the *RH* of 74% and temperature of 24^{o}C. After the product adsorbed water vapour for predetermined time, the sample was taken to examine its textural properties. The sample was placed on the hollow planar base and the test applied a direct force to the sample using a 5 mm spherical probe moving at a constant crosshead speed of 2 mm/s. Before the penetration test, the samples were exposed to the surrounding with *RH* of 35-45% for less than 20 s and it was expected that the textural property of the samples did not change. From the force deformation curve, the hardness was defined at the maximum force of the curve and the crispness was characterized by the number of peaks and the slope of the first peak. The data were analyzed by ANOVA using Duncan's multiple range test at $P < 0.05$. Twelve samples were used to determine the textural properties and the average values of hardness and crispness were presented.

160

161 **Determination of Effective Moisture Diffusivity**

162 The banana foam mat used in the experiments had a dimension of $43 \times 43 \times 4$ mm.
163 This sample size provided the transport of moisture in direction of thickness since the
164 material thickness was 10 times shorter than the other two dimensions. The change in
165 product size due to swelling was considered negligible during adsorption. Unsteady state
166 mass transfer equation for moisture diffusion within an isotropic material with flat slab
167 geometry is given by:

168

169 $$\frac{\partial(\rho M)}{\partial t} = \frac{\partial}{\partial x}\left(D_{eff}(M) \frac{\partial(\rho M)}{\partial x} \right) \quad (1)$$

170 or

171 $$\frac{\partial(\rho M)}{\partial t} = D_{eff}(M) \frac{\partial^2(\rho M)}{\partial x^2} + \frac{\partial(\rho M)}{\partial x} \cdot \frac{\partial(\rho D_{eff}(M))}{\partial x} \quad (2)$$

172

173 where ρ is the apparent density of dry banana foam (kg/m^3) M the moisture content
174 (kg/kg d.b.), t the time (s), $D_{eff}(M)$ the effective moisture diffusion coefficient (m^2/s) and
175 x the distance along the diffusion path (m). In this study, it was assumed that the moisture
176 distribution inside the sample at the beginning was spatially uniform and the migration of
177 water vapour from the surrounding air to the sample surface occurred at the top surface.
178 No moisture transferred at the bottom since the bottom surface was placed on an opaque
179 glass dish. From the above assumptions, the following initial and boundary conditions
180 can be setup:

181 $$M = M_{in} \quad 0 \le x \le L \ at \ t = 0 \quad (3)$$

182 $$D_{eff} \cdot \left(\frac{\partial(\rho M)}{\partial x} \right) = \frac{h_m M_w P_{vsat}}{RT} \left(RH_s(M) - RH_{air} \right) \quad x = 0 \; at \; t > 0 \tag{4}$$

183 $$\frac{\partial(\rho M)}{\partial x} = 0 \quad x = L \; at \; t > 0 \tag{5}$$

184 where M_{in} is the initial moisture content (kg/kg d.b.), L thickness of material (m), M_w the
185 molecular wight of water (18 kg/kmol), P_{vsat} the saturated vapour pressure (Pa), T the
186 temperature of the solid (K), R the perfect gas constant (8314.3 J/kmol/K), $RH_s(M)$ and
187 RH_{air} are the relative humidity of air at the top surface of product and in the surrounding
188 air, respectively. $RH_s(M)$ can be determined from the moisture adsorption isotherms and
189 the data were not reported in the present work. h_m is the convective mass transfer
190 coefficient (m/s) which can be determined from the correlation proposed by:[22]

191 $$Sh = 0.646 \, \mathrm{Re}^{0.5} \times Sc^{1/3} \tag{6}$$

192 Because the density of dry banana foam did not change during adsorption, the density can
193 be cancelled out on the both sides of Eq. (2) and Eq. (2) can be written in a form of finite
194 difference using forward for the first term on the right hand side and central difference for
195 the second term:

196 $$\frac{M_i^{t+1} - M_i^t}{\Delta t} = D_{eff,i}^t \left(\frac{M_{i+1}^t - 2M_i^t + M_{i-1}^t}{(\Delta x)^2} \right) + \left(\frac{M_{i+1}^t - M_{i-1}^t}{2\Delta x} \right) \left(\frac{D_{eff,i+1}^t - D_{eff,i-1}^t}{2\Delta x} \right) \text{ for } i=1 \text{ to } N\text{-}1 \tag{7}$$

197 where Δt is the time increment (s) and Δx the distance between adjacent nodes (m). Eq.
198 (4) was discretized using the central difference and it can be expressed by

199 $$D_{eff,i}^t \cdot \rho \left(\frac{M_{i+1}^t - M_{i-1}^t}{2\Delta x} \right) = \frac{h_m M_w P_{vsat}}{RT} \left(RH_s(M_i^t) - RH_{air} \right) \text{ for } i=N \tag{8}$$

where M_{N+1}^{t} in Eq. (8) is the fictitious moisture content at a fictitious node and N the number of layer, as illustrated in Fig. 1. From Eq. (8), the value of M_{N+1}^{t} can be calculated and this value was used to determine the moisture content at the top surface, M_N, at t+1 using Eq. (7). The discretization of Eq. (5) with the backward difference formula gives $M_{i+1}^{t} = M_{i-1}^{t}$. Substituting M_{i-1}^{t} in Eq. (7) with M_{i+1}^{t} it can then be written as follows:

$$\frac{M_i^{t+1} - M_i^t}{\Delta t} = 2D_{eff,0}^t \left(\frac{M_{i+1}^t - M_i^t}{(\Delta x)^2} \right) \text{ for } i=0 \tag{9}$$

From Eq. (9), the value of M_0^{t+1} can be determined. In the moisture calculation, the time increment of 0.01 s was used and the sample thicknesses of 2.8, 3.2 and 3.4 mm for the respective foam densities of 0.21, 0.26 and 0.30 g/cm^3 were divided into 105, 120 and 128 layers.

After the moisture content at every node is known, the average moisture content $\overline{M}(t)_{pre}$ can be readily be calculated by integrating the calculated moisture profile throughout the sample thickness and the trapezoidal numerical integration was used:

$$\overline{M}(t)_{pre} = \frac{\int_0^L M(t)dx}{\int_0^L dx} \tag{10}$$

Because the dependence of diffusivity on moisture content cannot be described by any specific equation, three possible empirical equations obtained from the literature[23-25] were tested with the moisture adsorption data:

$$D_{eff}(M) = D_0 \exp\left(-\left(e_1 M + e_2 M^2\right)\right) \tag{11}$$

$$D_{eff}(M) = D_0 \cdot M^{D_x} \tag{12}$$

$$D_{eff}(M) = D_0 \exp(-a \cdot M) \tag{13}$$

where D_0, D_x, e_1, e_2, and a are the constant parameters. The accuracy of the models was evaluated by root mean square error (*RMSE*) and coefficient of determination (R^2) value. *RMSE* is defined as:

$$RMSE = \left[\frac{1}{NP - P}\sum_{n=1}^{P}(M(t)_{\exp} - \overline{M}(t)_{pre})^2\right]^{1/2} \tag{14}$$

where $M(t)_{\exp}$ is the experimental average moisture content of material at time t and $\overline{M}(t)_{pre}$ the predicted average moisture content, *NP* the number of data points and *P* the number of parameters.

The lower the value of *RMSE* is the better the goodness of fit. In this work, a modified Nelder-Mead simplex method was used to estimate the constant parameters in Eqs. (11), (12) and (13). The *RMSE* was set as the objective function with a tolerance of 10^{-9}. To help speeding up the convergence of optimization, the initial guess was therefore obtained from the least squares fits of the moisture diffusivity data calculated from the method of slopes.[26] The model with the lowest value of *RMSE* and highest value of R^2 was considered the best model to correlate the experimental data.

RESULTS AND DISCUSSION

Morphology of Dry Banana Foam

The microstructures of dry banana foam mats characterized by SEM are shown in Fig. 2 and the pore size distributions determined by the binary image of SEM for three banana foam densities are shown in Fig. 3. It is clear from both figures that the sample with a foam density of 0.21 g/cm^3 had a larger proportion of large pores than the higher foam densities whilst the foam density of 0.30 g/cm^3 exhibited larger proportion of smaller pores. The proportions of the pore size larger than 300 μm were about 24, 10 and 4% for the foam densities of 0.21, 0.26 and 0.30 g/cm^3, respectively. From their pore size distributions, the void area fractions for the banana foam densities of 0.21, 0.26 and 0.30 g/cm^3 were 31, 26 and 23%, respectively. The void area fraction of banana foam sample at the density of 0.30 g/cm^3 was relatively small because there are a small number of large pores.

Identification of Effective Moisture Diffusivity Model

Three empirical effective diffusivity models describing the relationship between the effective diffusivity and moisture content were proposed and validated against the moisture adsorption data. Two experimental data sets for the dry banana foam density of 0.21 g/cm^3 obtained at 40°C and 66% *RH* and at 35°C and 83% *RH* were used to validate the effective diffusivity models. Fig. 4 shows the effective diffusivity-moisture relationship estimated from Eqs. (11)-(13) and their predictions of moisture uptake. As shown in Figs. 4a and 4d, the effective diffusivity values obtained from the diffusion

models decreased with moisture content, but their values were not identical. The difference of D_{eff} values amongst the three models was due to mathematics but not physics. The constant parameters for each diffusion model are shown in Table 1. For all cases studied, the models predicted the experimental data with a reasonable agreement; the R^2-values of the three models were above 0.99 and their values of *RMSE* were lower than 0.008.

The predictions of moisture adsorption using three effective diffusivity models are shown in Figs. 4b and 4e, indicating that the moisture contents calculated from the diffusivity models were almost superimposed even though the effective diffusivity values determined from the models were different. This implied that the extent of such difference in the effective diffusivity values was insensitive to the moisture-content calculation, and this seemed more difficult to identify the suitable model for predicting the moisture content from the values of *RMSE* and R^2. One more criterion was thus needed to quantify the quality of estimated constant parameters. In this study, the local relative error (E) was used to identify the suitable diffusivity model and it is defined as:

$$E(t) = 100\frac{\left|M_{\exp}(t) - M_{pre}(t)\right|}{M_{\exp}(t)} \tag{15}$$

where $M_{exp(t)}$ is the experimental moisture content at time t and $M_{pre(t)}$ the moisture content from prediction. If the estimation of moisture content was perfect, the value of E at time t was zero. The values of E for the three empirical diffusion models are shown in Fig. 4c for the temperature of 40°C and 66% *RH* and Fig. 4f for the temperature of 35°C and 83% *RH*, indicating that the values of E for Eqs. (12) and (13) were less than 2% throughout the exposure time whilst the error from prediction using Eq. (11) relatively

283 varied during adsorption; the maximum error, with a significantly higher than 2%, was
284 found at the early adsorption.

285 The prediction of adsorbed moisture at the early adsorption period with high
286 accuracy is very important to crispy product since the product quickly loses its crispy
287 texture when the product adsorbs the water vapor up to certain moisture content. From
288 this study, the banana foam will lose its crispiness at moisture content about 0.078 kg/kg
289 d.b. as will be seen in the section of banana foam texture. From these results, it could be
290 deduced that Eq. (12) or (13) was reasonably used to describe the moisture adsorption of
291 banana foam. However, using Eq. (12) for predicting moisture content during adsorption
292 provided E values for all adsorption times slightly lower than that using Eq. (13). This
293 implied that Eq. (12) was a suitable empirical model for describing the relationship
294 between effective moisture diffusivity and moisture content for dry banana foam.

295

296 **Effect of Relative Humidity on Effective Moisture Diffusivity**

297 The empirical equation of Eq. (12) was selected to study the effect of relative
298 humidity on the effective moisture diffusivity. Fig. 5 shows the moisture adsorption at
299 35°C and RH range of 32 to 83% for the banana foam density of 0.21 g/cm^3. As expected,
300 the faster adsorption rate was accomplished with higher relative humidity. The
301 predictions of moisture content using Eqs. (1) and (12) agreed well with the experimental
302 data over a wide range of relative humidity values.

303 Fig. 6 shows the changes of D_{eff} with moisture content at different values of RH
304 and at adsorption temperatures of 35, 40 and 45°C for the dry banana foam densities of
305 0.21, 0.26 and 0.3 g/cm^3. The D_{eff} value for the dry banana foam densities was strongly

306 increased with increasing moisture content at the range of *RH* of 31-48% and at all
307 adsorption temperatures. The equilibrium moisture content of samples at these relative
308 humidities was given in a range of 0.08 to 0.15 kg/kg d.b. At this *RH* range, the water
309 molecules were adsorbed on the pore surface with a small thickness. The adsorbed water
310 acts as a plasticizer which increases molecular mobility of water in the solid matrix. In
311 addition to plasticization effect, the flow of water vapor into the porous banana form was
312 not limited. Hence, the effective moisture diffusivity was remarkably increased as the
313 moisture content increased during adsorption.

314 When the *RH* was higher than 48%, the plasticization and vapor flow effects
315 became less important and the trend of changing D_{eff} with moisture content had very
316 differences amongst dry foam densities and amongst adsorption conditions i.e.
317 temperature and *RH*. At the dry banana foam density of 0.21 g/cm^3, the value of D_{eff}
318 shown in Fig. 6a for the temperature of 35°C and values of *RH* of 67 and 75% increased
319 slightly with increasing moisture content. When the value of *RH* was 83%, on the other
320 hand, the value of D_{eff} for this banana foam density decreased with increasing moisture
321 content. At higher temperatures of 35°C together with *RH* above 65%, the D_{eff} decreased
322 with increasing moisture content as shown in Figs. 6b and 6c. For the other two dry
323 banana foam densities, the D_{eff} shown in Figs. 6d and 6e for the dry banana foam density
324 of 0.26 g/cm^{3}as well as 6f for the foam density of 0.3 g/cm^{3}were almost independent of
325 adsorbed moisture content at higher temperatures of 35°C and at higher *RH* values of
326 66%. Such different moisture diffusivity trends may be related to the combined effects of
327 physical characteristics of pore size and formation of liquid in pores of sample, both

328 factors affecting the flows of water vapor and liquid inside the porous food sample which
329 will be described below.

330 As the adsorption was carried out at 35°C and higher 50% *RH*, some amounts of
331 water vapor incorporated into the banana sample, and some formed a thicker liquid film
332 which results in smaller flux of water vapor flowing through the material and provided, in
333 turn, the slight increase of D_{eff} with increasing moisture content. When the adsorption
334 temperature increased to 40 or 45°C, implying an increase of partial pressure, the rate of
335 water vapor adsorption by the porous banana foam sample became faster, allowing more
336 exterior pores to be filled with water as compared to the adsorption at 35°C.
337 Consequently, the water vapor is more difficult to transport through the sample, resulting
338 in the D_{eff} decrease for the dry banana foam density of 0.21 g/cm^3 as the sample adsorbs
339 more water vapor. For the samples with higher foam densities i.e. 0.26 and 0.3 g/cm^3, the
340 relationship between D_{eff} and adsorbed moisture content was independent, which was not
341 similar to the case of the dry foam density of 0.21 g/cm^3. Such difference of the moisture
342 diffusivity curves is claimed to variation in porous structure between banana foam
343 densities as depicted in Fig. 3. With a larger proportion of small pores, corresponding to
344 the size in the range of 5-100 μm, for the banana foam densities of 0.26 or 0.3 g/cm^3, it
345 might be possible that these small pores are occupied by the water with a number close to
346 the percolation threshold at which the vapor flow inside the pores is blocked. Hence, the
347 flow of water into the pores inside the banana foam is only governed by capillary flow
348 and the D_{eff} value, in turn, changes slightly with moisture content. Roca et al.[27] was
349 carried out the adsorption experiment at the adsorption condition of 84% *RH* and 20°C
350 and found that the effective moisture diffusivity of sponge cake with porosity of 86%

exponentially decreased with increasing moisture content and decreased slightly for the sample of 52% porosity.

Effects of Temperature and Banana Foam Density on Effective Moisture Diffusivity

Fig. 7 shows the changes of D_{eff} with moisture content at the adsorption temperatures of 35, 40 and 45°C. As expected, the D_{eff} values increased with increasing temperature. Figs. 8a and 8b show the D_{eff} value for three foam densities at an illustrated temperature of 35°C and relative humidities of 32% and 50%, respectively. The D_{eff} values were relatively lower for the high banana foam density than for the low foam density. The difference in the D_{eff} values can be accounted for the morphological difference between three samples as already explained in the SEM section. High porous food provides less diffusional flux resistance and thus greatly facilitates the moisture transport to the high porous foods, yielding high value of D_{eff}.

Effect of Moisture Content on Banana Foam Texture

Fig. 9 shows the force deformation curves of the banana foam at adsorption temperature of 35°C and *RH* values of 48% and 74%. Eight banana foam mats at the density of 0.26 g/cm^3 were used to demonstrate how adsorption condition affects the textural property. The adsorption time required to reach the moisture content about 0.05 kg/kg d.b. was approximately 32 and 5 min for the corresponding values of 48 and 74% *RH*. The force deformation curves show irregular peaks that likely represent subsequent fracture events of the pore structure. When the direct force was applied to the sample, multiple fractures were occurred due to the force required for passing through the pore

voids of the dry banana foam sample, leading to the irregular jaggedness of curve. The jagged pattern of the force deformation curve reflects the crispy behavior of the banana foam mats. As observed from this figure, the irregular jagged force-deformation curves are noticeably different to the samples which were exposed to different values of *RH* and their curves can be classified into two groups, namely A and B. In group B for the sample exposed to 74% *RH*, it was less crispy and tough as indicated by low jagged force and high maximum force. On the other hand, group A sample stored at 48% *RH* had a high jagged force and low maximum force, implying sample with crispy texture. From the force deformation curves, it is clear that the adsorption rate affected the textural property although the product moisture content for testing was identical. This is because most water vapor adsorbed at high relative humidity is present near the sample surface, and the resulting surface is wetted, which provides further the less crisp product.

Fig. 10 shows the curves of the force versus displacement recorded by texture analyzer at different moisture contents. The dry banana foam mat before adsorbed the water vapor had moisture content of 0.039 kg/kg d.b. and it had multiple peaks of force deformation curve. The original samples with a moisture content of 0.039 kg/kg d.b. at the banana foam densities of 0.21, 0.26 and 0.30 g/cm^3 had differences in number of peaks, initial slope and maximum force as shown in Fig. 11. From this information, it indicates that the microstructure of banana foams plays an important role in the textural properties. When the sample adsorbs water vapor up to certain moisture content, the fracture pattern as shown in Fig. 10 is absent, revealing that the sample is not expected to have the crispness. In addition, its texture is tough.

396 Fig. 11 shows the textural properties of banana foam at moisture contents and the
397 statistical analysis results are also shown in Figs. 11a-11c. The number of peaks was
398 counted when the force amplitude is more than the threshold value, which was set at 30 g
399 (0.294 N). The number of peaks and initial slope for all foam densities significantly
400 decreased with increasing moisture content. In contrast to the number of peaks or the
401 initial slope, the maximum forces for samples with foam densities respond differently to
402 the moisture content. At the foam density below 0.26 g/cm^3, the insignificant change in
403 the maximum force is observed in the moisture range of 0.039-0.078 kg/kg d.b. but the
404 maximum force changes significantly with moisture content for the foam banana density
405 of 0.3 g/cm^3, showing higher maximum force as the moisture content of sample
406 increased.

407 From this study, it indicated that the number of peaks were almost absent at the
408 moisture content of 0.078 kg/kg d.b., and it may be expected that the banana foam
409 samples loss their crispy texture. This moisture content for the banana foam is given in
410 same range of other crisp products such as crispy breads, cereals, popcorn and puffed
411 corns[10], and it may be concluded that the moisture content of crisp products should not
412 be higher than 0.07-0.08 kg/kg d.b. in order to preserve their textures.

413

414 **CONCLUSION**

415 Three empirical equations describing the dependence of the effective moisture
416 diffusivity on moisture content were tested. The *RMSE*, R^2-value and local relative error
417 were suitably used as criterion to identify the appropriate effective diffusivity model.
418 From these criterions, among the three empirical models tested, the relation between the

D_{eff} and moisture content could be described adequately by Eq. (12). This proposed equation was its simplicity and ability to estimate the D_{eff} values over a whole adsorption range of moisture content of banana foam mat. From the analysis of adsorption data, it indicated that the banana foam density, adsorption temperature and relative humidity affected the D_{eff} value. The D_{eff} value of every banana foam density rapidly increased with increasing moisture content at low relative humidity and for all adsorption temperatures. When the *RH* increased to above 50%, the D_{eff} may be constant, increase or decrease with increasing moisture content. Such D_{eff} trends related to the capability of the dry banana foam to adsorb water vapor. Faster adsorption rate let to the filling of liquid to the pores, resulting in the decrease of D_{eff} with moisture content for the low density of banana foam. But, it was independent of moisture content for the high foam density. The value of D_{eff} was higher for adsorption at higher temperature and for lower foam density.

From the quality evaluation, it was found that the banana foam mat was very hygroscopic and its crispness was very sensitive to moisture migration. The increase of moisture content of banana foam mat during adsorption decreased the number of peaks and initial slopes, implying less crispiness, but the maximum force increased, indicating tough texture. The banana foam mats for all densities lost definitely their crispy texture at the moisture content of 0.078 kg/kg d.b.

ACKNOWLEDGMENTS

The authors would like to express their appreciation to the Commission on Higher Education, Thailand for supporting by grant fund under the program Strategic Scholarships for Frontier Research Network for the Ph.D. Program Thai Doctoral degree

for this research. This work was also supported in part by Thailand Research Fund and King Mongkut's University of Technology Thonburi and also the National Science and Technology Development Agency.

REFERENCES

1. Thuwapanichayanan, R.; Prachayawarakorn, S.; Sopornronnarit, S. Modeling of diffusion with shrinkage and quality investigation of banana foam mat drying. Drying Technology **2008**, *26(11)*, 1326-1333.
2. Muthukumaran, A.; Ratti, C.; Raghavan, V.G.S. Foam-mat freeze drying of egg white and mathematical modeling part I optimization of egg white foam stability, Drying Technology **2008a**, *26(4)*, 508-512.
3. Muthukumaran, A.; Ratti, C.; Raghavan, V.G.S. Foam-mat freeze drying of Egg White-Mathematical Modeling Part II: Freeze Drying and Modeling, Drying Technology **2008b**, *26(4*), 513-518.
4. Raharitsifa, N.; Genovese, D.B.; Ratti, C. Characterization of apple juice foams for foam-mat drying prepared with egg white protein and methylcellulose, Journal of Food Science **2006**, *71 (3)*, 142–151.
5. Rajkumar, P.; Kailappan, R.; Viswanathan, R.; Raghavan, G.S.V.; Ratti, C. Foam mat drying of alphonso mango pulp, Drying Technology **2007**, *25(2)*, 357-365.
6. Karim, A.A.; Wai, C.C. Foam-mat drying of starfruit (*Averrhoa carambola* L.) puree. Stability and air drying characteristics. Food Chemistry **1999**, *64 (3)*, 337-343.

464 7. Zheng, X.Z.; Liu, C.H.; Zhou, H. Optimization of parameters for microwave-assisted
465 foam mat drying of blackcurrant pulp, Drying Technology **2011**, *29(2)*, 230-238.
466 8. Zheng, X.Z.; Liu, C.H.; Zhou, H. Drying characteristics of blackcurrant pulp by
467 microwave-assisted foam mat drying, Transactions of the CSAE **2009**, *25(8)*, 288-
468 293.
469 9. Thuwapanichayanan, R.; Prachayawarakorn, S.; Soponronnarit, S. Drying
470 characteristics and quality of banana foam mat, Journal of Food Engineering **2008**, *86*
471 *(4)*, 573–583.
472 10. van Nieuwenhuijzen, N.H.; Primo-Martín, C.; Meinders M.B.J.; Tromp, R.H.; Hamer,
473 R.J.; van Vliet, T. Water content or water activity: What rules crispy behavior in
474 bread crust, Journal of Agricultural and Food Chemistry **2008**, *56(15)*, 6432-6438.
475 11. Mazumder, P.; Roopa, B.S.; Bhattachrya, S. Textural attributes of a model snack food
476 at different moisture contents, Journal of Food Engineering **2007**, *79(2)*, 511-516.
477 12. Roudaut, G.; Dacremont, C.; Le Meste, M. Influence of water on the crispness of
478 cereal based foods-acoustic, mechanical, and sensory studies, Journal of Texture
479 Studies **1998**, *29(2)*, 199-213.
480 13. Bustos, C.I.; Toledo, P. Pore-level modelling of gas and condensate flow in two- and
481 three-dimensional pore network: Pore size distribution effects on the relative
482 permeability of gas and condensate, Transport in Porous Media **2003**, *53(3)*, 281-315.
483 14. Tong, C.H.; Lund, D.B. Effective moisture diffusivity in porous materials as a
484 function of temperature and moisture content. Biotechnol. Prog. **1990**, *6(1)*, 67-75.
485 15. Zogzas, N.P.; Maroulis, Z.B.; Marinos-Kouris, D. Moisture Diffusivity Data
486 Compilation in Foodstuffs. Drying Technology **1996**, *14(10)*, 2225-2253.

16. Loulou, T.; Adhikari, B.; Lecomte, D. Estimate of concentration-dependent diffusion coefficient in drying process from the space-average concentration versus time with experimental data. Chemical Engineering Science **2006**, *61(22)*, 7185-7198.
17. Bourlieu, C.; Guillard, V.; Powell, H.; Vallès-Pàmies, B.; Guilbert, S.; Gontard, N. Modelling and control of moisture transfers in high, intermediate and low a_w composite food. Food Chemistry **2008**, *106(4)*, 1350-1358.
18. Chen, X.D. Moisture diffusivity in food and biological materials, Drying Technology **2007**, *25(7)*, 1203-1213.
19. Saravacos, G.D.; Maroulis, Z.B. *Transport properties of foods*; Marcel Dekker: New York, 2001.
20. Kaya, S.; Kahyaoglu, T. Thermodynamic properties and sorption equilibrium of pestil (grape leather). Journal of Food Engineering **2005**, *71(2)*, 200-207.
21. AOAC. *Official Methods of Analysis*, 16th Ed; Association of Official Agricultural Chemists: Washington, D.C., 1995.
22. Incropera, F.P.; Dewitt, D.P. *Fundamentals of Heat and Mass Transfer 5th Ed*; John Wiley & Sons: New York, 2002.
23. Olek, W.; Weres, J. Effects of the method of identification of the diffusion coefficient on accuracy of modeling bound water transfer in wood. Transport Porous Media **2006**, *66(1-2)*, 135-144.
24. Guillard, V.; Broyart, B.; Bonazzi, C.; Guilbert, S.; Gontard, N. Moisture diffusivity in sponge-cake as related to porous structure evaluation and moisture content. Journal of Food Science **2003**, *68(2)*, 555-562.

25. Sakin, M.; Kaymak-Ertekin, F.; Ilicali, C. Modeling the moisture transfer during baking of white cake. Journal of Food Engineering **2007**, *80(3)*, 822-831.
26. Karathanos, V. T.; Villalobos, G.; Saravacos, G. D. Comparison of two methods of estimation of the effective moisture diffusivity from drying data. Journal of Food Science **1990**, *55(1)*, 218-233.
27. Roca, E.; Guillard, V.; Guilbert, S.; Gontard, N. Moisture migration in a cereal composite food at high water activity: Effects of initial porosity and fat content, Journal of Cereal Science **2006**, *43(2)*, 144-151.

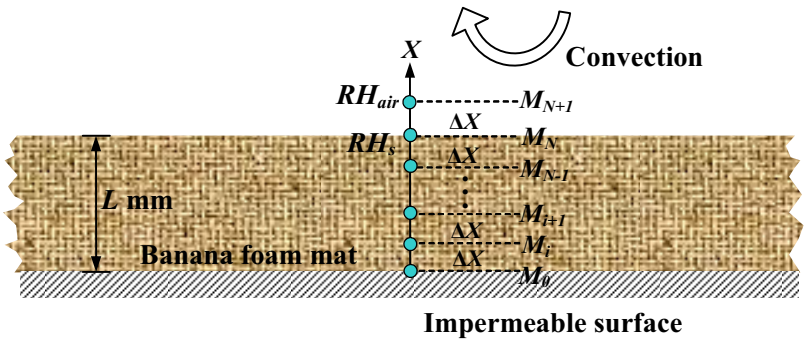

FIG. 1. Illustration for node positions in a banana foam mat

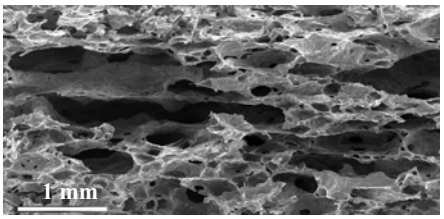

(a) 0.21 g/cm^3

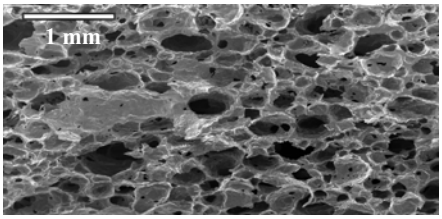

(b) 0.26 g/cm^3

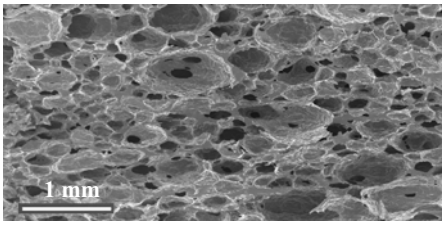

(c) 0.30 g/cm^3

FIG. 2. SEM micrographs of dry banana foam mats at different initial foam densities (Baseline is 1 mm)

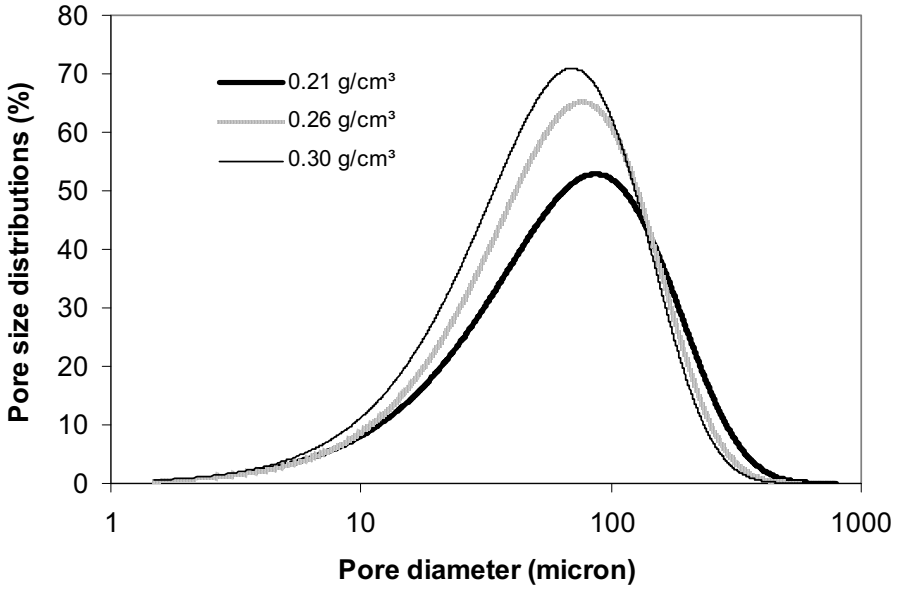

FIG. 3. Pore size distribution of dry banana foam at various densities.

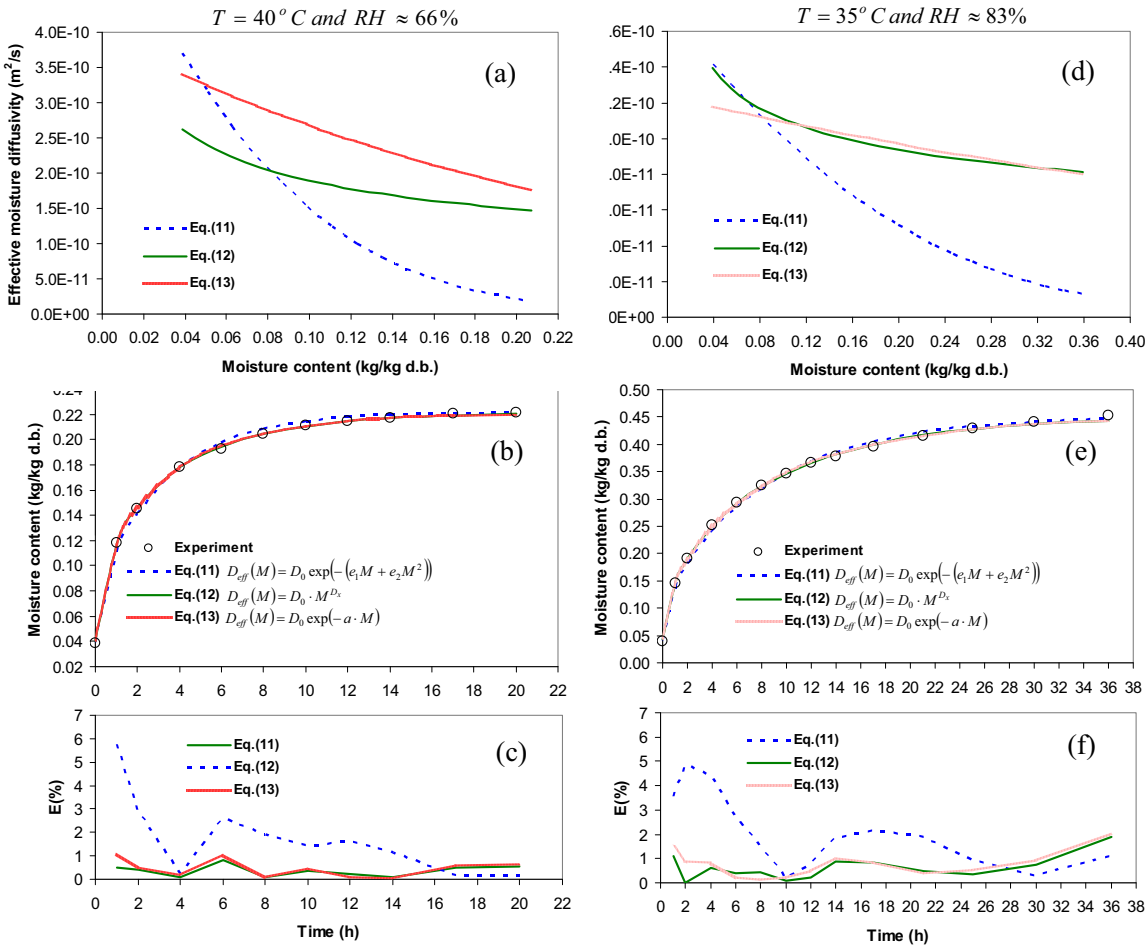

FIG. 4. Validation of the experimental and estimated moisture uptakes and the variation of effective diffusivity with moisture content of two selected example cases: 40°C, 66 %*RH* at left-hand side and 35°C, 83 %*RH* at right-hand side.

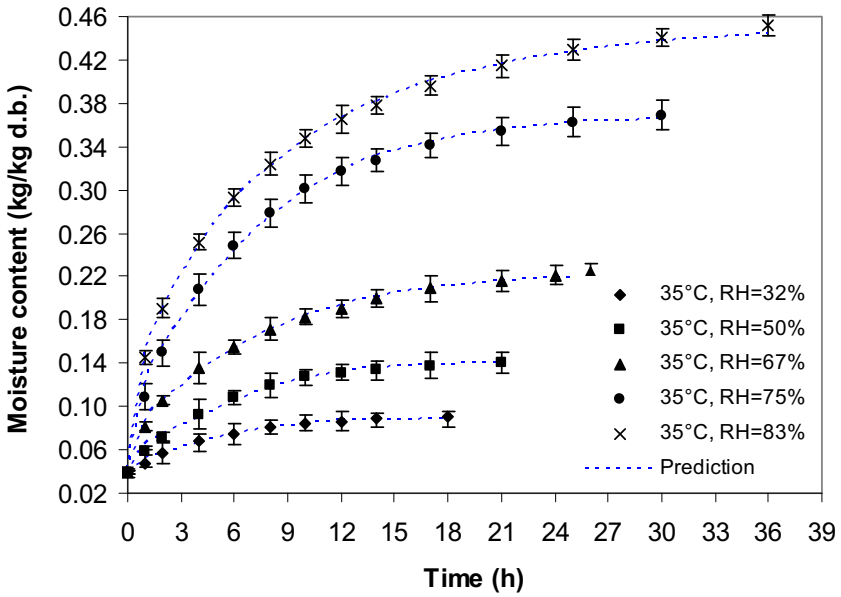

FIG. 5. Effect of values of relative humidity on moisture adsorption kinetics at 35°C for the foam density of 0.21 g/cm^3. Dash lines are the predictions; symbols represent experimental data.

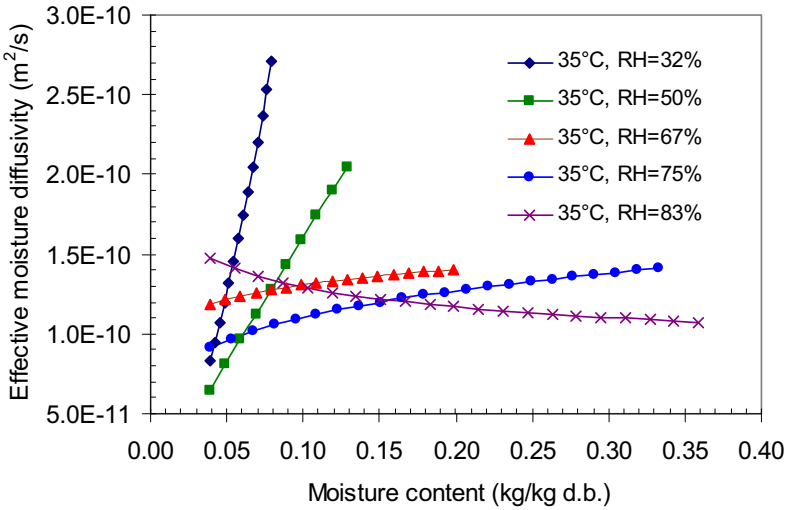

(a) Density of 0.21 g/cm^3

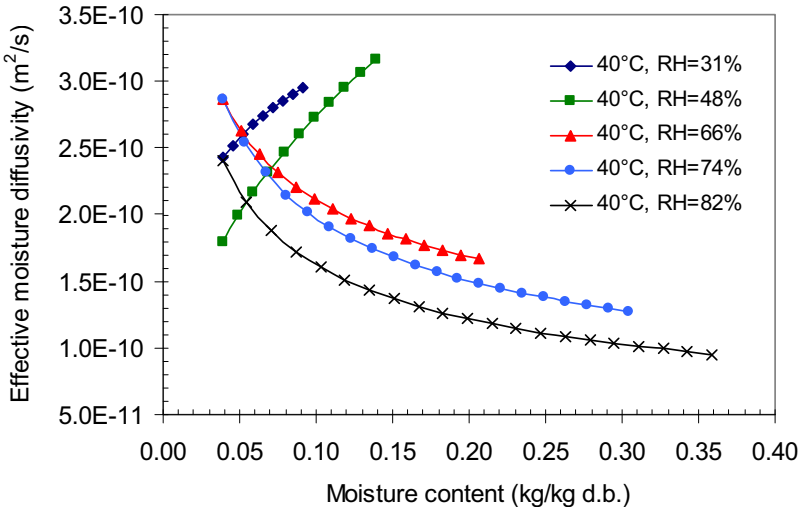

(b) Density of 0.21 g/cm^3

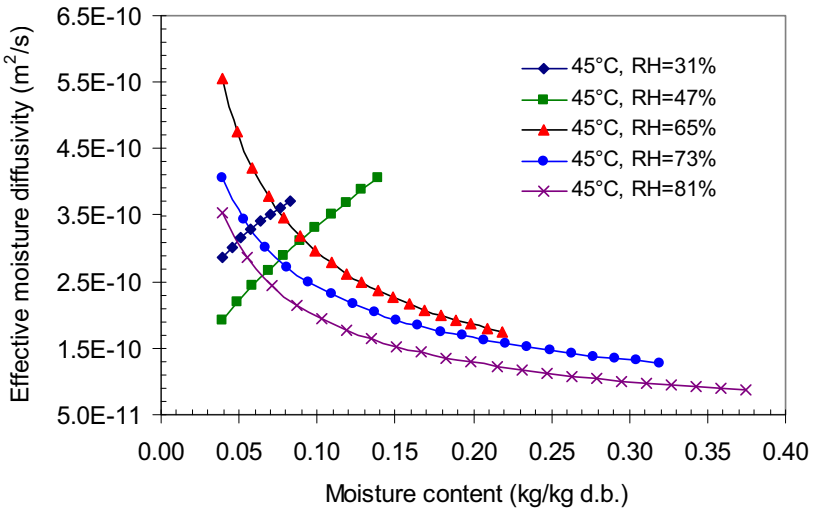

(c) Density of 0.21 g/cm^3

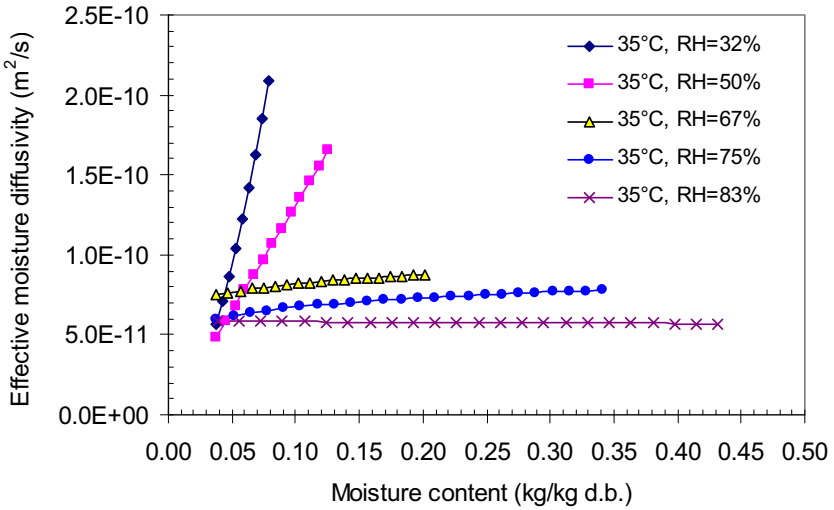

(d) Density of 0.26 g/cm^3

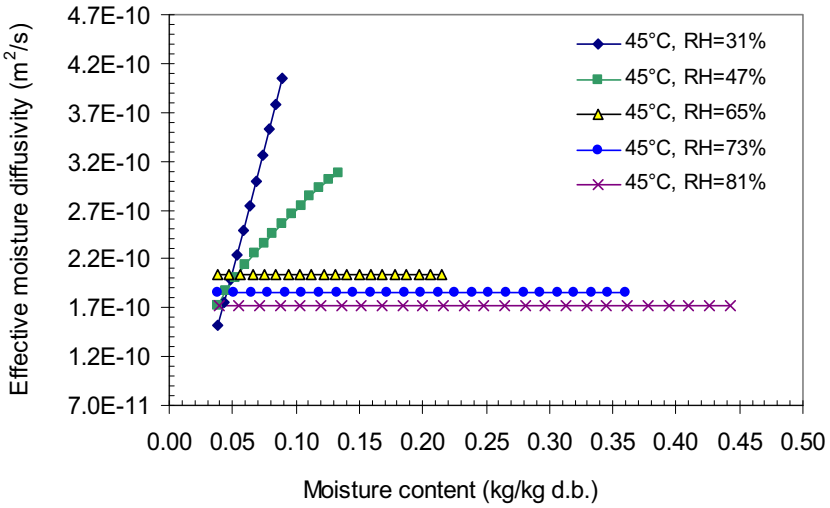

(e) Density of 0.26 g/cm^3

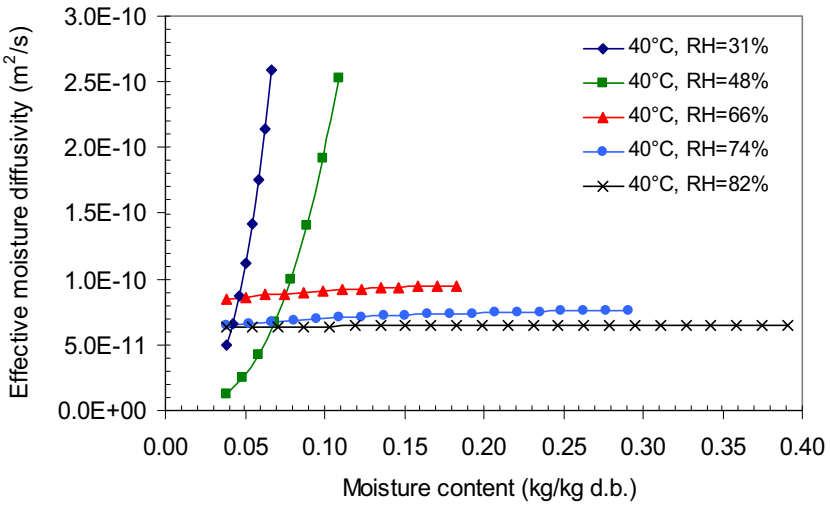

(f) Density of 0.30 g/cm^3

FIG. 6. Variation of effective diffusivity with moisture content at various relative humidities for the foam density of 0.21, 0.26 and 0.30 g/cm^3.

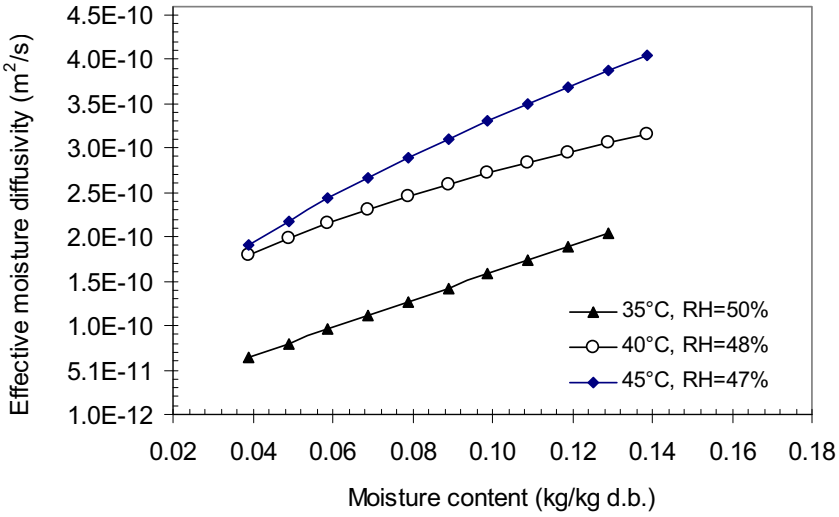

(a) $\rho = 0.21$ g/cm^3

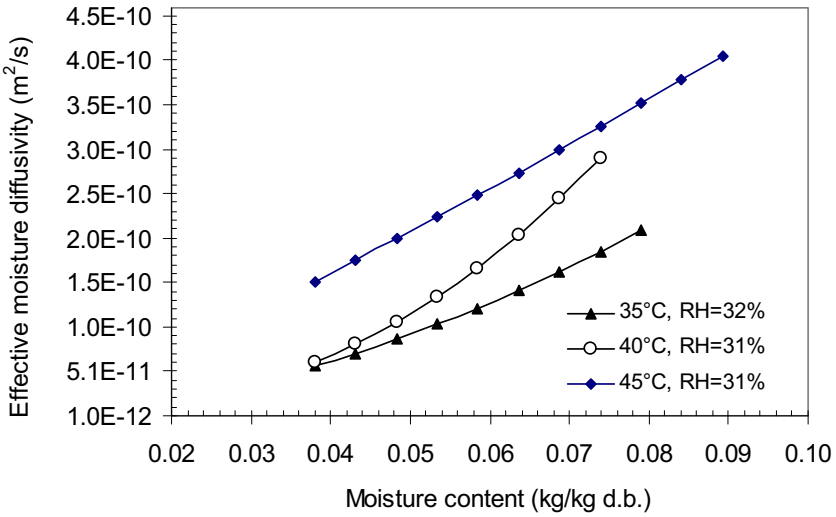

(b) $\rho = 0.26$ g/cm^3

FIG. 7. Effect of temperatures on the effective moisture diffusivity.

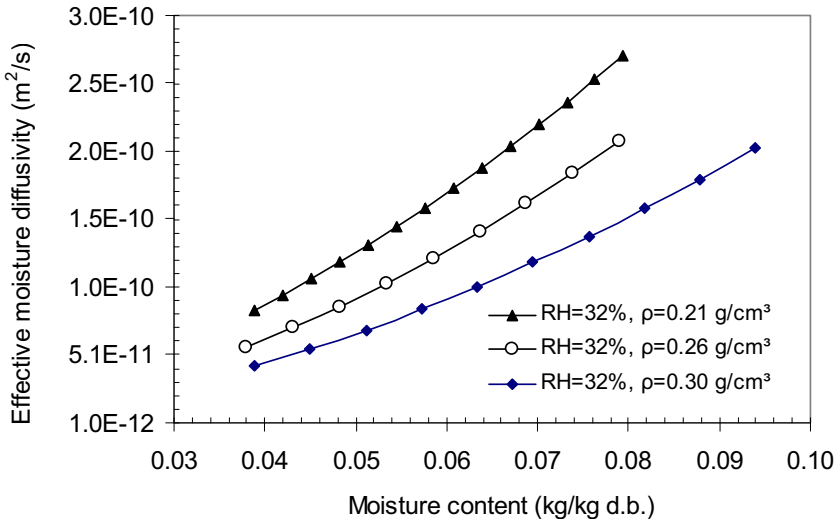

(a) 32% RH

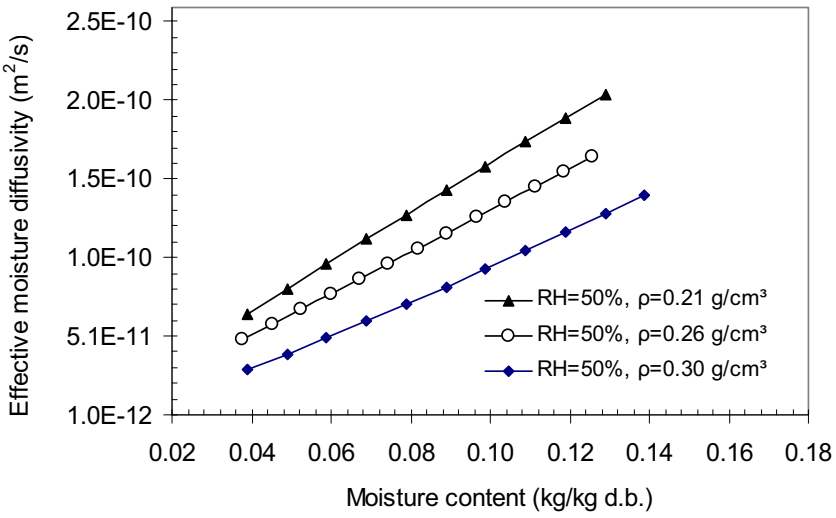

(b) 50% RH

FIG. 8. Effect of initial foam densities on effective diffusivity at the temperature of 35°C, relative humidities of 32% and 50%.

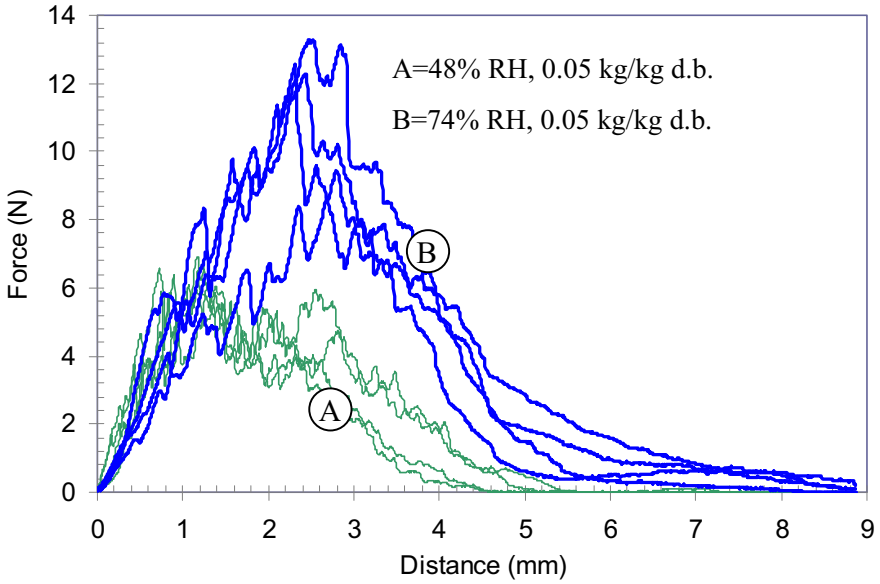

FIG. 9. The effect of adsorbed moisture on force-deformation curve for foam density of 0.26 g/cm^3.

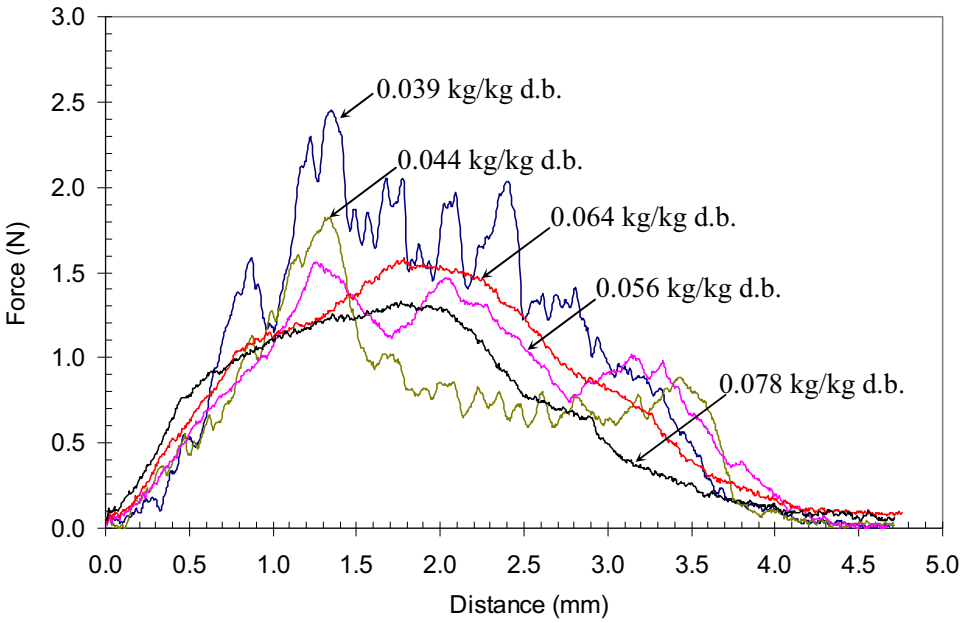

FIG. 10. Variation in force-deformation curve during compression test at various moisture content levels for foam density of 0.21 g/cm^3.

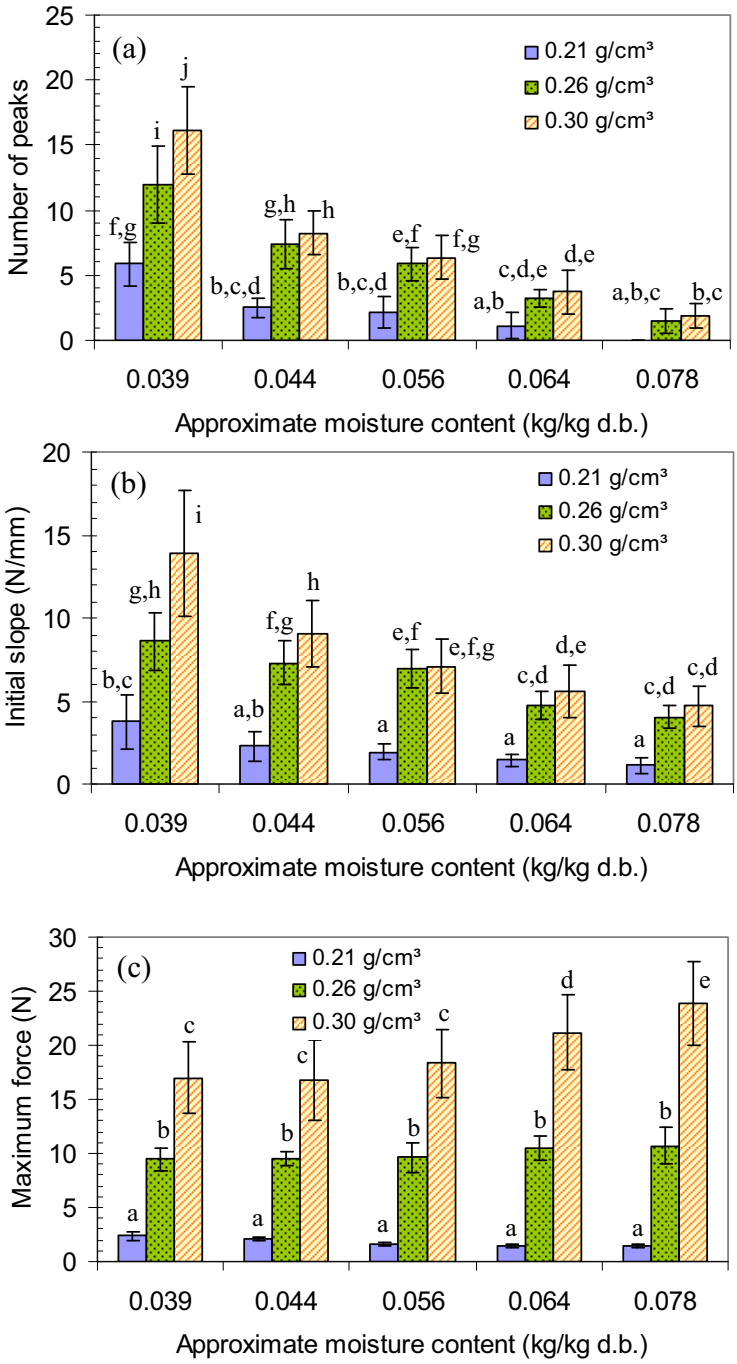

FIG. 11. Effect of moisture content and initial foam densities on (a) number of peaks (b) initial slope and (c) maximum force of the banana foam mats: the same letter means insignificant difference at $P>0.05$.

Effects of foaming agents and foam densities on drying characteristics and textural property of banana foam

Ratiya Thuwapanichayanan[1,*], Somkiat Prachayawarakorn[2], and Somchart Soponronnarit[3]

[1]Department of Farm Mechanics, Kasetsart University,

50 Phaholyothin Road, Bangkok 10900, Thailand

[2]Department of Chemical Engineering, King Mongkut's University of Technology Thonburi,

126 Pracha u-tid Road, Bangkok 10140, Thailand

[3]School of Energy, Environment and Materials, King Mongkut's University of Technology Thonburi, 126 Pracha u-tid Road, Bangkok 10140, Thailand

Abstract

Foaming technique can apply for producing porous structure which is an important requirement for crisp food. With this technique, foam density and foaming agent play a key role in drying kinetics and textural property of food. The influences of foam densities and foaming agents on the moisture diffusivity and the qualities of dried banana foam in terms of shrinkage, texture, microstructure and volatile loss were therefore investigated. Three foaming agents i.e. fresh egg albumen (EA), soy protein isolate (SPI) and whey protein concentrate (WPC) were used. The experimental results showed that the WPC banana foam after drying could retain more open structure during drying. This morphology encouraged the lower shrinkage and higher value of effective diffusivity than that of dried SPI and EA banana foams. For the textural properties of banana foam mats, the WPC and EA banana foams were spongy and less crisp than the SPI banana foam. The samples with lower foam densities for

* Corresponding author. Tel.: +662 561 3482; fax +662 561 3482.
E-mail address: t_ratiya@yahoo.com, agrrty@ku.ac.th (Ratiya Thuwapanichayanan).

all foaming agents had higher effective diffusivity and smaller hardness than those with higher foam densities. However, the crispness was lower. The volatile substances lost during the foaming and drying steps, the main loss occurring during foaming.

Keywords: crispness; drying; foaming agent; shrinkage; volatile loss

1. Introduction

Bananas are often consumed as fresh and sometimes processed to produce new products, i.e., snacks, puree and powder, etc. Because of the increasing consumer demand for snack foods, bananas have the potential to commercially produce a snack at a small scale industry. Drying of banana may take a long time and thus consume a large amount of energy sine the tissue structure of banana is very dense. Such dense structure may not present a good quality for producing a banana snack for which the crisp texture is preferred. A crisp food is characterized by a structure that consists of cellular assembly or a porous structure. Porous structure can also improve the hardness of food. There are several techniques to create the porous structure. Foaming technique, one of the methods, can be used to produce porous structure in foods. This technique is practically applied for many foods including bread, cake, cracker and confectionery products (Campbell and Mougeot, 1999). The combination of foam formation and drying may be a good method for producing crisp banana chips.

Foam is a dispersion of gas bubbles within liquid or semi-solid continuous phase. It is thermodynamically unstable. Two types of foaming agent are used in foods: low-molecular weight emulsifiers (lipids, phospholipids, surfactants etc.) and high-molecular weight biopolymers (proteins and polysaccharides). Proteins are widely used as an ingredient for foam formation and stabilization. The primary function of proteins in foam is to decrease the interfacial tension at the air/liquid interface which promotes the bubble formation (Davis and

Foegeding, 2007). The protein-protein attractions at the interface can result in the network formation which promotes the bubble stability, and contribute to texture of food foams.

One of the most difficult problems in the drying of foamed biological materials is the instability of the foam during heating (Ratti and Kudra, 2006). If the foam is unstable, the collapse of porous structure occurs resulting in the serious problem of drying operation and the foamed product quality. There are many variables involving the foam density and stability, and these variables include chemical nature of fruits, total soluble solids and concentration and type of foaming agent (Hart et al., 1963). The selection of foaming agent is thus the most important factors in preparation of the foam that can withstand processing, i.e., spreading and drying (Eduardo et al., 2001).

During drying of food foam, moisture gradient induces the material shrinkage. The volume change is larger than the volume of removed water during early period of drying, which corresponds to the semi-liquid state, and it closes to the volume change of removed water when the food foam becomes rigid (Thuwapanichayanan et al., 2008a). Thuwapanichayanan et al. (2008a), who investigated the drying of banana foam using egg white as foaming agent, described such volume change by the collapse of gas bubbles. This represents the bubble instability when using egg white.

The objectives of this work were therefore to study the effect of foaming agents, i.e., soy protein isolate, egg white and whey protein concentrate on the effective diffusivity of moisture and the qualities of the final product regarding to shrinkage, texture, microstructure and volatile compounds.

2. Materials and methods

2.1 Preparation of the banana puree and foam

Gros Michel bananas at a mature stage of 5, which contained total soluble solids of approximately 23-25ºBrix, were used. Soy protein isolate (SPI) and whey protein concentrate

(WPC) were used as foaming agents in this study. The SPI contained 90.2% protein (dry basis), 6% moisture content, 4.5% ash and 0.32% fat. The WPC contained 80% protein (dry basis), 6.7% moisture content, 4.5% ash and 8.5% fat. Bananas were cut into slices with a slicing machine. To prevent discoloration during foaming, the sliced bananas were pretreated by immersing them in 1% (w/w) sodium metabisulphite solution for 2 min and then rinsed with distilled water for 30 s. The pretreated banana slices were chopped into small pieces and then blended with a blender (Waring, model no. 8011 BU, Torrington, CT) for 1 min. About 800 g of the banana puree was then poured into a mixing bowl and then added with different foaming agents. SPI and WPC were added as a dry solid at a concentration of 5%. The concentration of SPI and WPC used in this study was the same of fresh egg albumen (EA) used in the previous work (Thuwapanichayanan et al., 2008a). The banana puree with a foaming agent was whipped by a Kitchen Aid Mixer (model no. 5K5SS, Strombeek-Bever, Belgium) at a maximum speed (220 rpm) to foam densities of 0.3, 0.5 and 0.7 g/cm^3. Foam density was determined by measuring the mass of a fixed volume of the foam. The experiments were done in duplicate.

2.2 Drying of banana foam mats

Banana foam mats with a thickness of 5 mm were placed on a mesh tray, which was covered with aluminum foil, and then placed in the drying chamber. The samples were dried to about 0.03 kg/kg db using the drying air temperature of 80°C and a superficial air velocity of 0.5 m/s. This drying temperature was a minimum temperature that could reduce the sample moisture content to the desire value. Moisture loss from the samples was determined by weighing the sample tray outside the drying chamber using an electronic balance with an accuracy of ±0.01 g.

2.3 Determination of moisture diffusivity

The diffusion of moisture inside a single banana foam mat was described by Fick's second law and the shape of sample was assumed to be an infinite slab, implying that the transfer of moisture is occurred in one dimension and it can be expressed by the following equation:

$$\frac{\partial M}{\partial t} = \frac{\partial}{\partial x}\left(D_v^{eff} \frac{\partial M}{\partial x} \right), 0<x<L(t) \quad (1)$$

where D_v^{eff} is the effective moisture diffusivity (m^2/s), L is the sample thickness (m), M is the local moisture content (kg/kg d.b.), x is the coordinate along the diffusion path and t is the drying time (s).

Since the effective moisture diffusivity of banana foam varied with moisture content (Thuwapanichayanan et al., 2008a), the space derivative of the product of D_v^{eff} and $\frac{\partial M}{\partial x}$ on the right side of Eq. (1) can then be written as:

$$\frac{\partial M}{\partial t} = D_v^{eff} \frac{\partial^2 M}{\partial x^2} + \frac{\partial M}{\partial x} \frac{\partial D_v^{eff}}{\partial x}, 0<x<L(t) \quad (2)$$

Eq.(2) was digitized using variable grid central finite difference method in its explicit form. In order to know the moisture at positions inside the banana foam and at drying times, Eq.(2) must be solved with initial and boundary conditions. The top surface of banana foam mat was only exposed to hot air, and no evaporation took place at the bottom, thus the initial and boundary conditions are:

$$\text{initial: } M = M_0, \ 0 \le x \le L(t) \ \text{ at } t = 0 \quad (3)$$

$$\text{boundary: } M = Meq, \ x = L(t) \ \text{ at } t > 0 \quad (4)$$

$$\frac{\partial M}{\partial x} = 0, \ x = 0 \ \text{ at } t > 0 \quad (5)$$

Because of the couple effects of foam instability and stress formation, the size of drying sample was shrunk and the shrinkage occurred only in the direction of thickness or x,

thus providing a shorter distance for diffusion of moisture. This effect was included into the diffusion model in order to determine the effective diffusivity. In the present study, the moving boundary method was employed to solve the diffusion model including shrinkage (Thuwapanichayanan et al., 2008b). From the experimental shrinkage data, it was found that a decrease in the thickness of banana foam mat was in a linear relation with the moisture content, and the shrinkage was expressed in finite difference form as given below

$$\Delta x_i / \Delta x_0 = a + b(M_{av} / M_0) \quad (6)$$

where a and b are the constant parameters, which were obtained from the experiments. Δx_i is the spacing between each grid point (m), Δx_0 is the spacing between grid point at the beginning (m), M_{av} is the average moisture content of each section (kg/kg d.b.), M_0 is the initial moisture content (kg/kg d.b.). The values of constant parameters a and b in Eq. (6) obtained by linear regression analysis of the experimental data are given in Table 1. Both constant parameters depended on the initial foam densities and types of foaming agent.

Table 1 Values of a and b in Eq. (6) for various foam densities and foaming agents

	EA			SPI			WPC		
	0.3g/cm^3	0.5g/cm^3	0.7g/cm^3	0.3g/cm^3	0.5g/cm^3	0.7g/cm^3	0.3g/cm^3	0.5g/cm^3	0.7g/cm^3
A	0.349	0.496	0.503	N/A	0.319	0.411	0.509	0.632	0.606
B	0.702	0.521	0.507	N/A	0.645	0.609	0.472	0.360	0.390
R^2	0.977	0.983	0.984	N/A	0.982	0.994	0.991	0.997	0.999

N/A: not available since SPI could not form foams at density of 0.3 g/cm^3.

To determine the effective diffusion coefficient, the modified Nelder-Mead simplex optimization technique was used. By this technique, it is necessary to identify the equation describing the relationship between the moisture content and effective moisture diffusivity

and determine the constant parameters of that equation. An exponential form as given by Eq. (7) was used to describe the diffusion in banana foams (Thuwapanichayanan et al., 2008a)

$$D_{eff}(M) = a \exp\left(\sum_{i=1}^{4} \alpha_i M^i\right) \quad (7)$$

where a and α_i are the constant parameters. Initial guess values of such two constant parameters were obtained by the method of slopes.

After assuming the initial guess for the constant parameters in Eq. (7), the moisture contents of banana during drying were calculated and compared to the experimental values. The root mean square error (RMSE) was set as an objective function and the calculation was stopped when the value of RMSE was less than 10^{-6}.

2.4 Shrinkage measurement

Four banana foam mats taken at different drying times were measured for their volumes. The volume was determined by the volumetric displacement method using glass beads with a diameter in the range of 0.106-0.212 mm as a replacement medium (Hwang and Hayakawa, 1980). In each measurement, one sample piece was used and the mean value of four samples was reported.

Shrinkage or volume change of sample at different drying times (ΔV) can be defined as:

$$\Delta V = V_0 - V \quad (8)$$

where V is the volume of the sample at different drying times (cm^3) and V_0 is the initial volume of the sample before drying (cm^3).

2.5 Texture measurement

The texture of dried banana foam mats was evaluated by a compressive test using a texture analyzer model TA.XT.plus (Stable Micro Systems, Surrey, UK). The sample was

placed on the hollow planar base. The test applied a direct force to the sample using a 5 mm spherical probe at a constant crosshead speed of 2 mm/s. The hardness was defined as the maximum force in the force-deformation curve while the crispness was characterized by the number of peaks and the slope of the first peak. Eight samples were tested and the average values of hardness and crispness were reported.

2.6 Microstructure evaluation

A scanning electron microscope (JEOL JSM-5600LV, Tokyo, Japan) was used to study the microstructure of dried banana foam mats. The dried banana foam mats were placed on two-side adhesive tape attached to metal stubs and were coated with gold. SEM micrographs were taken at an accelerating voltage of 10 kV and a magnification of 35×.

2.7 Analysis of volatiles

2.7.1 Sample preconcentration

The volatile components of fresh banana, foamed banana and dried banana foam mat were isolated by solid phase micro-extraction. Each sample was done in duplicate. Each sample was homogenized, placed in a 20 ml vial and then weighed with precision of ± 0.01 g; 4 g for fresh and foamed bananas, and 1 g for dried banana foam mat. The sample with a mass of 4 g was filled up with 6 mL of distilled water while the sample with a size of 1 g was filled up with 9 ml of distilled water. The internal standard, which consists of 0.2 µl of caproic acid ethyl ester in 0.1% (v/v) methanol solution, was added to those samples. The vial was then covered with a silicone Teflon-lined septum. A stainless steel needle covered with an 85 µm length carboxane/polydimethyl siloxane fiber penetrated the septum. The fiber was then pushed into the headspace above the sample for absorption at 30°C for 30 min.

2.7.2 Gas chromatography-mass spectrometry analysis (GC-MS)

Sample analysis was carried out with a Hewlett-Packard 6890 gas chromatography (GC). A HP5 column (30 m, 0.25 mm diameter, 0.25 μm thickness) was used. Helium was used as the carrier gas at a flow rate of 1 ml/min. Thermal desorption of the components from the fiber was carried out in the GC split injector (1:10) at 200°C for 5 min. The oven temperature was programmed from 40°C (1 min) to 120°C at 3°C/min. The volatile compounds were analyzed by mass spectrometry with electronic impact (EI) 70 eV quadripolar filter and identified by comparison with spectra stored in a data bank.

2.8 Statistical analysis

The data were analyzed using the analysis of variance (ANOVA). Duncan's test was used to establish the multiple comparisons of mean values. Mean values were considered at 95% significance level ($p<0.05$).

3. Results and discussion

3.1 Foam density

The foam ability can simply be measured by the foam density (Wilde and Clark, 1996). Lower foam density indicates more air to be entrapped in the foam. Figure 1 shows the effect of foaming agents on the foam ability, indicating that foaming agents took an effect on the foam ability. The additions of EA and WPC at 5% could produce the minimum foam density of 0.3 g/cm^3 whereas the addition of SPI at the same concentration could produce the minimum foam density of 0.8 g/cm^3 as shown in Fig. 1. The higher SPI foam density is probably because SPI might not be adequate to decrease the interfacial tension at the air/liquid interface due to the lower protein solubility. The protein solubilities of WPC and SPI at the present study were

When SPI was added at 10%, banana puree could be foamed to the minimum density of 0.5 g/cm^3. The more addition of SPI could not reduce banana foam density to be lower than 0.5 g/cm^3 significantly (data not shown) and thus the 10% SPI was enough for foaming banana.

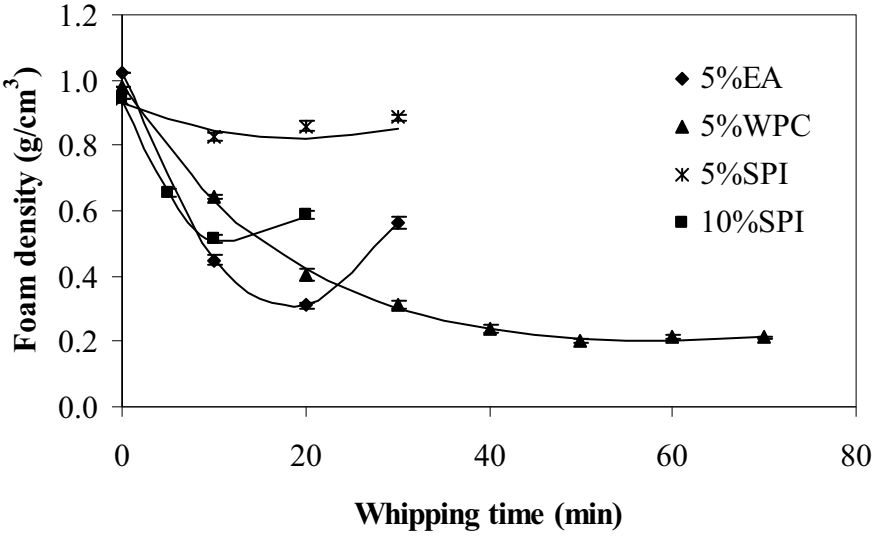

Fig. 1 Effects of foaming agent and whipping time on the foam density

It is interesting to that although the WPC and EA at 5% can produce the foam density of 0.3 g/cm^3, but the whipping time used was different. The whipping time for EA was significantly shorter than that of WPC; the whipping times were 20 and 50 min for EA and WPC, respectively. From this result, it implies that the proteins in egg white can be more rapidly absorbed at the air-liquid interface and more denatured than the WPC (Townsend and Nakai, 1983). However, the foams produced from EA was less stable than that from WPC as depicted in Fig.1, showing the increase of EA banana foam density at whipping time beyond 20 min whilst the WPC foam density did not change after it reached the minimum density even though the whipping time was continued. The instability of SPI banana foam was also found. These results corresponded to the experimental results reported by Mott et al. (1999). In their work, the whey protein foams could maintain the overrun during the extended whipping whereas the overrun of egg white foams decreased foam quickly. The increase in foam

density when using EA was explained by a result of protein aggregation caused by electrostatic interactions of the negatively charged lysozyme proteins (Phillips et al., 1990). Whey protein does not have the basic protein lysozyme and thus does not exhibit the electrostatic interactions. Hence, the foams are quite stable.

3.2 Drying characteristics of banana foams

Fig. 2 shows the drying curves of banana foam mats obtained from three foaming agents. The initial moisture contents of foamed banana samples added with different foaming agents were different; the initial moisture contents of EA, SPI and WPC banana samples were in the range of 3.2-3.5, 2.0-2.2 and 2.6-2.9 kg/kg db, respectively. This is because the SPI and WPC were added as a dry solid form while the EA was added as a liquid form. From their drying kinetics shown in Fig. 2, it indicated that the moisture content decreased exponentially with time, implying that the drying rate of banana foam mat is controlled by the internal diffusion process. Similarly, drying of star fruit foam mat was also controlled by diffusion (Karim & Wei, 1999). On the other hand, the drying rate of tomato foam was governed by both convection and diffusion (Brygidyr et al., 1977). From these facts, it reveals that the drying mechanisms depend on the product characteristic. Each fruit has differences in the chemical composition and the solid content.

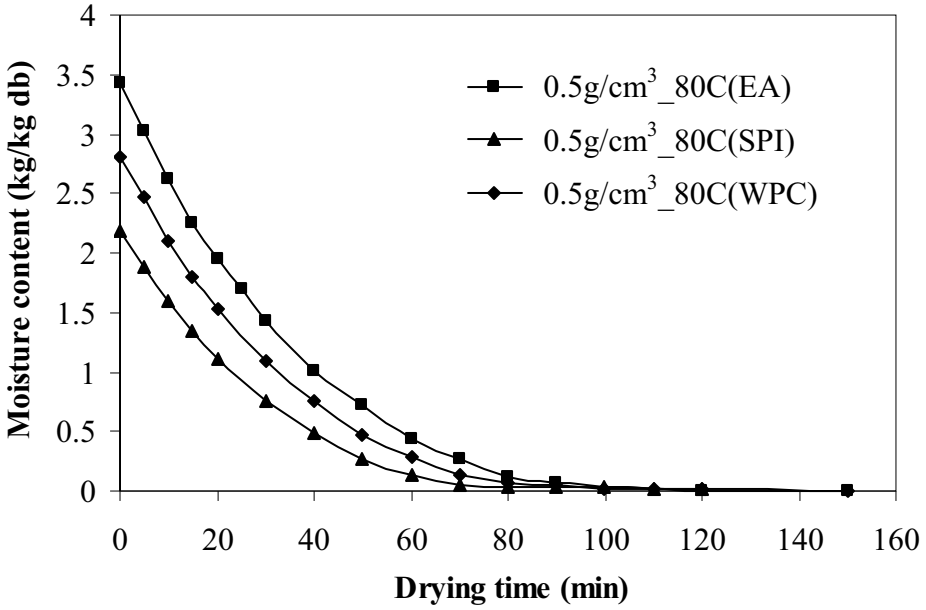

Fig. 2 Drying curves of banana foam mats at different foaming agents

Table 2 shows the effects of foaming agents and foam densities on the drying times of banana foam mat used for reducing moisture content to 3% d.b.at the drying temperature of 80°C. It was found that the drying of banana foam mats at lower initial foam densities took shorter time for all foaming agents because of the larger void area fraction at lower initial foam densities which facilitate the moisture moving from inside to the surface.

Considering the foaming agent effect, it can be seen that the drying time was different amongst foaming agents as compared at the same foam density and the same dying temperature. The difference in drying time is caused by differences in initial moisture content, effective moisture diffusivity and material shrinkage. The drying time for the SPI banana foam mat was shortest as compared to the WPI or EA banana foam mats. The lower initial moisture content of sample and the larger shrinkage provides the shorter drying time. The final thicknesses of EA, SPI and WPC banana foams are given in Table 2.

Table 1 Drying time of banana foam mats at different foaming agents and foam densities

Foam density (g/cm^3)	Drying time (min)		
	EA	SPI	WPC
0.3	60	N/A	80
0.5	150	120	150
0.7	270	180	270

N/A : not available since SPI could not form foams of density of 0.3 g/cm^3.

3.3 Shrinkage

Table 2 shows the thickness of EA SPI and WPC banana foams at the drying end. The banana foam mats before drying were prepared at a 5 mm thickness and when the drying was finished, the banana foam mat thickness was different amongst foam densities and amongst foaming agents. In the case of foam density, it is clear that the banana foam mat produced from the lower foam density had a thinner material or had a higher shrinkage. This can be explained by the fact that as observed from the experiment, the gas bubbles created during the preparation of banana foam at lower density had larger sizes and they were adjacent together. When it was subject to be dried, these gas bubbles were rather unstable and collapsed easily, resulting in the higher shrinkage of banana foam mat with the lower density.

As presented in Table 2, the thickness of the finished WPC banana foam mat had a largest value as compared to the other two foaming agents i.e. EA and SPI. This result indicated that the banana foams added with WPC had more stability than those with additions of EA and SPI. This result is contrast to that reported by several researchers (Devilbiss et al., 1974, Yang & Foegeding, 2010). From their works, the results have been shown that the egg white protein was better foam stability than the WPC. Such contradict results might possibly be due to the fact that the egg white protein used in this study was in the fresh form and thus, it had lower amount of proteins than the WPC. For SPI foam, however, though the amount of

protein for SPI was not very different from that of WPC as already reported in section 2.1, but the SPI foam was less stable than the WPC. This could be attributed to compact tertiary structure of the soy protein which provides the poor foaming properties i.e. foam formation and foam drainage (Martínez et al., 2009).

Table 2 Final thickness of EA SPI and WPC banana foams

Foam density (g/cm^3)	Sample thickness (mm)		
	EA	SPI	WPC
0.3	1.7	N/A	2.7
0.5	2.5	1.7	3.2
0.7	2.6	2.1	3.1

N/A: not available since SPI could not form foams at density of 0.3 g/cm^3.

3.3 Moisture diffusivity of banana foams

Fig. 3 illustrates the moisture diffusivities of EA, SPI and WPC banana foams at various initial foam densities. It was found that at the early drying time of the first 25 min drying time, corresponding to the higher moisture ratio of 0.5, the effective moisture diffusivity was highest for the SPI banana foam, followed by EA and WPC banana foams, respectively. The difference in the effective moisture diffusivity at this drying time range was not caused by the foaming agent effect but it might be related to the product temperature. As shown in Fig. 4, the product temperatures of SPI, EA and WPC at drying times were different. The SPI banana foam temperature was highest during course of drying, followed by the EA and WPC banana foam temperatures, respectively. The highest temperature for the SPI banana foam is due to the fact that the SPI banana foam had lowest initial moisture content, and when it was dried, the evaporation of moisture was not faster than the EA or WPC banana foam. Hence, heat transferring from drying air to the sample was utilized for warming up the sample, thereby providing the higher temperature of the SPI banana foam and, in turn, the higher value of effective diffusivity of SPI banana foam than the other two banana foams.

When the drying time was longer than 25 min, corresponding to lower moisture ratio of 0.5, the banana foam mat changed the state from semi-liquid to solid. At this later drying time, the SPI banana foam temperature was still relatively higher as compared to that of the other two foaming agents, but the value of moisture diffusivity became lower. This result was unexpected since the temperature is a main factor to the diffusion coefficient; the diffusion coefficient is higher at higher temperature. The lower moisture diffusivity for the SPI banana foam is possibly due to the different morphologies for the banana foam produced from SPI, EPC and WPI. Fig. 5 demonstrates the cross sectional views of morphology of dried banana foam, showing different morphologies of dried banana foam samples produced from foaming agents. The microstructure of dried SPI banana foam was more compact and the solid matrices were more compacted than the EA and WPC banana foams. The compact structure for the SPI banana foam resulted in the moisture present at inner area travelling to the sample surface with more difficulty, hence the lower moisture diffusivity for the SPI banana foam. As shown in Fig. 3, the moisture diffusion coefficient for the WPI banana foam at moisture ratio lower than 0.5 was highest. This result corresponded to the WPC banana foam structure, exhibiting very high porous structure.

It is also seen from Fig. 5 that the pore shape of dried EA and SPI banana foams was more elongate than that of died WPC banana foam. This is probably due to the fact that the stability of gas bubbles produced from EA and SPI is less which leads to more bubble collapse and subsequent greater shrinkage, as compared to the shrinkage of the WPC banana foam. The high shrinkage caused some distortion of material and, in turn, resulted in the microstructural change such as elongation of pores.

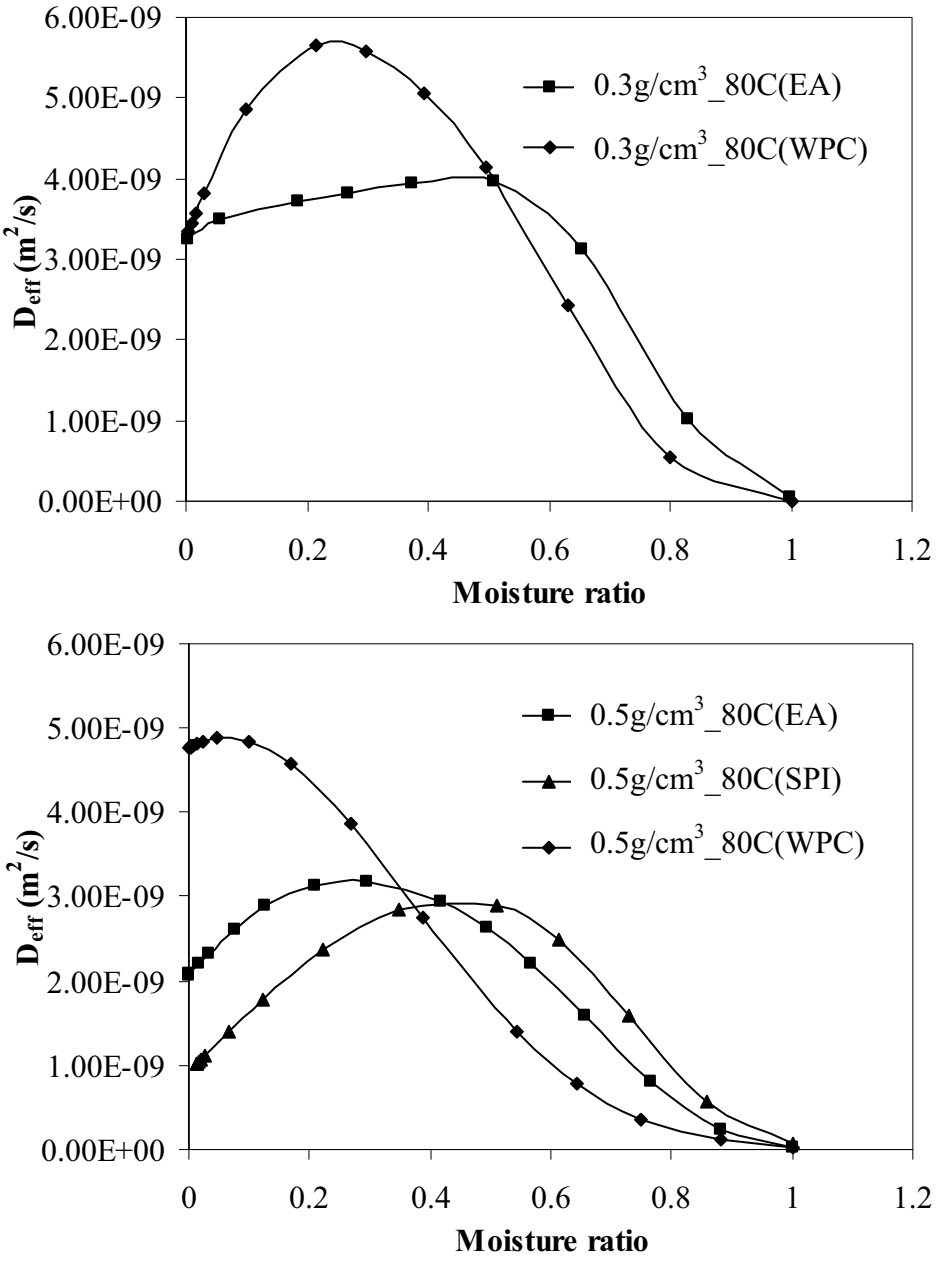

(b)

Fig. 3 Moisture diffusivity of banana foam mats at different banana foam densities and drying temperature of 80°C

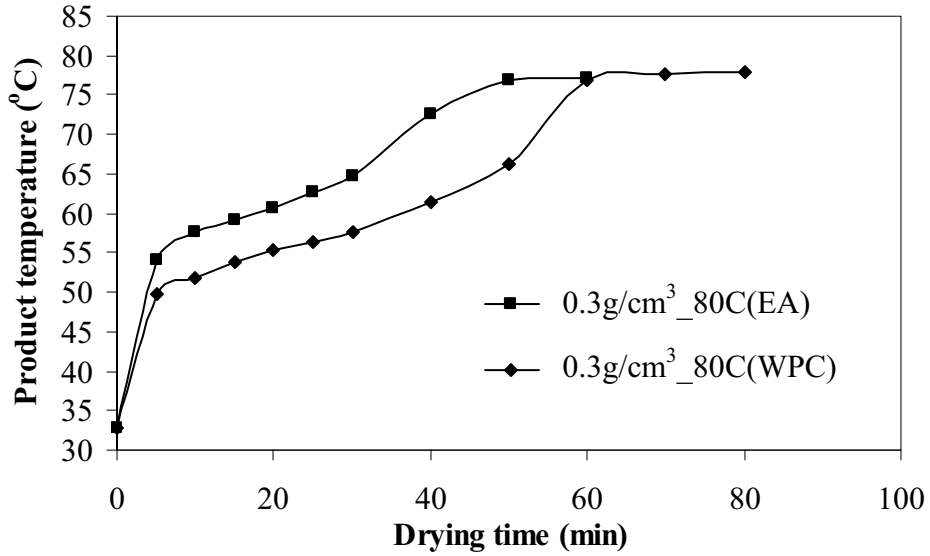

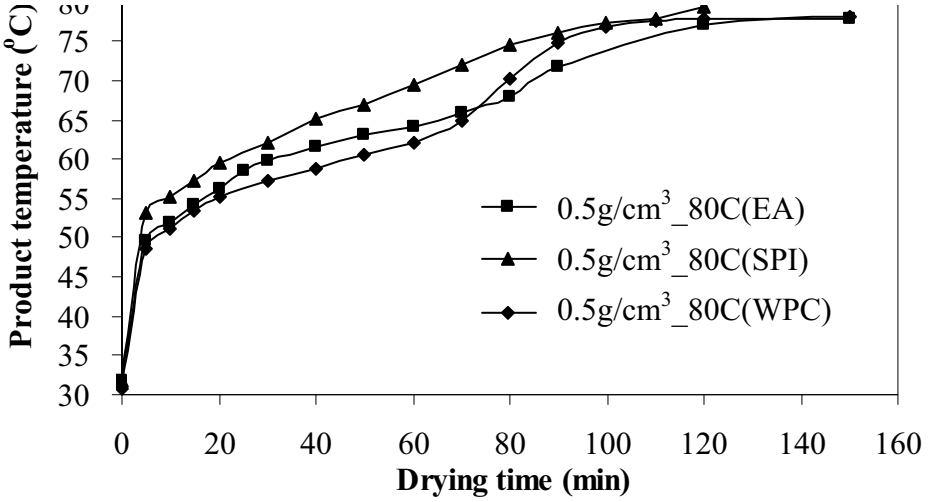

(b)

Fig. 4 Change in temperature of banana foam mats at 80°C

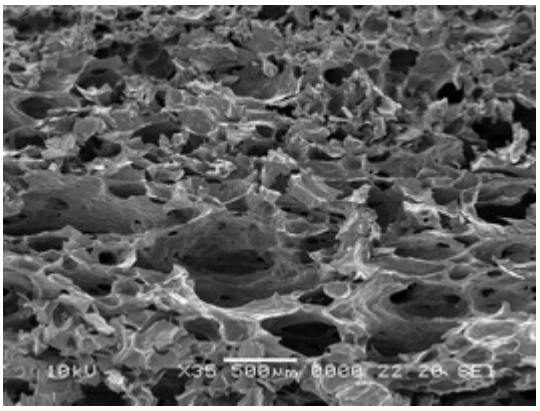

(a) EA

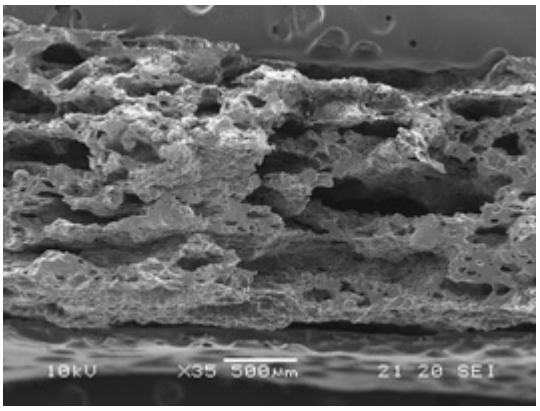

(b) SPI

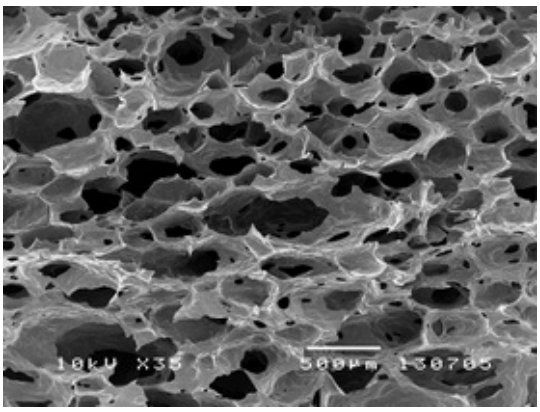

(c) WPC

Fig. 5 SEM micrographs of dried banana foam mats added with different foaming agents (initial foam density of 0.5 g/cm^3)

3.5 Textural properties

Fig. 6 shows the results of textural properties of dried banana foam mats produced from different foaming agents and foam densities. The hardness was defined as the maximum force in the force-deformation curve and the crispness was characterized by the number of peaks and the slope of the first peak from force curve. It was noted that the textural properties were strongly affected by the porous structure. The samples with lower initial foam densities, characterized by a number of large pores and more limited number of small pores, was very porous. Hence, the hardness was smaller as compared with those samples with higher initial foam densities. In terms of crispness as characterized by number of peaks and initial slope shown in Figs. 6b and 6c, respectively, the samples with lower initial foam densities, for each foaming agent, had smaller numbers of peaks and lower slopes of the first peak for all foaming agents as shown in Fig. 6, both textural characteristics showing less crispy at the lower banana foam density.

Considering the effect of foaming agent for a given banana foam density, it was found that the foaming agents i.e. SPI, EA and WPC strongly affected the crispy characteristics of dried banana foam, but they did not take an effect on the hardness. The SPI banana foam was significantly larger initial slope than the EA and WPC banana foams, but it was lower fracture points or number of peaks, both textural properties presenting rather crispier and less porous material for the SPI banana foam. For the EA and WPC banana foams, in spite of the larger number of peaks, their texture was not crisp but was relatively spongy. The different crispiness amongst three foaming agents may be related to different morphological features. Fig. 7 shows the pore size distributions of the dried banana foam mats with different foaming agents. These pore sizes were determined by image analysis and the details could be seen from Thuwapanichayanan, Prachayawarakorn and Soponronnait (2008a). As shown in Fig. 7, the dried EA banana foam had a range of pore size of 10-160 μm with a larger number than

the SPI and WPC dried banana foams. At this pore size range, the number of pores was 594, 270 and 350 for the samples produced from EA, SPI and WPC, respectively. In addition, the numbers of pores with diameters larger than 240 μm were 17, 8 and 24 for EA, SPI and WPC banana foams. Because of a greater number of large pore assemblies in the WPC sample, the void area fraction of the samples added with WPC was higher than that of the samples added with EA and SPI. The void area fractions of EA, SPI and WPC banana foam were 18%, 13% and 20%, respectively. From theses pore size distribution, it clearly indicated that the SPI banana foam possessed the smallest number of pores and consequently provided the smallest number of fracture points.

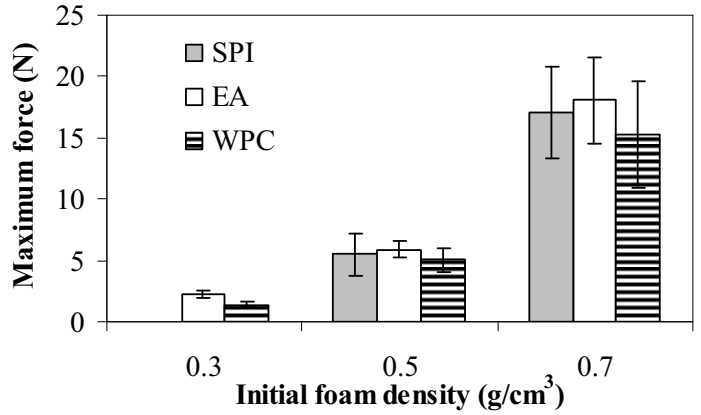

(a)

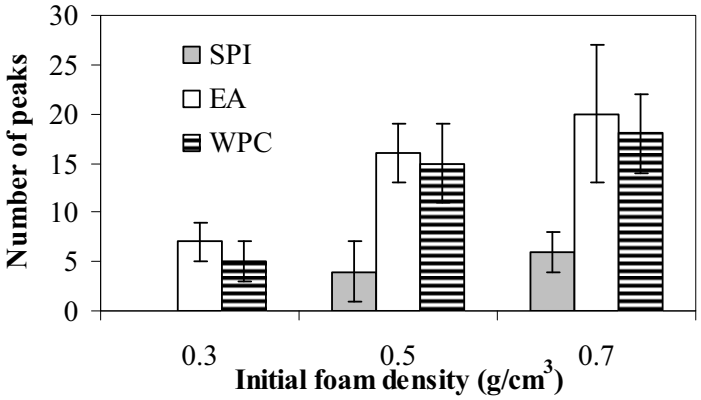

(b)

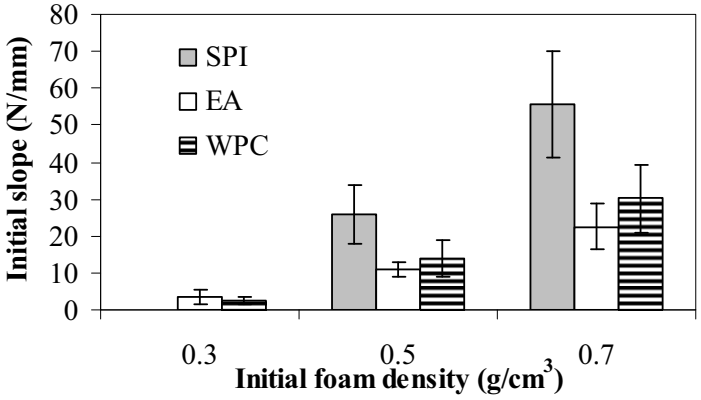

(c)

Fig. 6 Effects of foaming agents and initial foam densities on (a) Maximum force, (b) Number of peaks and (c) Initial slope of dried banana foam mat

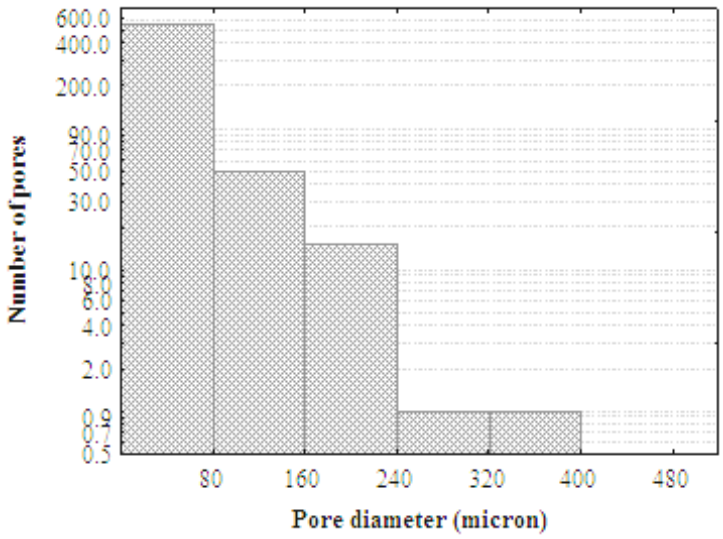

a) EA

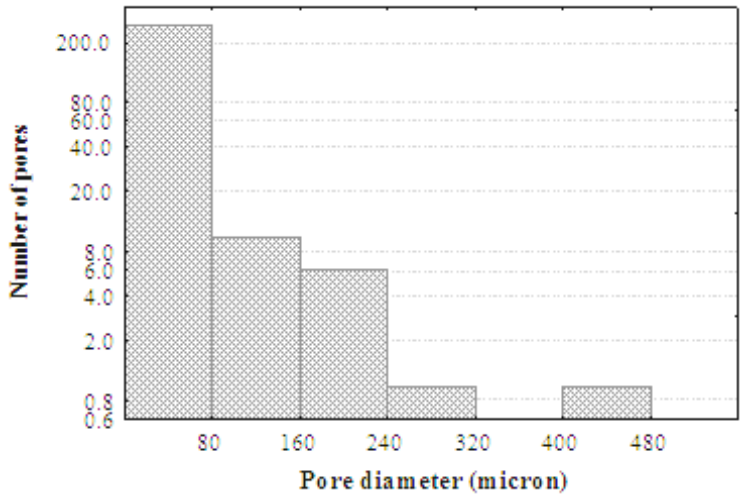

b) SPI

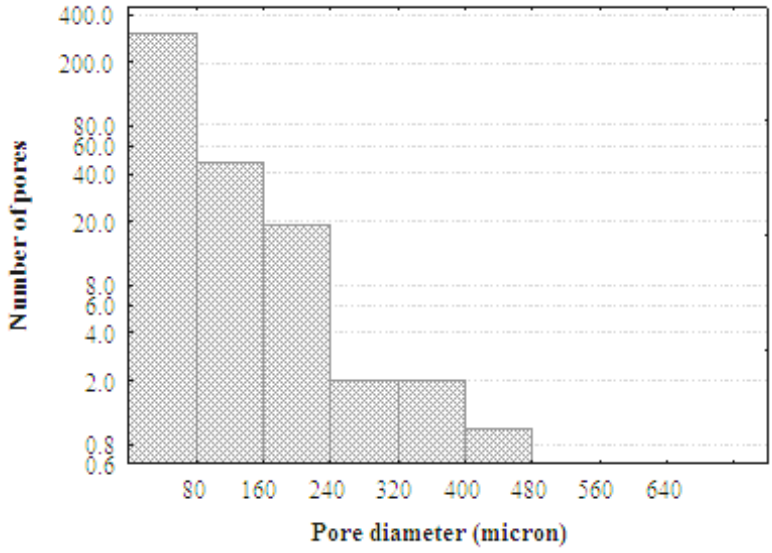

c) WPC

Fig. 7 Pore size distribution of dried banana foam mats using different foaming agents (initial foam density of 0.5 g/cm^3 and drying temperature of 80°C)

3.7 Volatile compounds

Fig. 8 (a-c) shows the chromatogram profiles obtained from fresh banana, foamed banana and dried foamed banana. The dried foamed banana was prepared by drying at 80°C. The volatile compounds extracted from the banana samples were identified by GC-MS. It was found that the most significant volatile compounds in fresh banana were the isoamyl acetate, isobutyl butanoate, butyl butyrate, isoamyl butyrate and isoamyl isovalerate. The retention times of these compounds were 6.75±0.1, 9.72±0.1, 11.46±0.1, 14.15±0.1 and 16.41±0.1 min, respectively. Among these five esters, only isoamyl acetate, isoamyl butyrate and isoamyl isovalerate, are the key components of the banana's fruity odor (Salmon et al., 1996).

From Fig. 8 (a-c), it can be seen that the substantial loss of volatile substances occurred during the foaming process although the foaming was performed at room temperature. The volatile fractions of fresh banana, banana foam and dried banana foam are shown in Table 4 for different foam densities and foaming agents. The whipping time strongly affected the loss of volatile compounds during foaming process; the longer the whipping time, the higher the evaporation of volatile compounds. This is because air was brought into the liquid puree during the whipping process and thus the evaporation of volatile compounds from the liquid phase to the air phase could occur easily. The isoamyl acetate, which is the lowest molecular weight, exhibited the highest loss during the foaming process.

In addition to the loss during foaming, the volatiles also lost during drying. As shown in Table 4, the losses of each volatile compound that was present in each banana foam sample seemed to be not the same in quantity although the samples were dried at the same drying temperature. At the initial foam density of 0.5 g/cm^3, for example, the losses of isoamyl acetate, isobutyl butanoate, butyl butyrate, isoamyl butyrate and isoamyl isovalerate were respectively 10.97, 6.45, 10.95, 16.31, 25.67% for EA banana foam, and 10.85, 20.26, 26.93, 31.80, 35.47% for SPI banana foam. The lower volatile retention for the SPI banana foam is

possibly due to the lower thickness of the SPI sample, as previously shown in Table 2; the volatile compounds diffused through the sample surface in a shorter time for the sample with lower thickness. In this case, the morphology of SPI banana foam, characterized by the dense porous structure as previously shown in Fig. 5 (b), could not retard the diffusion of volatile compounds. This is because the molecular sizes of such volatile compounds are very smaller than the pore sizes of the SPI banana foam, causing them to transport through pores easily.

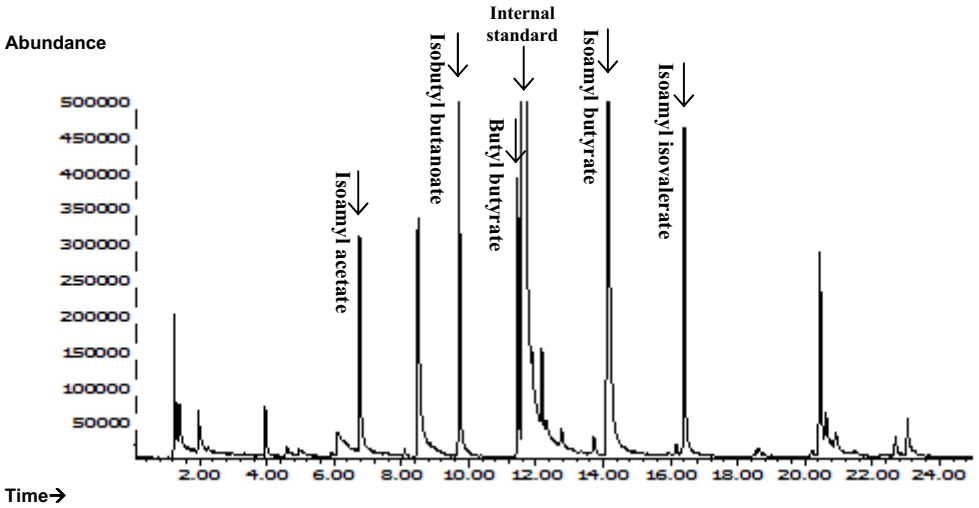

(a) Fresh banana

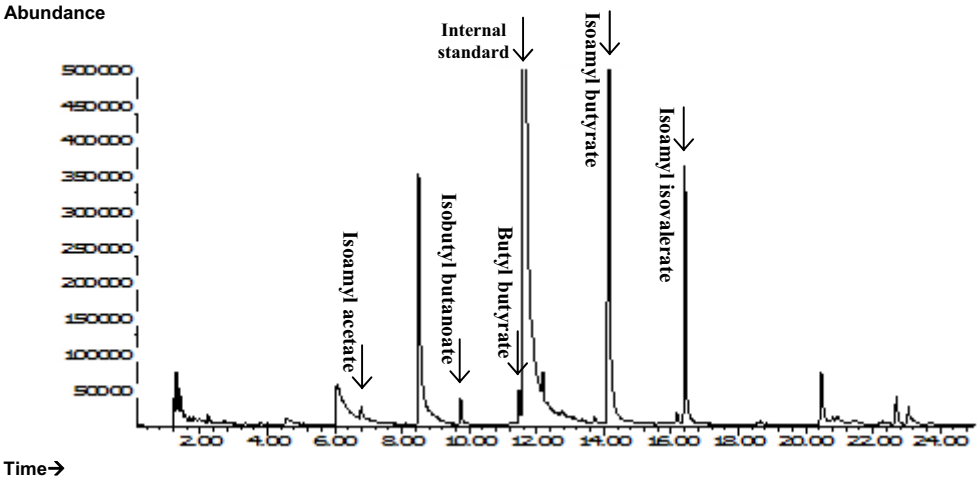

(b) Banana foam (before drying)

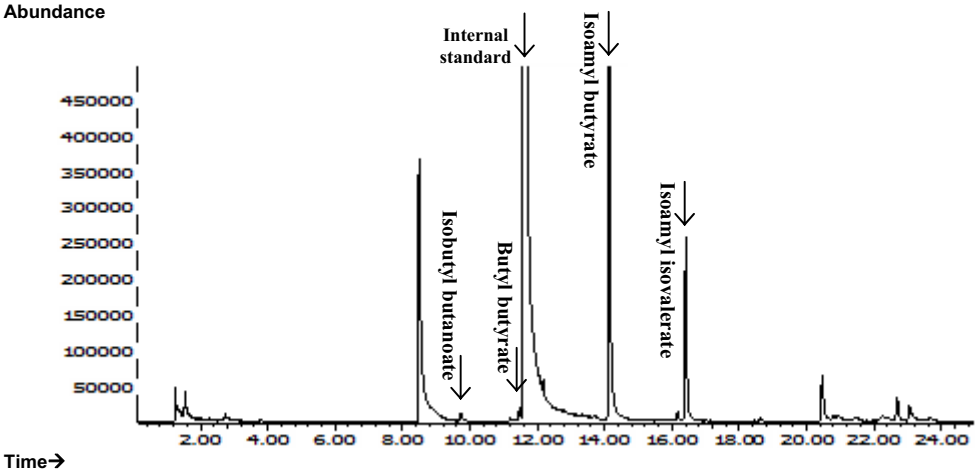

(c) Dried banana foam

Fig. 8 Chromatograms of fresh, foamed and dried bananas (using EA as a foaming agent and whipping to foam density of 0.5 g/cm^3)

Table 4 Losses of five major components of banana odor during processing

Whipping condition	Volatile compounds	Fraction (%)			%loss during foaming	%total loss
		Fresh	Foamed	Dried		
EA with initial foam density of 0.3 g/cm^3, Whipping time 20 min	Isoamyl acetate	4.35	0.00	0.00	100.00	100.00
	Isobutyl butanoate	5.82	0.11	0.00	98.14	100.00
	Butyl butyrate	8.75	0.29	0.03	96.68	99.68
	Isoamyl butyrate	54.64	4.57	0.16	91.63	99.70
	Isoamyl isovalerate	3.72	1.61	0.08	56.64	97.92
	Total components	100.00	10.92	0.57	89.08	99.43
EA with initial foam density of 0.5 g/cm^3, Whipping time 9 min	Isoamyl acetate	4.35	0.48	0.00	89.03	100.00
	Isobutyl butanoate	6.88	0.60	0.16	91.28	97.73
	Butyl butyrate	4.55	0.72	0.22	84.14	95.08
	Isoamyl butyrate	56.46	21.11	11.90	62.62	78.93
	Isoamyl isovalerate	6.27	5.08	3.47	18.94	44.61
	Total components	100.00	36.93	19.69	63.07	80.31
WPC with initial foam density of 0.5 g/cm^3, Whipping time 15 min	Isoamyl acetate	4.23	0.00	0.00	100.00	100.00
	Isobutyl butanoate	4.55	0.42	0.00	90.80	100.00
	Butyl butyrate	2.89	0.60	0.08	79.03	97.10
	Isoamyl butyrate	59.54	15.91	7.16	73.27	87.98
	Isoamyl isovalerate	8.08	4.47	3.08	44.70	61.87
	Total components	100.00	27.59	9.97	72.41	90.03
SPI with initial foam density of 0.5 g/cm^3, Whipping time 10 min	Isoamyl acetate	2.97	0.32	0.00	89.15	100.00
	Isobutyl butanoate	5.07	1.09	0.07	78.45	98.71
	Butyl butyrate	5.20	1.51	0.11	71.01	97.94
	Isoamyl butyrate	60.53	25.48	6.24	57.90	89.70
	Isoamyl isovalerate	5.17	3.18	1.35	38.45	73.92
	Total components	100.00	38.12	8.32	61.88	91.68

Note: Fractions of each component (%) = $\frac{\text{Peak area of a component}}{\text{Total peak area of all components in fresh banana}} \times 100$

4. Conclusions

EA and WPC at 5% by weight were found to be efficient foam inducer, decreasing banana foam density to 0.3 g/cm^3, whilst the addition of SPI at this percent weight or higher could not produce at this foam density. Banana foams produced using WPC had more stability during whipping than another two foaming agents and this, in turn, provided less shrinkage during drying, higher void area fraction and higher value of effective moisture diffusivity than the EA and SPI banana foam mats. However, banana foams produced by the EA and WPC were less crisp than the SPI one. The foams produced at lower densities had higher value of moisture diffusivity, and had lower values of hardness and crispness. The substantial loss of volatile substances occurred during foaming process. The SPI banana foam, which had high shrinkage value, provided a greater loss of volatile compounds during drying than another two foaming agents.

Acknowledgements

The authors express their sincere appreciation to the Thailand Research Fund (TRF), King Mongkut's University of Technology Thonburi and the National Science and Technology Development Agency (NSTDA) for their financial support.

References

Brygidyr, A. M., Rzepecka, M. A. and McConnel, M. B. (1977). Characterization and drying of tomato paste foam by hot air and microwave energy. Canadian Institute of Food Science and Technology Journal, 10, 313±319.

Campbell, G.M., & Mougeot, E. (1999). Creation and characterisation of aerated food producs. *Trend in Food Science and Technology*, 10, 283-296.

Davis, J.P. & Foegeding, E.A.(2007). Comparisons of the foaming and interfacial properties of whey protein isolate and egg white proteins. Colloids and Surfaces B: Biointerfaces, 54, 200-210.

Eduardo, J.V.C., Gilberto, E.P., Cesar, I.B., & Hipolito, R.T. (2001). Effect of foaming agents on the stability, rheological properties, drying kinetics and flavour retention of tamarind foam-mats. *Food Research International*, 34, 587-598.

Garcia, R., Leal, F., & Rolz, C. (1988). Drying of bananas using microwave and air ovens. *International Journal of Food Science and Technology*, 23, 73-80.

Hart, M. R., Graham, R. P., Ginnette, L. E. and Morgan, A. I. (1963), Foams for foam-mat drying. Food Technology 17(10), 90±92.

Hutton, C.W., & Campbell, A.M. (1981). Water and fat absorption. In J.P. Cherry (Ed.) *Protein Functionality in Foods* (pp. 177-200). Washington, D.C.: American Chemical Society.

Hwang, M.P., & Hayakawa, K.I. (1980). Bulk densities of cookies undergoing commercial baking processes. *Journal of Food Science*, 45, 1400-1402.

Karim, A.A. & Way, C.C. (1999). Foam-mat drying of starfruit (Averrhoa carambola L.) puree. Stability and air drying characteristics. Food Chemistry, 64, 337-343.

Kinsella, J.E. (1976). Functional properties of proteins in foods: A survey. *Critical Reviews in Food Science and Nutrition*, 7, 219-280.

Martínez, K.D., Sánchez, C. C., Patino, M.R. & Pilosof, A.M.R. (2009). Interfacial and foaming properties of soy protein and their hydrolysates. *Food Hydrocolloids*, 23, 2149-2157.

Mott, C.L., Hettiarachchy, N.S., & Qi, M. (1999). Effect of Xanthan gum on enhancing the foaming properties of whey protein isolate. *Journal of the American Oil Chemists' Society*, 76, 1383-1386.

Phillips, L.G., German, J.B., O'Neill, T.E., Foegeding, E.A., Harwalkar, V.R., Kilara, A., Lewis, B.A., Mangino, M.E., Morr, C.V., Regenstein, J.M., Smith, D.M., & Kinsella, J.E. (1990). Standardised procedure for measuring foaming properties of three proteins, a collaborative study. *Journal of Food Science*, 55, 1441-1444&1453.

Ratti, C. & Kudra, T. (2006) Drying of foamed biological materials: opportunities and challenges. Drying Technology, 24, 1101-1108.

Salmon, B., Martin, G.J., Remaud, G., & Fourel, F. (1996). Compositional and isotopic studies of fruit flavours. Part I. The banana aroma. *Flavour and Fragrance Journal*, 11, 353-359.

Sankat, C.K., & Castaigne, F. (2004). Foaming and drying behaviour of ripe bananas. *Lebensmittel-Wissenshaft und-Technologie*, 37, 517-525.

Thuwapanichayanan, R., Prachayawarakorn, S., & Soponronnarit S. (2008a). Drying Characteristics and Quality of Banana Foam Mat. *Journal of Food Engineering*, 86, 573-583.

Thuwapanichayanan, R., Prachayawarakorn, S., & Soponronnarit S. (2008b). Modeling of Diffusion with Shrinkage and Quality Investigation of Banana Foam Mat Drying. *Drying Technology*, 26, 1326-1333.

Townsend, A.A., & Nakai, S. (1983). Relationships between hydrophobicity and foaming characteristics of food proteins. *Journal of Food Science*, 48, 588-594.

Wilde, P.J., & Clark, D.C. (1996). Foam formation and stability. In G.M. Hall (Ed.) *Methods of testing protein functionality* (pp. 110-152). London: Blackie Academic & Professional.

Journal of Food Engineering 96 (2010) 119–126

Contents lists available at ScienceDirect

Journal of Food Engineering

journal homepage: www.elsevier.com/locate/jfoodeng

Modelling of moisture diffusion in pores of banana foam mat using a 2-D stochastic pore network: Determination of moisture diffusion coefficient during adsorption process

Preeda Prakotmak [a,*], Somchart Soponronnarit [a], Somkiat Prachayawarakorn [b]

[a] School of Energy, Environment and Materials, King Mongkut's University of Technology Thonburi126 Pracha u-tid Road, Bangkok 10140, Thailand
[b] Department of Chemical Engineering King Mongkut's University of Technology Thonburi126 Pracha u-tid Road, Bangkok 10140, Thailand

ARTICLE INFO

Article history:
Received 23 November 2008
Received in revised form 1 July 2009
Accepted 6 July 2009
Available online 31 July 2009

Keywords:
Adsorption kinetics
Banana foam mat
Pore diffusivity
Pore network

ABSTRACT

The purpose of this research was to determine the diffusion coefficient of moisture in the pores of banana foam mat using stochastic pore network. A 2-D pore network was used to represent the pore voids inside the banana foam sample and the moisture movement inside the individual pore segments was described by Fick's law. To determine the moisture diffusion coefficient, the adsorption experiments were carried out with standard static method using saturated salt solutions. Two banana foam densities of 0.21 and 0.26 g/cm^3 were used to adsorb the water vapour. The interactions between moisture and pore structure were illustrated using a 3-D pictorial representation of network concentration gradients in spaces with colour representing the moisture content. The network model described the experimental results relatively well. The diffusion coefficient of moisture in pores was in order of 10^{-9} m^2/s which was nine times higher than the effective diffusion coefficient calculated from the continuum model. The value of moisture diffusion coefficient was dependent on the temperature and independent of the foam densities and the relative humidity, except for the diffusivity determined from the condition at higher relative humidity of 70%.

1. Introduction

Moisture migration during storage is of great importance to food quality, in particular for dried crispy products such as biscuits, ready-to-eat cereals and snacks. An increase in the product moisture content, which in turn leads to the loss of crispness, generally occurs by migration of water vapor from the ambient into the product. The rate of moisture adsorption into porous food is governed by the environmental conditions, i.e., temperature and relative humidity. The rate also relies upon the porous structure of the food (Guillard et al., 2003; Roca et al., 2006). Therefore, an ability to model water migration in porous food is of great interest. To date, two different approaches have been developed for studying moisture movement in porous foods.

The first modeling is based on a continuum model. In this type of model, porous spaces are considered as a continuum, consistent with its appearance on the macroscopic scale. In this case, the effective moisture diffusivity includes in itself all microscopic complexities of the porous structure (e.g., sizes of pores and their connectedness) as well as mechanisms of mass transfer, which may occur by molecular diffusion or capillary flow, etc. (Efremov and Kudra, 2004; Roca et al., 2006). When a dried porous food is subject to humid air, water vapor transports from the air to the sample surface and is then assumed to diffuse into the internal area of the sample via the pores by assuming that the solid act as an impermeable surface. This adsorption phenomenon is described by the Fick's second law of diffusion. Under isothermal condition, moisture transport in a porous food with an infinite slab geometry (Chen, 2007) can be described by:

$$\frac{\partial M}{\partial t} = \nabla(D_{eff}\nabla M) \tag{1}$$

where M is the moisture content (kg/kg d.b.), t the time (s), D_{eff} the effective moisture diffusivity (m^2/s), which can be expressed by:

$$D_{eff} = \frac{\varepsilon D_p}{\tau} \tag{2}$$

where ε is the porosity of the material (dimensionless), D_p the actual diffusivity in the pore voids (m^2/s) and τ the tortuosity factor (dimensionless). Tortuosity factor accounts for the fact that the pore

* Corresponding author. Tel.: +662 470 8695; fax: +662 470 8663.
E-mail address: preeda_list@hotmail.com (P. Prakotmak).

0260-8774/$ - see front matter © 2009 Elsevier Ltd. All rights reserved.
doi:10.1016/j.jfoodeng.2009.07.004

spaces do not provide straight line paths through, thereby lengthening the diffusive path and reducing the internal diffusional fluxes.

The second approach is based on the discrete model or pore network model. In this type of model, the pore sizes and topology of a porous material are taken into account by mapping them onto an equivalent network of the interconnected pores. Network models represent void spaces of a porous medium by a simple two- or more realistic three-dimensional lattice in which large and small pores are randomly interconnected. Each pore can be assumed to be cylindrical, slit, triangular and polygonal shapes. Segura and Toledo (2005) found that pore shapes used in the network model had an insignificant effect on the drying characteristic curves, vapour relative diffusivity, and liquid relative permeability. The pore network model is more useful and flexible than the first approach since the moisture calculation using continuum model requires use of the effective moisture diffusivity, which varies from material to material, whilst the pore network model requires only the structural parameters of the material such as total pore volume or pore size distribution (providing that the actual moisture diffusivity in the pore voids is known). However, at present, there is no available information on the actual diffusion coefficient of moisture in pore voids, D_p. To be able to estimate the actual diffusion coefficient, first the pore network model needs to be constructed, where more or less simplified geometries, and pore size distributions are used to describe the topology of the pore structure of a real material (Mann, 1993; Hollewand and Gladden, 1992; Androutsopoulos and Mann, 1979). Diffusion equation is then applied to an individual pore of the network; the flow of substances through pore segments can then be numerically predicted (Blunt, 2001; Yiotis et al., 2005; Prachayawarakorn et al., 2008) and compared with the experimental results. Although, theoretically, either experimental data on desorption (or drying) or adsorption could be used to calculate the moisture diffusivity in the pore voids, the adsorption experiment is preferred since the transfer rate of heat is usually faster than the transport rate of moisture and hence the temperature of the porous material remains close to the temperature of the experiment. Also, the morphology of porous food changes only slightly during adsorption experiment whilst it significantly changes during drying (Saravacos and Maroulis, 2001).

As the data on the moisture diffusivity in the pore voids of any porous food are not available, the aim of the present investigation was to determine the pore diffusivity by using a two-dimensional stochastic pore network. Banana foam mat was used as a representative porous medium. The Fick's second law was used to describe the moisture diffusion in individual pore segments and an optimization technique was implemented to determine the pore diffusivity under adsorption conditions. The actual moisture diffusion coefficient in pore voids obtained in this work may be applied to other porous foods as well.

2. Materials and methods

2.1. Dried banana foam preparation

The banana puree with 5% of fresh egg albumen used as foaming agent was foamed to densities of 0.3 and 0.5 g/cm^3. The selected foam densities were suitable to produce the snack since its texture provided the low hardness and crispiness as reported by Thuwapanichayanan et al. (2008a,b).

The density was determined by measuring the mass of a fixed volume of the prepared foam. The banana foam was poured slowly into a steel block with a dimension of $43 \times 43 \times 4$ mm^3 and then placed on a mesh tray, which was covered with aluminium foil. After that, it was dried to about 3% dry basis (d.b.) at a temperature of 80 °C and a 0.5 m/s superficial air velocity. The banana foam prepared from the initial foam densities of 0.3 and 0.5 g/cm^3 can produce the dried banana densities of 0.21 ± 0.02 and 0.26 ± 0.02 g/cm^3, respectively. The product thicknesses after drying were 2.8 mm and 3.2 mm for the densities of 0.21 and 0.26 g/cm^3, respectively.

2.2. Adsorption experiment

Moisture adsorption experiments were carried out using the static method. Samples were placed into the glass jars contained the saturated salt solutions ($MgCl_2{\cdot}6H_2O$, $Mg(NO_3)_2{\cdot}6H_2O$, KI, NaCl and KCl) which provided the relative humidity (RH) in range of 32–82% at the temperatures of 35, 40 and 45 °C. The glass jars were kept in the hot air oven that controlled the temperature with an accuracy of ±1 °C (UFE500, Memmert, Germany). Samples were weighed at different exposure times ranging from 1 to 120 h. At RH > 74%, a small amount of toluene held in a vial was fixed in the glass jars in order to prevent microbial spoilage of the samples (Kaya and Kahyaoglu, 2005). Moisture content of each sample after reaching the equilibrium condition was determined by drying it with the hot air oven at a temperature of 103 °C for 3 h. Under this moisture content determination condition, the percentage error was approximately 0.4% when compared to the result obtained by the standard vacuum method (AOAC, 1995) at a temperature of 70 °C and at a negative pressure of 13.3 kPa for 24 h. This error might be caused by the vaporization of volatile compounds. Thuwapanichayanan (2007) reported that the loss of volatile compounds after drying of banana foam was approximately 90%. The experiment at each sorption condition was repeated three times and the mean value was reported.

2.3. SEM photograph

The morphologies of dried banana foam mats were characterized using scanning electron microscope (SEM) with an accelerating voltage of 10 kV. Before photographing, the specimens were cut into a dimension of 5×5 mm^2 and then glued on the metal stub. The samples were coated with gold, scanned, and photographed at 15× magnification.

To quantify the porous banana foam characteristics such as pore diameter and pore area, Image J software was used. Each pixel of the SEM micrograph was assigned a value of gray intensity between 0 and 255 and the binary images were generated. The pixels with gray levels lower than the selected threshold were assigned as pore, which appeared as black colour, and the pixels with gray levels above the selected threshold were set as solid phase, which appeared as white colour in binary image. The pore diameter was estimated from the known pore area by counting the number of pixels filled in the specified space.

2.4. Estimation of activation energy

The diffusion coefficient of moisture was related with the temperature through the following Arrhenius equation:

$$D_p = D_0 \exp\left(\frac{-E_a}{RT}\right) \quad (3)$$

where D_0 is the constant value (m^2/s), E_a is the activation energy (kJ/mol), R is the universal gas constant and T is the temperature (K). In this work, the pore diffusivity data obtained from the experimental conditions at the relative humidity below 70% and at the temperatures of 35–45 °C were used to determine the values of E_a and D_0. Under the specified conditions, the moisture content of banana foam ranged between 0.038 and 0.37 kg/kg d.b.

3. Generation of the pore network

When the pore size distribution of material is known, these pores are assigned according to its distribution and allocated randomly onto a lattice. In this work, the pore was assumed to be of cylindrical geometry and each pore in the network had the same length. The pores with different sizes were randomly placed onto the network and this approach provided pore at any positions within the network independent to the neighboring pores. Such random arrangement of pore assemblies was referred to stochastic pore network. Fig. 1 illustrates an example of a 2-D stochastic pore network with a small size of 23 × 50, defined by the number of pore junctions in the vertical direction multiplied by the number of pore junctions in the horizontal direction. This network size consists of 2373 pores obeying a pore size distribution of dried banana foam shown in Fig. 6 for the density of 0.21 g/cm^3. The pores in this figure were represented by black colour and solid by white colour. In addition, each pore junction, where the pores are intersected, had a connectivity of 4. However, for calculating the pore diffusivity, we used a larger network size, with a number of pores of the network corresponding to those pores in the cross-sectional area of sample.

In this work, the network size of 20 × 231 for the foam density of 0.21 g/cm^3, accounting for 9491pores, and the size of 23 × 264 for the density of 0.26 g/cm^3, accounting for 12 431 pores, were used. These numbers of pores were estimated from the known number of pores in the unit area of sample that was obtained from SEM. The length of each pore, L, was calculated by dividing the thickness of banana foam sample by number of vertical pores in each row; 21 for the network size of 20 × 231 and 24 for the network size of 23 × 264. The average value of L was equal to 133 μm.

3.1. Single pore

In this work, moisture adsorption between surrounding air and banana foam mat occurred under isothermal condition. The water vapor from the air will be adsorbed at the sample surface and then moves in the liquid form through interior area via the pores. The moisture diffusing through each pore in the network, whether the pore is allocated in horizontal or vertical direction, can be described by Fick's second law:

$$\frac{\partial M}{\partial t} = D_p \frac{\partial^2 M}{\partial x^2} \tag{4}$$

where M is the moisture content (kg/kg d.b.), t the adsorption time (s), D_p the water diffusivity in pore (m^2/s), and x the distance along the pore length (m). The migration of moisture from the surrounding air to the banana foam surface occurred specifically at the top surface and no moisture transferred at the bottom surface of the network since the banana foam mat was placed on an opaque glass dish. The samples had the length and width about 11 times of its thickness and thus, the banana foam mats were reasonably assumed to be an infinite slab. Accordingly, moisture movement during adsorption process occurred along the material thickness direction. The constant diffusion coefficient at a given condition was assumed and the moisture profile in the pores at the beginning was uniform along the pore axis:

$$M = M_i \quad : t = 0, \quad 0 \le x \le L \tag{5}$$

where M_i is the initial moisture content (kg/kg d.b.). From the prepared sample size, it indicated that the surface area at each sample side was remarkably smaller than that at the top surface. Hence, the moisture transferring from the surrounding to the pores allocated at the two sides of sample was small. Accordingly, the boundary condition for the pores allocated at both sides of the network (see Fig. 1) is set as:

$$\left.\frac{\partial M}{\partial x}\right|_{r_{i,j}} = 0 \quad : t > 0 \tag{6}$$

where r is the pore radius (m) and subscripts i and j are the position of the pores in the network as can be seen in Fig. 1. The positions of pore, $r_{i,j,}$ at the left edge of network are $r_{1,2}$, $r_{1,4}$, … $r_{1,V+1}$, at the right edge are $r_{H,2}$, $r_{H,4}$, …, $r_{H,V+1}$, and at the bottom edge are $r_{2,1}$, $r_{4,1}$, …, $r_{H+1,1}$. Subscripts H and V are the number of columns and rows of the pores on the network, respectively. For the periphery pores positioned on the top of the network, such as $r_{2,V}$, $r_{4,V}$, …, $r_{H+1,V}$, the moisture moving from the surrounding to those pores was occurred by convection and the boundary condition is set by:

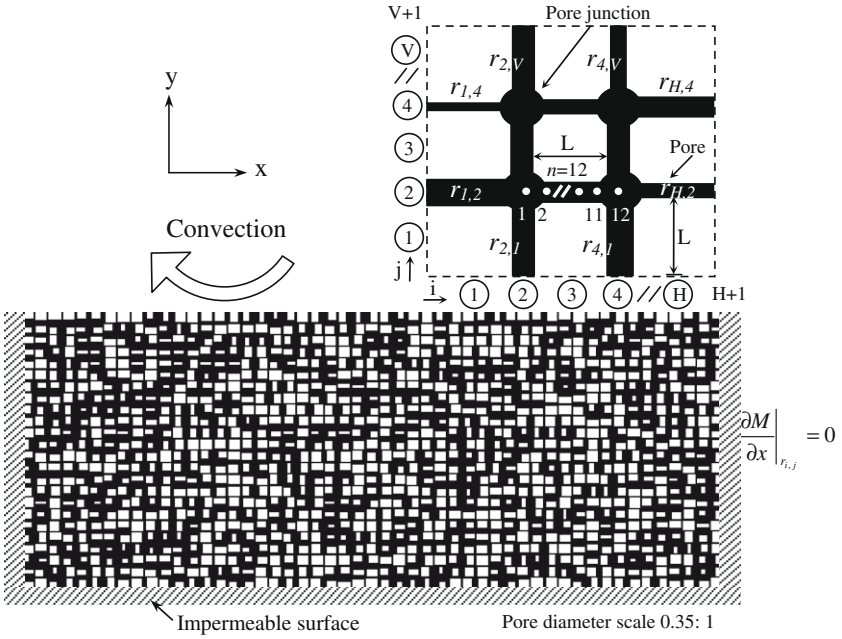

Fig. 1. Illustration of a simple 2-D stochastic pore network and boundary conditions.

$$D_p\left(\frac{\partial M}{\partial x}\right)_{r_{i,j}} = h_m(M_e - M_s) \quad : t > 0 \tag{7}$$

where h_m is the convective mass transfer coefficient (m/s), M_e the equilibrium moisture content (kg/kg d.b.) and M_s the moisture content at the sample surface (kg/kg d.b.). To calculate the moisture concentration of the pores, a finite difference method was used. An individual pore in the network was divided into n intervals (n = 12 as shown in Fig. 1) and Eq. (4) was discretized using the explicit method as follows:

$$M^{p+1}_{n,r_{ij}} + M^{p}_{n,r_{ij}}(2\alpha - 1) - \alpha(M^{p}_{n+1,r_{ij}} + M^{p}_{n-1,r_{ij}}) = 0 \tag{8}$$

where $\alpha = D_p\Delta t/\Delta x^2$ is the Fourier number, p and n the respective indexes of the present time and of nodal position along the pore axis. Eq. (8) is used to calculate the moisture content for the inner pores of network. The boundary conditions in Eqs. (6) and (7) can be written respectively as:

$$M^{p+1}_{n,r_{ij}} + M^{p}_{n,r_{ij}}(2\alpha - 1) - 2\alpha(M^{p}_{n+1,r_{ij}}) = 0 \tag{9}$$

$$M^{p+1}_{n,r_{ij}}(\gamma + 1) - M^{p}_{n-1,r_{ij}} - \gamma M^{p+1}_{e} = 0 \tag{10}$$

Where $\gamma = h_m\Delta x/D_p$. The moisture adsorption rate $Q_{i,j}$ (kg/s) for the individual pores can be calculated by:

$$Q_{r_{ij}} = \rho \cdot \pi r^2_{ij} \cdot D_P\left(\frac{dM_{r_{ij}}(x,t)}{dx}\right)_{x=L} \tag{11}$$

The finite difference approximation of Eq. (11) is

$$Q_{r_{ij}} = \rho \cdot \pi r^2_{ij} \cdot D_P\left(\frac{M^{p+1}_{n} - M^{p+1}_{n-1,r_{ij}}}{\Delta x}\right)_{x=L} \tag{12}$$

where ρ is the dried banana densities (kg/m^3) and M^{p+1}_n is the moisture contents at pore junctions.

3.2. Mass balance in the network

To determine the moisture contents at the pore junctions for the inner pores of the network, the mass balance of moisture content at the inner nodes of network was made, assuming no accumulation of moisture at each pore junction within the network, which is thus expressed by:

$$\sum_{\{u,v\}} Q_{r_{ij}} = 0 \tag{13}$$

where sum is over all the pores, $r_{i,j}$, that connected to the pore junction (u,v), and u,v are the coordinate for a pore junction in the network. Substituting Eq. (12) into Eq. (13) and solve it for the moisture contents at the pore junctions. After the moisture contents at nodes of the network were known, the average moisture content $\overline{M}_{network}$ of network can then be calculated using the following equation:

$$\overline{M}(t)_{netwotk} = \frac{\sum_{n=1}^{Z} r^2_{ij}\int_0^L M_{r_{ij}}(x,t)dx}{Z \cdot L\sum_{n=1}^{Z} r^2_{ij}} \tag{14}$$

where Z is number of pores in the network. To estimate the pore diffusion coefficient, D_p, the optimization technique using a golden-search method was used. The root mean square error (RMSE) for the residuals of the measured and predicted values of average moisture content was set as the objective function with a tolerance of 10^{-5}. The RMSE is defined as:

$$RMSE = \left[\frac{1}{K}\sum_{n=1}^{K}(M(t)_{exp} - \overline{M}(t)_{network})^2\right]^{1/2} \tag{15}$$

where $M(t)_{exp}$ is the experimental moisture content of material at time t, $\overline{M}(t)_{network}$ is the predicted moisture content, and K is the number of the experimental data. The lower the value of RMSE, the better the goodness of fit. All computations were implemented using Intel C++ Compiler (Intel® Software Network, 2009) and run on a PC compatible with 3.0 GHz dual-processor and 2 GB of RAM.

4. Results and discussion

4.1. Effects of temperature and relative humidity

Figs. 2 and 3 show the effects of temperature and relative humidity on the adsorption rate, respectively. As observed from the experimental results, the rate of moisture uptake was very fast during the early period of time and gradually decreased as the moisture content approached the moisture equilibrium. The higher adsorption rate was clearly evident when the temperature and relative humidity increased.

At the equilibrium state, the equilibrium moisture content tended to decrease with increasing temperature; these values were 0.1384, 0.1368 and 0.1308 kg/kg d.b. for the corresponding temperatures of 35, 40 and 45 °C and respective humidities of 50%, 48% and 47% as shown in Fig. 2. The decrease of equilibrium moisture content with temperature can be attributed to the excitation states of water molecules. At elevated temperature, the water molecules are in higher states of excitation, thus increasing their distance apart and, in turn, decreasing the attractive forces between them (Jamali et al., 2006). The experimental results found in this study were similar to those reported by Kim and Okos (1999) and Palou et al. (1997). In their works, the sorption capacity or equilibrium moisture content of crackers and cookies decreased with increasing temperature.

4.2. Effect of foam densities

Fig. 4 shows the moisture adsorption kinetics at temperature of 45 °C for the banana foam densities of 0.21 and 0.26 g/cm^3. It can be seen that the foam density strongly affects the moisture adsorption rate; the lower the foam density, the faster the adsorption rate. The different moisture adsorption rates are due to the fact that the void area fractions of both banana foam samples were different; the void area fractions of the banana foam densities of 0.21 and 0.26 g/cm^3 were 31% and 26%, respectively.

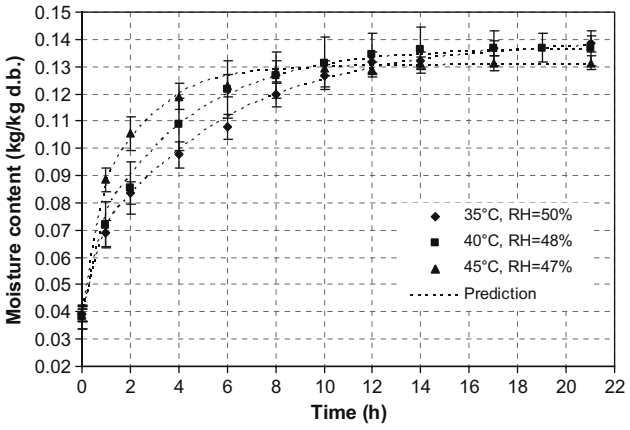

Fig. 2. Kinetics data of moisture adsorption at different temperatures and relative humidities for the foam density of 0.21 g/cm^3.

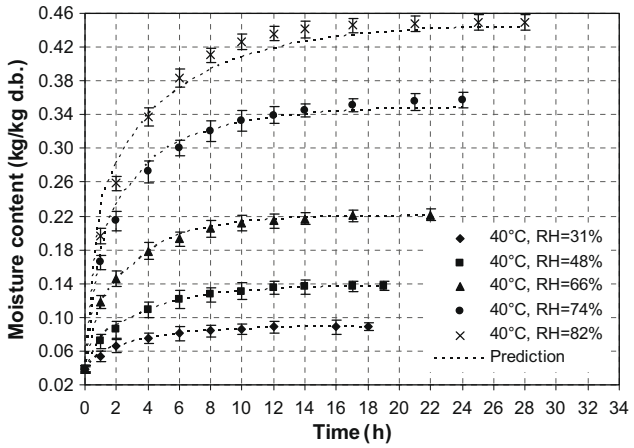

Fig. 3. Kinetics data of moisture adsorption at 40 °C and relative humidities of 31%, 48%, 66%, 74% and 82% for the foam density of 0.21 g/cm^3.

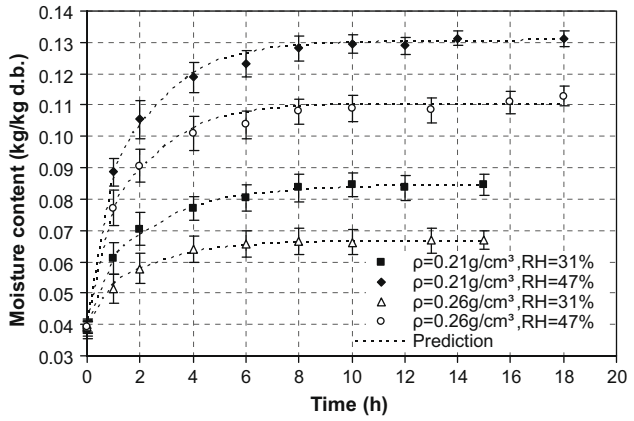

Fig. 4. Moisture adsorption kinetics at 45 °C and relative humidities of 31% and 47% for the banana foam densities of 0.21 and 0.26 g/cm^3.

High porosity in porous foods provides less diffusional flux resistance and thus greatly facilitates the moisture transport to those porous foods. In the porous banana foam studied, the higher void area fraction for the banana foam density of 0.21 g/cm^3 was a result of the assembly of the giant pores with sizes larger than 150 μm which had a larger number (38%) than that at the foam density of 0.26 g/cm^3 as will be seen in Fig. 6. These huge pores, serving as a massive transport of moisture through the interior pores, may possibly be interconnected into almost all parts of the whole network. Hence, the rapid moisture adsorption is obviously evident in the foam density of 0.21 g/cm^3.

The efficient communication of large pores in the network provided not only faster adsorption, but also faster drying. Prachayawarakorn et al. (2008) studied the effect of pore assembly architecture on the drying rate and found that different arrangements of pores exhibited different drying rates. When the large pores are positioned at the network exterior and the smaller pores assigned to the interior, the drying rate is remarkably faster in such a network archetype than in the network, with smaller pores allocated on the network exterior.

As shown in Fig. 4, the moisture uptakes of the banana foams after the elapsed time of 10 h vary slightly and this indicated that the system reaches the equilibrium state. At the equilibrium, the moisture content of banana foam at density of 0.21 g/cm^3 was apparently higher than that at 0.26 g/cm^3 due to higher porosity.

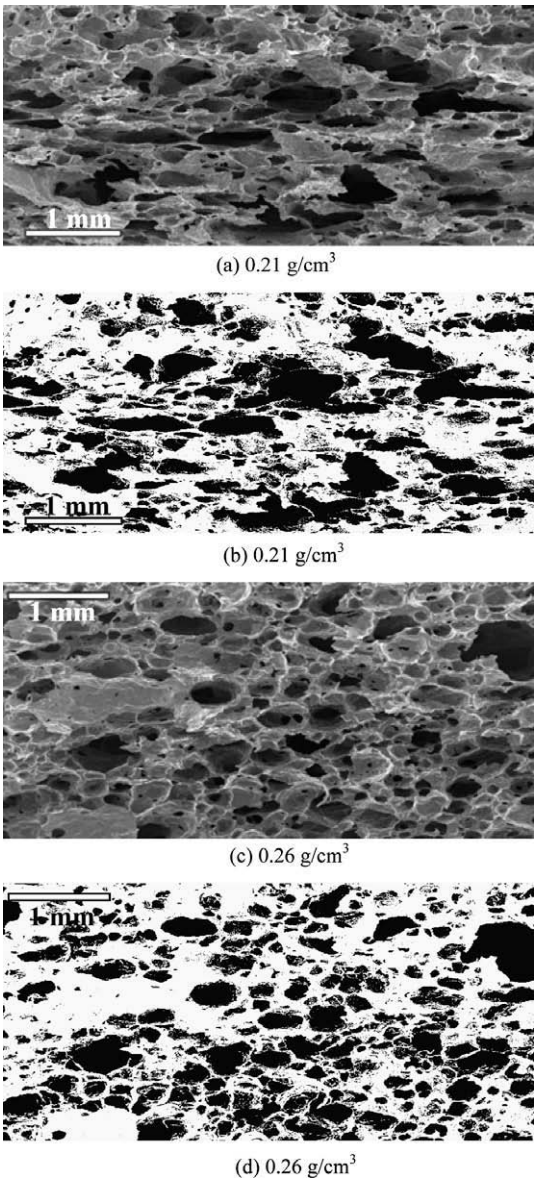

Fig. 5. (a and c) SEM micrographs of dried banana foam mats at different initial foam densities and binary images (b and d).

4.3. Pore size distribution

The microstructures of dried banana foam mats characterized by SEM are shown in Figs. 5a and c for several foam densities. The corresponding binary images are illustrated in Figs. 5b and d. The reconstructed porous structures of the banana foams in binary image reasonably represented their original images. The pores in the banana foam were random in sizes, irregular in shape and interconnected. This pore structure results in the movement of moisture into the interior; some pores may have high or low moisture content even though the pores are positioned at the same horizontal plane. Such moisture transport behavior cannot be formulated through a continuum model since the model did not take the pore structure effect into account.

Fig. 6 shows the pore size distributions of the dried banana foams at the densities of 0.21 and 0.26 g/cm^3, both distributions obtained from the binary image of SEM. The sample with a foam density of 0.21 g/cm^3 had small pore assembly in the range 6 to 150 μm accounting for 62% of the whole number of pores and for 38% with the pores larger than 150 μm. For the density of 0.26 g/

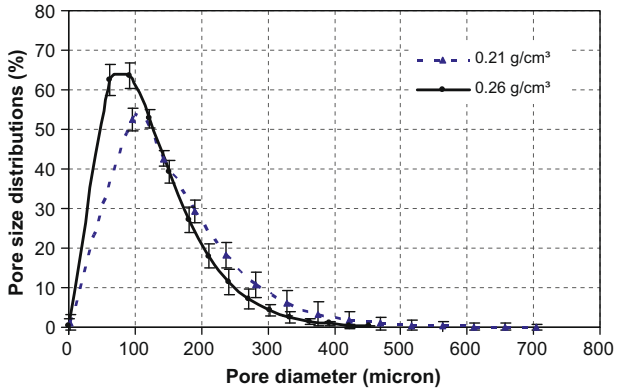

Fig. 6. Pore size distributions of dried banana foam at different densities.

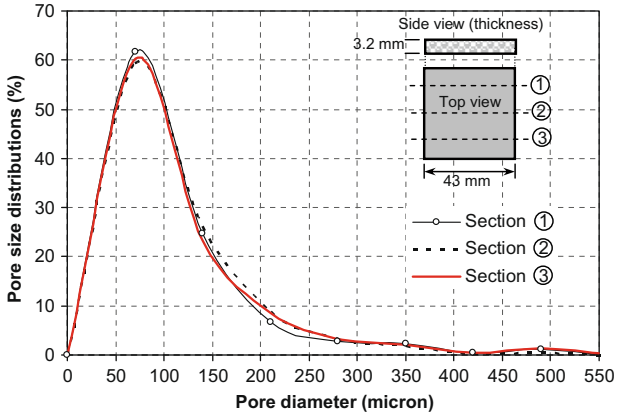

Fig. 7. Pore diameter distributions at different cross-section areas of a banana foam mat (foam density of 0.26 g/cm^3).

cm^3, it appears the proportion of small pores accounting for 71% which was higher than that of the sample at the density of 0.21 g/cm^3. However, the porosity of sample at the density of 0.26 g/cm^3 was relatively smaller because the large pores had a smaller number.

Fig. 7 shows the pore size distributions at three cross-sectional areas of a banana foam mat at the density of 0.26 g/cm^3. A sample was divided into three parts and each part was morphologically characterized by SEM. It indicated that the characteristics of pore size distribution were identical throughout the sample and this may reasonably be assumed that the moisture distributions at any cross-sectional area of sample were not different. Hence, the average moisture content at any cross-sectional area of sample can represent the moisture data of sample.

4.4. Moisture diffusivity in pores

The values of pore diffusivity for two banana foam densities at different temperatures and relative humidities are shown in Table 1 and the results also show in Fig. 8. At a given temperature, most values of moisture diffusion coefficient, except for the value at the relative humidity higher than 70%, presented only a slight change with the relative humidity. These values, when analyzed statistically using Duncan's test, showed an insignificant difference. The mean values of pore diffusivity were in the order of 10^{-9} m^2/s. In fact, the orders of magnitude of the diffusion coefficients depend on the state of substance: for gases, approximately 10^{-5} m^2/s; for liquids, approximately 10^{-9} m^2/s (Aguilera and Stanley, 1999). From this information, it might be indicated that the transport of moisture through the banana foam mat is similar to liquid. Roca et al. (2006) also reported that the adsorption of water vapour in sponge cake occurred mainly in the liquid form.

Table 1
Estimated pore diffusivity for two banana foam densities at different adsorption conditions with R^2-values above 0.96.

T(°C)	Approximate RH (%)	ρ (g/cm^3)	
		0.21	0.26
		Pore diffusivity $\times 10^{-9}$ *(m^2/s)*	
35	32	2.276 ± 0.231	2.072 ± 0.193
	50	2.304 ± 0.211	2.149 ± 0.238
	67	2.204 ± 0.185	1.990 ± 0.183
	75	1.941 ± 0.219	1.686 ± 0.241
	83	1.747 ± 0.166	1.544 ± 0.227
40	31	3.152 ± 0.182	2.906 ± 0.236
	48	3.210 ± 0.275	3.084 ± 0.179
	66	3.350 ± 0.231	3.112 ± 0.233
	74	2.922 ± 0.191	2.678 ± 0.164
	82	2.680 ± 0.179	2.464 ± 0.166
45	31	4.602 ± 0.190	4.334 ± 0.190
	46	4.961 ± 0.214	4.538 ± 0.211
	65	5.053 ± 0.188	4.623 ± 0.265
	74	4.255 ± 0.227	4.139 ± 0.191
	81	4.015 ± 0.162	3.794 ± 0.150

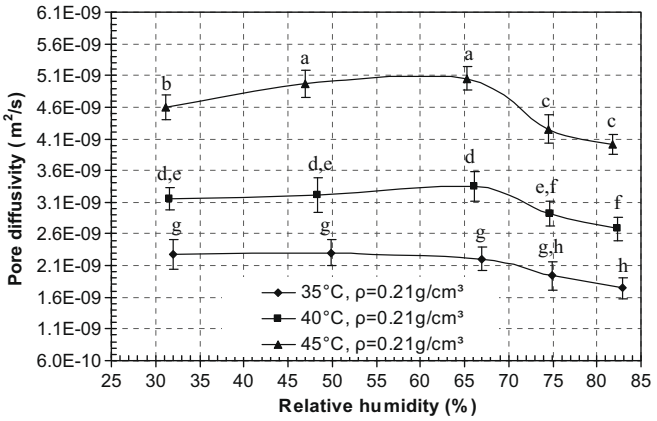

Fig. 8. Effects of temperatures and relative humidities on the pore diffusivities for the banana foam density of 0.21 g/cm^3: the same letter means insignificant difference at P>0.05.

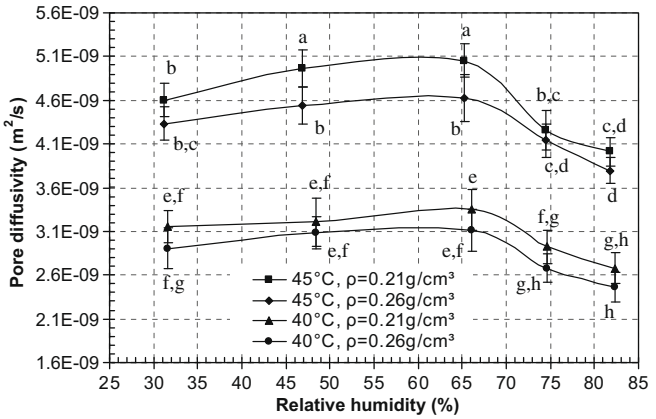

Fig. 9. Effect of initial foam densities on the pore diffusivities at different relative humidities and temperatures of 40 and 45 °C: the same letter means insignificant difference at P>0.05.

Table 2
Constant parameters in Eq. (3) for D_{eff} of banana foam at two foam densities.

Foam density (g/cm^3)	Constant parameters		R^2-value
	D_0 (m^2/s)	E_a (kJ/mol)	
0.21	488.94	74.00	0.98
0.26	148.39	71.68	0.98

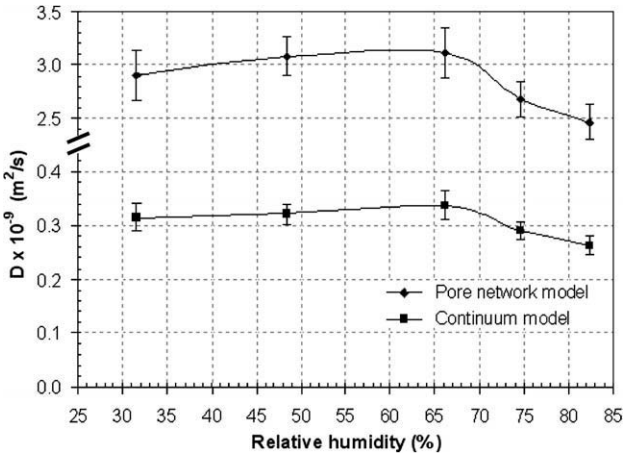

Fig. 10. Comparison between pore diffusivities and effective diffusivities of banana foam mat at 40 °C and relative humidities for foam density of 0.26 g/cm^3.

Moreover, the pore diffusivity determined by stochastic pore network is much closed to the water self-diffusion coefficient for all temperature range studied. For example, the moisture diffusion coefficient found in this study was $(3.06 \pm 0.27) \times 10^{-9}$ m^2/s at temperature of 40 °C and the water self-diffusion coefficient for pure liquid water was 3.222×10^{-9} m^2/s (Holz et al., 2000). In their work, they measured the water self-diffusion coefficient by using pulsed gradient NMR spin-echo technique. These results implied that transport of moisture during adsorption condition can reasonably be described by molecular diffusion equation.

Once the relative humidity was higher than 70%, however, the pore diffusivity relatively decreased with increase in the relative humidity. At this relative humidity range, the banana foam mat could adsorb a large amount of moisture. Subsequently, the sample was softened and shrunk due to the collapse of pores. This may cause the decrease of moisture diffusion coefficient as shown in Fig. 8. From the statistical analysis, it indicated that the moisture diffusion coefficient at a given temperature was significantly different to those values determined from the relative humidity below 70%.

Fig. 8 also presents the effect temperature on pore diffusivity. As expected, the pore diffusivity significantly increased with increase in temperature ($P < 0.05$).

4.5. Effect of foam densities on diffusion coefficient

Fig. 9 shows the diffusivity of moisture in pores for the samples at the foam densities of 0.21 and 0.26 g/cm^3. The pore diffusivity was slightly lower at the foam density of 0.26 g/cm^3 than at the density of 0.21 g/cm^3 for all experimental conditions. However, the statistical analysis of these pore diffusivity data showed the insignificant difference among the two foam densities.

4.6. Comparison of pore diffusion coefficient and effective diffusion coefficient

Fig. 10 shows the comparison of the pore diffusivity and the effective diffusivity. The value of effective diffusion coefficient was determined using Eq. (1) assuming that the moisture migration occurred in one dimension and the water vapour transported from the air to the top surface by convection. It can be seen that the effective moisture diffusivity was approximately 3.3×10^{-10} m^2/s at the temperature of 40 °C and relative humidity in the range of 30–70%. The calculated value was approximately 9 times lower than the diffusivity of moisture in pores.

4.7. Activation energy of pore diffusivity

From the statistical fitting, the Arrhenius equation can suitably describe the relationship between moisture diffusion coefficient in pores and temperature as indicated by R^2 value of 0.97. The values of E_a and D_0 were 64.7 kJ/mol and 193.91 m^2/s, respectively. However, if the effective moisture diffusion coefficient was used to correlate with temperature, the fitting results of E_a and D_0 for the effective diffusivity of moisture are shown in Table 2 for two foam

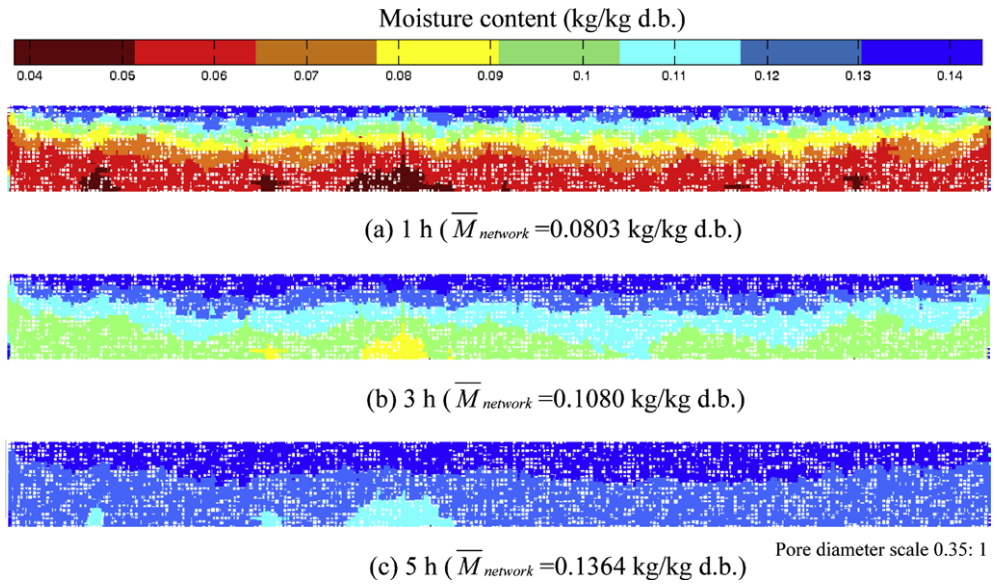

Fig. 11. Visualization of moisture contents in pores of banana foam at temperature of 35 °C, initial foam density of 0.21 g/cm^3 and relative humidity of 50%.

densities. The value of the activation energy determined from the pore diffusivity data was relatively lower than the case of using the effective moisture diffusivity data.

4.8. Validation

As previously shown in Figs. 2 and 3, the pore network model showed a good fit to the experimental data throughout the exposure time, with R^2-values above 0.98 at the relative humidity below 67%. Beyond 67%, however, the accuracy of prediction was slightly smaller (R^2-values varying between 0.96 and 0.97); the model predicted the change of moisture content of sample relatively faster than the experiment at the early exposure time and became relatively slower afterwards.

4.9. Graphical visualization

Fig. 11 shows the moisture distribution in 2-D pore network during adsorption process. Each pore was colored according to the moisture content. The representative colours with 8 shades from red to blue were used for the corresponding range of moisture from 0.038 to 0.138 kg/kg d.b.

At the beginning, every pore within the network presumably contained the moisture content of 0.038 kg/kg d.b. When the sample was subject to adsorption condition, the capability of moisture diffusing through the pores positioned at the same horizontal plane was different, reflecting the pore shielding effect (Mann, 1993). This can be seen easily at the exposure time of 3 h; some pores located near the bottom surface of the pore network have moisture content of 0.08–0.09 kg/kg d.b. as indicated by yellow colour whilst the other pores were coloured by green corresponding to the moisture contents of 0.095–0.105 kg/kg d.b. The yellow-coloured pore assembly had a size relatively larger than the surrounding nearby pores. Hence, the moisture diffusing through those large pores is restricted by the smaller ones since the cross-sectional area available for moisture diffusion is reduced in the surrounding nearby small pores.

5. Conclusions

A 2-D stochastic pore network has been developed to represent the pore structure of banana foam and the transport of moisture in the pores of the network was described by Fick's second law. The optimization technique with a golden-search method was used to determine the diffusivity of moisture in the pores of banana foam. The experimental results showed that the pore network model could describe the moisture migration inside the banana foam relatively well. The pore diffusivity was not changed with the relative humidity, except for the case of relative humidity higher than 70% at which the value of moisture diffusion had a decreasing trend. The actual moisture diffusion coefficient in pore voids determined from this work may be applied to other porous foods. Moisture in void spaces and interaction between layers of banana foam mat was visualized using colour codes.

Acknowledgments

The authors would like to express their appreciation to the Commission on Higher Education, Thailand for supporting by grant fund under the program Strategic Scholarships for Frontier Research Network for the Ph.D. Program Thai Doctoral degree for this research. This work was also supported in part by the Thailand Research Fund and King Mongkut's University of Technology Thonburi.

References

Aguilera, J.M., Stanley, D.W., 1999. Microstructure and Mass Transfer: Solid–liquid Extraction. Microstructural Principles of Food Processing and Engineering. Aspen Publishers, Gaithersburg, MD. p. 329.

AOAC, 1995. Official Methods of Analysis, 16th ed. Association of Official Agricultural Chemists, Washington, DC.

Androutsopoulos, G.P., Mann, R., 1979. Evaluation of mercury porosimeter experiments using a network pore structure model. Chemical Engineering Science 34, 1203–1212.

Blunt, M., 2001. Flow in porous media-pore-network models and multiphase flow. Current Opinion in Colloid & Interface Science 6, 197–207.

Chen, X.D., 2007. Moisture diffusivity in food and biological materials. Drying Technology 25, 1203–1213.

Efremov, G., Kudra, T., 2004. Calculation of the effective diffusion coefficients by applying a quasi-stationary equation for drying kinetics. Drying Technology 22, 2273–2279.

Guillard, V., Broyart, B., Bonazzi, C., Guilbert, S., Gontard, N., 2003. Moisture diffusivity in sponge-cake as related to porous structure evaluation and moisture content. Journal of Food Science 68, 555–562.

Hollewand, M.P., Gladden, L.F., 1992. Modeling of diffusion and reaction in porous catalysts using a random three-dimensional network model. Chemical Engineering Science 47, 1761–1770.

Holz, M., Heli, S.R., Sacco, A., 2000. Temperature-dependent self-diffusion coefficients of water and six selected molecular liquids for calibration in accurate ^{1}H NMR PFG measurements. Physical Chemistry Chemical Physics 2, 4740–4742.

Intel® Software Network. (2009). Available at: http://software.intel.com/en-us/articles/intel-c-compiler-professional-edition-for-windows-evaluation/.

Jamali, A., Kouhila, M., Mohamed, L.A., Idlimam, A., Lamharrar, A., 2006. Moisture adsorption–desorption isotherms of citrus reticulate leaves at three temperatures. Journal of Food Engineering 77, 71–78.

Kaya, S., Kahyaoglu, T., 2005. Thermodynamic properties and sorption equilibrium of pestil (grape leather). Journal of Food Engineering 71, 200–207.

Kim, M.K., Okos, M.R., 1999. Some physical, mechanical, and transport properties of crackers related to checking phenomenon. Journal of Food Engineering 40, 189–198.

Mann, R., 1993. Developments in chemical reaction engineering: issues relation to particle pore structures and porous materials. Chemical Engineering Research and Design 71, 551–562.

Palou, E., Lopez-Malo, A., Argiz, A., 1997. Effect of temperature on the moisture sorption isotherms of some cookies and corn snacks. Journal of Food Engineering 31, 85–93.

Prachayawarakorn, S., Prakotmak, P., Sopornronnarit, S., 2008. Effect of pore size distribution and pore-architecture assembly on drying characteristics of pore networks. International Journal of Heat and Mass Transfer 51, 344–352.

Roca, E., Guillard, V., Guilbert, S., Gontard, N., 2006. Moisture migration in a cereal composite food at high water activity: Effects of initial porosity and fat content. Journal of Cereal Science 43, 144–151.

Saravacos, G.D., Maroulis, Z.B., 2001. Transport of Water in Food Materials. Transport Properties of Foods.. Marcel Dekker, New York. p. 128.

Segura, L.A., Toledo, P.G., 2005. Pore-level modeling of isothermal drying of pore networks: Effects of gravity and pore shape and size distributions on saturation and transport parameters. Chemical Engineering Journal 111, 237–252.

Thuwapanichayanan, R., 2007. Drying of foam-mat ripe banana using tray dryer. PhD Thesis, King Mongkut's University of Technology Thonburi, Thailand.

Thuwapanichayanan, R., Prachayawarakorn, S., Sopornronnarit, S., 2008a. Drying characteristics and quality of banana foam mat. Journal of Food Engineering 86, 573–583.

Thuwapanichayanan, R., Prachayawarakorn, S., Sopornronnarit, S., 2008b. Modeling of diffusion with shrinkage and quality investigation of banana foam mat drying. Drying Technology 26, 1326–1333.

Yiotis, A.G., Stubos, A.K., Boudouvis, A.G., Tsimapanogiannis, I.N., Yortsos, Y.C., 2005. Pore-network modeling of isothermal drying in porous media. Transport in Porous Media 58, 63–86.

Effects of Osmotic Treatment and Puffing Superheated Steam Temperature on Drying Characteristics and Texture Properties of Banana Slices

S. Tabtiang[1] , S. Prachayawarakon[2] S. and Soponronnarit[1]

[1]Energy Technology Division, School of Energy Environment and Materials, King Mongkut's University of Technology Thonburi, Suksawat 48 Road, Tungkru, Bangkok 10140, Thailand

[2]Faculty of Engineering, King Mongkut's University of Technology Thonburi, Suksawat 48 Road, Tungkru, Bangkok 10140, Thailand

[*]Corresponding author: somkiat.pra@kmutt.ac.th

ABSTRACT

Porous structure as an important characteristic of crisp food can be produced alternatively by puffing process. However, the color of puffed product may have intense brown. To limit the brown reaction, the banana slice needs to be treated osmotically before puffing. This research was therefore to study on the effect of osmotic treatment on quality of puffed banana. The banana with 20-23°Brix total soluble solid was immersed into sucrose solution concentrations at 30, 35 and 40°Brix and dried at 90°C using hot air until the sample moisture content reduced to 30% dry basis (d.b.). After that, the banana slices were puffed by superheated steam at 180, 200 and 220°C for 150 s and dried again at 90°C until the sample moisture content reached 4% d.b. From the experimental results, it was found that the osmotic dehydration could improve the color of banana. The

puffed osmotic banana was less brown than the puffed non osmotic banana as indicated by the L-, a- and b- values and hue angle. The puffing temperature and osmotic concentrations did not enhance the browning rate. The sucrose impregnation for the osmotic banana caused longer drying time than for the non osmotic one and limited the banana cell wall expansion, resulting in the significantly higher shrinkage of osmotic sample and the less porous structure as viewed by scanning electron microscope. Such morphology of osmotic banana directly affected the texture properties in terms of hardness, initial slope and number of peaks.

Keywords: Color, Drying, Osmotic dehydration, Snack, Texture

INTRODUCTION

Bananas deteriorate rapidly after harvest. To reduce their losses, bananas are processed to various kinds of product such as fried banana, osmotic banana and puree banana. The fried banana chips, one of the most popular products, possess crispy texture[1,2] and it can serve as a snack food.[3] However, the fried product contains high oil content and can not be kept for an extended period of time due to possible lipid oxidation leading to rancidity. Hence the free oil crisp banana is an alternative product. The free oil crisp banana may also be received more attention to the conscious consumers. The free oil banana can be produced by drying method. To obtain the crisp texture, the food material requires high porosity. There are several drying techniques for producing high porous food material such as high temperature and short time drying,[4,5] microwave drying,[6,7] and low pressure superheated steam drying.[8,9] In this work, the high temperature and short time drying technique or puffing technique was interested. The operating cost of this puffing technique is rather economics as compared to the other methods.

During puffing process, food is subject to high temperature for a short period of time, which allows some amounts of moisture inside the food vaporizing suddenly. The internal vapor pressure can thus be increased and this forces the food structure to be expanded, thereby producing the porous structure of food products. Porous structure and thickness of solid between pores generated by puffing process strongly affect the properties of puffed products such as bulk density and texture.[4,10] In addition, the puffing process can save drying time[4,11]

and provide 40% energy saving as compared to the conventional hot air dehydration.[11]

The puffing or heating medium normally uses the hot air since it is convenient in practice. Recently, several works have been reported that the superheated steam provides more efficient heat transfer rate than the hot air.[12,13] Also, during superheated steam drying steam condensation at the material surface is taken place and this releases the latent heat from the phase change which results in the rapid rise in material temperature to stay at the boiling point temperature of water.[14] From such previous works, it is expected that using superheated steam may increase rapidly vapor pressure inside the product and provides a high expansion of product accordingly. However, up to now, the application of superheated steam for puffing and its effect on the crispiness has not been fully studied. Saca and Lozano[4] studied the puffing of banana using superheated steam at temperature of 152-175°C and steam pressure of 7.84×10^4-27.45×10^4 Pa. It was found that the superheated steam puffed banana had higher porosity than the conventional air dried product, but the product color was browner and this might not be favored by the consumers. Such browning in food is caused by the non-enzymatic browning reactions and pigment degradations.

One way of improving color of product can be done by osmotic pretreatment. During osmosis the natural solutes existing in food material such as reducing sugar, acid and minerals flow out from food during osmotic dehydration[15,16] and those solutes are replaced by osmotic agent. Sucrose is frequently used as osmotic agent.[17-19] The decrease of reducing sugars i.e. glucose and fructose in the osmotic product can limit brown color development

because these monosaccharide are more reactive for the brown reactions than the sucrose.[20] The food pretreated with sucrose solution before drying can also reduce shrinkage during thermal processing. Many researchers have studied the effect of sugar on shrinkage properties of puffed products i.e. rice and corn,[21,22] and found that the puffed osmotic products were lower shrinkage than non osmotic ones.

As mentioned-above, the osmotic dehydration of banana before puffing may help to improve the color of puffed product, but the information of effect of osmotic pretreatment on chemical and physical qualities of puffed product has been limited. The objective of this work was therefore to study the effects osmotic solution concentrations and puffing conditions on the drying characteristics and quality of puffed banana. The quality parameters were considered in terms of color, shrinkage and texture properties.

MATERIALS AND METHODS

Material Preparation

Fresh bananas were obtained from local market and their soluble solid contents were given in the range of 20-23°Brix. Before processing, the banana was sliced into 3.5 mm thickness and blanched by hot water at 95°C for 1 min. Blanching increased the plasticity of food material which allows the samples to expand during puffing.[23] Also, blanching decreased the permeability of water vapor and this obstructed the transport of moisture inside the bananas when it vaporized during puffing step. This resulted in the increasing vapor pressure

inside the banana samples and the corresponding expansion of the walls of the material.

Osmotic Treatment

Osmotic solution was prepared using commercial sucrose with concentrations of 30, 35 and 40°Brix. The banana slices were immersed into various sucrose solution concentrations and the mass ratio of osmotic media to the sample was about 30:1 to avoid the dilution effect. The samples were immersed into the osmotic solution until the banana moisture content was not changed.

Puffing Method

Process for producing crispy banana used in this study was consisted of 3 main steps. In the first step, the banana was dried by a hot air tray dryer to certain level, puffed by a superheated steam tray dryer and dried by the hot air tray dryer again. From the preliminary study, it was found that the banana moisture content before puffing and the puffing time were less affected on the volume expansion than the puffing temperature. In addition, the intermediate moisture content of sample of 30% dry basis (d.b.) and puffing time for 150 s were suitable for puffing banana. Before puffing, the banana was dried at 90°C to the recommended moisture content. Drying banana at this temperature did not form the brown color.[24] After reducing moisture content to 30% d.b., the osmotic banana was puffed at temperatures of 180, 200 and 220°C for 150 s and dried by hot air again at the same temperature as the first stage drying. The final moisture content required at 4% d.b. At the end of each experiment, the moisture content of

140 samples was determined by drying them in the oven at 103°C for 3 h. The
141 moisture content determined by this method was closed to the vacuum oven
142 method 934.06 (AOAC, 1995)[25] as reported by Thuwapanichayanan et al.[26]

143

144 **Texture Property Evaluation**.

145 The puffed banana slices were kept in aluminium foil bag at room
146 temperature for 3 days before texture test. The banana samples were measured by
147 the texture analyzer (Stable Micro System, TA. XT. Plus, UK) with a 5 N load
148 cell. The samples were fractured by a cutting probe (HDP-BSK type) at a constant
149 crosshead speed of 2 mm/s. The maximum compressive force, the initial slope and
150 the number of peaks from force deformation curve were considered as hardness,
151 stiffness and crispness, respectively. The number of peak was counted when the
152 peak was higher than the threshold value which was set at 30 g.

153 **Color Evaluation**

154 The color of dried samples was measured using a colorimeter (Hunter Lab,
155 ColorFlex, UK). The color of a banana sample was measured on the banana
156 surface at six different positions and the average value was reported. Twenty
157 banana samples were used to represent the color of sample lot from an
158 experimental condition. The color was expressed as L-value (Brightness), a-value
159 (redness/greenness) and b-value (yellowness/blueness). The overall color of dried
160 banana sample was presented by hue angle (°h) which is calculated by
161 $h^o = \tan^{-1}(b/a)$ .The angle at 0°, 60°, 120°, 180° and 240° corresponds to red,

yellow, green, cyan and blue colors, respectively. The color was calibrated with a standard white plate (L*=96.98, a*=0.03 and b*=1.84).

Shrinkage Determination

Twenty samples were used to determine shrinkage. The volume of each sample was determined by the volumetric displacement method using n-heptane as the replacement medium.[4] The shrinkage was defined as the ratio of the dried sample volume to the original sample volume

$$\% \text{ shrinkage} = \frac{V}{V_i} \times 100$$

where V_i and V are the volume of the fresh sample and the volume of dried sample.

Glucose, Fructose and Sucrose Determination

Determination of sugar content was performed according to AOAC method 982.14 (1995)[25] with some modification. 5-10 g sample was pulverized and mixed with 50 mL water in a 100 mL volumetric flask. 1 mL 15% $K_4(Fe(CN_6))\bullet 3H_2O$ and 1 mL 30% $ZnSO_4\bullet 7H_2O$ was added into the solution in order to extract protein. After that, it was filtered through filter paper No. 42. The filtered solution from the last step was filtered again through 0.45 μm nylon syringe filter. The final volume of the filtered solution was kept in refrigerator until chromatographic analysis. The 10 μL aliquots of the filtered solution were injected into High Performanace Liquid Chromatography (HPLC). The HPLC consists of a Prevail Carbohydrate ES column (4.6 mm, 25 cm; 5μm) (Alltech,

Derfield, USA), a pump and a controller (Agilent, 1100, USA), autosampler (Agilent, 1100, USA) and a evaporative light scattering detector (ELSD detector) (Alltech , 500 ELSD, USA).

The fructose and glucose present in the banana can clearly be separated by gradient elution.[27] Acetonitrile and water was used as mobile phase and flowed through the column at 1 mL/min. The column temperature was kept at 30°C, the detector was controlled at drift tube temperature of 50°C. Nitrogen flowed through the column with a rate of 1.5 L/min. Peaks of samples were quantified with standard.

Statistical Analysis

The experimental data of color, texture properties and shrinkage was analyzed by an analysis of variance (ANOVA) to indicate how operating conditions affected those qualities. Duncan's test was used to establish the multiple comparisons of the mean values. The mean values were considered significantly different when p-value ≤ 0.05

RESULTS AND DISCUSSION

Effect of Osmotic Concentrations on Water Loss and Solid Gain

Table 1 shows the moisture loss, solid gain and the losses of native sugars of banana slices immersed in sucrose solutions at 30, 35 and 40°Brix. The banana slices immersed into the higher sucrose concentrations lost the larger amounts of their moisture content. The possible explanation in this case related to the osmotic pressure difference between intracellular fluid in banana and osmotic solution. When the banana sample was immersed into the higher sucrose concentration, the osmotic pressure difference increased, resulting in the larger loss of moisture content. Although the larger amount of moisture lost, the solid gain also increased. The increase of solid gain is caused by the diffusion of sucrose from the solution into the sample. From the experimental results, it was found that the ratios of water loss to solid gain increased with the increased sucrose solution concentrations, implying loss of moisture content larger than the solid gain. This is because the size of sucrose molecule is larger than that of water molecules.[18,28] Hence, the water molecule can move with a rate faster than the sucrose molecule.

Table 1 also shows that the native sugars i.e. glucose and fructose disappeared during osmosis. The remaining amounts of glucose and fructose in samples immersed into the sucrose solution concentrations were not rather different; the percent looses were 84-86% for glucose and 83-85% for fructose. From these results, it indicated that the losses of glucose and fructose were nearly the same amount. This can be described by the fact that the glucose and fructose have the same molecular weight and this would be expected to have the same diffusion coefficient. Gekas et al.[29] reported that the diffusion coefficients of glucose and fructose in water at 25°C were equal and had a value of 69×10^{-11} m^2/s.

Effect of Osmotic Solution Concentration and Puffing Temperature on Drying Characteristics

Fig. 1 illustrates the changes of moisture contents of the osmotic banana slices during the processing steps consisting of drying and puffing. The osmotic samples obtained from the sucrose solution concentrations of 30, 35 and 40°Brixs and puffing temperature of 200°C were demonstrated. It can be seen that the changes of moisture content did not showed a smooth curve throughout the entire process. The decrease of moisture content showed an exponential decay in the first stage drying, followed a rapid decrease during puffing stage and stayed on the exponential curve again at the last drying step. The abrupt change of moisture content during puffing step is due to the fact that the sample was subject to high temperature and this enhanced the diffusion of moisture through the banana tissue.

From these drying curve results, it indicated that the drying time was spent mostly in the last drying stage where the sample moisture content was rather low, yielding the low rate of drying. Acceleration in drying rate for the last drying stage using higher temperature of 90°C was not appropriate since the moisture content of banana was rather low and this led to a rapid rise in sample temperature, which induces the brown pigment formation.[30]

Fig 2 shows the drying rates of osmotic and non osmotic samples at the last stage drying. The samples were puffed at the superheated steam temperature of 200°C. The drying rate was relatively lower in osmotic sample than in the sample without osmotic. This is because the solid gain in the osmotic sample increases the internal resistance to water movement during drying.[10,19]

Fig. 3 shows the effects of sucrose solution concentrations and puffing temperatures on total drying time. The lower puffing temperature and higher concentration of sucrose solution provided the longer drying time. During puffing, the moisture content of sample was decreased faster at higher puffing temperature and this resulted further in the drying of banana at the final stage which took a shorter drying time for the sample puffed at higher temperature. In addition, the banana samples had a higher porosity when puffed at higher temperature, which could facilitate the movement of moisture.

When comparing the total drying time between osmotic and non osmotic bananas, it was found that the time required to reach the final moisture content for the osmotic samples was taken longer. In addition, the required drying time increased significantly as the sucrose solution concentration increased. The longer

277 drying time for the osmotic banana can be explained by a couple of reasons. The
278 osmotic samples possess the lower porous structure as will be seen in Fig. 6. Also,
279 the sucrose diffusing into the banana slice is bounded with moisture present at
280 banana tissue and this binding resulted in the low drying rate as already seen in
281 Fig. 2.[10,19]

282 **Color**

283 Table 2 shows the effect of the puffing temperatures and sucrose solution
284 concentrations on the color of the bananas slices in terms of lightness (L), redness
285 (a) and yellowness (b) and overall color. The change of color parameters during
286 puffing is related to the browning reactions where a decrease in L value, an
287 increase in a value and a decrease in hue angle indicate more browning.[31,32] The
288 color of the non osmotic product was rather brown, in particular when it was
289 puffed at the temperature of 220°C which shows the intense brown as interpreted
290 by the °h value of 69° and L-value of 49.5.

291 When the banana was treated by sucrose solution before processing steps,
292 the product color was improved, with less brown. Both the L- and b-values were
293 higher and the a-value was lower as compared to the corresponding color
294 parameters for the non osmotic banana processed at the same puffing conditions
295 as that of the osmotic banana. The color improvement for the osmotic banana can
296 be explained by the fact that the monosaccharide serving as a main active
297 component for non-enzymatic browning reactions[33] leaches out during the
298 osmotic dehydration as previously shown in Table 1. Subsequently the browning
299 rate is retarded and results in less brown for the osmotic samples than the non
300 osmotic sample. As shown in Table 2, the osmotic agent concentrations seemed to

be not affect the osmotic product color, as indicated by L-, a- and b- values and hue angle, whether it was puffed at 180 or 220°C. The product color had brownish-yellow.

Shrinkage

Fig. 4 shows the shrinkages of non osmotic and osmotic samples, both puffed at temperatures of 180, 200 and 220°C. The volume ratio of osmotic banana samples was significantly lower than that of the non-osmotic ones for all puffing temperatures, indicating larger shrinkage for the osmotic product. These results can be explained by the fact that the OH group of n-$C_6H_{12}O_6$ in the solution may interact with OH group in the banana tissue by hydrogen bonding.[34] Their interactions resulted in stronger tissue of the osmotic banana and the resulting tissue may relatively rigid, which leads to more difficulty of expansion of banana during puffing and subsequently provides larger shrinkage. To confirm the explanation of the osmotic banana tissue rigidity, both osmotic and non osmotic samples after the first stage drying were taken to examine their microstructure and their microstructures were shown in Fig. 5, exhibiting the different morphological features of the osmotic and non osmotic samples. The cell walls of the osmotic banana, especially at 35 and 40°Brix, less disrupted, showing very porous structure, whilst most their cell walls were shrunk or disrupted for the non osmotic one.

From the microstructure result of osmotic banana, it might be expected that the osmotic banana should have a high volume expansion or a small shrinkage at the process end. The experimental result, however, shows that the degrees of volume ratio for the osmotic bananas at the puffing temperatures of

180-220°C were significantly lower than those of the sample without osmotic. The shrinkage of the osmotic banana was in between 54.9 and 67.5%, depending on puffing temperature and sucrose solution concentration. The explanation of the higher shrinkage of the osmotic sample is due to the fact that the tissue of banana after osmotic is strong and rigid, both factors limiting the expansion of cellular structure during puffing.

Considering the puffing temperature effect, the degrees of shrinkage for both osmotic and non osmotic banana samples were lesser at higher puffing temperature. However, the degree of shrinkage, when the puffing temperature increased, was noticeably smaller for the non osmotic sample than for the osmotic sample. As shown in Fig. 6, for example, the volume ratio of non osmotic samples was 82.6% at puffing temperature of 180°C and increased to 103.6% at the puffing of 220°C. In the case of osmotic samples with 40°Brix, the volume ratio was 62.6% at 180°C and 67.5% at 220°C.

Fig. 6 demonstrates morphologies of non osmotic banana and osmotic banana samples prepared from sucrose solution concentrations of 30, 35 and 40°Brix and puffed at temperature of 200°C. The morphologies of osmotic and non osmotic banana samples were noticeably different. The structure of osmotic banana samples was dense and exhibited less porous, but it was very porous for the non osmotic sample. As shown in Fig. 6 (a), the non osmotic banana had a huge pore with size larger than 1 mm. at the internal area of the sample. The formation of huge pore implies that there was a rapid vaporization of moisture inside the non osmotic samples during puffing, resulting in increasing vapor pressure inside the banana sample and the subsequent cell wall expansion.

However, the cell wall expansion was occurred rarely in the osmotic banana samples. From their morphologies, it confirmed the shrinkage results, showing the high shrinkage for the osmotic bananas and the small shrinkage for the non osmotic ones.

Texture

The force deformation curve presents the texture characteristics of product. The product that has many fracture points indicates a crispy characteristic[35] and the number of jags on the force deformation curves indicate the porosity in sample. Fig. 7 shows the force deformation curves of osmotic and non osmotic samples at the puffing temperatures of 180, 200 and 220°C. The force deformation curves of the osmotic samples were clearly different from those of the non osmotic ones. While the cutting probe was acted on the osmotic samples, the force reached the maximum point of 250-270 N. after which it was dropped sharply to zero, without any jag appearance. For the non osmotic samples, on the other hand, the force acting on the samples after reaching the maximum point did not drop rapidly to zero: it still appeared the several smaller peaks. From these force behavior, it can be explained by the fact that the sucrose solution causes banana tissue loosing the elasticity which in turn provides a sharp drop of force after the maximum point. These force characteristics indicated that the osmotic banana after puffing was brittle.

Fig. 8 shows the fracture works of osmotic samples and non osmotic samples at puffing temperatures of 180 200 and 220°C. It was found that the fracture works of osmotic samples had significantly higher than the non osmotic

ones. The increase of sucrose solution concentration let to increase of fracture work whilst the puffing temperature did not affect the work.

Fig. 9 shows the effects of sucrose concentrations and puffing temperatures on the textural properties of non osmotic and osmotic banana samples. Considering at each sucrose solution, the puffing temperature given in a range of 180-220°C insignificantly affect the textural properties such as hardness, number of peaks and initial slope. The insignificant effect of puffing temperature on the textural characteristics for the non osmotic banana samples was also observed. On the other hand, the sucrose concentration strongly affected such textural characteristics. Increase in both of hardness and initial slope and decrease in number of peaks were found with increasing sucrose solution concentration. As shown in Fig. 9, the banana slices pretreated with 40°Brix sucrose solution had the highest values of hardness and initial slope but the smallest number of peaks. Such textural characteristics revealed that the osmotic banana product after puffing had a harder texture, less crispy and rather brittle than the non osmotic one. The harder texture in the osmotic banana is related to the interaction between the OH-groups of banana tissue and sucrose solution[34] which will improve the cellulose strength. These results corresponded to the morphological features as already mentioned.

From the experimental results, it indicated that although the osmotic dehydration with sucrose could retard the browning of banana after puffing, but the texture of banana at the process end might not be favored by the consumers because of very hard and less crispy of the osmotic banana.

CONCLUSION

Osmotic pretreatment of banana slices with sucrose can retard the browning reactions and the subsequent product color was less brown than that of product without osmotic treatment. The color of osmotic products obtained at sucrose solution concentrations and puffing temperatures were not notably different. The color improvement of the osmotic banana was due to the fact that the monosaccharide existing in the banana and serving as reactive component to browning was leached out during osmotic whilst the gain in sucrose during osmotic did not enhance the browning rates. The sucrose diffusing into the banana allowed more difficulty of moisture travelling to the exterior surface, hence lengthening the drying time as compared to that of the non osmotic banana. In addition, the impregnation of sucrose caused the stronger tissue of banana. This caused the less expansion of banana during puffing, resulting in low porous structure of osmotic banana after puffing and corresponding poor texture of product i.e. high hardness and less crisp. The shrinkage was also higher for the osmotic banana than the banana without osmotic. The increase of sucrose solution yielded the harder texture and lesser extent of shrinkage. The range of puffing temperature used in this study could not improve the aforementioned qualities.

ACKNOWLEDGEMENTS

The authors express their sincere thanks to Thailand Research Found, National Science and Technology Development Agency and King Mongkut's University of Technology Thonburi for supporting financially this project. Author Tabtiang thanks the Commission on Higher Education, Thailand for support the

grant fund under the Strategic Scholarships for Frontier Research Network of the Ph.D. program Thai doctoral degree.

REFERENCES

1. Yamsaengsung, R.; Ngamnuch, M. Transient change in temperatures and pressure during vacuum frying of banana in a pilot scale, Proceeding of the 15th annual conference of Thai chemical engineering and applied chemistry, Chonburi, Thailand, October 27-28, 2005, PE 18-11.

2. Singthong, J.; Thongkaew, C. Using hydrocolloids to decrease oil absorption in banana chip. LWT – Food Science and Technology **2009**, *42* (7), 1199-1203.

3. Nimitpornsuko, N. Changes in physical and chemical qualities of used fried oils for banana slices; M.S. Thesis, Mahidol University, Bangkok, Thailand, 2008.

4. Saca, A.S.; Lozano, E.J. Explosion puffing of bananas. International Journal of Food Science and Technology **1992,** *27* (4), 419-426.

5. Hofsetz, K.; Lopes, C.C.; Hubinger, M.D.; Mayor, L.; Sereno, A.M. Change in the physical properties of bananas on applying HTST pulse during air drying. Journal of Food Engineering **2007**, *83* (4), 531-540.

6. Alibas, I. Microwave, vacuum, and air drying characteristics of collard leaves. Drying Technology **2000**, *27* (11)*,* 1266-1273.

7. Hussain, A.; Li, Z.; Ramanah, D.R.; Niamnuy, C.; Raghavan, G.S.V. Microwave drying of ginger by online aroma monitoring. Drying Technology **2010**, *28* (1), 42-48.

8. Devahastin, S.; Suvarnakuta, P.; Soponronnarit, S.; Mujumdar, A.S. A comparative study of low-pressure superheated steam and vacuum drying of a heat-sensitive material. Drying Technology **2004**, *22* (8), 1845-1867.

9. Elustondo, D.; Elustondo, M.P.; Urbicain, M. J. Mathermatical modeling of moisture evaporation from foodstuffs exposed to subatmospheric pressure superheated steam. Journal of Food Engineering **2001**, *49* (1), 15-24.

10. Kim, M.H.; Toledo, T.R. Effect of osmotic dehydration and high temperature fluidized bed drying on properties of dehydrated rabbiteye blueberries. Journal of Food Science **1987**, *52* (4), 980-989.

11. Sullivan, J.F.; Craig, J.C.; Konstance, R.P.; Egoville, M.J., Aceto, N.C. Continuous explosion-puffing of apples. Journal of Food Science **1980**, *45* (6), 1550-1555.

461 12. Chow, L.C.; Chung, J.N. Evaporation of water into a laminar stream of air and
462 superheated steam. International Journal of Heat and Mass Transfer **1983**, *26*
463 (3), 373-380.

464 13. Deventer, H.C.; Heijmans R.M.H. Drying with superheated steam. Drying
465 Technolgy **2001**, *19* (8), 2033-2045.

466 14. Taechapairoj, C., Dhuchakallaya, I., Soponronnarit, S., Wetchacama, S.,
467 Prachayawarakorn, S. Superheated steam fluidised bed paddy drying. Journal
468 of Food Engineering **2003**, *58* (1), 67-73.

469 15. Shi, J.; Xue, J.S. Application and development of osmotic dehydration
470 technology in food processing. In *Advances in food dehydration*; Ratti, C.,
471 Eds.; Taylor & Francis Group, New York, 2009; 187-208.

472 16. Sagar, V.R.; Kumar, P.S. Improvement of some process variables in mass
473 transfer kinetics of osmotic dehydration of mango slices and storage stability.
474 Journal of Scientific & Industrial Research **2009**, *68*, 1043-1048.

475 17. Krokida, M.K.; Karathanos, V.T.; Maroulis, Z.B. Effect of osmotic
476 dehydration on color and sorption characteristics of apple and banana. Drying
477 Technology **2000**, *18* (4), 937-950.

478 18. Mandala, I.G.; Anagnostaras, E.F.; Oikonomou, C.K. Influence of osmotic
479 dehydrations on apple air drying kinetics and their quality characteristics.
480 Journal of Food Engineering **2005,** *69* (3), 307-316.

481 19. Antonio, G.C.; Alves, D.G.; Azoubel, P.M.; Murr, F.E.X.; Park, K.J. Influence
482 of osmotic dehydration and high temperature short time processes on dried

483 sweet potato (*Ipomoea batatas* Lam.). Journal of Food Engineering **2008,** *84*
484 (3), 375-382.

485 20. Marquez, G.; Anon, M.C. Influence of reducing sugars and amino acids in the
486 color development of fried potatoes. Journal of Food Science **1986**, *51* (1),
487 157-160.

488 21. Hsieh, F.; Hu, L.; Peng, I.C.; Huff, H.E. Pretreating dent corn grits for puffing
489 in a rice cake machine. Journal of Food Science **1990,** *55* (5), 1345-1355.

490 22. Orts, W.J.; Glenn, G.M.; Nobes, G.A.R.; Wood, D.F. Wheat starch effect on
491 the textural characteristics of puffed brown rice cakes. Cereal Chemistry **2000**,
492 *77* (1), 18-23.

493 23. Varnalis, A.I.; Brennan, J.G.; MacDougall, D.B. A proposed mechanism of
494 high-temperature puffing of potato. part II. Influence of blanching and initial
495 drying on the permeability of the partially dried layer to water vapour. Journal
496 of Food Engineering **2001**, *48* (4) 369-378.

497 24. Thuwapanichayanan, R.; Prachayawarakorn, S.; Kunwisawa, J.;
498 Soponronnarit, S. Determination of effective moisture diffusivity and
499 assessment of quality attributes of banana slices during drying. LWT - Food
500 Science and Technology 2011, 44, 1502-1510.

501 25. Association of Official Analytical Chemists. *Official Methods of Analysis of*
502 *the AOAC International*, 16th ed.; Gaithersburg, MD, 1995.

503 26. Thuwapanichayanan, R.; Prachayawarakorn, S.; Soponronnarit, S. Modeling
504 of diffusion and shrinkage and quality investigation of banana foam mat

505 drying. Drying Technology **2008**, *26* (11), 1326-1333.

506 27. Slimestad, R.; Vågen, I.M. Thermal stability of glucose and other sugar
507 aldoses in normal phase high performance liquid chromatography. Journal of
508 Chromatography A. **2006,** *1118* (2), 281-284.

509 28. Lerici, C.R.; Pinnavaia, G.; Dalla Rosa, M.; Bartolucci, L. Osmotic
510 dehydration of fruit: Influence of osmotic agents on drying behavior and
511 product quality. Journal of Food Science **1985,** *50* (5), 1217-1219.

512 29. Gekas, V.; Oste, R.; Lamberg, I. Diffusion in heated potato tissue. Journal of
513 Food Science **1993**, *58* (4), 827-831.

514 30. Baini, R.; Langrish, T.A.G. Assessment of colour development in dried
515 bananas-measurements and implication for modeling. Journal of Food
516 Engineering **2009**, *93* (2), 177-182.

517 31. Rocha, A.M.C.N.; Morais, A.M.M.B. Shelf life of minimally processed apple
518 (cv. Jonagored) determined by colour change. Food control **2003**, *14* (1), 13-
519 20.

520 32. Hii, C.L.; Law, C.L.; Cloke, M.; Suzannah, S. Thin layer drying kinetics of
521 cocoa and dried product quality. Biosystems Engineering **2009**, *102* (2), 153-
522 161.

523 33. Purlis, E. Browning development in bakery product-A review. Journal of Food
524 Engineering **2010**, *99* (3), 239-249.

525 34. Allan, G.G.; Stoyanov, A.P.; Ueda, M.; Yahiaoui, A. Sugar-cellulose
526 composites V. The mechanism of fiber strengthening by cell wall
527 incorporation of sugars. Cellulose **2001**, *8*, 127-138.

528 35. Hofsetz, K.; Lopes, C.C. Crispy banana obtained by the combination of a high
529 temperature and short time drying stage and a drying process. Brazilian
530 Journal of Chemical Engineering **2005**, *22* (2), 285-292.

531
532
533
534
535
536
537
538
539
540
541
542
543
544

545 **LIST OF FIGURES**

LIST OF TABLES

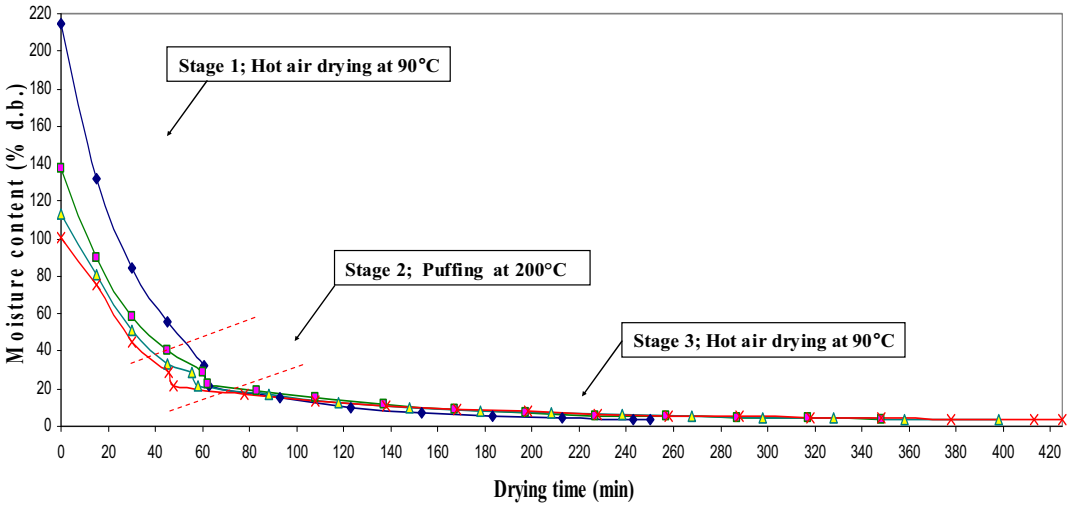

FIG. 1 Drying curve of banana sliced during processing steps [(●) non osmotic sample; (■) osmotic by sucrose 30°Brix; (▲) osmotic by sucrose 35°Brix and (×) osmotic by sucrose 40°Brix].

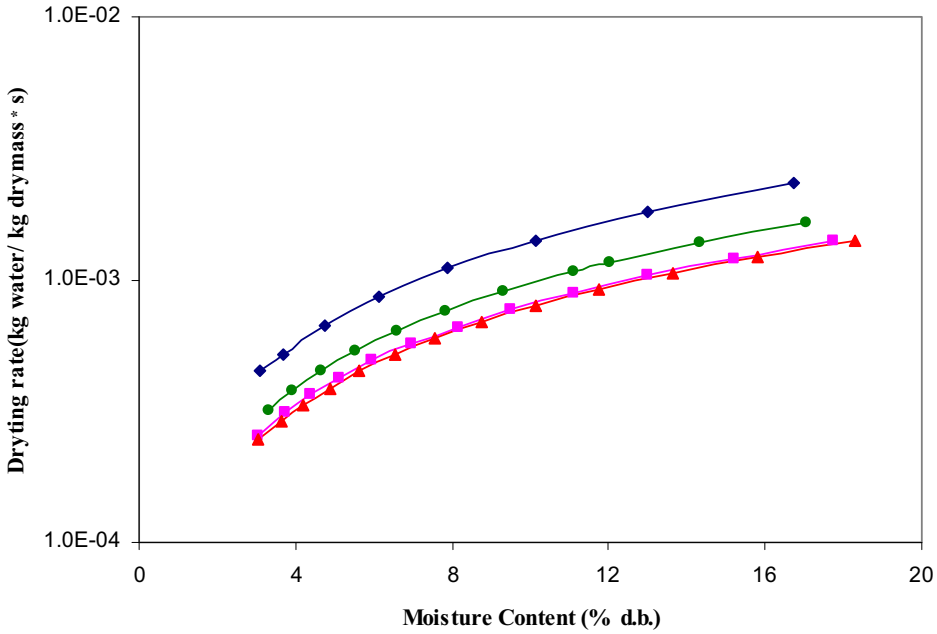

FIG. 2 Drying rate of banana sliced at the last drying stage for samples puffed at 200 °C [(♦) non osmotic; (●) osmotic by sucrose 30°Brix; (■) osmotic by sucrose 35°Brix; (▲) osmotic by sucrose 40°Brix].

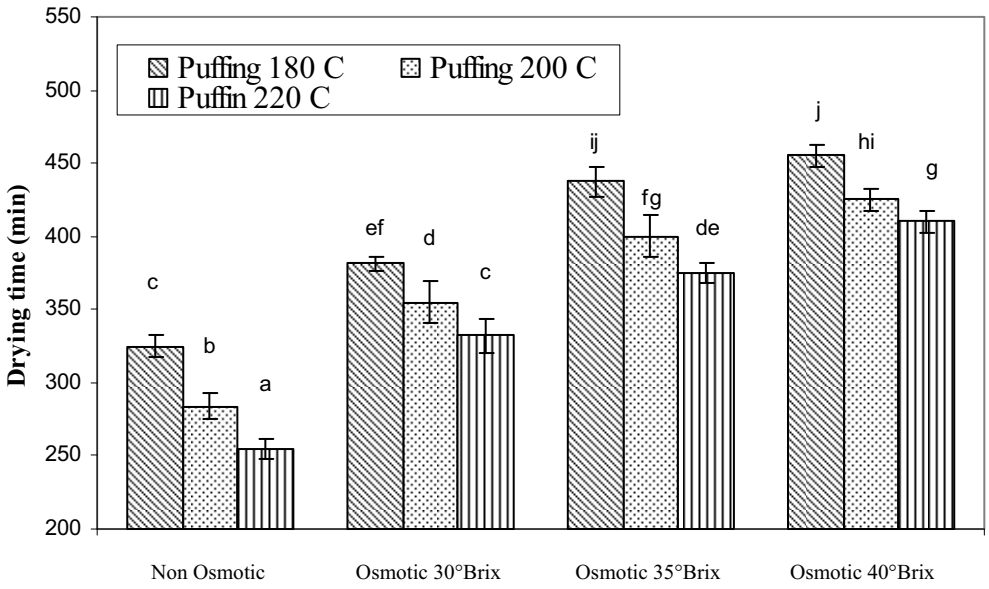

The different scripts presented over the bar mean the significant difference at $p \leq 0.05$.

FIG. 3 Drying time of banana slices undergoing puffing at 180, 200 and 220°C and osmotic pretreatment at 30, 35 and 40°Brix.

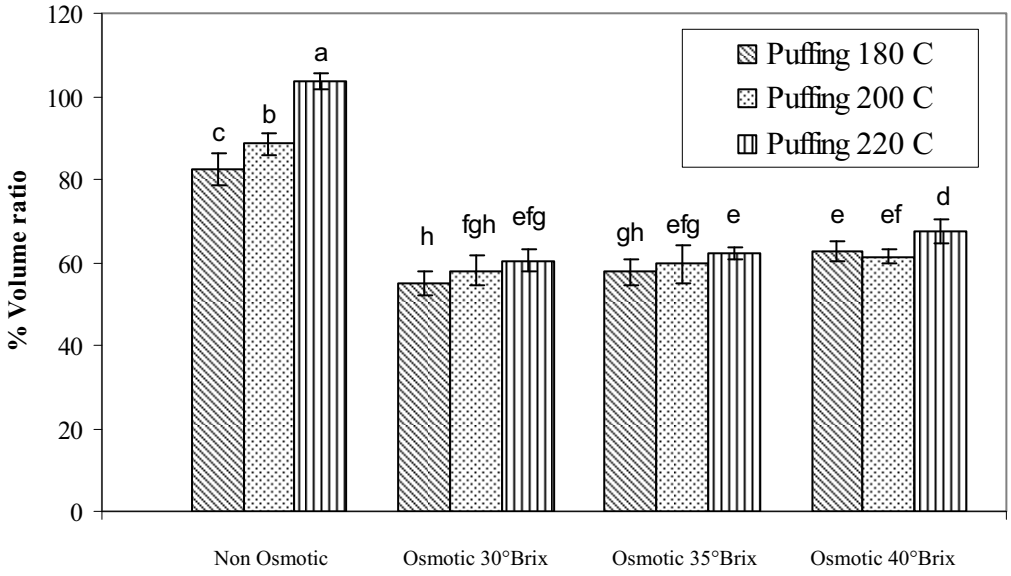

The different scripts presented over the bar mean the significant difference at $p \leq 0.05$.

FIG. 4 Effects of puffing temperatures and osmotic solution concentrations on volume ratio.

602

603

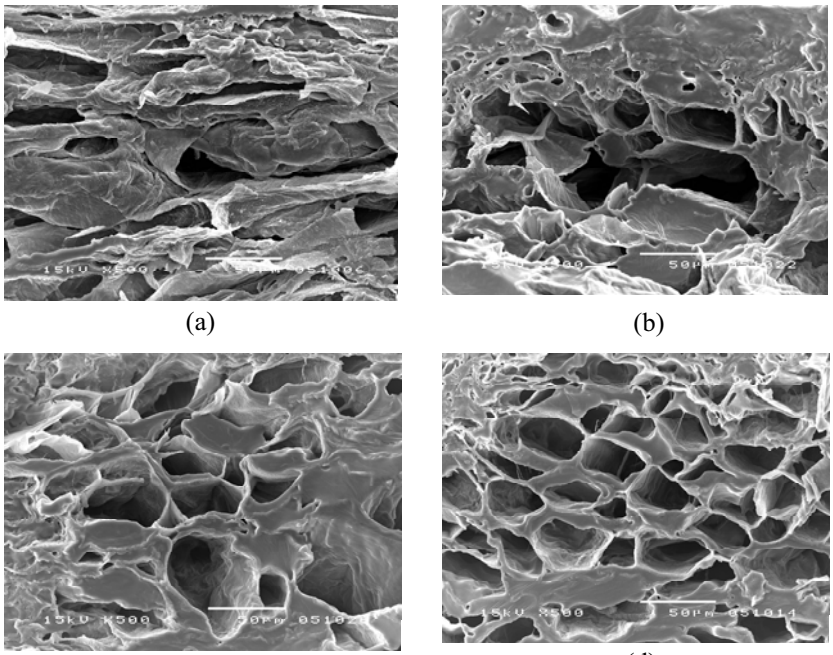

(a) (b)

(c) (d)

604

605 **FIG. 5** SEM photographs showing cross section of banana slices after first stage
606 drying; (a) non osmotic; (b) 30°Brix; (c) 35°Brix; and (d) 40°Brix.

607

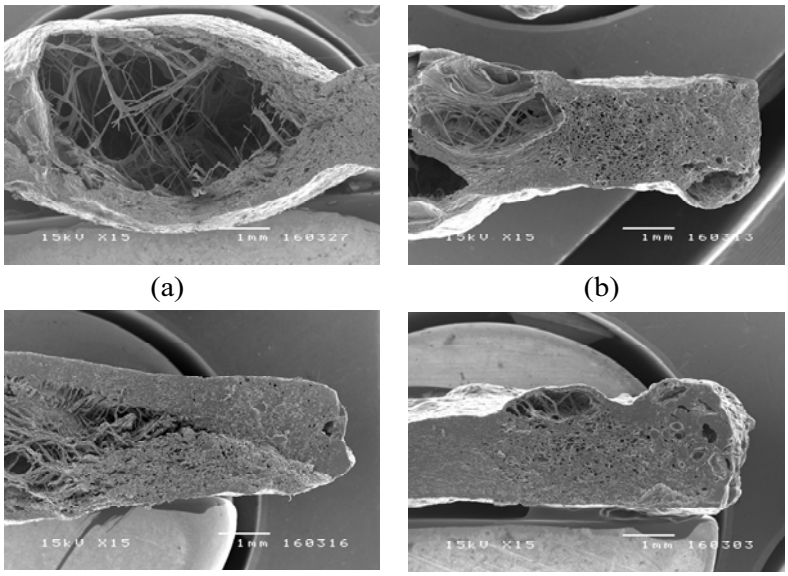

(a) (b)

(c) (d)

608

609 **FIG. 6** SEM photographs showing cross section of banana slices puffed at 200°C; (a)
610 non osmotic; (b) 30°Brix; (c) 35°Brix; and (d) 40°Brix.

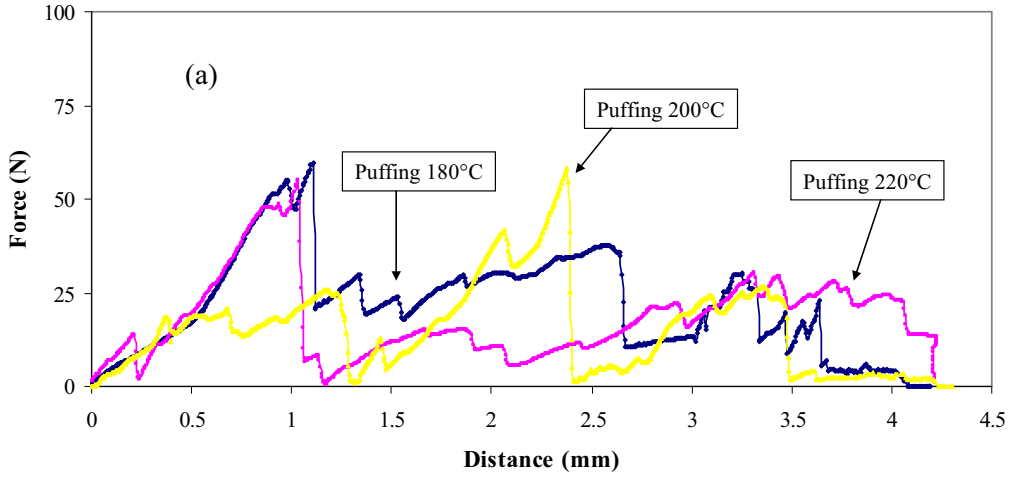

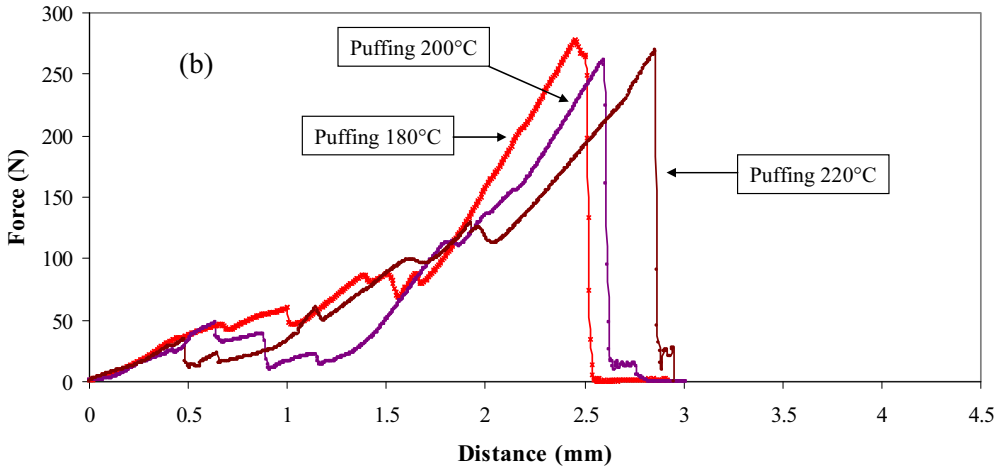

FIG. 7 Force deformation curves: (a) the none osmotic banana and (b) the osmotic banana.

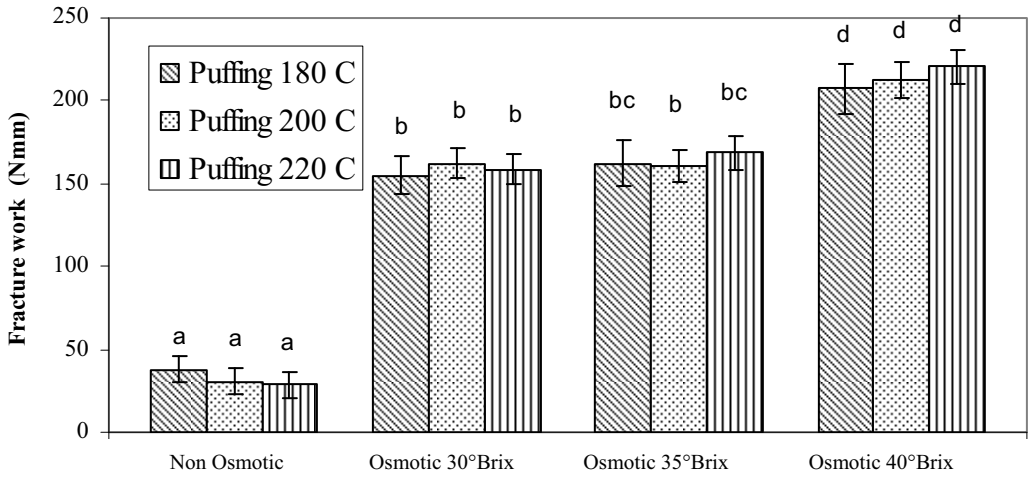

The different scripts presented over the bar mean the significant difference at $p \leq 0.05$.

FIG. 8 Fracture work of the osmotic banana and non osmotic banana at different puffing temperatures.

645

646

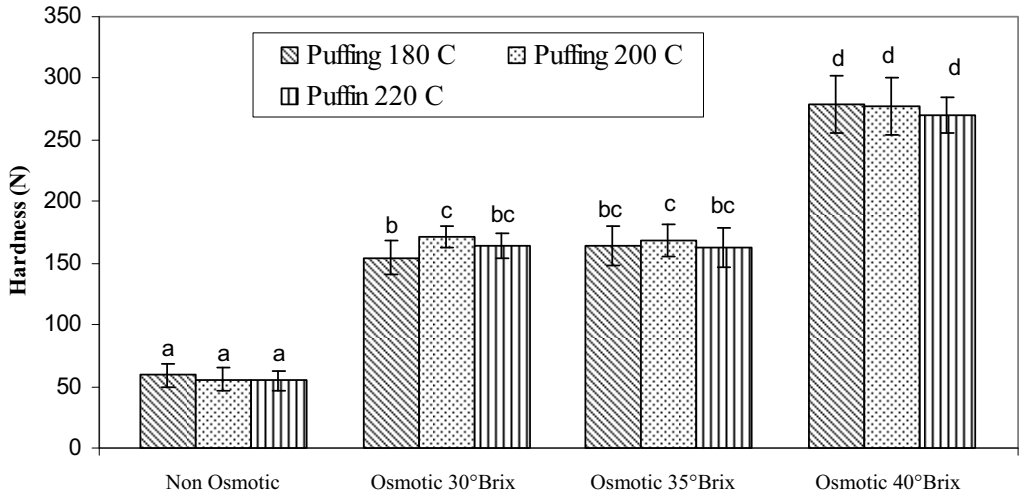

647

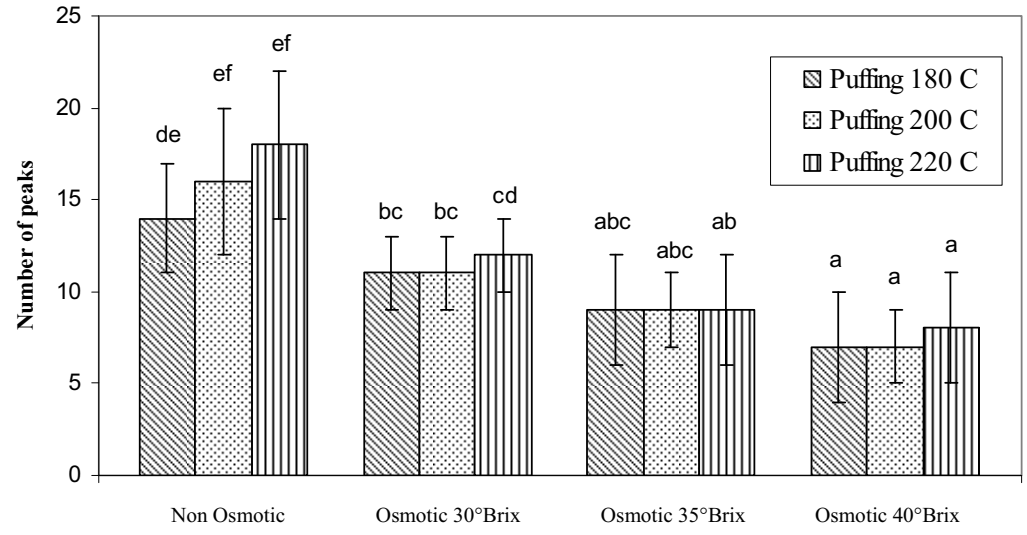

648

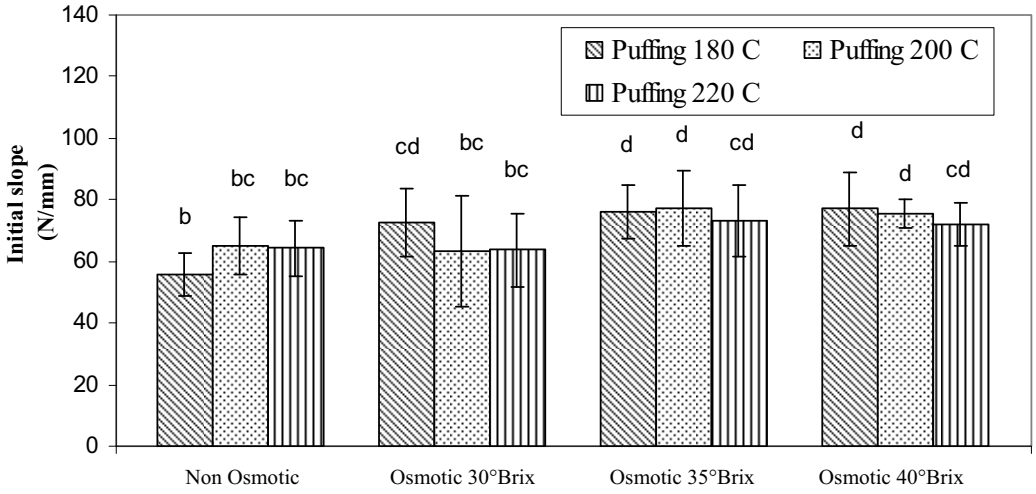

649

650 The different scripts presented over the bar mean the significant difference at $p \leq 0.05$.

651 **FIG. 9** Texture properties of the osmotic banana and non osmotic banana.

Table 1 Immersion time, amount of water loss, amount of solid gain, moisture content, amount of sucrose, amount of fructose and amount of glucose of banana slice at various sucrose concentration.

Sucrose Concentration (°Brix)	Immersion time (min)	Water loss (g water/ g dry mass)	Solid gain (g solid/ g dry mass)	Water loss/ Solid gain	Moisture content (% d.b.)	Amount of sucrose (g/100 g banana)	Amount of glucose (g/100 g banana)	Amount of fructose (g/100 g banana)
none osmotic	-	-	-	-	210.1 ± 3.5	7.43	1.04	1.12
30°Brix	240	0.321	0.248	1.29	134.1 ± 2.4	16.41	0.14	0.17
35°Brix	290	0.539	0.303	1.78	116.4 ± 3.7	18.45	0.16	0.19
40°Brix	330	0.772	0.326	2.37	102.4 ± 3.1	22.86	0.14	0.16

Table 2 Color of osmotic banana and none osmotic banana slices at different puffing temperatures.

Puffing temperature (°C)	Osmotic concentration (°Brix)	L	a	b	°h	Product
180°C	0	$52.1^{ab} \pm 1.02$	$5.32^{cd} \pm 0.3$	$16.81^{a} \pm 0.83$	$72.41^{bc} \pm 1.20$	
	30	$59.29^{f} \pm 1.51$	$4.87^{abc} \pm 0.26$	$19.97^{cd} \pm 0.74$	$76.30^{h} \pm 0.62$	
	35	$57.01^{ef} \pm 3.02$	$5.02^{abc} \pm 0.32$	$16.65^{a} \pm 0.9$	$73.21^{cd} \pm 0.59$	
	40	$57.43^{ef} \pm 1.28$	$5.02^{abc} \pm 0.28$	$18.68^{bc} \pm 0.97$	$74.91^{efg} \pm 1.19$	
200°C	0	$51.3^{ab} \pm 1.66$	$5.66^{cd} \pm 0.25$	$16.85^{a} \pm 0.85$	$71.48^{b} \pm 0.62$	
	30	$59.1^{ef} \pm 2.73$	$4.93^{abc} \pm 0.21$	$18.89^{bc} \pm 1.11$	$75.35^{fgh} \pm 0.73$	
	35	$58.35^{ef} \pm 1.7$	$5.40^{cd} \pm 0.51$	$18.15^{bc} \pm 0.50$	$73.42^{cd} \pm 1.82$	
	40	$57.31^{ef} \pm 1.3$	$5.2^{cd} \pm 1.3$	$18.71^{bc} \pm 0.83$	$74.32^{def} \pm 1.02$	
220°C	0	$49.5^{a} \pm 1.5$	$6.11^{e} \pm 0.21$	$16.3^{a} \pm 0.83$	$69.44^{a} \pm 1.78$	
	30	$57.22^{ef} \pm 2.1$	$5.41^{cd} \pm 0.33$	$18.68^{bc} \pm 0.5$	$73.71^{cde} \pm 1.24$	
	35	$56.36^{de} \pm 2.45$	$5.06^{abcd} \pm 0.3$	$18.39^{bc} \pm 0.54$	$74.60^{def} \pm 0.93$	
	40	$54.19^{bcde} \pm 4.22$	$5.27^{bcd} \pm 0.32$	$17.7^{b} \pm 1.14$	$73.75^{cde} \pm 1.19$	

The different scripts values in the same column mean the significant different at $p \leq 0.05$

17th International Drying Symposium (IDS 2010)
Magdeburg, Germany, 3-6 October 2010

POROUS STRUCTURE DESIGN OF BANANA FOAM TO RESIST MOISTURE ADSORPTION USING A 2-D STOCHASTIC PORE NETWORK: EXPERIMENT AND SIMULATION

P. Prakotmak [1], S. Soponronnarit [1], S. Prachayawarakorn [2]

[1] *Energy Technology Division, School of Energy Environment and Materials, King Mongkut's University of Technology Thonburi, Suksawat 48 Road, Tungkru, Bangkok 10140, Thailand*
E-mail: preeda_list@hotmail.com

[2] *Faculty of Engineering, King Mongkut's University of Technology Thonburi, Suksawat 48 Road, Tungkru, Bangkok 10140, Thailand*
E-mail: somkiat.pra@kmutt.ac.th

Abstract: High porosity of dried banana foam could quickly adsorb the moisture from the air during storage**,** leading to the lost of quality and textural property. The purpose of this research was to design banana foam porous structure that can resist moisture adsorption using a stochastic pore network. The textural quality of the structured banana foams regarding to hardness and initial slope was also determined. A 2-D network of cylindrical pores was used to represent the voids inside the banana foam and the moisture movement inside the individual pore segments was described by Fick's law. A network size of 23×264 accounting for 12431 pores was used. The pore size distributions of dried banana foam for the foam densities of 0.21, 0.26 and 0.31 g/cm^3 were characterized by binary image of SEM. The result shows that the stochastic pore network could qualitatively describe the adsorption experimental results. The rate of moisture adsorption depends on both pore size distribution and the arrangement of pores within network.

Keywords: adsorption**,** pore structure, snack, texture property

INTRODUCTION

Moisture migration plays a part in almost all of the chemical and physical changes that occur in the production of dried crispy products e.g. ready to eat cereals, biscuits and snack foods. (Cauvain and Young, 2000). Quality change is, for example, texture and color. The rate of moisture migration into porous food is governed by the environmental conditions, i.e. relative humidity and temperature. Also, it depends on the porous food structure. The dried crispy products try to achieve moisture equilibrium with their surroundings so that the moisture may be lost or gained with time. If moisture adsorption occurred from any exposed surfaces, the relative humidity would not be uniform throughout the product. This RH gradient means that moisture will gradually migrate from the outside to the centre of the product through the porous structure in order to restore equilibrium atmosphere.

The moisture transport in porous foods can be governed by different mechanisms. Diffusion of moisture may be divided into molecular diffusion, capillary diffusion, Knudsen diffusion, etc. Among these, molecular diffusion is the most important phenomenon that has a major influence. In molecular diffusion, gases or liquid molecules transferred from a region of high concentration to a region of low concentration due to the random motion of the substance. In general, the Fick' s law can describe the diffusing molecular within pores and other interconnected voids in the porous solid. The molecular diffusion is defined as the net transport of gases and liquids on a molecular scale due to a concentration or partial pressure gradient throughout a medium (Saravacos and Maroulis, 2001). Each of these diffusion mechanisms is difficult to study independently and the effect of porous microstructure is lumped into effective parameters. However, more recent works studied the discrete model (or pore network model) to overcome the limitations of continuum model by mapping pore sizes and topology of porous food onto the network model (Yiotis et al., 2005; Prat and Bray, 1999; Blunt, 2001; Segura and Toledo, 2005).

Pore network models represent porous media as simplified randomly connected sets of large and small pores with fluid flow. The network models have been applied mostly in theoretical study and used to describe the experimental observations. Banana foam mat in this study is considered to be a high porous and this product could quickly adsorb the moisture from the air when exposed to the

surrounding, leading to the loss of crispness. A better understanding relation of moisture transfer and its microstructure can therefore reduce or prevent the quality change in the banana foam. The effect of porous structures on moisture migration is of great interest. The study of the effect of porous structure on the moisture migration in porous foods during adsorption has limited in the literature. Prakotmak et al. (2010) studied the effect of densities of banana foam mats, characterizing different porous structures, on the moisture adsorption rate.

In addition to the porous structure, the arrangement of pores within network is also important to transport of moisture. Prachayawarakorn et al. (2008) theoretically studied the effect of pore architecture assembly on moisture evaporation rate and found that the minimum shielding network, large pore assembly exposed to the exterior surface, enhanced greatly the drying rate. On the other hand, the maximum shielding network, which is small pores allocated onto the network exterior, exhibits the slowest drying rate. Similarly, Pillai et al. (2009) studied moisture evaporation in dual-porosity porous medium using square network model and found that when the lower porosity material (smaller pore) covered the material containing large pore can limit the evaporation rate and the result became converse when the high porosity material (larger pore) exposed to the drying air.

Limited information concerning the effect of two-layer products on moisture transport is available in the literature. The objective of the present study was to design the banana foams structure to resist moisture migration using a two dimensional stochastic pore network. The network model results were then compared with the adsorption experiments. The textural property of dried banana foam was also characterized by initial slope, number of peaks and maximum force**.**

DRIED BANANA FOAM PREPARATION

The banana puree with 5% fresh egg albumen, used as foaming agent, were foamed to densities of 0.3, 0.5 and 0.7 g/cm^3. The density was determined by measuring the mass of a fixed volume of the foam. The banana foams was poured slowly into a steel block and then placed on a mesh tray, which was covered with aluminium foil. After that, it was dried to about 3% kg/kg d.b. using 80^{o}C and a 0.5 m/s superficial air velocity. The banana foam prepared from the initial foam densities of 0.3, 0.5 and 0.7 g/cm^3 can produce the dried banana densities of 0.21 ± 0.02, 0.26 ± 0.02 and 0.31 ± 0.01 g/cm^3, respectively. The product thicknesses after drying were 2.8, 3.2 mm and 3.5 mm for the densities of 0.21, 0.26 and 0.31 g/cm^3, respectively. For dual density preparation, the first density of banana foams was poured into a steel block with a thickness of 2 mm and dried by hot air for 1 h. After that, the second density of banana foam was poured on it and dried again by the hot air for 2 h.

ADSORPTION EXPERIMENT

Moisture adsorption experiments were carried out using the static method. Samples were placed into the glass jars contained a saturated potassium iodine solution (KI) which provided the relative humidity (RH) in a range of 66-68% at the temperatures of 35^{o}C. The jars were placed in the temperature-controlled oven with a precision of ±1°C (UFE500, Memmert, Germany). Samples were weighed at different exposure times ranging from 1 to 80 h. A small amount of toluene held in a vial was fixed in the glass jars in order to prevent microbial spoilage of the samples. Moisture content of each sample after reaching the equilibrium condition was determined by drying it with the hot air oven at a temperature of 103°C for 3 h. As compared to the AOAC procedure (AOAC, 1995), the error from this method was approximately 0.4% as reported by Thuwapanichayanan et al. (2008). The experiment at each sorption condition was repeated three times and the mean value was reported.

SEM PHOTOGRAPH

The morphologies of dried banana foam mats were characterized using scanning electron microscope (SEM) with an accelerating voltage of 10 kV. Before photographing, the specimens were cut into a dimension of 5×5 mm and then glued on the metal stub. The samples were coated with gold, scanned, and photographed at $15\times$ magnification.

TEXTURE ANALYSIS

The effects of moisture content and porous foam configuration on the product texture were determined quantitatively. The initial moisture content of the banana foam was about 0.038 kg/kg d.b. A compressive force was applied to the sample using a 5 mm spherical probe moving down at a constant crosshead speed of 2 mm/s. The hardness was defined as the maximum force of the force-deformation curve and the crispness was characterized by the number of peaks and the slope of the first peak. Eight samples were tested and the average values of hardness and crispness were presented. All experiments were performed at 24^{o}C.

GENERATION OF THE PORE NETWORK

In this study, the microstructure of single banana foam mat can be represented by a two dimensional network of randomly connected pores. Each pore in the network had a constant connectivity of 4. In this work, pores are assumed to be cylindrical shape with their diameter assigned according to the experimental pore size distribution, and each pore in the network had the same pore length and was denoted as L. The pore diameters determined from this study was

characterized by SEM. Fig. 1 illustrates an example of a 2-D stochastic pore network with a small size of 16× 40, defined as the number of pore junctions in the vertical direction multiplied by those pore junctions in the horizontal direction. This network size consists of 1336 pores. The pores in this figure were presented by black color and solid by white color.

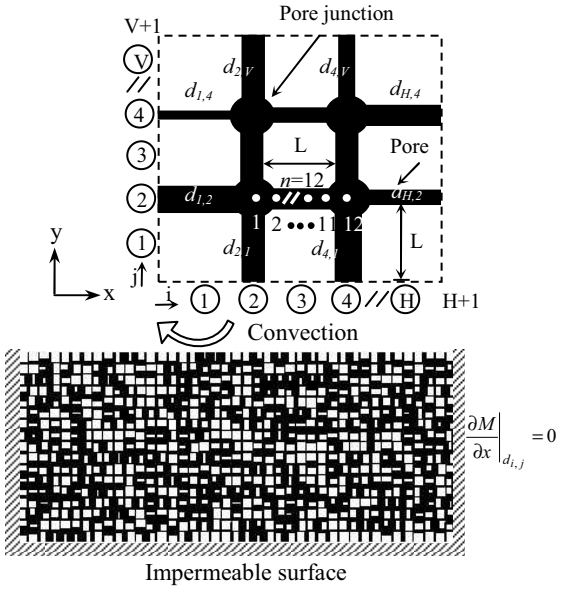

Fig. 1. An Illustration of 2- D stochastic pore network with a size of 16×40

However, for calculating the pore diffusivity, we used a large network size, with a number of pores of the network corresponding to number of pores in the real sample. The single foam densities of 0.31, 0.26 and 0.21 g/cm^3 had the network sizes of 26× 291, 23× 264 and 20× 231, respectively, and their sizes were accounted for 15449, 12431 and 9491 pores, respectively. These numbers of pores were estimated from the number of pores in the unit area of sample that was obtained from SEM. The length of each pore, L, was calculated by dividing the thickness of banana foam sample by number of vertical pores in each row. The average value of L was equal to 133 μm.

DIFFUSION IN A SINGLE PORE

In this work, moisture adsorption between surrounding air and banana foam mat occurred under isothermal condition. The water vapor from the air will be adsorbed at the sample surface and then moves in the liquid form through interior area via the pores. The moisture diffusing through each pore in the network, whether the pore is allocated in horizontal or vertical direction of the network, can be described by Fick's second law:

$$\frac{\partial M}{\partial t} = D_p\left(\frac{\partial^2 M}{\partial x^2}\right) \qquad (1)$$

where M is the moisture content (kg/kg d.b.), t the adsorption time (s), D_p the water diffusivity in pore (m^2/s), and x the distance along the pore length (m). The migration of moisture from the surrounding air to the banana foam surface occurred specifically at the top surface and no moisture transferred at the bottom surface of the network since the banana foam mat was placed on an opaque glass dish. The constant diffusion coefficient at a given adsorption condition was assumed and the moisture profile in the pore at the beginning was uniform along the pore axis:

$$M = M_i \quad : t = 0, 0 \le x \le L \qquad (2)$$

where M_i is the initial moisture content (kg/kg d.b.).

Boundary condition for pores at edges of network

From the prepared sample size, it indicated that the surface area at each sample side was remarkably smaller than that at the top surface. Hence, the moisture transferring from the surrounding to the pores allocated at the three sides of sample was small, as can be seen in Fig. 1, and the three sides of the pore network are reasonably presented as impermeable surface. Accordingly, the boundary condition for the pores allocated at these three sides of the network is set as:

$$\left.\frac{\partial M}{\partial x}\right|_{d_{i,j}} = 0 \quad : t > 0 \qquad (3)$$

where d is the pore diameter (m) and subscripts i and j are the positions of the pore in the network. The positions of outer pores are represented as $d_{1,2}$, $d_{1,4}, \ldots, d_{1,V+1}$ for the pores at the left edge of network, $d_{H,2}$, $d_{H,4}, \ldots, d_{H,V+1}$, for the pore at the right edge and $d_{2,1}$, $d_{4,1}, \ldots, d_{H+1,1}$ for the pores at the bottom edge. Subscripts H and V are the number of columns and rows of the pores on the network, respectively.

Boundary condition for the pores at top surface of network

For the periphery pores positioned on the top of the network, such as $d_{2,V}$, $d_{4,V}, \ldots, d_{H+1,V}$, the moisture moving from the surrounding to those pores was occurred by convection and the boundary condition is set by:

$$D_p\left(\frac{\partial M}{\partial x}\right)_{d_{i,j}} = h_m\left(M_e - M_s\right) \quad : t > 0 \qquad (4)$$

where h_m is the convective mass transfer coefficient (m/s), M_e the equilibrium moisture content (kg/kg d.b.) and M_s the moisture content at the sample surface (kg/kg d.b.). To calculate the moisture concentration of the pores inside the network, a finite difference method was used. An individual pore in the network was divided into $n=12$ intervals as shown in Fig 1 and Eq. (1) was discretized using the explicit method as follows:

$$M_{n,d_{i,j}}^{p+1} + M_{n,d_{i,j}}^{p}(2\alpha - 1) - \alpha\left(M_{n+1,d_{i,j}}^{p} + M_{n-1,d_{i,j}}^{p}\right) = 0 \quad (5)$$

where $\alpha = D_p \Delta t / \Delta x^2$ is the Fourier number, p and n the respective indexes of the present time and of nodal position along the pore axis. The Eq. (5) is used to calculate the moisture content for the inner pores of network. The boundary conditions in Eqs. (3) and (4) can be written respectively as:

$$M_{n,d_{i,j}}^{p+1} + M_{n,d_{i,j}}^{p}(2\alpha - 1) - 2\alpha\left(M_{n+1,d_{i,j}}^{p}\right) = 0 \quad (6)$$

$$M_{n,d_{i,j}}^{p+1}(\gamma + 1) - M_{n-1,d_{i,j}}^{p+1} - \gamma M_e^{p+1} = 0 \quad (7)$$

where $\gamma = h_m \Delta x / D_p$. The moisture adsorption rate $Q_{i,j}$ (kg/s) for the individual pores can be calculated by:

$$Q_{d_{i,j}} = \rho \cdot \frac{\pi}{4} d_{i,j}^2 \cdot D_p \left(\frac{dM_{d_{i,j}}(x,t)}{dx} \right)_{x=L} \quad (8)$$

The finite difference approximation of Eq. (8) is

$$Q_{d_{i,j}} = \rho \cdot \frac{\pi}{4} d_{i,j}^2 \cdot D_p \left(\frac{M_n^{p+1} - M_{n-1,d_{i,j}}^{p+1}}{\Delta x} \right)_{x=L} \quad (9)$$

where ρ is the dried banana densities (kg/m^3) and M_n^{p+1} is the moisture contents at pore junctions.

Mass balance for the network

To determine the moisture contents at the pore junctions for the inner pores of the network, the mass balance of moisture content at the inner nodes of network was made, assuming no accumulation of moisture at each pore junction within the network, which is thus expressed by:

$$\sum_{\{u.v\}} Q_{d_{i,j}} = 0 \quad (10)$$

where Σ is over all the pores, $d_{i,j}$, that connected to the pore junction (u,v), and u,v are the coordinate for a pore junction in the network. Substituting Eq. (9) into Eq. (10) and solve it for the moisture contents at the pore junctions. After the moisture contents at nodes of the network were known, the average moisture content $\overline{M}_{network}$ of network can then be calculated using the following equation:

$$\overline{M}(t)_{network} = \frac{\sum_{n=1}^{Z} \frac{d_{i,j}^2}{4} \int_0^L M_{r_{i,j}}(x,t)dx}{Z \cdot L \sum_{n=1}^{Z} \frac{d_{i,j}^2}{4}} \quad (11)$$

where Z is number of pores in the network. All computations were implemented using Intel C++ Compiler (Intel® Software Network, 2009).

RESULT AND DISCUSSION

Pore size distribution

The pore size distributions of the dried banana foam at densities were shown in Fig. 2. These pore size distributions were determined from the cross-sectional view of samples from SEM using image analysis. The sample with a foam density of 0.31 g/cm^3 had small pores in the range of 7-120 μm accounting for 63% of the whole number of pores and for 37 % with the pores larger than 120 μm. For the densities of 0.26 and 0.21 g/cm^3, it had the proportions of small pores accounting for 57% and 43% respectively, which was lower than that of sample at the density of 0.31 g/cm^3. The porosity of sample at the density of 0.31 g/cm^3 was relatively higher due to higher number of large pores. The void area fractions for the banana foam densities of 0.21, 0.26 and 0.31 g/cm^3 obtained by counting the pore area of binary images, were 31, 26 and 22%, respectively. From these characterizations of porous banana foam, it indicated that the high void area fraction for the low banana foam density resulted from the large pore size assembly although the number of pores in the sample was smaller.

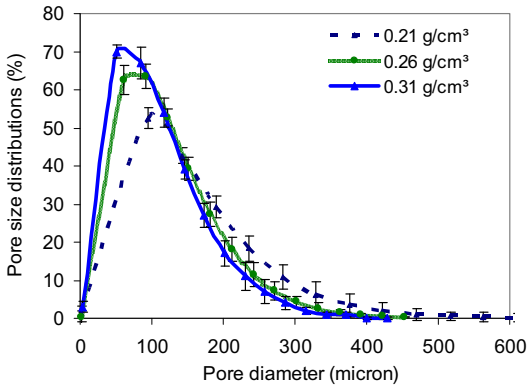

Fig. 2. Pore size distributions of single banana foam

Diffusion in single foam density

The pore diffusion coefficients for three banana foam densities at 35°C and different relative humidities are shown in Table. 1. The diffusion coefficients were obtained by using the optimization technique with the golden search.

Table 1. Estimated pore diffusivity for three banana foam densities at 35°C and relative humidities with R^2-values above 0.96

RH	$D_p \times 10^{-9}$ (m^2/s)		
(%)	0.21 g/cm^3	0.26 g/cm^3	0.31 g/cm^3
32	2.276 ± 0.230^{a}	2.072 ± 0.193^{ab}	0.903 ± 0.295^{c}
50	2.304 ± 0.210^{a}	2.149 ± 0.238^{ab}	1.024 ± 0.480^{c}
67	2.204 ± 0.185^{ab}	1.990 ± 0.183^{ab}	1.102 ± 0.280^{c}
75	1.941 ± 0.219^{ab}	1.686 ± 0.241^{b}	0.876 ± 0.405^{c}

Values in the table with different superscripts mean that the values are significantly different ($p < 0.05$).

The root mean square error RMSE was set as the objective function. The calculation will be stop when the value of RMSE was lower than 10^{-6} The RMSE is defined as:

$$RMSE = \left[\frac{1}{K} \sum_{n=1}^{K} (M(t)_{\exp} - \overline{M}(t)_{network})^2 \right]^{1/2} \quad (12)$$

where $M(t)_{exp}$ is the experimental moisture content of material at time t, $\overline{M}(t)_{network}$ is the predicted moisture content, and K is the number of the experimental data.

The effects of relative humidity and banana foam density as well as their interactions on the values of moisture diffusion coefficient were examined by the univariate full factorial analysis of variance (ANOVA). Duncan's multiple range test was used to indicate the difference of means at a confidence level of 95%. The results from the statistical analysis shows that the relative humidity did not affect the moisture diffusion coefficient, but the banana foam density significantly affect the diffusion coefficient.

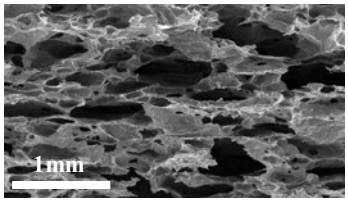

(a) 0.21 g/cm^3

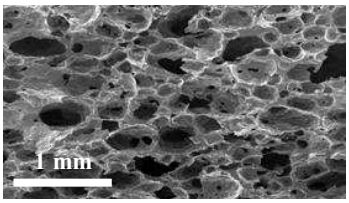

(b) 0.26 g/cm^3

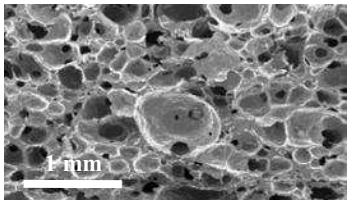

(c) 0.31 g/cm^3

Fig. 3. SEM micrographs of dried banana foam mats at different foam densities

The later result is rather interesting that even though the pore size distribution was included into the network model, the diffusion coefficient still varied amongst foam densities. The strong influence of banana foam density on the diffusivity may be caused by the different morphologies amongst banana foam densities. As shown in Fig. 3, shape of pores for the dried banana foam at density of 0.31 and 0.26 g/cm^{3}is rather circle. However, when the foam density was lower particularly at 0.21 g/cm^3, pore shape was elongate. Different pore shapes may affect the transport property. This is because the difference of pore shapes can result in the different arrangements of solid matrix in the porous material and provides further the different length scales of travelling path of fluid and the resulting mass transport property (Segular and Toledo, 2005; Stewart et al., 2006). Stewart et al. (2006) theoretically studied the pore geometry effect on intrinsic hydraulic permeability of porous material using lattice-Boltzmann method and found that porous material, with the same porosity but different pore geometries, provided different values of hydraulic permeability.

Fig. 3 shows typical scanning electron micrographs of cross-sectional views of three banana foam densities, 0.21, 0.26 and 0.31 g/cm^3. The pore shape was rather more circular at the foam density of 0.31 g/cm^{3}than at the other two foam densities, which exhibited more elliptical. The higher gas bubbles were produced at lower foam density and these bubbles were presented near together which can then be coalesced simply. The large gas bubble size is thus not quite stable and collapse easily. In addition, its shape can be changed, due to the stress formation during drying.

Adsorption kinetics and validation

Fig. 4 shows the moisture adsorption kinetics at temperature of 35^{o}C and 67% RH for the banana foam densities of 0.21, 0.26 and 0.31 g/cm^3. The adsorption rate was high at the beginning of adsorption, and gradually decreased as the moisture content increased.

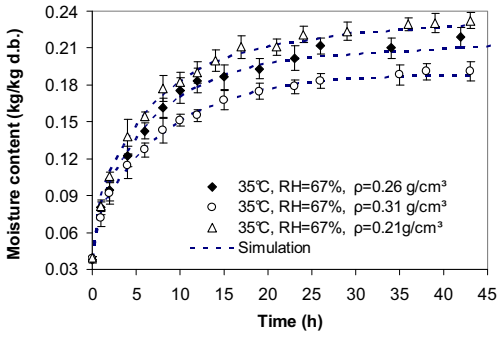

Fig. 4. Moisture adsorption kinetics at 35^{o}C and relative humidity of 67% for banana foam densities of 0.21, 0.26 and 0.31 g/cm^3

The rate of moisture adsorption was highest for the foam density of 0.21 g/cm^3 and became slower with the higher banana foam density. The low adsorption rate for the high banana foam density can be attributed to the low porosity. When the moisture content of product was changed with the exposure time or in the equilibrium with the exposed condition, the moisture content at the equilibrium were not identical amongst the banana foam densities, presenting the strong influence of porous

structure on the equilibrium moisture content. As shown in Fig. 4, the lower equilibrium moisture content was observed at the higher banana foam density, which corresponded to the lower porosity. The moisture diffusion coefficients shown in Table 1 were used to calculate the moisture content of banana foams and found that the stochastic pore network can predict the moisture content in agreement with the experiments.

Porous structure design

From the results in the previous section, it indicated that the porosity or the porous structure play an important role in moisture migration in food. If the pore assembly taking from the different pore size distributions was arranged onto the 2-D network in order to produce the two-layer network, it is interesting to see how such a porous structure affected the adsorption rate. To achieve this, we proposed two types of two-layer network, small pore assembly or large pore assembly at the upper layer network. For the lower layer, the pore assembly was assigned from a particular pore size distribution, and the pore size distribution from the dried banana foam density of 0.26 g/cm^3 was chosen because the texture at this density was rather crispy and not very hard, which was suitable for the snack as reported by Thuwapanichayanan et al. (2008). For the upper layer, the pores were assigned from the pore size distributions at foam densities of 0.21 and 0.31 g/cm^3. The pore size distribution from the foam density of 0.31 g/cm^3 was allocated randomly onto the upper half layer of the pore network with a size of 23×264, and this porous structure appeared the dense layer at the upper part of pore network as illustrated in Fig. 7b. On the other hand, if pores at the upper half layer of the pore network were allocated with the distributive size from the density of 0.21 g/cm^3, the structure exhibited very porous at the outer network as depicted in Fig. 7c.

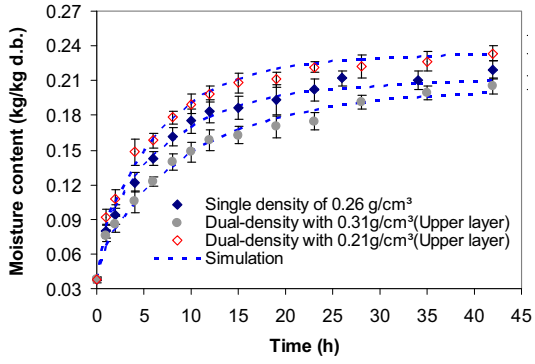

Fig .5. Moisture adsorption kinetics at 35°C and relative humidity of 67% of the single and dual-density of the banana foams and its simulation curve

Fig. 5 shows the simulation results of moisture uptake of banana foam samples exposed to the static air at temperature of 35°C and 67% RH. The moisture diffusion coefficients from Table 1 were used for calculating the moisture uptake in the two-layer networks. The slowest adsorption rate was evident in the two-layer network of which the pore sizes obtained from the foam density of 0.31 g/cm^3 was laid at the upper half. On the other hand, the fastest adsorption rate was found in the case that the pore sizes from the foam density of 0.21 g/cm^3 was laid on the upper half layer.

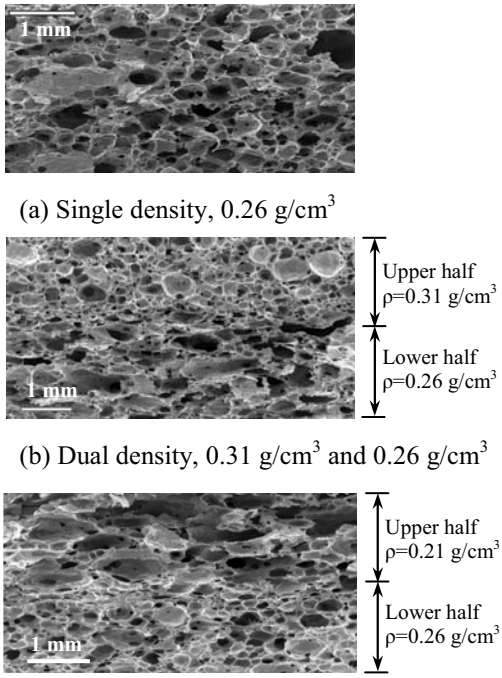

Fig. 6. SEM micrographs of single and dual-density of dried banana foam mats

To validate the simulation results, the two layer banana foams were produced and their morphologies are shown in Figs. 6b and 6c, showing low porosity and high porosity at the upper layer respectively. From the experiments, it indicated that the 2-D stochastic pore network can predict the moisture uptake throughout the exposure time in agreement with experiments, with the R^2-value of 0.95. The results from both simulation and experiments revealed that as the small pore assembly was positioned near the surface which is exposed to the humid air, it can limit the water vapor diffusing into the porous material, thus delaying the moisture uptake in the porous food. On the other, when small pore assembly in a porous food is covered with layers of porous material with large pores, such a porous structure provides less diffusional flux resistance and thus greatly facilitates the moisture transport to the porous foods. As shown in Fig. 5, the moisture uptake of the two-layer banana foam in the case of foam density of 0.21 g/cm^3 laid on the upper layer was faster than that in the single foam density of 0.26

g/cm^3 and this porous structure is not preferred for the crispy food, which is sensitive to moisture.

Graphical visualization

The visualization using colour represented the moisture content helped understanding of the interactions between moisture and pore structure. For calculating the moisture content, we used a large network size with 23×264. However, middle part of the large network was selected to represent the moisture movement in the idealised porous food and the visualization is shown in Fig. 7.

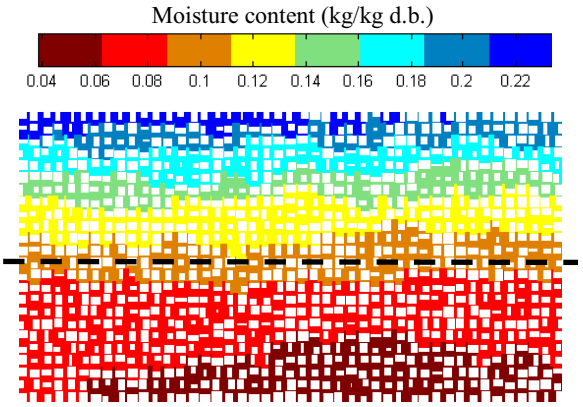

(a) Banana foam mats with single density of 0.26 g/cm^3 (0.109 kg/kg d.b.)

(b) Banana foam mats with dual density of 0.31 g/cm^3 on top (0.092 kg/kg d.b.)

(c) Banana foam mats with dual density of 0.21 g/cm^3 on top (0.127 kg/kg d.b.)

Fig. 7. Visualization of moisture contents in pores of banana foam mats at 3h of adsorption time

Each pore was colored according to its moisture content. The representative colours with 8 shades from dark red to blue were used for the corresponding range of moisture from 0.038 to 0.210 kg/kg d.b. At the beginning of adsorption, every pore within the network contained the moisture content of 0.038 kg/kg d.b. When the moisture migrated to the porous food, the concentration of moisture diffusing through pores positioned at the same horizontal plane was different, implying the different fluxes of moisture into pores due to the random assembly of pore sizes.

The moisture diffusing through the pores positioned at the same horizontal plane in Fig. 7a was different. When moisture migration to the network, moisture diffusing through the pores positioned at the same horizontal plane was different, reflecting the random assembly of pore sizes. With the two-layer networks, transport of moisture through pores was noticeably different from the single layer network. The moisture is difficult to reach the pores allocated at the lower part of network as shown in Fig. 7b, pores at the bottom half network coloured by dark brown corresponding to the moisture contents of 0.04-0.06 kg/kg d.b. On the other hand, it can arrive easily as the large pore assembly was dominant at upper part: moisture content in the pores at the lower part as shown in Fig. 7c was given in the range of 0.06-0.13 kg/kg.d.b.

Texture of dried banana foams

From Fig. 8a shows the curves of the force versus displacement recorded by texture analyzer of single and dual foam density. The direct force was applied until the sample has completely cracked. The jagged pattern of the force-deformation curve reflects the crispy behavior of the banana foam mats.

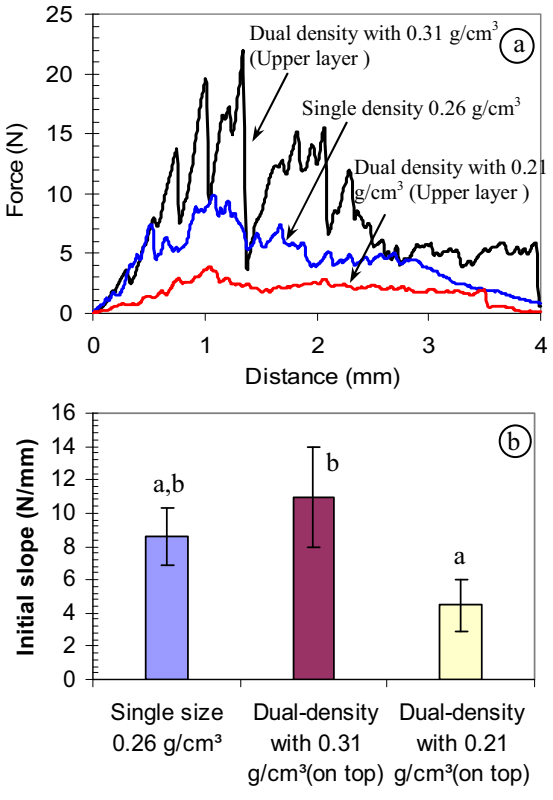

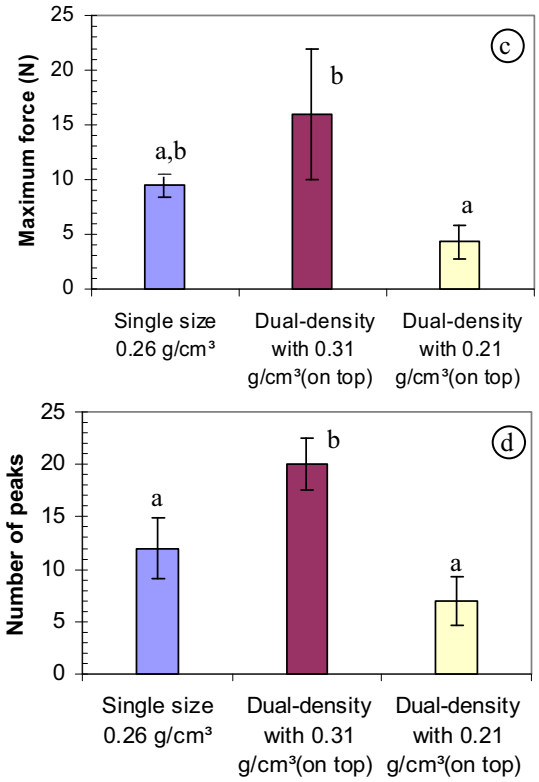

Fig. 8. Variation in force-deformation curve during compression test (a) and the textural parameters (b-d) at initial moisture content of dried banana foams (0.038 kg/kg d.b.)

As shown in Fig. 8a, the force curves were different the banana foam samples, presenting the strong effect of porous structure on textural property. The initial slope, maximum forces and number of peaks of single foam density and dual density were significantly different.

The dual density with high density of 0.31 g/cm^3 laid on the upper layer was crispier than the single density of banana foam as indicated by the number of peaks which showed higher than 20 for the dual density while it was 12 for the single density. In contrast, it is not crispy for the dual density with density of 0.21 g/cm^3 laid on the upper layer.

CONCLUSIONS

- The 2-D pore networks comprised of the cylindrical pore segments have been developed to determine the diffusion coefficient of moisture in pore and found that the diffusion coefficient determined from the moisture adsorption kinetics did not vary with the relative humidity but varied with the banana foam density, due to different pore shapes at the dried banana foam densities.
- The transport of moisture, from the humid air, through the 2-D stochastic pore network is highly complex. The diffusion rate of moisture moving through the individual pores within network was very different, indicating that the inherently random assembly of pores with different sizes governs the moisture migration. Such complex can be demonstrated through the visualization with the color code.
- The stochastic pore network can be applied successfully to design the porous structure and is able to predict the results in agreement with the experiment.
- The characteristic of porous structure was important to textural property of food besides the moisture migration. The two-layer porous structure of banana foam mats with the high foam density having most small pores laid on the upper layer of sample could resist the moisture adsorption and provided the crispy texture. On the other hand, the low crispness and rapid moisture migration was found in the banana foam mat with the low foam density characterizing most large pores laid on the upper layer of sample.

ACKNOWLEDGEMENTS

The authors would like to express their appreciation to the Commission on Higher Education, Thailand for supporting by grant fund under the program Strategic Scholarships for Frontier Research Network for the Ph.D. Program Thai Doctoral degree for this research. This work was also supported in part by the National Science and Technology Development Agency and King Mongkut's University of Technology Thonburi.

REFERENCES

AOAC. Official Methods of Analysis, 16th ed. (1995), Association of Official Agricultural Chemists, Washington, DC.

Blunt, M. (2001), Flow in porous media-pore-network models and multiphase flow. Current Openion in Colliod & Interface Science, Vol.6, pp. 197-207.

Bustos, C.I., and Toledo, P.G. (2004), Pore shape effects on the relative permeability of gas and condensate in three-dimensional pore networks. Transport in Porous Media, Vol. 55, pp. 247-251.

Cauvain, S. and Young, L. (2000), Bakery food manufacture and quality: Water control and effects, Blackwell Science, Oxford, UK.

Intel® Software Network. Available (2009) at: http://software.intel.com/en-us/articles/intel-c-compiler-professional-edition-for-windows-evaluation/

Pillai, K.M., Part, M. and Marcoux, M. (2009), A study on slow evaporation of liquids in a dual-porosity porous medium using square network

model, Internationnal Journal of Heat and Mass Transfer, Vol. 52, pp. 1643-1656.

Prat, M. and Bray, Y., Le. (1999), Three dimensional pore network simulation of drying in capillary porous media. Internationnal Journal of Heat and Mass Transfer, Vol. 42, pp. 4207-4224.

Prakotmak, P., Soponronnarit, S. and Prachayawarakorn, S. (2010), Modelling of moisture diffusion in pores of banana foam mat using a 2-D stochastic pore network: Determination of moisture diffusion coefficient during adsorption process, Journal of Food Engineering, Vol. 96, pp. 119-126.

Saravacos, G.D. and Maroulis, Z.B. (2001), Transport properties of foods, Marcel Dekker, New York.

Segura, L. A., and Toledo, P. G. (2005), Pore-level modeling of isothermal drying of pore networks: Effects of gravity and pore shape and size distributions on saturation and transport parameters, Chemical Engineering Journal, Vol. 111, pp. 237-252.

Stewart, M.L., Ward, A.L. and Rector, D.R. (2006), A study of pore geometry effects on anisotropy in hydraulic permeability using the lattice-Boltzmann method. Advances in Water Resources, Vol. 29, pp. 1328-1340.

Thuwapanichayanan, R., Prachayawarakorn, S. and Sopornronnarit, S. (2008), Modeling of diffusion with shrinkage and quality investigation of banana foam mat drying, Drying Technology, Vol. 26, pp. 1326-1333.

Yiotis, A.G., Stubos, A. K., Boudouvis, A. G., Tsimapanogiannis, I. N. and Yortsos, Y. C. (2005), Pore-network modeling of isothermal drying in porous media. Transport in Porous Media, Vol. 58, pp. 63-86.

การหาสภาวะที่เหมาะสมของการพัฟฟิงกล้วยด้วยไอน้ำร้อนยวดยิ่ง

Optimization of the superheated steam puffing of banana

คำพัน บัวละพัน[1] สมเกียรติ ปรัชญาวรากร[2] สมชาติ โสภณรณฤทธิ์[3] วารุณี เตีย[4]

Khamphanh Boualaphanh[1] Somkiat Prachayawarakorn[2] Somchart Soponronnarit[3] Warunee Tia[4]

Abstract

The purpose of this research was to investigate the effects of superheated steam temperature and puffing time and moisture content of banana before puffing on physical properties of banana slice i.e. shrinkage, texture and color. The banana was dried with three drying steps, hot air drying at a temperature of 90°C and a velocity of 2 m/s in order to reduce moisture contents to the range of 20-30% d.b. followed by puffing it with superheated steam at temperatures of 160, 170 and 180°C and puffing time of 1, 2 and 3 minutes. After puffing step the samples were dried by hot air at the same conditions at the first step until its final moisture content reduced to 3% d.b. The results showed that the high puffing temperature and long puffing time caused high values of redness (a) and low values of both lightness (L) and yellowness (b). In addition, high puffing temperature resulted in low shrinkage, low hardness and high crispiness. The optimal puffing conditions were at the superheated steam temperatures of 180°C, puffing time of 1.4 min and moisture content of banana before puffing 26.16. %d.b.

Keyword: Banana/ Color/ Puffing/ Shrinkage / Superheated steam/ Texture

บทคัดย่อ

งานวิจัยนี้มีวัตถุประสงค์เพื่อศึกษาปัจจัยของอุณหภูมิของไอน้ำร้อนยวดยิ่ง เวลาในการพัฟฟิง(puffing) และ ความชื้นของกล้วยก่อนการพัฟฟิง ที่มีผลต่อคุณสมบัติทางกายภาพของกล้วยแผ่นในด้านต่าง ๆ ได้แก่ การหดตัว เนื้อสัมผัส (ความแข็ง และความกรอบ) และ สี โดยใช้เทคนิคการอบแห้งด้วยลมร้อนร่วมกับการพัฟฟิงด้วยไอน้ำร้อนยวดยิ่ง ซึ่งแบ่งออกเป็น 3 ขั้นตอนได้แก่ ในขั้นตอนแรกทำการอบแห้งด้วยลมร้อนที่อุณหภูมิ 90°C ความเร็วลม 2 m/s เพื่อลดความชื้นของกล้วยให้เหลือระหว่าง 20-30% d.b. ตามด้วยการพัฟฟิงด้วยไอน้ำร้อนยวดยิ่งที่อุณหภูมิ 160, 170 และ 180°C เป็นเวลา 1, 2 และ 3 นาที และในขั้นสุดท้ายนำไปอบแห้งด้วยลมร้อนที่สภาวะเดียวกันกับในขั้นตอนแรกให้เหลือความชื้นสุดท้ายประมาณ 3 % d.b. จากผลการทดลองพบว่า เมื่อใช้อุณหภูมิของไอน้ำร้อนยวดยิ่งสูงขึ้นและเวลาในการพัฟฟิงมากขึ้น ผลิตภัณฑ์กล้วยแผ่นที่ได้มีค่าความเป็นสีแดง (ค่า a) เพิ่มขึ้น ค่าความสว่าง (ค่า L) และ ค่าความเป็นสีเหลือง (b) ลดลง การพัฟฟิงด้วยไอน้ำร้อนยวดยิ่งที่อุณหภูมิสูง ทำให้ผลิตภัณฑ์ที่ได้มีการหดตัวน้อย มีค่าความแข็งต่ำ มีความกรอบมาก สภาวะที่เหมาะสมของการพัฟฟิงของกล้วยอยู่ที่อุณหภูมิของไอน้ำร้อนยวดยิ่งเท่ากับ 180°C เวลาที่ใช้ในการพัฟฟิงเท่ากับ 1.4 นาที และ ความชื้นของกล้วยก่อนการพัฟฟิงเท่ากับ 26.16 %d.b.

คำสำคัญ: กล้วย/ การพัฟฟิง/ การหดตัว/ เนื้อสัมผัส/ สี/ ไอน้ำร้อนยวดยิ่ง

---

1) Graduated student,

2) Associate Professor, Faculty of Engineering,

3) Professor, School of Energy and Materials,

4) Associate Professor, School of Energy and Materials,

King Mongkut's University of Technology Thonburi, 126 Prachautid, Tungkru, Bangkok 10140

*Corresponding author. Tel.:0-0-2470-8695 ext.112; E-mail address: khamphans@hotmail.com

บทนำ

กล้วยเป็นผลไม้ที่นิยมบริโภคในรูปของผลสดโดยเฉพาะกล้วยหอม แต่เนื่องจากกล้วยเป็นผลไม้ที่เน่าเสียได้ง่าย จึงนิยมนำมาแปรรูปเป็นผลิตภัณฑ์ในรูปแบบต่าง ๆ เช่น กล้วยอบ กล้วยตาก กล้วยฉาบ กล้วยแผ่น เป็นต้น การแปรรูปมีความสำคัญยิ่งต่อการรักษาคุณภาพ ลดความสูญเสีย ยืดเวลาการเก็บผลิตภัณฑ์ให้ได้นานขึ้น และทำให้ผลิตภัณฑ์หลังการแปรรูปมีมูลค่าเพิ่มมากขึ้นด้วย ผลิตภัณฑ์กล้วยแผ่นที่มีขายตามท้องตลาดส่วนใหญ่ทำการแปรรูปโดยการทอดในน้ำมัน ผลิตภัณฑ์ที่ได้มักจะมีสีเข้ม สีไม่สม่ำเสมอ เมื่อเก็บไว้นานกล้วยแผ่นจะเกิดกลิ่นหืนเนื่องจากปฏิกิริยาออกซิเดชันของไขมันกับออกซิเจน ในปัจจุบันผลิตภัณฑ์อาหารว่างที่มีปริมาณไขมันสูงอาจไม่เป็นที่ต้องการของผู้บริโภคที่ใส่ใจในสุขภาพ เพราะไขมันก่อให้เกิดโรคหัวใจ ความดันโลหิตสูงและโรคอ้วน ผลิตภัณฑ์กล้วยแผ่นที่มีขายตามท้องตลาดส่วนมากจะผลิตโดยการทอดในน้ำมันที่ใช้อุณหภูมิประมาณ 177 ถึง 200°C ผลิตภัณฑ์ที่ได้มักจะมีสีน้ำตาลเข้มและมีปริมาณไขมันสูง ในการผลิตอาหารว่างประเภทขนมขบเคี้ยวที่มีลักษณะพองกรอบ นั้นจะเกี่ยวข้องกับปริมาณความชื้น อุณหภูมิของตัวกลาง และเวลาที่ใช้ในกระบวนการ เช่น การทำข้าวเกรียบ โดยความชื้นที่เหมาะสมของข้าวเกรียบดิบคือ 12 % เมื่อทอดในน้ำมันร้อนที่อุณหภูมิ 180 °C โดยใช้เวลาสั้นมากจะได้ผลิตภัณฑ์ข้าวเกรียบที่มีรูพรุนสม่ำเสมอ ความหนาแน่นต่ำ ถ้าทอดในน้ำที่อุณหภูมิต่ำข้าวเกรียบจะไม่พอง เพราะอุณหภูมิไม่สูงพอที่จะให้น้ำกลายเป็นไอได้อย่างรวดเร็ว ขณะเดียวกันหากความชื้นของข้าวเกรียบดิบสูงจะได้ผลิตภัณฑ์ข้าวเกรียบที่มีรูพรุนใหญ่บ้างเล็กบ้างไม่สม่ำเสมอ ซึ่งเป็นลักษณะของข้าวเกรียบคุณภาพต่ำ (เพลินใจ ตังคณะกุล, 2546) ดังนั้นในงานวิจัยนี้จึงมีวัตถุประสงค์เพื่อหาสภาวะที่เหมาะสมในการผลิตกล้วยแผ่นให้เป็นผลิตภัณฑ์อาหารขบเคี้ยวที่ไม่มีไขมัน โดยจะทำการศึกษาถึงอิทธิพลของความชื้นของกล้วยแผ่นก่อนกระบวนการพัฟฟิง อุณหภูมิของไอน้ำร้อนยวดยิ่งและเวลาที่ใช้ ในกระบวนการพัฟฟิง

อุปกรณ์และวิธีการทดลอง

อุปกรณ์การทดลอง

เครื่องอบแห้งด้วยลมร้อนและไอน้ำร้อนยวดยิ่งที่ใช้ในการทดลอง ดังรูปที่ 1 ประกอบด้วยอุปกรณ์หลักคือ เครื่องกำเนิดไอน้ำ เพื่อผลิตไอน้ำความดันสูงกว่าบรรยากาศเล็กน้อย อุปกรณ์ให้ความร้อน เพื่อให้ความร้อนกับอากาศและทำให้ไอน้ำอิ่มตัวกลายเป็นไอน้ำร้อนยวดยิ่ง ขนาด 13.5 kW โดยการควบคุมด้วย PID มีค่าความถูกต้อง ± 1°C ห้องอบแห้ง ขนาด 30 x30 x10 cm^3 พัดลมเป็นแบบเหวี่ยงใบพัดโค้งหลัง อัตราการไหลของตัวกลางที่ใช้ในการอบแห้งควบคุมโดยการปรับความเร็วรอบของพัดลม และในระบบอบแห้งยังประกอบด้วยอุปกรณ์อื่น ๆ เช่น วาล์ว ควบคุมและมาตรวัดความดัน

การออกแบบการทดลอง และการหาสภาวะที่เหมาะสม

การทดลองอบแห้งกล้วยแผ่นด้วยลมร้อนร่วมกับการพัฟฟิงด้วยไอน้ำร้อนยวดยิ่งโดยมี 3 ขั้นตอนคือ ในขั้นตอนแรกอบแห้งกล้วยแผ่นด้วยลมร้อนที่อุณหภูมิ 90 °C โดยใช้ความเร็วเฉลี่ยของอากาศเข้าห้องอบแห้งประมาณ 2 m/s อบกล้วยแผ่นให้เหลือความชื้นประมาณ 20, 25 และ 30% d.b. ตามด้วยการพัฟฟิงด้วยไอน้ำร้อนยวดยิ่งที่อุณหภูมิ 160, 170 และ 180 °C ที่เวลาพัฟฟิง 1, 2 และ 3 นาที และในขั้นตอนสุดท้ายนำไปอบ

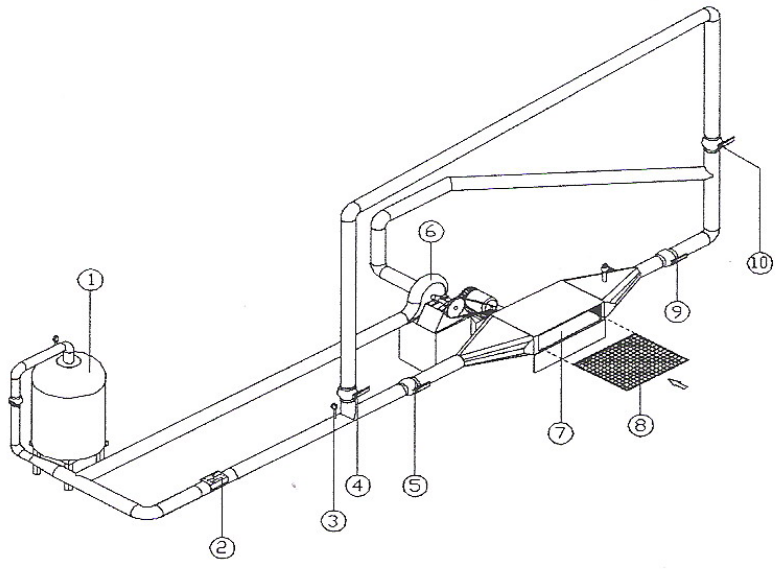

1. เครื่องกำเนิดไอน้ำ (Boiler)
2. อุปกรณ์ให้ความร้อน (Heater)
3. มาตรวัดความดัน (Pressure gauge)
4., 5., 9.,10. วาล์ว(Valve)
6. พัดลม(Blower)
7. ห้องอบแห้ง (Drying chamber)
8. ถาดอบแห้ง

รูปที่ 1 ไดอะแกรมระบบอบแห้งด้วยลมร้อนและไอน้ำร้อนยวดยิ่ง

ตารางที่ 1 แสดงตัวแปรและระดับของตัวแปรที่ต้องการศึกษา

Independent Variable	Symbol		Levels	
	Uncoded	Coded	Uncoded	Coded
Steam Temperature (°C)	Temperature	x_1	160	1
			170	2
			180	3
Puffing time (min)	time	x_2	1	1
			2	2
			3	3
Moisture content (% d.b.)	Moisture	x_3	20	1
			25	2
			30	3

แห้งด้วยลมร้อนที่สภาวะเดียวกันกับในขั้นตอนแรก อบแห้งกล้วยแผ่นให้เหลือความชื้นประมาณ 3%d.b. ในการออกแบบการทดลองเป็นแบบ Full Factorial โดยมีการศึกษา 3 ตัวแปร 3 ระดับ จำนวนการทดลองทั้งหมด 27 การทดลอง ดังแสดงในตารางที่ 1

การอบแห้งกล้วยหอมแผ่น ด้วยลมร้อนร่วมกับการพัฟฟิงด้วยไอน้ำร้อนยวดยิ่ง ปัจจัยที่ต้องการศึกษาได้แก่ อุณหภูมิของไอน้ำร้อนยวดยิ่ง ความชื้นก่อนการพัฟฟิง และเวลาพัฟฟิง ที่มีผลต่อคุณภาพของกล้วยด้าน เนื้อสัมผัส (Hardness, Number of peaks และ Initial slope) การหดตัว (Shrinkage) และสี (L, a และ b) ของกล้วยแผ่น ในงานวิจัยนี้ทำการหาสภาวะที่เหมาะสมด้วยวิธี Response Surface Methodology (RSM) การหาความสัมพันธ์ระหว่างตัวแปรกับผลตอบสนองในรูปสมการโพลิโนเมียลกำลังสอง โดยมีรูปแบบทั่วไปดังดังสมการ (1)

$$y = \beta_0 + \sum_{i=1}^{k} \beta_i x_i + \sum_{i=1}^{k} \beta_{ii} x_i^2 + \sum_{i=1}^{k} \sum_{j=1}^{k} \beta_{ij} x_i x_j + \varepsilon \quad (1)$$

โดยตัวแปรที่ต้องการศึกษามี 3 ตัวคือ อุณหภูมิของไอน้ำร้อนยวดยิ่ง (x_1) เวลาพัฟฟิง (x_2) และความชื้นของกล้วยก่อนการพัฟฟิง (x_3) จากสมการ (1) สามารถเขียนสมการได้ดังสมการ (2)

$$y = \beta_0 + \beta_1 x_1 + \beta_2 x_2 + \beta_3 x_3 + \beta_4 x_1^2 + \beta_5 x_2^2 + \beta_6 x_3^2 + \beta_7 x_1 x_2 + \beta_8 x_1 x_3 + \beta_9 x_2 x_3 \quad (2)$$

เมื่อ $\beta_0, \beta_1, \ldots\ldots \beta_9$ เป็นค่าคงที่

การวิเคราะห์ความแปรปรวน (ANOVA) ของสัมประสิทธิ์ถดถอยในสมการที่ (2) โดยการฟิตกับข้อมูลที่ได้จากการทดลอง เพื่อวิเคราะห์หานัยสำคัญทางสถิติในแต่ละเทอมของแบบจำลอง

สำหรับการหาสภาวะที่เหมาะสมของตอบสนองหลายค่า (Multiple response) จะใช้ฟังก์ชันความพึงพอใจโดยรวม (Desirability Function) (Myers & Montgomery, 2002) เพื่อหาค่าที่เหมาะสมของปัจจัย ดังสมการที่ (3)

$$D = \left[d_1(y_1) \bullet d_2(y_2) \bullet \ldots\ldots \bullet d_k(y_k) \right]^{\frac{1}{k}} \quad (3)$$

โดย k คือ จำนวนของผลตอบสนอง

$d_1(y_1)$, $d_2(y_2)$ และ $d_k(y_k)$ คือ ความพึงพอใจของผลตอบสนอง y_1, y_2 และ y_k ตามลำดับ

การเตรียมตัวอย่าง

กล้วยหอมทองระยะสุกที่ 3 ซึ่งพิจารณาได้จากสีของเปลือกจากเขียวออกเหลืองมากขึ้นแต่ยังมีสีเขียวมากกว่าสีเหลือง โดยความหวานของเนื้อกล้วยมีค่าประมาณ 14-18 %Brix ขนาดเส้นผ่านศูนย์กลางประมาณ 25 mm ความชื้นเริ่มต้นของกล้วยแผ่นก่อน การพรีทรีทเมนต์เท่ากับ 250-300 %d.b. ปอกเปลือกและหั่นตามขวางด้วยเครื่องหั่น ความหนาของชิ้นตัวอย่างมีขนาด 35 mm ก่อนการทดลองทำการพรีทรีทเมนต์ตัวอย่างด้วยสารละลายกรดแอสคอร์บิคความเข้มข้น 0.1% (w/w) นาน 1 นาที (Demirel และ Turhan, 2003) หลังจากนั้นนำตัวอย่างมาล้างด้วยน้ำกลั่นนาน 30 วินาที ซับน้ำให้แห้งแล้วทิ้งไว้ 5 นาที จากนั้นนำไปจัดเรียงบนตะแกรงก่อนเข้าเครื่องอบแห้ง

วิธีการทดลอง

ทำการอบแห้งกล้วยแผ่น ที่ผ่านการพรีทรีทเมนต์ด้วยสารละลายกรดแอสคอร์บิคด้วยอากาศร้อนในขั้นตอนแรกที่อุณหภูมิ 90°C ให้เหลือความชื้นเท่ากับ 20, 25 และ 30 %d.b แล้วทำให้พองตัว (puffing) ด้วยไอน้ำร้อนยวดยิ่งที่อุณหภูมิ 160, 170 และ 180°C โดยใช้เวลา 1, 2 และ 3 นาที และในขั้นตอนสุดท้ายนำ

กลับไปอบแห้งด้วยลมร้อนที่สภาวะเดิมกับในตอนเริ่มต้นจนเหลือความชื้นสุดท้ายประมาณ 3% d.b. จากนั้นนำผลิตภัณฑ์กล้วยแผ่นที่ได้ไปทดสอบคุณภาพในด้านสี การหดตัว และเนื้อสัมผัส

การทดสอบคุณภาพด้านสี

สีของกล้วยแผ่นทำการวัดโดยใช้เครื่องวัดสีอาหาร HunterLab รุ่น ColorFlex โดยวัดค่าสีของกล้วยแผ่นตามระบบ Hunter ซึ่งแสดงในเทอมของตัวแปร L, a และ b โดยค่า L แสดงค่าความสว่าง, a แสดงค่าสีแดงและสีเขียว, b แสดงค่าสีเหลืองและน้ำเงิน การทดสอบจะใช้กล้วยแผ่นอบแห้ง 3 ตัวอย่างและวัดสีตัวอย่างละ 6 ครั้ง โดยก่อนจะวัดสีของกล้วยแผ่นด้วยเครื่องวัดสีดังกล่าว ต้องทำการทดสอบเปรียบเทียบ (Calibrate) ด้วยแผ่นสีมาตรฐานที่มีลักษณะเป็นแผ่นสีดำและสีขาว

การทดสอบคุณภาพด้านการหดตัว

การทดสอบคุณภาพด้านการหดตัวของกล้วยแผ่นใช้วิธีแทนที่ปริมาตรกล้วยแผ่นในของแข็งทั้งก่อนและหลังการอบแห้ง ตัวอย่างละ 10 ชิ้น โดยของแข็งที่ใช้ทดสอบคือ Glass beads ซึ่งมีขนาดมีเส้นผ่านศูนย์กลาง 0.106-0.212 mm (Hwang และ Hayakawa, 1980) ร้อยละการหดตัวเทียบกับปริมาตรของกล้วยสด สามารถคำนวณได้จากสมการ (4)

$$\%Shrinkage = \frac{V_0 - V}{V_0} \times 100 \qquad (4)$$

โดย V_o คือ ปริมาตรของกล้วยแผ่นสด, cm^3

V คือ ปริมาตรของกล้วยแผ่นหลังจากการอบแห้ง, cm^3

การทดสอบคุณภาพด้านเนื้อสัมผัส

การทดสอบคุณภาพด้านเนื้อสัมผัสของกล้วยแผ่นหลังการอบแห้งโดยใช้เครื่อง Texture Analyzer รุ่น TA.XT.plus (Stable Microsystems Texture Technologies Inc.,UK) ค่าความถูกต้อง ± 0.001 N โดยจะทำการทดสอบในลักษณะของแรงกดใช้หัวกดแบบตัด (Cutting probe) และความเร็วในการกด 2 mm/s กดจนกระทั่งตัวอย่างแยกออกจากกัน พิจารณาคุณภาพด้านเนื้อสัมผัสของกล้วยแผ่นจากค่าความแข็ง (Hardness) จำนวนยอด (Number of peaks) ที่มีค่า Theshold force ตั้งแต่ 30 g ขึ้นไป และความชันเริ่มต้น (Initial slop)

ผลการทดลองและวิจารณ์

การวิเคราะห์ความแปรปรวนของปัจจัยที่ต้องการศึกษา คือ อุณหภูมิของไอน้ำร้อนยวดยิ่ง เวลาพัฟฟิง และความชื้นของกล้วยแผ่นก่อนการพัฟฟิงต่อคุณภาพของกล้วยแผ่นดังตารางที่ 2 โดยเป็นผลการวิเคราะห์การถดถอยของแบบจำลองพบว่า เวลาพัฟฟิงมีอิทธิพลต่อคุณภาพด้านสี (ค่า L, a, b) มากที่สุด โดย

ตารางที่ 3 ค่าคงที่ต่าง ๆ ของสมการที่ (2) ซึ่งได้จากการวิเคราะห์การถดถอยสำหรับคุณภาพด้านต่าง ๆ

Coefficient	Texture			shrinkage	Color		
	Hardness	Number of Peaks	Initial slope		L-value	a-value	b-value
Intercept							
β_0	4208.59*	-1027.46*	-774.44*	1834.90*	517.61*	-17.368*	57.799*
Linear							
β_1	-52.166*	13.478*	10.458*	-17.981*	-5.72	0.431	-0.467
β_2	92.081	9.083	-38.625	-12.698*	3.648*	-6.614*	-0.206
β_3	17.614	-10.211	-6.293	-16.933*	1.893*	-0.714	0.206
Quadratic							
β_4	0.166*	-0.046	-0.035	0.049*	0.017	-0.0014	0.0014
β_5	-1.718	-4.278	-3.888	4.007	-1.209	0.212	-0.611*
β_6	0.208	-0.131	-0.037	0.261*	-0.049	0.0244	-0.0014
Interaction							
β_7	-0.468*	0.058	0.304	-0.139	-0.039	0.060*	0.011
β_8	-0.165*	0.100*	0.048	0.023	-0.0016	-0.0016	-0.0013
β_9	-0.211	-0.1	0.075	0.541	0.249	-0.135*	0.025
R^2	0.8	0.59	0.53	0.87	0.6	0.69	0.52

* Significant at 95% level

อิทธิพลที่มีต่อค่า L นั้น คือ เวลาพัฟฟิงและความชื้นก่อนการพัฟฟิง สำหรับอิทธิพลที่มีต่อค่า a มากที่สุดคือ เวลาพัฟฟิง โดยเฉพาะผลรวมของเวลาพัฟฟิงกับอุณหภูมิของไอน้ำร้อนยวดยิ่ง (ในเทอมของ Interaction) จะมีอิทธิพลต่อค่า a มาก สำหรับอิทธิพลของปัจจัยต่อค่า b ไม่เด่นชัดนัก จากการทดสอบจะได้ว่าค่าสัมประสิทธิ์การตัดสินใจ (R^2) ของสมการถดถอยคุณภาพของกล้วยแผ่นด้านความแข็ง และการหดตัวเท่ากับ 0.80 และ 0.87 ตามลำดับ ซึ่งทำให้สามารถใช้สมการที่ได้ไปทำนายคุณภาพของกล้วยแผ่นที่สภาวะต่าง ๆ ได้อย่างมีประสิทธิภาพ แต่สำหรับสมการถดถอยคุณภาพของกล้วยแผ่น ด้านอื่น ๆ ค่าสัมประสิทธิ์การตัดสินใจค่อนข้างต่ำ ซึ่งอาจจะทำให้มีความคลาดเคลื่อนอยู่บ้างเมื่อนำไปใช้

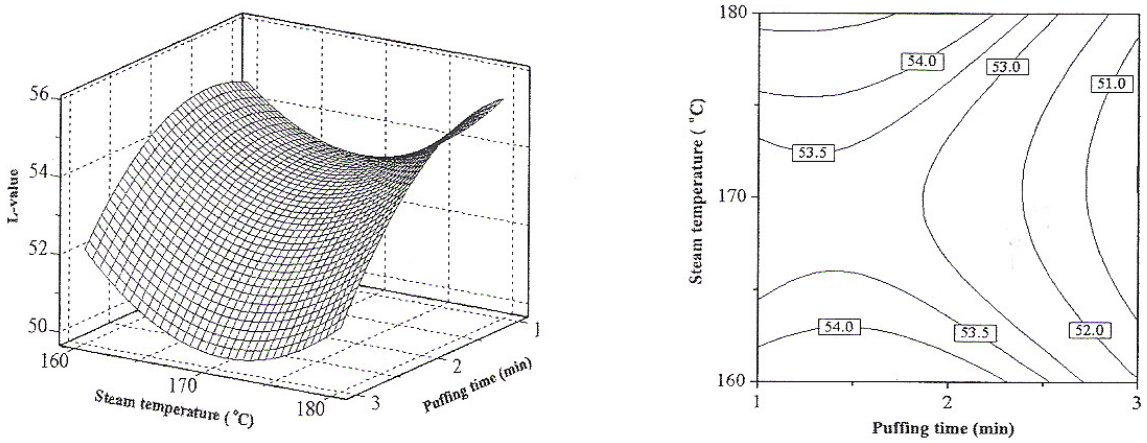

(ก) การเปลี่ยนแปลงค่า L ของกล้วยแผ่น

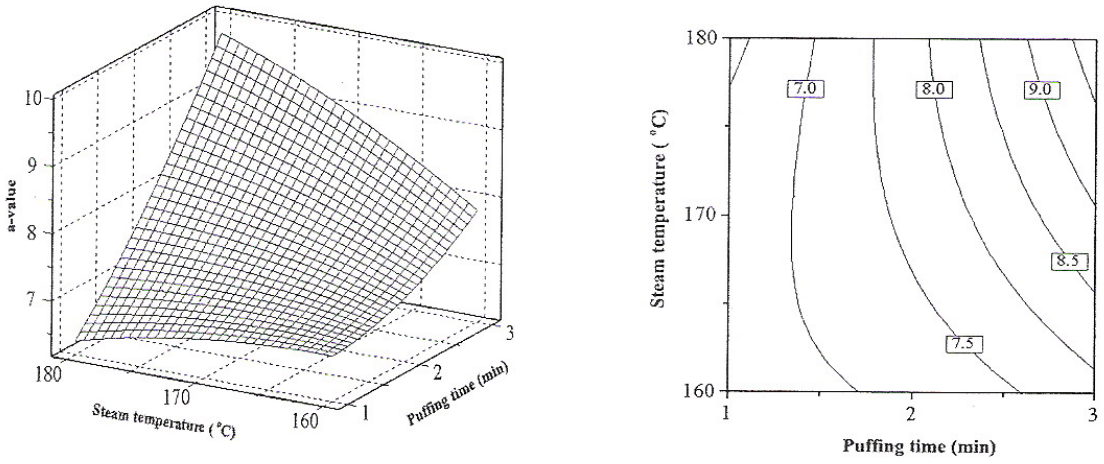

(ข) การเปลี่ยนแปลงค่า a ของกล้วยแผ่น

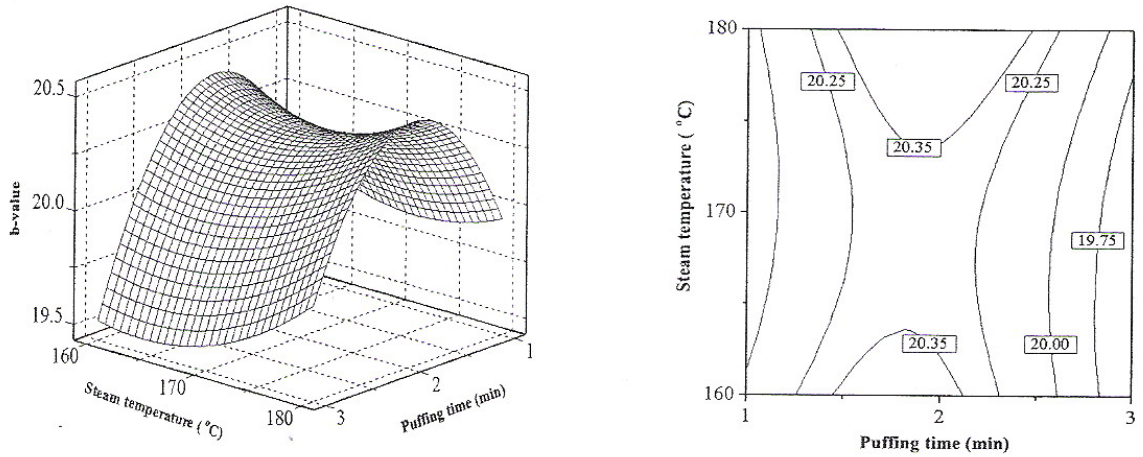

(ค) การเปลี่ยนแปลงค่า b ของกล้วยแผ่น

รูปที่ 2 ผลของอุณหภูมิและเวลาพัฟฟิงต่อการเปลี่ยนสีของกล้วยแผ่น (ความชื้นของกล้วยแผ่นก่อนการพัฟฟิง 25%d.b.)

คุณภาพด้านสีของกล้วยแผ่น

จากการทดลองพบว่าก ารเปลี่ยนสีของกล้วยแผ่นที่ได้หลังการอบแห้งด้วยลมร้อนอย่างเดียว และการอบแห้งด้วยลมร้อนร่วมกับการพัฟฟิงด้วยไอน้ำร้อนยวดยิ่งจะมีสีโดยรวมเป็นสีเหลืองปนน้ำตาล โดยบริเวณรอบจุดศูนย์กลางของกล้วยแผ่นจะมีสีน้ำตาลเข้มมากที่สุด เนื่องจากมีปริมาณน้ำตาลมากกว่าบริเวณอื่น ๆ โดยผลของอุณหภูมิ เวลาพัฟฟิง และความชื้นของกล้วยแผ่นก่อนการพัฟฟิงต่อการเปลี่ยนแปลงสีของกล้วยแผ่นในเทอมของ L, a และ b ดังแสดงในรูปที่ 2 ซึ่งจะประกอบด้วย surface plot และ contour plot

รูปที่ 2 (ก) แสดงผลของอุณหภูมิของไอน้ำร้อนยวดยิ่งและเวลาพัฟฟิงต่อการเปลี่ยนแปลงสีของกล้วยแผ่น พบว่าเวลาพัฟฟิงมีอิทธิพลต่อความสว่าง (ค่า L) มากกว่าอิทธิพลของอุณหภูมิไอน้ำร้อนยวดยิ่ง เมื่อเวลาพัฟฟิงมากขึ้นค่า L ลดลง เนื่องมาจากที่เวลาพัฟฟิงนานขึ้นทำให้เกิดปฏิกิริยาสีน้ำตาลเพิ่มขึ้น สำหรับอิทธิพลของอุณหภูมิไอน้ำร้อนยวดยิ่งนั้นพบว่าการเพิ่มอุณหภูมิในช่วงระหว่าง 160-170°C ค่า L มีค่าลดลงหลังจากนั้นค่า L มีแนวโน้มเพิ่มขึ้น ทั้งนี้เนื่องจากที่อุณหภูมิพัฟฟิงต่ำนั้นหลังสิ้นสุดกระบวนการพัฟฟิงความชื้นของกล้วยแผ่นยังเหลืออยู่มากทำให้การอบแห้งในขั้นตอนที่ 3 นั้น ใช้ระยะเวลานานขึ้น

รูปที่ 2 (ข) แสดงอิทธิพลของอุณหภูมิไอน้ำร้อนยวดยิ่งและเวลาพัฟฟิงต่อการเปลี่ยนแปลงค่า a ของกล้วยแผ่น พบว่าเมื่อเวลาพัฟฟิงนานและอุณหภูมิพัฟฟิงสูงขึ้น ค่าของ a ซึ่งแสดงความเป็นสีแดงมีค่าสูงขึ้น จากรูปจะเห็นว่า ที่เวลาพัฟฟิง 3 นาที เมื่ออุณหภูมิของการพัฟฟิงสูงขึ้น การเปลี่ยนแปลงของ a จะเป็นไปอย่างรวดเร็ว แต่ผลของอุณหภูมิอาจไม่เด่นชัดนักเมื่อเวลาในการพัฟฟิงสั้น (1 นาที) จากรูปค่า a มีค่าต่ำสุดเท่ากับ 6.12±0.7 ที่อุณหภูมิของไอน้ำร้อนยวดยิ่ง 180°C และ เวลาในการพัฟฟิง 1 นาที

รูปที่ 2 (ค) แสดงอิทธิพลของอุณหภูมิไอน้ำร้อนยวดยิ่งและวลาพัฟฟิงต่อการเปลี่ยนแปลงค่า b ของกล้วยแผ่น พบว่าเวลาพัฟฟิงจะมีอิทธิพลต่อค่า b มากกว่าอิทธิพลของอุณหภูมิไอน้ำร้อนยวดยิ่ง แต่อย่างไรก็ตามช่วงของค่า b ที่เปลี่ยนแปลงจะแคบมากโดยค่า b อยู่ระหว่าง 19.25 และ 20.29 ตลอดเงื่อนไขการทดลอง

การหดตัวของกล้วยแผ่น

รูปที่ 3 แสดงอิทธิพลของเวลาพัฟฟิงและอุณหภูมิของไอน้ำร้อนยวดยิ่งต่อร้อยละการหดตัวของกล้วยแผ่น พบว่า เมื่ออุณหภูมิของไอน้ำร้อนยวดยิ่ง และเวลาพัฟฟิงนานขึ้น ส่งผลให้ร้อยละการหดตัวของกล้วยแผ่นน้อยลง เนื่องจากที่อุณหภูมิสูงและเวลาพัฟฟิงนานขึ้นนั้นจะทำให้น้ำในกล้วยแผ่นเดือดกลายเป็นไออย่างรวดเร็ว เกิดความดันไอขึ้นภายในกล้วยแผ่น โครงสร้างมีการพองตัวขึ้น ในการพัฟฟิงที่อุณหภูมิสูง และเวลาพัฟฟิงนานนั้น ความชื้นของกล้วยแผ่นหลังกระบวนการพัฟฟิงจะเหลืออยู่น้อยมากทำให้โครงสร้างมีเสถียรภาพมากขึ้นเมื่อนำไปอบแห้งในขั้นตอนสุดท้ายโครงสร้างจะไม่มีการยุบตัวอีก ทำให้ร้อยละการหดตัวมีน้อย

คุณภาพด้านเนื้อสัมผัสของกล้วยแผ่น

คุณภาพด้านเนื้อสัมผัสของกล้วยแผ่น จะพิจารณาจากค่าความแข็ง จำนวนยอด และ ความชันเริ่มต้น โดยที่จำนวนยอดและความชันเริ่มต้น แสดงถึงความกรอบของผลิตภัณฑ์ หากจำนวนยอดและความชันเริ่มต้นมาก ก็แสดงว่าผลิตภัณฑ์มีความกรอบมาก เนื่องจากยอดเกิดจากการเปลี่ยนแปลงความชันของกราฟความสัมพันธ์ระหว่างแรงกับระยะทาง ซึ่งการเปลี่ยนแปลงความชันเกิดจากผลิตภัณฑ์มีช่องว่างหรือโพรงอากาศภาย

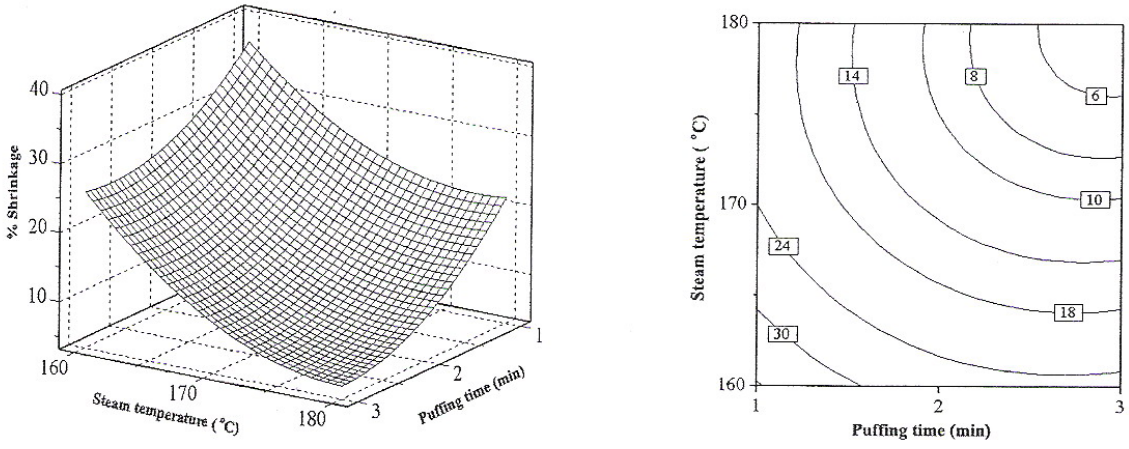

รูปที่ 3 ผลของอุณหภูมิและเวลาพัฟฟิงต่อการหดตัวของกล้วยแผ่น(ความชื้นของกล้วยแผ่นก่อนการพัฟฟิง 25% d.b.)

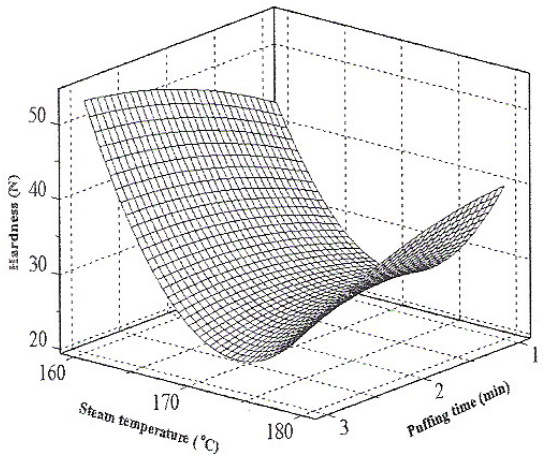

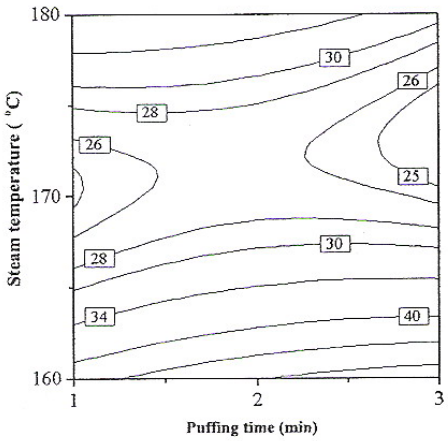

(ก) ผลของอุณหภูมิและเวลาพัฟฟิงต่อความแข็งของกล้วยแผ่น

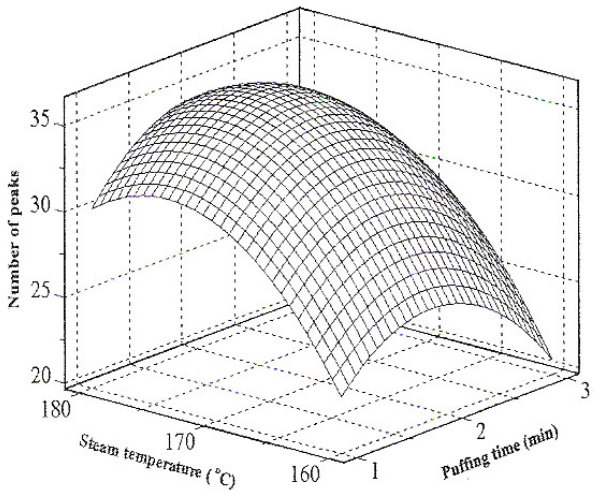

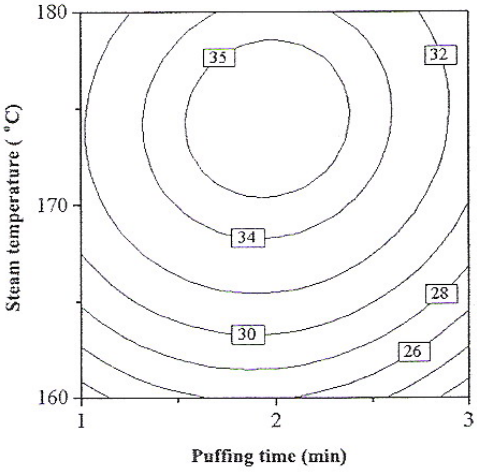

(ข) ผลของอุณหภูมิและเวลาพัฟฟิงต่อจำนวนยอดของกล้วยแผ่น

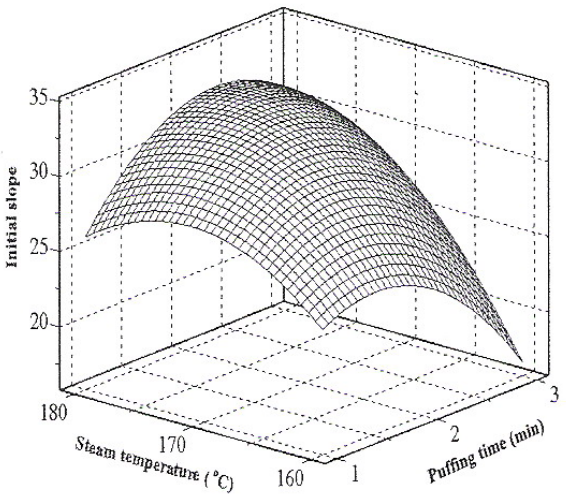

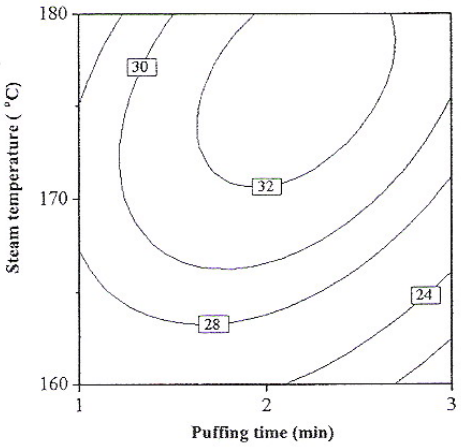

(ค) ผลของอุณหภูมิและเวลาพัฟฟิงต่อความชันเริ่มต้นของกล้วยแผ่น

รูปที่ 4 ผลของอุณหภูมิ และเวลาพัฟฟิงต่อเนื้อสัมผัสของกล้วยแผ่น (ความชื้นของกล้วยแผ่นก่อนการพัฟฟิง 25%d.b.)

ตารางที่ 4 ผลที่ได้จากการทำ optimization

	Hardness	Peaks	slope	Shrinkage	L-value	a-value	b-value
Optimal value	37.081	33.982	30.025	17.019	54.615	7.000	20.238
Individual Desirability (d_i)	0.996	0.999	1.000	0.999	0.9777	1.000	0.981
Composite Desirability (D)			0.994				

ใน ผลิตภัณฑ์ที่มีความกรอบมากจะมีจำนวนยอดมากและมีค่าความแข็งน้อย

รูปที่ 4 (ก) แสดงความสัมพันธ์ระหว่างอุณหภูมิของไอน้ำร้อนยวดยิ่งและเวลาพัฟฟิงต่อคุณภาพด้านความแข็งโดยพิจารณาที่ความชื้นของกล้วยแผ่นก่อนการพัฟฟิง 25 %d.b. พบว่าอุณหภูมิของไอน้ำร้อนยวดยิ่งมีผลต่อความแข็งของกล้วยแผ่นมากกว่าเวลาพัฟฟิง ซึ่งสังเกตได้จากความชันของเส้นกราฟ โดยที่พัฟฟิงด้วยไอน้ำร้อนยวดยิ่งที่อุณหภูมิต่ำกล้วยแผ่นจะมีความแข็งมาก เนื่องจากที่อุณหภูมิต่ำน้ำในวัสดุจะเดือดได้น้อย โครงสร้างเกิดการพองตัวได้น้อย ดังนั้นหลังกระบวนการพัฟฟิงกล้วยแผ่นเมื่อนำมาอบแห้งต่อทำให้ โครงสร้างที่ไม่มีเสถียรภาพจะยุบตัวลง (collapse) ซึ่งสอดคล้องกับข้อมูลของการหดตัวที่ได้กล่าวมาแล้ว โดยการหดตัวมากทำให้โครงสร้างมีรูพรุนน้อย มีความหนาแน่นมาก ทำให้กล้วยแผ่นมีความแข็งมาก

รูปที่ 4 (ข) และ (ค) แสดงความสัมพันธ์ระหว่างอุณหภูมิของไอน้ำร้อนยวดยิ่งและเวลาพัฟฟิงต่อจำนวนยอด และความชันเริ่มต้นของกล้วยแผ่นที่ความชื้นของกล้วยแผ่นก่อนการพัฟฟิง 25 %d.b. พบว่า อุณหภูมิไอน้ำร้อนยวดยิ่งมีอิทธิพลต่อจำนวนยอด และความชันเริ่มต้นของกล้วยแผ่นมากกว่าอิทธิพลของเวลาพัฟฟิง กล่าวคือเมื่ออุณหภูมิของไอน้ำร้อนยวดยิ่งสูงขึ้นจำนวนยอด และความชันเริ่มต้นมีค่ามากขึ้น เนื่องจากที่อุณหภูมิไอน้ำร้อนยวดยิ่งสูงนั้น น้ำภายในวัสดุจะเกิดการเดือด ทำให้เกิดความดันไอขึ้นภายในกล้วยแผ่นมาก กล้วยแผ่นจะเกิดการพองตัว โครงสร้างมีรูพรุนเกิดขึ้นมากทำให้กล้วยแผ่นกรอบมากขึ้น และที่เวลาพัฟฟิงมากขึ้นจำนวนยอดและความชันเริ่มต้นจะไม่เปลี่ยนแปลงมากนัก

การหาสภาวะที่เหมาะสมของการทดลอง

การหาจุดที่เหมาะสมของคุณภาพกล้วยอบกรอบ จะใช้ความพึงพอใจโดยรวม (Desirability Function) เพื่อหาค่าที่เหมาะสมของปัจจัยโดยการกำหนดค่า Weight function ของแต่ละผลตอบสนองด้านคุณภาพได้แก่ คุณภาพด้านสี และการหดตัว กำหนดค่า Weight เป็น 0.5 ด้วยเหตุผลที่ว่าในขั้นตอนการวัดสี และ การหาค่าการหดตัวของกล้วยแผ่นนั้นอาจมีความผิดพลาดอยู่บ้างทำให้ข้อมูลมีความแปรปรวนค่อนข้างมาก สำหรับคุณภาพด้านเนื้อสัมผัสกำหนดค่า Weight เป็น 0.1 ด้วยเหตุผลที่ว่าลักษณะการพองตัวของกล้วยแผ่นไม่สม่ำเสมอ ทำให้ข้อมูลที่ได้จากการวัดด้านเนื้อสัมผัสมีความแปรปรวนมาก และการกำหนด Importance ในงานวิจัยนี้จะให้ความสำคัญกับทุกผลตอบสนองเท่า ๆ กัน โดยค่า defaults ที่โปรแกรมกำหนดมาคือ 1

ตารางที่ 4 แสดงผลของคุณภาพกล้วยแผ่นที่ได้จากการทำ Optimization โดยสภาวะที่เหมาะสมสำหรับการพัฟฟิงกล้วยด้วยไอน้ำร้อนยวดยิ่งคือ อุณหภูมิของไอน้ำร้อนยวดยิ่งเท่ากับ 180 °C เวลาพัฟฟิงเท่ากับ 1.41 นาที และความชื้นก่อนการพัฟฟิงเท่ากับ 26.16%d.b.ที่สภาวะเงื่อนไขของกล้วยโดยความพึงพอใจโดยรวม (Composite Desirability) เท่ากับ 0.994

สรุปผล

จากการศึกษาปัจจัยต่าง ๆ ในกระบวนการพัฟฟิง คือ อุณหภูมิของไอน้ำร้อนยวดยิ่ง เวลาพัฟฟิง และความชื้นของกล้วยแผ่นก่อนการพัฟฟิงที่มีอิทธิพลต่อคุณภาพของกล้วยแผ่น พบว่า อุณหภูมิของไอน้ำร้อนยวดยิ่งมีอิทธิพลต่อคุณภาพของกล้วยแผ่นมากกว่าอิทธิพลของเวลาพัฟฟิง สำหรับความชื้นของกล้วยแผ่นก่อนการพัฟฟิงมีอิทธิพลต่อคุณภาพของกล้วยแผ่นน้อยมาก เมื่อพัฟฟิง กล้วยแผ่นที่อุณหภูมิสูงขึ้นและเวลาพัฟฟิงนานคุณภาพด้านสี ค่า a เพิ่มขึ้น และค่า L และ ค่า b ลดลง และเมื่อพัฟฟิงกล้วยแผ่นด้วยไอน้ำร้อนยวดยิ่งที่อุณหภูมิสูง(เวลาพัฟฟิงสั้น ๆ) ทำให้คุณภาพของกล้วยแผ่นด้าน การหดตัว และความแข็งลดลง แต่ความกรอบเพิ่มขึ้น และคุณภาพด้านสีค่าความเป็นสีแดง(ค่า a) ต่ำ สภาวะที่เหมาะสมของกระบวนการพัฟฟิงที่ให้ค่าการหดตัวน้อย ค่าความแข็งต่ำ มีความกรอบมาก และ สีดีที่สุด คือที่อุณหภูมิของไอน้ำร้อนยวดยิ่งเท่ากับ 180°C เวลาที่ใช้ในการพัฟฟิงเท่ากับ 1.4 นาที และ ความชื้นของกล้วยก่อนการพัฟฟิงเท่ากับ 26.16%d.b.

คำขอบคุณ

ผู้วิจัย ขอขอบคุณสำนักงานคณะกรรมการอุดมศึกษาและ

สำนักงานกองทุนสนับสนุนการวิจัย (สกว.) ที่ให้ทุนอุดหนุนการวิจัย และ ขอขอบคุณสำนักงานความร่วมมือเพื่อการพัฒนาระหว่างประเทศ (สพร.) ที่ให้ทุนสนับสนุนงานวิจัย

เอกสารอ้างอิง

เพลินใจ ตังคณะกุล. 2546. การทำข้าวเกรียบเป็นผลิตภัณฑ์คุณภาพ. อาหาร. 33(2): 90-93.

Demirel, D. and Turhan, M. (2003). Air-drying behavior of dawrf cavendish and Gros Michel banana slices. Journal of Food Engineering., 59(1), 1-11.

Hwang, M.P., & Hayakawa, K.I. (1980). Bulk densities of cookies undergoing commercial baking processes. Journal of Food Science., 45(5), 1400-1402.

Myers,R., & Montgomery,D.C. (2002). Response surface Methodology. New York, USA: Wiley.

Prachayawarakorn, S., Soponronarit, S., Wetchacama, S.and Jaisut, D. (2002). Desorption isotherms and drying characteristics of shrimp in superheated steam and hot air. Drying Technology., 20(3), 669-684.

Tang, Z. and Cenkowski, S. (2000). Dehydration dynamics of potatoes in superheated steam and hot air. Canadian Agricultural Engineering., 42(1), 6.1-6.13.

Proceedings of 5th International Conference On Innovations In Food and Bioprocess Technology, 7-9 December 2010

Effect of Osmotic Treatment and Puffing Temperature on Textural Properties of Banana Slices

S. Tabtiang[1] , S. Soponronnarit[1] and S. Prachayawarakon[2]

[1]Energy Technology Division, School of Energy Environment and Materials, King Mongkut's University of Technology Thonburi, Suksawat 48 Road, Tungkru, Bangkok 10140, Thailand, E-mail: ohmpare@hotmail.com

[2]Faculty of Engineering, King Mongkut's University of Technology Thonburi, Suksawat 48 Road, Tungkru, Bangkok 10140, Thailand, E-mail: somkiat.pra@kmutt.ac.th

[*]Corresponding author: somkiat.pra@kmutt.ac.th

Porous structure in food, a very important characteristic to crisp product, can be produced by intensive heating technique. However, the color of puffed product may have intense brown. To limit the brown reaction, the banana slice needed to be treated before puffing. This research was therefore to study on the effect of osmotic treatment on quality of puffed banana. The banana with 20-23°Brix total soluble solid was immersed into sucrose solution concentrations at 30, 35 and 40°Brix and dried at 90°C using hot air until the sample moisture content reduced to 30% dry basis (d.b.). After that, the banana slices were puffed by superheated steam at 180, 200 and 220°C for 150 s and dried again at 90°C until the sample moisture content reached 4% d.b. From the experimental results, it was found that the osmotic dehydration can improve the color of banana. The puffed osmotic banana was less brown than the puffed none osmotic banana as indicated by the L-, a- and b- values. The puffing temperature and osmotic concentrations did not enhance the browning rate. The osmotic dehydration limited the banana cell wall expansion, and resulted in the significantly larger shrinkage of osmotic sample than the none osmotic one. . In addition, the osmotic product had less porous as visually observed by scanning electron

microscope. Such morphology of osmotic banana directly affected the textural properties in terms of hardness, initial slope and number of peaks.

Keywords: Puffing, Banana, Drying, Osmotic dehydration, Texture, Color

Introduction

Bananas, one of the most popular fruits in tropical climate country, deteriorate rapidly after harvest. To reduce their losses, bananas are processed to various types of product such as fried banana, osmotic banana and puree banana. The fried banana is the one of those products which is more favourite because it attain crispy texture (Ali, 2008). However, the obtained product contains high oil content and can not be kept for an extended period of time due to possible lipid oxidation leading to rancidity. Thus, the free oil crisp banana is an alternative product. To obtain the crisp texture, the food material needs high porosity.

There are several drying techniques to produce high porous food material such as high temperature and short time drying (Saca and Lozano, 1992; Hofsetz *et al*., 2007; Varnalis *et al.*, 2001), microwave drying (Maskan 2000; Erle and Schubert, 2001) and low pressure superheated steam drying (Devahastin *et al.*, 2004; Elustondo *et al.*, 2001). In this work, the high temperature and short time drying technique was chosen.

During puffing process, some amounts of moisture or gas inside the food suddenly vaporize or expand. It can build up pressure and force the food structure to be expanded, thereby producing the porous structure of food products. The product characteristics after puffing has low bulk density (Kim and Toledo, 1987; Saca and Lozano, 1992). Moreover, the puffing process can save drying time (Sullivan *et al*, 1980; Saca and Lozano, 1992) and provide 40% energy saving as compared to the conventional hot air dehydration (Sullivan, *et al* , 1980).

The puffing medium normally uses the hot air since it is convenient in practice. For this research, the superheated steam will be used because the steam condensation at the material surface during the initial drying period can release the latent heat which results in the rapid rise in temperature of food material to stay at boiling point temperature of water. (Taechapairoj *et al*., 2003; Rordprapat *et al*., 2005) This may increase rapidly vapor pressure inside the product and thus provides a high expansion of product. However, the study of puffing with superheated steam has been limited in literature. Saca and Lozano, (1992) studied the puffing of banana using superheated steam at temperature of 152-

175°C and steam pressure at 0.8-2.8 kg/cm. It was found that the puffed banana had higher porosity than the conventional air dried product. Although, the product contained very porous structure, the product color was brown. Such browning in food is caused by the none enzymatic browning reaction and pigment degradation.

The way to improve the color of product can be done by osmotic pretreatment. Sucrose is frequency used as osmotic agent (Krokida *et al.*, 2000; Mandala *et al.*, 2005; Antonio *et al*., 2008). During osmotic dehydration, the natural solutes existing in food material such as reducing sugar, acid and minerals flow out from food (Islam and Flink, 1982; Shi and Xue, 2009; Sagar and Kumar, 2009) and they are replaced by osmotic agent. Marquez and Anon (1986) found that monosaccharide, glucose and fructose, had more influent on brown color development than sucrose.

Moreover, the sugar pretreatment before puffing process can improve shrinkage properties. Many researchers studied the effect of sugar on shrinkage properties of puffed products such as rice (Hsieh *et at*., 1990; Orts *et al*., 2000). They found that the osmotically puffed products had lower shrinkage or higher expansion volume than the none osmotically puffed products.
As mentioned-above, the objective of this work therefore was to study the effects osmotic solution concentrations and puffing conditions on the drying characteristics and quality of puffed banana. The quality parameter were considered in terms of color, shrinkage and textural properties.

2. Materials and methods

2.1 Material preparation

Fresh bananas were obtained from local market and their soluble solid contents were given in the range of 20-23°Brix. Before processing, the banana was sliced into 3.5 mm thickness and blanched by hot water at 95°C for 1 min.

2.2 Osmotic pretreatment

Osmotic solution was prepared by using commercial sucrose with concentrations of 30 35 and 40°Brix. The banana slices were immersed into various sucrose solution concentrations and the mass ratio of osmotic media to the sample was 30:1 to avoid the dilution effect. The samples were immersed into the osmotic solution until the moisture content of banana was not changed.

2.3 Puffing method

Puffing process used in this studies was consisted of 3 step; drying, puffing and drying. In the first step, the banana was dried by hot air at temperature of 90°C and air velocity of 2 m/s. When the moisture content reached to 30% d.b., the sample was puffed by superheated steam at temperatures of 180, 200 and 220°°C for 150 s. In the last drying stage, the banana was dried with hot air at the same temperature as the first stage drying. The final moisture content required at 4% d.b. At the end of each experiment, the moisture content of samples was determined by drying them in the oven at 103°C for 3 hr.

2.5 Textural property evaluation.

The puffed banana slices were kept in aluminium foil bag at room temperature for 3 day before texture test. The banana sample were measured by using the texture analyzer (Stable Micro System, TA. XT. Plus, UK) with a 5 N load cell. The samples were fractured with a cutting probe (HDP-BSK type) using blade speed of 2 mm/s. The probe move down to the banana sample with a speed of 2 mm/s. The maximum compressive force, the initial slope and the number of peaks (over 50 g force threshold) from force deformation curve were considered as an hardness, stiffness and crispness, respectively.

2.6 Color measurement

The color of dried samples were measured using a colorimeter (HunterLab, ColorFlex, UK). In each sample, the measurement were performed at different six positions and the measurement value was reported as the average value. The color were expressed as L-value (Brightness), a-value (redness/greenness) and b-value (yellowness/blueness).

2.6 Shrinkage determination

Ten samples were used to determine shrinkage. The volume of each sample was determined by the volumetric displacement method using n-heptane as the replacement medium (Saca and Lozano, 1992). The shrinkage was defined as the ratio of the dried sample volume to the original sample volume

$$\% \text{ shrinkage} = \frac{V}{V_i} \times 100$$

where V_i and V are the volume of the fresh sample and the volume of dried sample.

2.7 Glucose, fructose and sucrose determination

Determination of sugar content was performed according to AOAC method 982.14 with some modification. The sample of 5-10 g was pulverised and mixed with 50 mL water in a 100 mL volumetric flask. 1 mL 15% $K_4(Fe(CN_6))3H_2O$ and 1 mL 30% $ZnSO_4$ $7H_2O$ was added into the solution in order to extract

protein. After that, it was filtered through filter paper No. 42. The filtered solution from the last step was filtered through 0.45 μm nylon syringe filter. The final volume of solution kept at refrigerator until its chromatographic analysis. The 10 μL aliquots of the filtered solution were injected into HPLC.
The High Performanace Liquid Chromatography consist of a Prevail Carbohydrate ES column (4.6 mm, 25 cm; 5μm)(Alltech, Derfield, USA), a pump and a controller (Agilent, 1100, USA), autosampler (Agilent, 1100, USA) and a evaporative light scattering detector (ELSD detector) (Alltech , 500 ELSD, USA).

The fructose and glucose which are sugar isomers can clearly separate peaks by gradiant elution in column at 1 mL/min flow rate. The gradient elution was varied the portion of mobile phase. The mobile phase used contained acetonitrile and water. The column temperature was kept 30°C and the detector was carried out at drift tube temperature at 50°C and nitrogen flow rate 1.5 L/min. Peaks of samples were quantified with standard.

2.8 Statistical analysis
The experimental data of color, textural and shrinkage properties was analyzed by using an analysis of variance (ANOVA) and presented as mean value with standard deviations. Duncan's test was used to establish the multiple comparisons of the mean values. The mean values were considered significantly different when $p \leq 0.05$

Results and discussion

1. Effect of Osmotic Concentrations on Water loss and Solid Gain

Table 1 shows the moisture loss, solid gain and the losses of native sugars of banana slices immersed into sucrose solutions at 30, 35 and 40°Brix. The banana slices immersed into the higher sucrose concentrations lost the larger amounts of their moisture content. The possible explanation was related to the osmotic pressure difference between intracellular fluid in banana and osmotic solution. When the sample was immersed into the higher sucrose concentration, the osmotic pressure difference was higher, resulting in the larger loss of moisture content. At the same time, the solid gain increased, due to the diffusion of sucrose from the solution into the sample. As shown in Table 1, the solid gain increased from 24.8% to 32.6% when the osmotic concentration increased from 30°Brix to 40°Brix. From these results, the ratios of water loss to solid gain increased with the increased sucrose solution concentrations, implying loss of moisture content larger than the solid gain. This is because the size of sucrose

molecule is larger than that of water molecules. Hence, the water molecule can move with a rate faster than the sucrose molecule.

Table 1 also shows that the native sugars i.e. glucose and fructose disappeared during osmosis. The remaining amounts of glucose and fructose in the samples immersed into the sucrose solution concentrations were not rather different; the percent looses were 84-86% for glucose and 83-85% for fructose. From these results, it can be observed that the losses of glucose and fructose were nearly the same amount. This can be described by the fact that the glucose and fructose have the same molecular weight and this would be expected to have the same diffusion coefficient. Gekas *et al*. (1993) reported that the diffusion coefficients of glucose and fructose in water at 25°C were equal and had a value of 69×10^{-11} m^2/s.

Table 1 Immersion time, amount of water loss, amount of solid gain, moisture content, amount of sucrose, amount of fructose and amount of gluco of banana slice at various sucrose concentration.

Sucrose concentration (°Brix)	Immersion time (min)	Water loss (g water/ g dry mass)	Solid gain (g solid/ g dry mass)	Water loss/ Solid gain	Moisture content (% d.b.)	Amount of sucrose (g/100 g banana)	Amount of glucose (g/100 g banana)	Amount of fructose (g/100 g banana)
none osmotic					210.1 ± 3.5	7.43	1.04	1.12
30°Brix	240	0.321	0.248	1.29	134.1 ± 2.4	16.41	0.14	0.17
35°Brix	290	0.539	0.303	1.78	116.4 ± 3.7	18.45	0.16	0.19
40°Brix	330	0.772	0.326	2.37	102.4 ± 3.1	22.86	0.14	0.16

2. Shrinkage

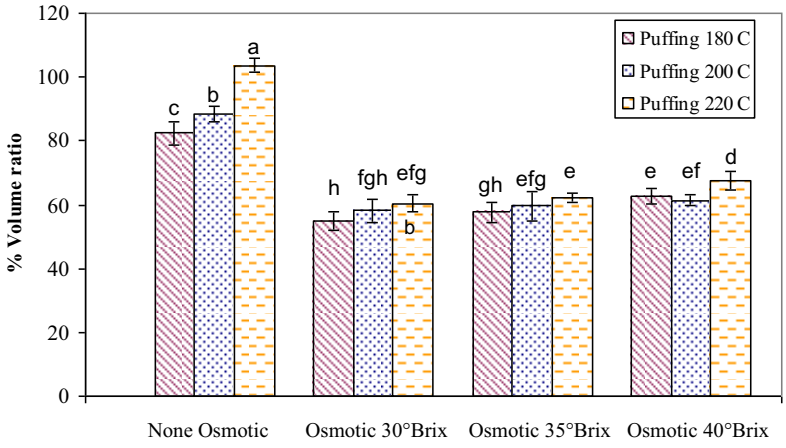

The different scripts presented over the bar mean the significant difference at $p \leq 0.05$.

Figure 1 Effects of puffing temperatures and osmotic solution concentrations on volume ratio.

Fig. 1 shows the shrinkages of none osmotic and osmotic samples both puffed at 180 200 and 220°C. The volume ratio of osmotic banana samples was significantly lower than that of the none osmotic ones for all puffing temperature. These results can be explained by the fact that the OH group of n-$C_6H_{12}O_6$ may bound with OH group in the cellulose of banana by hydrogen bonding (Allan *et al*, 2001). Consequently, the banana cell wall become stronger, allowing the small expansion of cellular structure during puffing and subsequently providing higher degree of banana shrinkage. The sucrose solution concentration affect on degree of banana shrinkage.

Considering the puffing temperature effect, it affected significantly the degree of shrinkage for both osmotic and none osmotic banana samples. The high puffing temperature provided lower degree of shrinkage. As showing in Fig 1, the volume ratio of none osmotic sample was 82% at puffing temperature of 180°C and increased to 103% at the puffing of 220°C.

Fig. 2 demonstrates morphologies of osmotic banana samples prepared from sucrose solution concentrations of 30, 35 and 40°Brix and puffed at temperature of 200°C. The morphologies of osmotic and non osmotic banana samples were noticeably different. The structure of osmotic banana samples was dense and exhibited less porous, but it was very porous for the none osmotic sample. As shown in Fig. 2 (a), the none osmotic banana had a huge pore with size larger than 1 mm. at the internal area of the sample. The formation of huge pore implies that there was a rapid vaporization of moisture inside the none osmotic samples during puffing, resulting in increasing vapor pressure inside the banana sample and the subsequent cell wall expansion. However, the cell wall expansion was occurred rarely in the osmotic banana samples. From their morphologies, it confirmed the shrinkage results, showing the higher shrinkage for the osmotic banana.

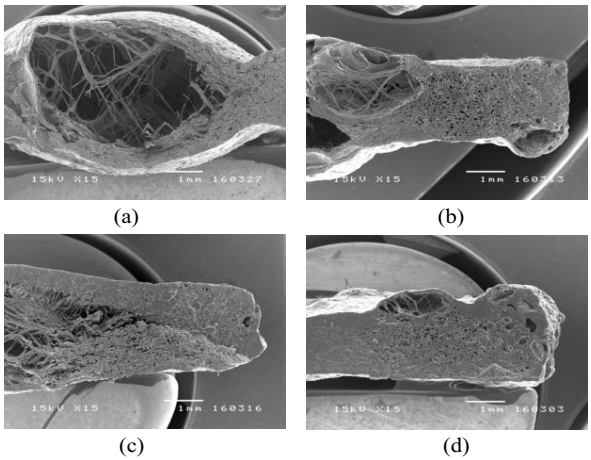

Figure 2 SEM photographs showing cross section of banana slices puffed at 200°C; (a) none osmotic; (b) 30°Brix; (c) 35°Brix; and (d) 40°Brix.

3. Texture

The force deformation curves represents the characteristics of crisp product. The product that was many fracture points indicate a crispy characteristic (Hofsetz and Lopes, 2005) and the number of jags on the force deformation curves indicate the porosity in samples. Fig. 3 shows the force deformation curve of osmotic and none osmotic samples at puffing temperatures of 180, 200 and 220°C. The force deformation curves of the osmotic samples were clearly different from those of the none osmotic ones. While the cutting probe was acted on the osmotic samples, the force reached the maximum point about 250-270 N. after which it was dropped sharply to zero, without any jag appearance. For the none osmotic samples, on the other hand, the force acting on the samples after reaching the maximum point did not drop rapidly to zero: it still appeared the several peaks. This can be explain by the fact that the sucrose solution causes banana tissue loosing the elasticity which in turn provides a sharp drop of force after the maximum point. This force characteristic indicated that the osmotic banana after puffing was brittle.

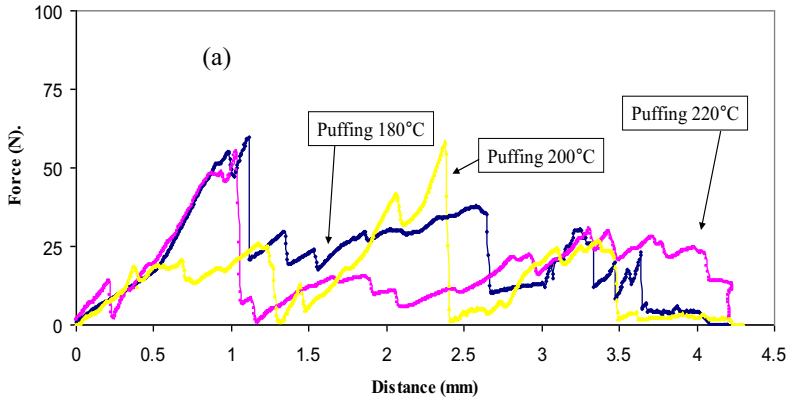

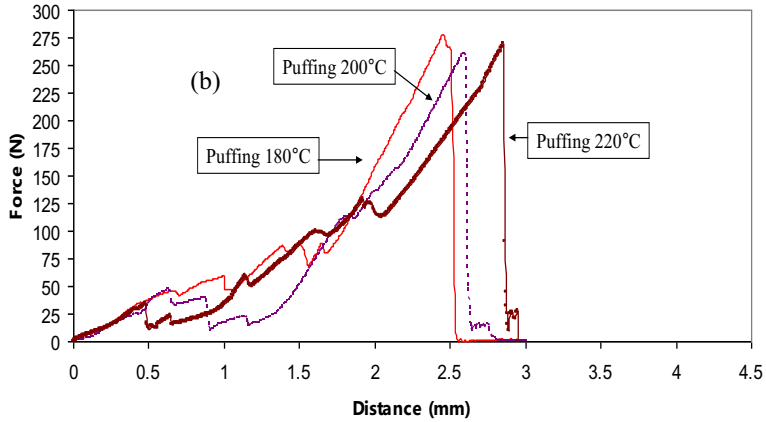

Figure 3 Force deformation curves: (a) the none osmotic banana and (b) the osmotic banana.

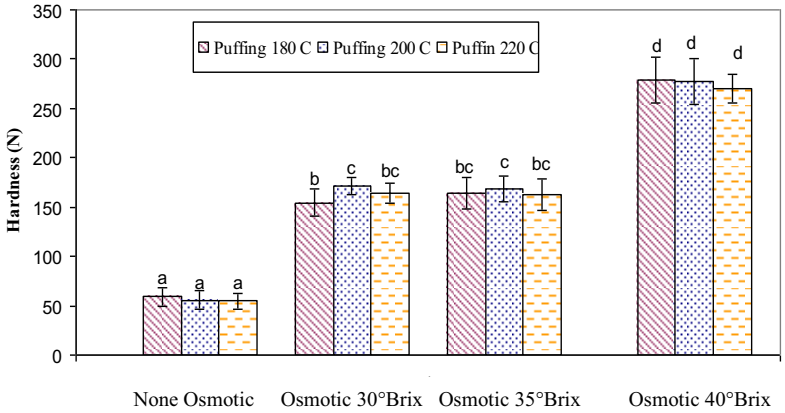

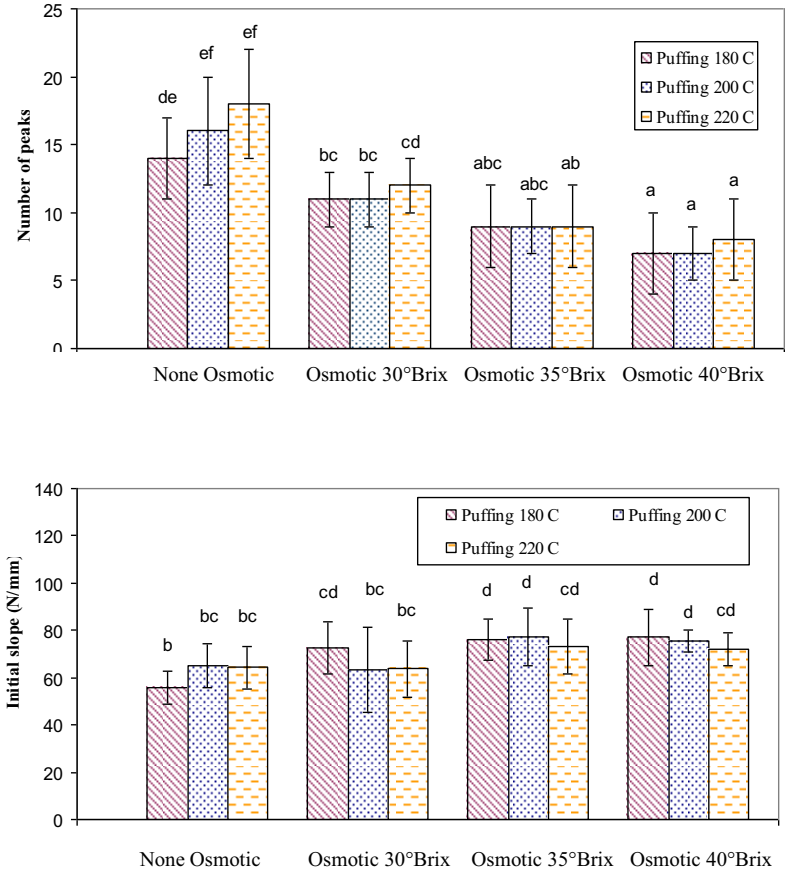

The different scripts presented over the bar mean the significant difference at $p \leq 0.05$.

Figure 4 Texture properties of the osmotic banana and the none osmotic banana.

Fig. 4 shows the effects of sucrose concentrations and puffing temperatures on the textural properties of none osmotic and osmotic banana samples. Considering at each sucrose solution, the puffing temperature given in a range of 180-220°C insignificantly affect the textural properties such as hardness, number of peaks and initial slope. The insignificant effect of puffing temperature on the textural characteristics for the none osmotic banana samples was also observed. On the other hand, the sucrose concentration strongly affected such textural

characteristics. Increase in both of hardness and initial slope and decrease in number of peaks were found with increasing in sucrose solution concentration.

As shown in Fig. 4, the banana slices pretreated with 40°Brix sucrose solution had the highest values for the of hardness initial slope but the smallest number of peaks. Such textural characteristics revealed that the osmotic banana product after puffing had a harder texture, less crispy and rather brittle than the osmotically untreated banana. The harder texture in the osmotic banana is related to the interaction between the OH groups of cellulose and sucrose solutions (Allan *et al*, 2001) which will improve the cellulose strength. These results corresponded to the morphological features as already mentioned.

4. Color

Table 2 shows the effect of the puffing temperatures and sucrose solution concentrations on the color of the bananas slices in terms of lightness (L), redness (a) and yellowness (b).

It was found that osmotic pretreatment can improve the color of banana samples compared with the color of samples without osmotic pretreatment. The color of osmotic samples had brownish-yellow but it had yellowish-brown for the banana without osmotic dehydration. It can indicated by the osmotic sample had higher of L- and b- values and lower of a-value than the none osmotic samples.

The color improvement of osmotic banana can be explain by the fact that the monosaccharide which is the main active component for none-enzymatic browning reaction (Pulis, 2010), leak out during the osmotic dehydration. Thus the browning rate is retarded and resulted in less brown for osmotic samples than the none osmotic sample. The osmotic concentration had not affect on the color of the osmotic samples indicated by L-, a- and b- values which shows insignificant difference among the samples at various sucrose concentrations.

Considering the effect of puffing temperature, it was found that the puffing temperature affect on the color of none osmotic samples. The color of none osmotic samples trend to intensive brown when the puffing temperature was increased as indicated by higher a value. In contrast, the puffing temperature did not affect on the product color of osmotic samples.

Table 2 color of dried osmotic banana slices and puffed none osmotic banana slices.

Drying Condition	L	a	b	Product color
Puffing 180°C	52.1^{ab} ±1.02	5.32^{cd} ± 0.3	16.81^{a} ± 0.83	
Puffing 200°C	51.3^{ab} ± 1.66	5.66^{cd} ± 0.25	16.85^{a} ± 0.85	
Puffing 220°C	49.5^{a} ± 1.5	6.11^{e} ± 0.21	16.3^{a} ± 0.83	
Puffing 180°C (30 °Brix)	59.29^{f} ±1.51	4.87^{abc} ±0.26	19.97^{cd} ±0.74	
Puffing 200°C (30 °Brix)	59.1^{ef} ± 2.73	4.93^{abc} ± 0.21	18.89^{bc} ± 1.11	
Puffing 220°C (30 °Brix)	57.22^{ef} ± 2.1	5.41^{cd} ± 0.33	18.68^{bc} ± 0.5	
Puffing 180°C (35 °Brix)	57.01^{ef} ±3.02	5.02^{abc} ± 0.32	16.65^{a} ± 0.9	
Puffing 200°C (35 °Brix)	58.35^{ef} ± 1.7	5.40^{cd} ± 0.51	18.15^{bc} ± 0.50	
Puffing 220°C (35 °Brix)	56.36^{de} ± 2.45	5.06^{abcd} ± 0.3	18.39^{bc} ± 0.54	
Puffing 180°C (40 °Brix)	57.43^{ef} ± 1.28	5.02^{abc} ± 0.28	18.68^{bc} ± 0.97	
Puffing 200°C (40 °Brix)	57.31^{ef} ± 1.3	5.2^{cd} ± 1.3	18.71^{bc} ± 0.83	
Puffing 220°C (40 °Brix)	54.19^{bcde} ± 4.22	5.27^{bcd} ± 0.32	17.7^{b} ± 1.14	

Different superscripts values are significantly different at 95% confidence level.

Conclusions

Osmotic pretreatment of banana slices can limit the browning reaction so the color of final osmotic product can improve. The color of osmotic product obtained at sucrose solution concentrations and puffing temperatures were not different. In spite of color in product, the osmotic pretreatment provided the texture of product to be harder and less crispy than the none osmotic banana. This is because the osmotic product had less porous as revealed by scanning electron microscope. The shrinkage was also high for the osmotic banana. Increase of sucrose solution concentration provided lesser extent of shrinkage whilst increase of puffing temperature did not affect on the textural properties of product.

Acknowledgements

The authors express their sincere thanks to Thailand Research Found, National Science and Technology Development Agency and King Mongkut's University of Technology Thonburi for supporting this financially project. Author Tabtiang thanks the Commission on Higher Education, Thailand for support the grant fund under the Strategic Scholarships for Frontier Research Network of the Ph.D. program Thai doctoral degree.

Reference

Ali, A. S. (2008). Banana chips [Online]. Available: www.practicalaction.org/practicalanswers/product: [5/10/2010].

Allan, G. G., Stoyanov, A. P., Ueda, M. and Yahiaoui, A. (2001). Sugar-cellulose composites V. The mechanism of fiber strengthening by cell wall incorporation of sugars. Cellulose **8**: 127-138.

Antonio, G. C., Alves, D. G., Azoubel, P.M., Murr, F. E. X. and Park, K. J. (2008). Influence of osmotic dehydration and high temperature short time processes on dried sweet potato (Ipomoea batatas Lam). Journal of Food Engineering **84**: 375-382.

AOAC (2006). Official method of analysis (18th ed.). Gaitherburg, Maryland: AOAC.

Devahastin, S., Suvarnakuta, P., Soponronnarit, S. and Mujumdar, A. S. (2004). A comparative study of low-pressure superheated steam and vacuum drying of a heat-sensitive material. Drying Technology **22**: 1845-1867.

Elustondo, D., Elustondo, M. P. and Urbicain, M. J. (2001). Mathermatical modeling of moisture evaporation from foodstuffs exposed to subatmospheric pressure superheated steam. Journal of Food Engineering **49**: 15-24.

Erle, U. and Schubert, H. (2001). Combine osmotic and microwave-vacuum dehydration of apples and strawberries. Journal of Food Engineering **49**: 193-199.

Gekas, V., Oste, R. and Lamberg, I. (1993). Diffusion in heated potato tissue. Journal of Food Science **58**: 827-831.

Hofsetz, K. and Lopes, C. C. (2005). Crispy banana obtained by the combination of a high temperature and short time drying stage and a drying process. Brazilian Journal of Chemical Engineering **22**: 285-292.

Hofsetz, K., Lopes, C. C., Hubinger, M. D., Mayor, L. and Sereno, A. M. (2007). Change in the physical properties of bananas on applying HTST pulse during air drying. Journal of Food Engineering **83**: 531-540.

Hsieh, F., Hu, L., Peng, I. C. and Huff, H. E. (1990). Pretreating dent corn grits for puffing in a rice cake machine. Journal of Food Science **55**: 1345-1355.

Islam, M. N. and Flink, J. M. (1982). Dehydration of potato II. Osmotic concentration and its effect on air drying behavior . Journal of Food Technology **17**: 387-403.

Kim, M. H. and Toledo, T. R. (1987). Effect of osmotic dehydration and high temperature fluidized bed drying on properties of dehydrated rabbiteye blueberries. Journal of Food Science **52**: 980-989.

Krokida, M. K., Karathanos, V. T. and Maroulis, Z. B. (2000). Effect of osmotic dehydration on color and sorption characteristics of apple and banana. Drying Technology **18**: 937-950.

Mandala, I. G., Anagnostaras, E. F. and Oikonomou, C. K.. (2005). Influence of osmotic dehydrations on apple air –drying kinetics and their quality characteristics. Journal of Food Engineering **69**: 307-316.

Marquez, G. and Anon, M. C. (1986). Influence of reducing sugars and amino acids in the color development of fried potatoes. Journal of Food Science **51**: 157-160.

Maskan, M. (2000). Microwave/air and microwave finish drying of banana. Journal of Food Engineering **44**: 71-78.

Orts, W. J., Glenn, G. M., Nobes, G. A. R., and Wood, D. F.(2000). Wheat starch effect on the textural characteristics of puffed brown rice cakes. Cereal Chemistry **77**: 18-23.

Purlis, E. (2010). Browning development in bakery product-A review. Journal of Food Engineering **99**: 239-249.

Rordprapat , W., Nathakaranakule, A., Tia, W. and Soponronnarit, S. (2005). Comparative study of fluidized bed paddy drying using hot air and superheated steam. Journal of Food Engineering **71**: 28-36.

Saca, A. S. and Lozano, E. J. (1992). Explosion puffing of bananas. International Journal of Food Science and Technology **27**: 419-426.

Sagar, V. R. and Kumar, P. S. (2009). Improvement of some process variables in mass transfer kinetics of osmotic dehydration of mango slices and storage stability. Journal of Scientific & Industrial Research **68**: 1043-1048.

Shi, J. and J. S. Xue (2009). Application and development of osmotic dehydration technology in food processing. In Advances in food dehydration; Ratti, C., Ed.; Taylor & Francis Group, LLC, New York, U.S.A.

Sullivan, J. F., Craig, J. C., Konstance, R. P., Egoville, M. J. and Aceto, N. C. (1980). Continuous explosion-puffing of apples. Journal of Food Science **45**: 1550-1558.

Taechapairoj, C., Dhuchakallaya, I., Soponronnarit, S., Wetchacama, S., Prachayawarakorn, S. (2003). Superheated steam fluidised bed paddy drying. Journal of Food Engineering **58**: 67-73.

Varnalis, A. I., Brennan, J. G. and MacDougall, D. B. (2001). A proposed mechanism of high-temperature puffing of potato. part I. the influence of blanching and drying conditions on the volume of puffed cubes. Journal of Food Engineering **48**: 361-367.

16th International Drying Symposium (IDS 2008)
Hyderabad, India 9-12 November 2008

DETERMINATION OF APPARENT DIFFUSIVITY OF MOISTURE IN PORES OF DRIED FOAM BANANA USING 2-D STOCHASTIC PORE NETWORKS

P. Prakotmak[1,*], S. Prachayawarakon[1], S. Soponronnarit[2]

[1,2] School of Energy, Environment and Materials, King Mongkut's University of Technology Thonburi, 126 Pracha-utit Rd., Bangmod, Thungkru, Bangkok, Thailand 10140 E-mail: preeda_list@hotmail.com, somkiat.pra@kmutt.ac.th*

[1] Department of Chemical Engineering, King Mongkut's University of Technology Thonburi, 126 Pracha-utit Rd., Bangmod, Thungkru, Bangkok, Thailand 10140

Abstract: Moisture diffusivity is an important parameter to predict the shelf life of food products. The main purpose of this research was therefore to determine the apparent diffusivity of moisture in pores of banana foam mat. 2-D stochastic pore network was used to represent the pore voids inside the banana foam sample and the moisture movements inside the individual pore segments were described by Fick's law. To obtain the moisture diffusivity, the experiments were carried out with standard static method using saturated salt solutions over a wide range of relative humidities and a temperature range of 35 to 45°C. Two banana foam densities of 0.3 and 0.5 g/cm^3, both having different porosities, were used to adsorb water vapor under the controlled condition. The interactions of transport processes within the pore network were illustrated using a 3-D pictorial representation of network concentration gradients in spaces with colour representing the moisture content. The network model could describe the experimental results relatively well. The diffusivity of water in pores was in order of 10^{-9} m^2/s which was 9 times higher than the apparent effective diffusivity. For a given temperature, the pore diffusivities were independent of the foam densities and relative humidity, except for the case of higher relative humidity of 70%. Moreover, the diffusivity depended strongly on the temperature.

Keywords: adsorption kinetics, banana foam mat, pore diffusivity, pore network

INTRODUCTION

Moisture migration during food storage is greatly important to many dry crispy products, such as biscuits, ready to eat cereals and snack foods, because the loss of their crispness strongly correlated to the moisture content. Rate of moisture adsorption in porous foods depends not only on the environmental conditions but also on their pore structures. Hence, understanding and capability to predict the moisture migration through their void spaces at different conditions are the main aspects that cannot be avoided in order to preserve their quality and to extend their shelf life as long as possible. To achieve this, model of porous food material is required and equation of moisture transfer is needed.

The moisture transport in porous foods can be mathematically by either a continuum or a discrete approach. In a continuum model, the porous spaces are considered as a continuum consistent with its appearance on macroscopic scale and effective macroscopic properties lump all the microscopic complexities of real pore network, including mechanisms of mass transfer which may be occurred by molecular diffusion and capillary flow etc. For adsorption under isothermal condition, moisture adsorption occurring in an infinite slab geometry can be described by

$$\frac{\partial M}{\partial t} = \nabla\left(D_{eff}\nabla M\right) \qquad (1)$$

By using eq.(1), the effective diffusivity, D_{eff}, can simply be determined from the adsorption experiments. The effective diffusivity can be expressed as

$$D_{eff} = \frac{\varepsilon D_A}{\tau} \qquad (2)$$

Tortuosity factor, τ, accounts for the fact that the pore spaces do not provide straight line paths through the particle, thereby lengthening the diffusive path and reducing the internal diffusional fluxes. At the present, however, there is no reference of the actual

diffusivity of water in pore voids, D_A. To estimate the water diffusivity in the pores, the model must include the information details about the interactions between internal diffusional fluxes and pores, which determine the pathways of moisture movement. The diffusivity of water can be estimated by first constructing the discrete network models, where more or less simplified geometry and pore size distribution are used to describe topology of pore structure of real material (Mann, 1993; Hollewand and Gladden, 1992; Androutsopoulos and Mann, 1979). Diffusion equation is then applied to individual pores of these simulated structures and the flow of substances through pore segments can be numerically predicted (Blunt, 2001; Yiotis et al, 2005; Prachayawarakorn, Prakotmak and Soponronnarit, 2008).

Network models represent the void spaces of a porous medium by a simple two-or more realistic three-dimensional lattice in which the large and small pores are randomly interconnected. Each pore can be assumed to be cylindrical, slit, triangular and polygonal shapes. Segura and Toledo (2005) found that pore shapes used in the network model had an insignificant effect on the drying characteristic curves, vapor relative diffusivity and liquid relative permeability.

As mentioned above, diffusivity data of water in the pores of the porous foods have not been available in the literature. The aim of the present investigation was therefore to determine the pore diffusivity by using a two dimensional stochastic pore network. The banana foam mat was used as a representative porous medium. The Fick's second law was used to describe the moisture diffusion in individual pore segments and an optimization technique was implemented to determine the pore diffusivity under adsorption conditions.

DRIED BANANA FOAM PREPARATION

The banana puree with 5% of fresh egg albumen used as foaming agent was foamed to densities of 0.3 and 0.5 g/cm^3. The banana foams was poured slowly into a steel block with a dimension of $43 \times 43 \times 4$ mm and then placed on a mesh tray, which was covered with aluminium foil. After that, it was dried to about 3% dry basis (d.b.) using 80^{o}C and a 0.5 m/s superficial air velocity. The sample thicknesses after drying were 2.8mm and 3.2mm for the banana foam densities of 0.3 and 0.5 g/cm^3, respectively.

ADSORPTION EXPERIMENT

Moisture adsorption experiments were carried out using the static method. Samples were placed into the glass jars contained the saturated salt solutions which ($MgCl_2$ 6·H_2O, $Mg(NO_3)_2$ 6·H_2O, KI, NaCl and KCl) give the relative humidity (RH) in range of 32-82% for the temperatures of 35, 40 and 45^{o}C. The glass jars were kept in the hot air oven with an accuracy of ±1°C (UFE500, Memmert, Germany). Samples were weighed at different exposure times until the moisture content of samples did not change. At high relative humidity (RH > 74%), a small amount of toluene was added into a small tube which was fixed in the glass jars in order to prevent microbial spoilage of the samples (Kaya and Kahyaoglu, 2005). Moisture content of each sample after reaching the equilibrium condition was determined by drying it with an oven at a temperature of 103°C for 3 h. The experiment at each sorption condition was repeated three times and the mean value was reported.

SEM PHOTOGRAPH

The morphologies of dried banana foam mats were characterized using scanning electron microscope (SEM) with an accelerating voltage of 10 kV. Before photographing, the specimens were cut into a dimension of 5×5 mm and then glued on the metal stub. The samples were coated with gold, scanned, and photographed at $15 \times$ magnification.

To quantify the porous banana foam characteristics such as pore diameter and pore area, Image J software was used. Each pixel of the SEM micrograph was assigned a value of gray intensity between 0 and 255 and the binary images were generated. The pixels with gray levels lower than the selected threshold were assigned as pore, which appeared as black colour, and the pixels with gray levels above the selected threshold were set as solid phase, which appeared as white colour in binary image. The pore diameter was estimated by the known pore area by assuming a spherical shape.

PORE NETWORK MODEL

When the pore size distribution of material is known, these pores are assigned according to their distribution and allocated randomly onto a lattice. In this work, the pore was assumed to be cylindrical geometry and each pore in the network had the same length. The pores with different sizes were randomly placed onto the network and this approach provided pore at any positions within the network independent to the neighbouring pores. Such random arrangement of pore assemblies was referred to as stochastic pore network. Figure 1 shows an illustrative 2-D stochastic pore network with a size of 23×50 consisting of 2373 pores obeying a pore size distribution of dried banana foam shown in Figure 6 for the initial density of 0.3 g/cm^3, but in calculating the pore diffusivity, we used a larger network size. In this work, we considered the 2-D parallelogram pore networks with a size of 20×231 consisting of 9491 pores for the sample at the initial foam density of 0.3 g/cm^3 and a size of 23×264 consisting of 12431

pores for the density of 0.5 g/cm^3. The distance between two pore bodies (L) was equal to 128 μm .

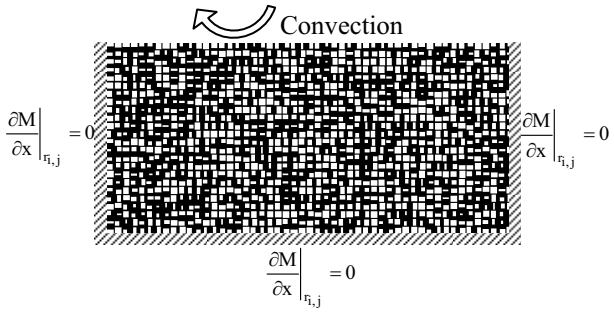

Fig. 1. Illustration of a simple 2-D stochastic pore network and boundary conditions.

Single Pore

In this work, moisture adsorption between surrounding air and banana foam mat occurred under isothermal condition. The moisture moved along the pore axis and it can be described by Fick's second law for the individual pores in the network:

$$\frac{\partial M}{\partial t} = D_p\left(\frac{\partial^2 M}{\partial x^2}\right) \qquad (3)$$

The migration of moisture from the surrounding air to the banana foam surface occurred specifically at the top surface and no moisture transferred at the bottom surface of the network since the banana foam mat was placed on an opaque glass dish. The samples had the length and width about 11 times of its thickness and thus, the banana foam mats were reasonably assumed to be an infinite slab. Accordingly, moisture movement during adsorption occurred along the material thickness direction. The constant diffusion coefficient at a given condition was assumed and the moisture profile in the pores at the beginning was uniform along the pore axis,

$$M = M_i \quad : t = 0, 0 \le x \le L \qquad (4)$$

The length of each pore, L, was calculated by dividing width of material by NV+1 where NV is the number of pores in each row of the network; 264 for the network size of 23×264 and 231 for the network size of 20×231 were used. Because the surface area at each sample side was remarkably smaller than that at the top surface, the moisture transferring from the surrounding to the pores allocated at the two sides of sample was small. Hence, the boundary condition for the pores allocated at both sides of the network is set as

$$\frac{\partial M}{\partial x} = 0 \quad : t > 0 \qquad (5)$$

For the periphery pores allocated on the top of the network, the moisture moving from the surrounding to those pores was occurred by convection and the boundary condition is set as

$$D_p\left(\frac{\partial M}{\partial x}\right) = h_m\left(M_e - M_s\right) \quad : t > 0 \qquad (6)$$

To calculate the moisture concentration of the pores, a finite difference method was used. An individual pore in the network was divided into n intervals (N=12) and Eq. (3) was discretized using the explicit method as follows:

$$M^{p+1}_{n,r_{i,j}} + M^{p}_{n,r_{i,j}}(2\alpha - 1) - \alpha\left(M^{p}_{n+1,r_{i,j}} + M^{p}_{n-1,r_{i,j}}\right) = 0 \qquad (7)$$

where $\alpha = D_p \Delta t / \Delta x^2$ is the Fourier number, p and n the respective indexes of the present time and of nodal position along the pore axis. The boundary conditions in Eqs. (5) and (6) can be written as:

$$M^{p+1}_{n,r_{i,j}} + M^{p}_{n,r_{i,j}}(2\alpha - 1) - 2\alpha\left(M^{p}_{n+1,r_{i,j}}\right) = 0 \qquad (8)$$

$$M^{p+1}_{n,r_{i,j}}(\gamma + 1) - M^{p+1}_{n-1,r_{i,j}} - \gamma M^{p+1}_{e} = 0 \qquad (9)$$

where $\gamma = h_m \Delta x / D_p$. The moisture adsorption rate $Q_{i,j}$ for the pore with radius of $r_{i,j}$, can be calculated by

$$Q_{r_{i,j}} = \pi r^2_{i,j} D_p\left(\frac{dM_{r_{i,j}}(x,t)}{dx}\right)_{x=L} \qquad (10)$$

Mass balance in the network

To determine the moisture contents at the pore junctions, the mass balance of moisture content at the inner nodes of network was made, assuming no accumulation at the pore junctions within the network, which is thus expressed by

$$\sum_{j \in \{i\}} Q_{r_{i,j}} = 0 \qquad (11)$$

where {i} refers to the set of i-adjacent nodes which are connected to node (i) in the network. After the moisture contents at every nodes of the network were known, the average moisture content $\overline{M}_{network}$ of network can then be calculated using the following equation

$$\overline{M}(t)_{network} = \frac{\sum_{n=1}^{Z} r^2_{i,j} \int_0^L M_{r_{i,j}}(x,t)dx}{Z \cdot L \sum_{n=1}^{Z} r^2_{i,j}} \qquad (12)$$

To estimate the apparent pore diffusion, D_p, the optimization technique using a golden-search method was used. The root mean square error (RMSE) for the residuals of the measured and predicted values of average moisture content was set as the objective

function with a tolerance of 10^{-5}. The RMSE is defined as

$$RMSE = \left[\frac{1}{K} \sum_{n=1}^{K} (M(t)_{exp} - \overline{M}(t)_{network})^2 \right]^{1/2} \quad (13)$$

where $M(t)_{exp}$ is the experimental moisture content of material at time t, $\overline{M}(t)_{network}$ is the predicted moisture content, and K is the number of the experimental data. The lower the value of RMSE is the better the goodness of fit. All computations were implemented using Intel C++ Compiler (http://www.intel.com) to run on a PC compatible with 3.0 GHz dual-processor and 2 GB of RAM.

RESULT AND DISCUSSION

Effect of temperature and relative humidity

Generally, if the partial vapor pressure or vapor concentration is greater in the surrounding atmosphere than in the porous materials, the moisture is then transferred from the air to the materials. The adsorption rate is extremely rapid when there is a great vapor pressure difference between the water in the air and the water in the adsorbent. The process of adsorption continues until the adsorbed layer is in thermodynamical equilibrium with gas or vapour.

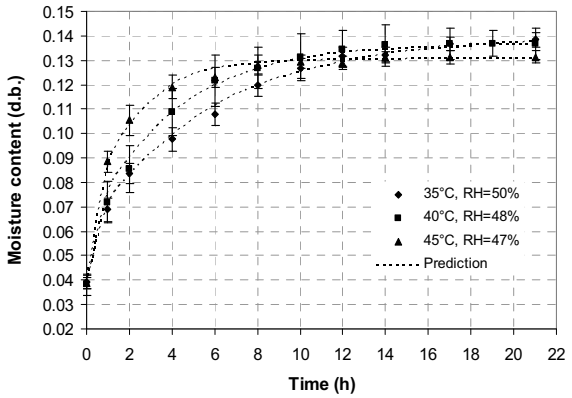

Fig. 2. Kinetics data of moisture adsorption at different temperatures and relative humidities for the initial banana foam density of 0.3 g/cm^3

The effect of partial vapour pressure on the adsorption rate can be studied by changing the temperature or relative humidity and the experimental results are shown in Figure 2 for the temperature effect and Figure 3 for the relative humidity effect.

As shown in Figure 2, the rate of moisture uptake was very fast during the early period of time and gradually decreased as the moisture content approached the moisture equilibrium. The higher adsorption rate was evident in elevated temperature and relative humidity. From the preliminary test, the banana foam mat lost its textures at the moisture content of 0.07 d.b. From this result, it indicated that the banana foam will lost the crispiness when it exposed to air about 40 minutes under the operating conditions at the relative humidity and temperature lower than 75% and 40°C, respectively.

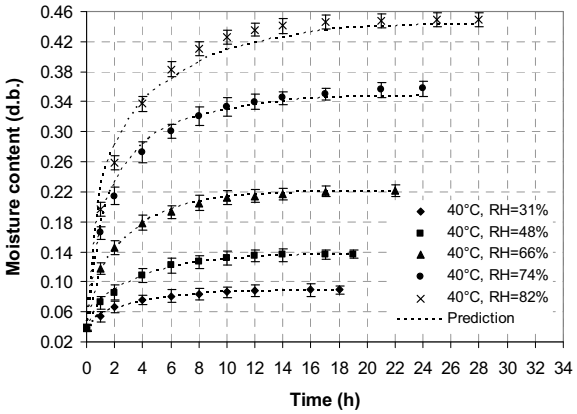

Fig. 3. Kinetics data of moisture adsorption at 40^{o}C and relative humidities of 31, 48, 66, 74 and 82% for the initial banana foam density of 0.3 g/cm^3

At the equilibrium state, the equilibrium moisture content tended to decrease with increasing temperature; these values were 0.1384, 0.1368 and 0.1308 d.b. for the temperatures of 35, 40 and 45^{o}C, respectively. This may attribute to the excitation states of water molecules. At elevated temperature, the molecules are in higher states of excitation, thus increasing their distance apart and, in turn, decreasing the attractive forces between them (Jamali et al., 2006). Similarly, Kim et al. (1999) and Palou et al. (1997) found that the sorption capacity or equilibrium moisture content of crackers and cookies decreased with increasing temperature.

Effect of initial foam density

Figure 4 shows the moisture adsorption kinetics at temperature of 45°C for the initial foam densities of 0.3 and 0.5 g/cm^3. It can be seen that the initial foam density strongly affects the moisture adsorption rate; the lower the initial foam density, the faster the adsorption rate. This is because the porosities of both banana foams were different; the void area fractions for the banana foam densities of 0.3 and 0.5 g/cm^3 were 31 and 26 %, respectively.

High porosity in porous foods provides less diffusional flux resistance and thus greatly facilitates the moisture transport to those porous foods. In the porous banana foam studied, the higher void area fraction for the banana foam density of 0.3 g/cm^3 is a result of the assembly of the giant pores with sizes larger than 150 μm which had a larger number (38%) than that at the foam density of 0.5 g/cm^3 as will be seen in Figure 6. These huge pores, serving as a massive transport of moisture through the interior pores, may be interconnected into almost all parts of the whole network. Hence, the rapid adsorption is

obviously evident for the foam density of 0.3 g/cm^3. Prachayawarakorn, Prakotmak and Soponronnarit (2008), who studied the effect of pore assembly architecture on the drying rate, found that full set of pores which were assembled in a different way exhibited different drying rates. As the network archetype with the large pore assembly allocated onto the network exterior and the smaller pores to the interior, the drying rate is very fast as compared to the other pore architectures.

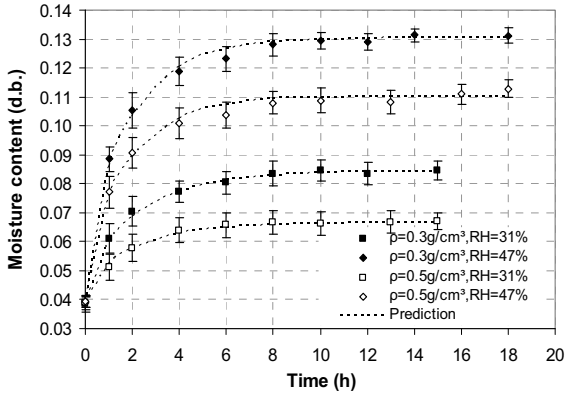

Fig. 4. Moisture adsorption kinetics at 45°C and relative humidities of 31 and 47% for the initial banana foam densities of 0.3 and 0.5 g/cm^3

As shown in Figure 4, the uptakes of moisture content into the banana foams after the elapsed time of 10 hours are very slightly and this indicated the system reaching the equilibrium state. At the equilibrium, the moisture content of banana foam at density of 0.3 g/cm^3 was apparently higher than that at 0.5 gm/cm^3 due to different porosities.

Pore size distribution

The microstructures of dried banana foam mats characterized by SEM are shown in Figures 5a and 5b for various initial foam densities. The corresponding binary images are illustrated in Figures 5b and 5d. The reconstructed porous structures of the banana foams in binary image reasonably represented their original images. As shown in Figures 5a and 5c, the pores were random in sizes and irregular in shape. Moreover, the porosity appears to form a mass of interconnecting pores in the banana foam sample. This would be clear that it is very task to understand the interactions between pore structure and diffusional fluxes of moisture by using a simple mathematical model.

Figure 6 shows the pore size distributions of the dried banana foams at the densities of 0.3 and 0.5 g/cm^3, both distributions obtained from the reconstructed pore structures. The characteristic of distributive pore sizes was reasonably described by grammar distribution. The sample with an initial foam density of 0.3 g/cm^3 had small pore assembly in the range 6 to 150 μm accounting for 62% of the whole number of pores and for 38% with the pores larger than 150 μm. For the density of 0.5 g/cm^3, it appears the proportion of small pores accounting for 71% which was higher than the sample at the density of 0.3 g/cm^3 for the same pore size range. However, the porosity of sample at the density of 0.5 g/cm^3 was relatively smaller as mentioned before because the large pores had a smaller number.

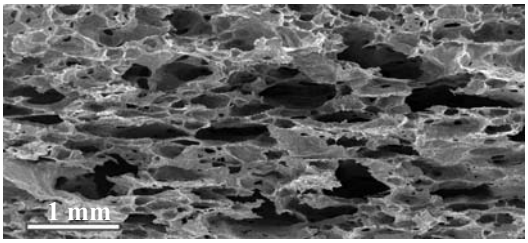

(a) 0.3 g/cm^3

(b) 0.3 g/cm^3

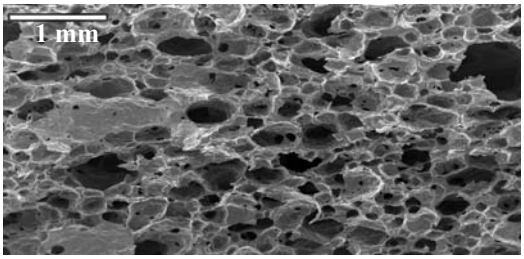

(c) 0.5 g/cm^3

(d) 0.5 g/cm^3

Fig. 5. (a,c) SEM micrographs of dried banana foam mats at different initial foam densities and binary images (b,d)

Apparent pore diffusivity

Figure 7 shows the values of pore diffusivity in banana foam at different temperatures and relative humidities. Considering at a given temperature, for example at 40°C, most moisture diffusivity data had a slight change for the humidity range below 70%, corresponding to the lower equilibrium moisture

contents than 0.2214 d.b. for all adsorption conditions used in this study. These results, when analyzed statistically with Duncan's test, showed an insignificant difference. The mean values of apparent pore diffusivity were in the order of 10^{-9} m^2/s. In fact, the orders of magnitude of the diffusion coefficients depend on the state of substance: for gases, approximately 10^{-5}; for liquids, approximately 10^{-9} (Aguilera and Stanley, 1999). From this information, it might be indicated that the transport of moisture through the banana foam mat mainly occurred in form of liquid. Similarly, Roca et al. (2006) reported that the adsorption of water vapor by sponge cake occurred mainly in liquid phase.

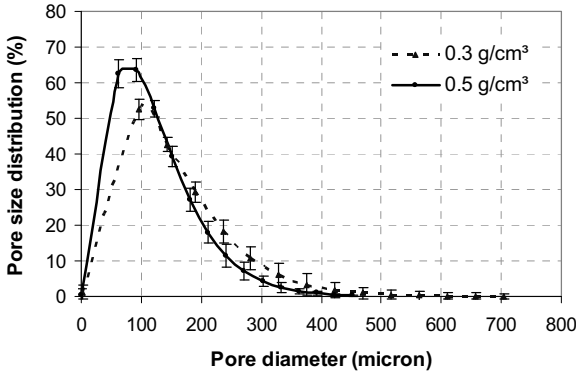

Fig. 6. Pore size distributions of dried banana foam at different densities

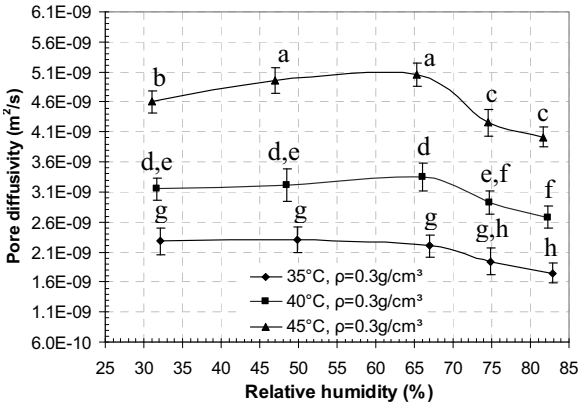

Fig. 7. Effects of temperatures and relative humidities on the pore diffusivities for the initial banana foam density of 0.3 g/cm^3: the same letter means insignificant difference (P>0.05)

Once the relative humidity was higher than 70% however, the pore diffusivity decreased relatively with increase in the relative humidity. In this case, the water vapor adsorption rate was very fast and the texture of banana foam was subsequently very soften as observed from the experiments, which leads to collapse of the pores and decrease of diffusivity as a consequent result. Figure 7 also presents the effect temperature on apparent pore diffusivity. As expected, the apparent pore diffusivity significantly increased with increase in temperature (P<0.05).

Figure 8 shows the apparent pore diffusivity of water for the samples at the initial foam densities of 0.3 and 0.5 g/cm^3. The pore diffusivity was slightly lower at the foam density of 0.5 g/cm^3 than at the density of 0.3 g/cm^3 for all experimental conditions. However, the statistical analysis of these pore diffusivity data showed the insignificant difference among the two initial foam densities.

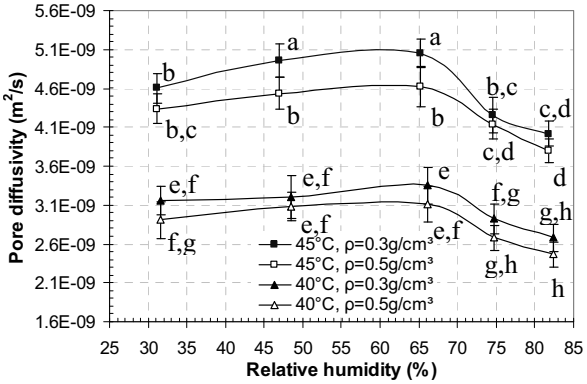

Fig. 8. Effect of initial foam densities on the apparent pore diffusivities at different relative humidities and temperatures of 40 and 45^{o}C: the same letter means insignificant difference (P>0.05)

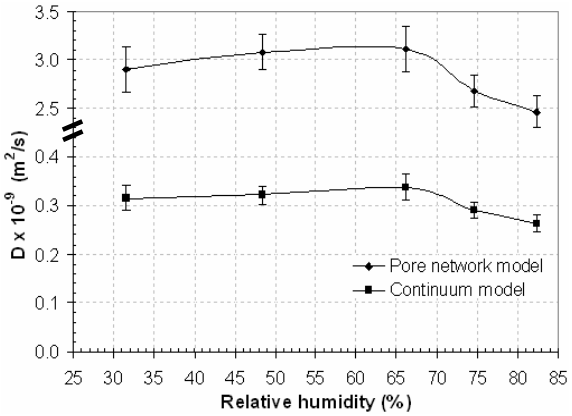

Fig. 9. Comparison between pore diffusivities and effective diffusivities of banana foam mat at 40 ^{o}C and relative humidities for the initial banana foam density of 0.5 g/cm^3

Figure 9 shows the comparison of the apparent pore diffusivity and the effective diffusivity. The value effective diffusivity was determined using Eq. (1) assuming that the moisture migration occurred in one dimension and the water vapour transported from the air to the top surface by convection. It can be seen that the effective diffusivity is approximately 9 times lower than the pore diffusivity. If the fraction void area for the banana foam density of 0.5 g/cm^3 was 0.26 as previously mentioned, the tortuosity factor calculated by Eq. (2) was 2.3.

.

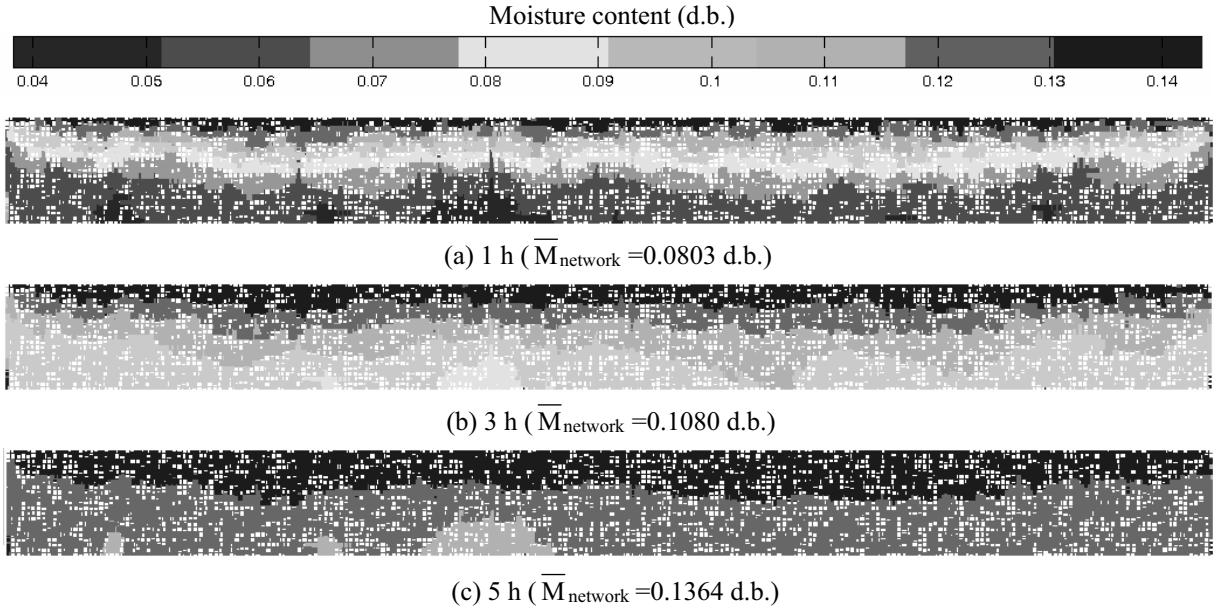

(a) 1 h ($\overline{M}_{network}$ =0.0803 d.b.)

(b) 3 h ($\overline{M}_{network}$ =0.1080 d.b.)

(c) 5 h ($\overline{M}_{network}$ =0.1364 d.b.)

Fig. 10. Visualization of moisture contents in pores of banana foam at temperature of 35^{o}C, initial foam density of 0.3 g/cm^3 and relative humidity of 50%

This value was in a normal range of porous materials (adsorbents and catalysts) for which the tortuosity factor varies between 2 and 6, corresponding to the porosity between 0.3 and 0.8 (Aguilera and Stanley, 1999)

Validation

As previously shown in Figures 2 and 3, the pore network model showed a good fit to the experimental data throughout the exposure time, with R^2-values above 0.98 at the relative humidity below 67%. Beyond 67%, however, the lower accuracy of prediction was found (R^2 values varying between 0.96-0.97); the model predicted the change of moisture content of sample relatively faster than the experiment at the early exposure time and became relatively slower at the later time.

Graphic visualization

Figure 10 shows the moisture distribution in 2-D pore network during adsorption process. Each pore was colored according its moisture content. The representative colours with 8 shades from red to blue were used for corresponding range of moisture from 0.038 to 0.138 d.b.

At the beginning, every pore within the network presumably contained the moisture content of 0.038 d.b. After 1 hour of adsorption, it can be seen in Figure 10a that the adsorption front moved from the top to the bottom and this confirmed the assumption used in the model. Moisture content near the surface reached the equilibrium value of 0.138 d.b. whilst the moisture content near the bottom was approximately 0.05-0.06 d.b., indicating that the liquid water only forms a thin liquid film near the pore walls and moisture transfer processes at this time may be dominated by molecular vapour diffusion.

In addition, it is clear from Figure 10 that the pattern of increasing moisture content at the same horizontal plane for a given time was irregular, reflecting the pore structure effect. As a result, the moisture contents were quite different and this can be seen clearly at the bottom surface of the pore network for the exposure time of 3 hours as an example, showing the moisture content of approximately 0.08-0.09 d.b in a small area as indicated by yellow colour (see Figure. 10b) whilst the other areas at the bottom surface were coloured by green corresponding to the moisture contents of 0.095-0.105 d.b. For the region of lower moisture content, the pores positioned at that region were relatively larger in sizes than the surrounding nearby pores. Hence, the moisture diffusing through those large pores was restricted by the smaller ones since the cross sectional area available for moisture diffusion is reduced in the surrounding nearby small pores.

CONCLUSIONS

- A 2-D stochastic pore network has been developed to represent the pore structure of banana foam and the transport of water vapour in the pores of the network was described by Fick's second law. The optimization technique with a

golden-search method was used to determine the diffusivity of pores. The experimental results showed that the pore network model could describe the moisture migration inside banana foam relatively well.

- The interactions between pore structure and moisture movement were relatively complicated and the visualization using colour coded moisture content helped understanding of their interactions.
- The pore diffusivity at a given temperature insignificantly changed with the relative humidities, except for the higher relative humidities of 70% at which the diffusivity had a decreasing trend. Moreover, the pore diffusivity depended strongly on the temperature, but was independent of the initial banana foam densities.

NOMENCLATURE

a_w	water activities	-
D_{eff}	effective diffusivity	m^2/s
D_A	actual diffusivity in the pore voids	m^2/s
D_p	apparent pore diffusivity	m^2/s
h_m	convective mass transfer coefficient	m/s
L	pore length	m
M	moisture content (dry basis)	kg/kg^{-1}
N	number of interval	-
$r_{i,j}$	pore radius	m
RH	relative humidity	%
RMSE	root mean square error	-
t	adsorption time	s
T	temperature	^oC
x	distance along the pore length	m
Z	number of pores in the network	-

Greek letters

ε	porosity	-
τ	tortuosity factor	-
ρ	initial foam density	g/cm^3

Subscripts

i	initial
m	mass
e	equilibrium
exp	experimental
s	surface

ACKNOWLEDGEMENTS

The authors express their appreciation to the Commission on Higher Education and the Thailand Research Fund (TRF) for financial support.

REFERENCES

Aguilera, J. M., Stanley, D. W. (1999), Microstructural principles of food processing and engineering. Aspen Publishers Inc, Maryland.

Androutsopoulos, G.P. and Mann, R. (1979), Evaluation of mercury porosimeter experiments using a network pore structure model, Chemical Engineering Science, Vol. 34, pp. 1203-1212.

Blunt, M. (2001), Flow in porous media-pore-network models and multiphase flow, Current Openion in Colliod & Interface Science, Vol. 6, pp. 197-207

http://www.intel.com/cd/software/products/asmo-na/eng/compilers/284132.htm

Hollewand and Gladden, L.F. (1992), Modeling of diffusion and reaction in porous catalysts using a random three-dimensional network model, Chemical Engineering Science, Vol. 47, pp. 1761-1770.

Jamali, A., Kouhila, M., Mohamed, L. A., Idlimam, A., Lamharrar, A. (2006), Moisture adsorption–desorption isotherms of citrus reticulata leaves at three temperatures, Journal of Food Engineering , Vol. 77, pp. 71–78.

Kaya, S., Kahyaoglu, T. (2005), Thermodynamic properties and sorption equilibrium of pestil (grape leather), Journal of Food Engineering, Vol.71, pp. 200-207.

Kim, M. K., Okos, M., R. (1999), Some physical, mechanical, and transport properties of crackers related to checking phenomenon, Journal of Food Engineering, Vol. 40, pp. 189-198.

Labuza, T.P., Hyman, C.R. (1998), Moisture migration and control in multi-domian foods, Food Science and Technology, Vol. 9, pp. 47-55.

Mann, R. (1993), Developments in chemical reaction engineering: issues relation to particle pore structures and porous materials, Chemical Engineering Research and Design, Vol. 71, pp. 551-562.

Palou, E., Lopez-Malo, A., Argiz, A. (1997) Effect of temperature on the moisture sorption isotherms of some cookies and corn snacks, Journal of Food Engineering , Vol. 31, pp. 85-93.

Prachayawarakorn, S., Prakotmak, P., Sopornronnarit, S. (2008), Effect of pore size distribution and pore-architecture assembly on drying characteristics of pore networks, International Journal of Heat and Mass Transfer, Vol. 51, pp. 344-352.

Roca, E., Guillard, V., Guilbert, S., Gontard, N. (2006), Moisture migration in a cereal composite food at high water activity: Effects of initial porosity and fat content, Journal of Cereal Science, Vol. 43, 144-151.

Segura, L.A., Toledo, P.G. (2005), Pore-level modeling of isothermal drying of pore networks:

Effects of gravity and pore shape and size distributions on saturation and transport parameters, Chemical Engineering Journal, Vol. 111, pp. 237-252.

Yiotis, A.G., Stubos, A.K., Boudouvis, A.G.,Tsimapanogiannis, I.N, Yortsos, Y.C. (2005), Pore-network modeling of isothermal drying in porous media. Transport in Porous Media, Vol. 58, pp. 63-86.

EFFECT OF MOISTURE ADSORPTION ON EFFECTIVE DIFFUSIVITY AND TEXTURAL PROPERTY OF BANANA FOAM MAT

*Preeda PRAKOTMAK[1], Somkiat PRACHAYAWARAKORN[2] and Somchart SOPONRONNARIT[1]

[1] *School of Energy, Environment and Materials, King Mongkut's University of Technology Thonburi*
126 Pracha u-tid Road, Bangkok 10140, Thailand

[2] *Department of Chemical Engineering, King Mongkut's University of Technology Thonburi*
126 Pracha u-tid Road, Bangkok 10140, Thailand

Corresponding author: Somkiat PRACHAYAWARAKORN. E-mail: somkiat.pra@kmutt.ac.th

Keywords: adsorption kinetics; banana foam mat; crispness; effective moisture diffusivity

ABSTRACT

Foam-mat drying technique can improve the mass transfer rate. However, the high porous of dried product could quickly adsorb the moisture from the air during storage, leading to the lost of textural property. The main purpose of this research was therefore to study moisture adsorption kinetics of banana foam mat and its quality. The adsorption isotherms experiments were carried out with standard static method using saturated salt solutions over a wide range of relative humidities from 31 to 82%, and a temperature range of 35 to 45°C. Two different banana foam densities of 0.21 and 0.26 g/cm^3 were used to adsorb water vapor under the controlled conditions. A Fick's second law and the optimization technique were used to estimate the effective moisture diffusivity (D_{eff}) at adsorption conditions. Three empirical equations i.e. a power-law, and two exponential forms for describing the dependence of the effective moisture diffusivity on moisture content were tested. The power-law function was suitably described the variation of the effective moisture diffusivity with moisture content. The force deformation curve obtained from a penetration test of the samples showed that an increase of moisture content of sample decreased number of peaks and initial slope.

INTRODUCTION

The foam mat drying can enhance the drying rate of banana since its structure is very porous. The textural properties in particular hardness and crispiness are better in the dried foamed banana than the non foamed banana; the foamed banana provides less hardness and more crispy. However, the product is very hygroscopic and its texture could be lost quickly if it keeps undergoing undesirable condition. To circumvent the undesirable property, the understanding of moisture adsorption for the banana foam at conditions is necessary. Application of food texture analysis and moisture diffusivity will help to improve food product quality adsorption conditions and understand the movement of moisture.

Many dry crispy products are sensitive to moisture migration. Moisture transport in porous foods is very complicated since the pore system is very complex and irregular. Generally, the diffusion of gases or liquids through the complex structure can be simply described by classical Fick's second law in which the overall mass transports are lumped into an effective diffusivity. The wide ranges of effective moisture diffusivity in different physical structure of food materials have been reported in the literature [1] and it has been known to be either independent or function of moisture content. Nevertheless, general model for evaluating the effective diffusivity of food materials have not existed [2]. Many empirical such as power-law, polynomial and exponential forms were frequently used to describe the relation of effective moisture diffusivity with moisture content in the foodstuffs [3, 4 and 5]. The different result in effective moisture diffusivity values would be attributed to the difference in food structure.

The objectives of this study were to select a suitable empirical equation of effective moisture diffusivity, to investigate the influence of relative humidity, temperature and initial foam density on the effective moisture diffusivity. The effect of moisture content on product textures was also determined. The textural property was characterized by initial slope, number of peaks and maximum force.

DRIED BANANA FOAM PREPARATION

The banana puree with 5% of fresh egg albumen used as foaming agent were foamed to density of 0.3 and 0.5 g/cm^3. The density was determined by measuring the mass of a fixed volume of the foam. The banana foams was poured slowly into a steel block and then placed on a mesh tray, which was covered with aluminium foil. After that, it was dried to about 3% kg/kg d.b. using 80°C and a 0.5 m/s superficial air velocity. The banana foam prepared from the initial foam densities of 0.3 and 0.5 g/cm^3 can produce the dried banana densities of 0.21 ± 0.02 and 0.26 ± 0.02 g/cm^3, respectively. The product thicknesses after drying were 2.8 mm and 3.2 mm for the densities of 0.21 and 0.26 g/cm^3, respectively. Five replicates were performed.

ADSORPTION EXPERIMENT

Moisture adsorption experiments were carried out using the static method. Samples were placed into the glass jars contained the saturated salt solutions ($MgCl_2$ $6{\cdot}H_2O$, $Mg(NO_3)_2$ $6{\cdot}H_2O$, KI, NaCl and KCl) which provided the relative humidity (RH) in range of 32-82% at the temperatures of 35, 40 and 45°C. All the jars were placed in the temperature-controlled oven at the operating temperature with a precision of ±1°C (UFE500, Memmert, Germany). Samples were weighed at different exposure

times ranging from 1 to 120 h. At RH > 74%, a small amount of toluene held in a vial was fixed in the glass jars in order to prevent microbial spoilage of the samples [6]. Moisture content of each sample after reaching the equilibrium condition was determined by drying it with the hot air oven at a temperature of 103°C for 3 h. The moisture content determined by the hot air oven was used instead of the AOAC method [7], the percentage error from two methods approximately 0.4% [8]. The experiment at each sorption condition was repeated three times and the mean value was reported.

SEM PHOTOGRAPH

The morphologies of dried banana foam mats were characterized using scanning electron microscope (SEM) with an accelerating voltage of 10 kV. Before photographing, the specimens were cut into a dimension of 5 × 5 mm and then glued on the metal stub. The samples were coated with gold, scanned, and photographed at 15X magnification

TEXTURE ANALYSIS

The effects of moisture content on product textures were studied. The initial moisture content of the banana foam was about 0.038 kg/kg d.b. The dried banana foam mats adsorbed water vapour in the glass jars which controlled relative humidity about 75% by using saturated NaCl solutions at temperature of 24°C. After moisture adsorbed for determined time, the test applied a direct force to the sample using a 5 mm spherical probe at a constant crosshead speed of 2 mm/s. The hardness was defined as the maximum force of the force-deformation curve and the crispness was characterized by the number of peaks and the slope of the first peak. The data were analyzed by ANOVA using Duncan's multiple range test at $p<0.05$. Eight samples were tested and the average values of hardness and crispness were presented. Moisture content of each sample after the texture analysis was determined. All experiments were performed at 24°C.

DETERMINATION OF EFFECTIVE MOISTURE DIFFUSIVITY

The banana foam mats used in the experiments has a dimension of 43 × 43 × 4 mm. This sample size may provide the transport of moisture in direction of thickness. The transport of moisture can be described by Fick's equation:

$$\frac{\partial M(x,t)}{\partial t} = \frac{\partial}{\partial x}\left(D_{eff}(M)\frac{\partial M(x,t)}{\partial x} \right) \quad (1)$$

or

$$\frac{\partial M(x,t)}{\partial t} = D_{eff}(M)\frac{\partial^2 M(x,t)}{\partial x^2} + \frac{\partial M(x,t)}{\partial x}\cdot\frac{\partial D_{eff}(M)}{\partial x} \quad (2)$$

where $D_{eff}(M)$ is the effective moisture diffusion coefficient (m^2/s), M the moisture content (kg/kg d.b.), t the time (s) and x the distance along the diffusion path (m). In this study, it was assumed that the initial moisture distribution inside the sample was spatially uniform and the migration of water vapor from the surrounding air to the foam mat surface occurred at the top surface and no moisture transferred at the bottom since the sample surface was placed on an opaque glass dish. Initial moisture distribution in the sample was assumed to be uniform. From the above assumptions, the following initial and boundary conditions can be setup:

$$M(x,t) = M_{in} \quad 0 \le x \le L \ at\ t = 0 \quad (3)$$

$$D_{eff}(M)\left(\frac{\partial M(L,t)}{\partial x}\right) = h_m\left(M_e - M_s\right) \quad x = 0 \ at\ t > 0 \quad (4)$$

$$\frac{\partial M(x,t)}{\partial x} = 0 \quad x = L \ at\ t > 0 \quad (5)$$

where M_{in} is the initial moisture content (kg/kg d.b.), M_s and M_e the moisture content at the surface and at the equilibrium (kg/kg d.b.), respectively, L thickness of material (m), h_m the convective mass transfer coefficient (m/s). Eqs. (2), (4) and (5) can be, respectively written in a finite difference form as follows:

$$\frac{M_i^{t+1} - M_i^t}{\Delta t} = D_i\left(\frac{M_{i+1}^t - 2M_i^t + M_{i-1}^t}{(\Delta x)^2}\right) + \left(\frac{M_{i+1}^t - M_{i+1}^t}{2\Delta x}\right)\left(\frac{D_{i+1}^t - D_{i-1}^t}{2\Delta x}\right) \quad (6)$$

$$D_N^t\,\frac{M_N^{t+1} - M_{N-1}^{t+1}}{\Delta x} = h_m\left(M_e^{t+1} - M_N^{t+1}\right) \quad (7)$$

$$\frac{M_0^{t+1} - M_0^t}{\Delta t} = 2D_0^t\left(\frac{M_{i-1}^t - M_i^t}{(\Delta x)^2}\right) \quad (8)$$

In the calculation of moisture content, the sample thicknesses of 2.8 and 3.2 mm for the respective foam densities of 0.21 and 0.26 g/cm^3 were divided in 105 and 120 layers and the time step of 0.01 sec was chosen.

After the moisture content at every node is known, the average moisture content $\overline{M}(t)_{pre}$ can be readily be calculated by integrating the predicted moisture profile though out the sample thickness and the trapezoidal numerical integration was used:

$$\overline{M}(t)_{pre} = \frac{\left(M_0^t + M_N^t + 2\sum_{i=1}^{N-1} M_i^t\right)\Delta x}{2L} \quad (9)$$

where N is number of layer. The dependence of diffusivity on moisture content can not be described by any specific equation. To find the suitable form of equation, three possible empirical equations obtained from the literature [9, 10, and 11] were tested with the moisture adsorption data.

$$D_{eff}(M) = D_0 \exp\left(-\left(e_1 M + e_2 M^2\right)\right) \quad (10)$$

$$D_{eff}(M) = D_0 \cdot M^{D_x} \quad (11)$$

$$D_{eff}(M) = D_0 \exp(-a \cdot M) \quad (12)$$

where D_0, D_x, e_1, e_2, and a are the constant parameters.

The accuracy of the models was evaluated by root mean square error (RMSE) and coefficient of determination (R^2) value. The RMSE is defined as

$$RMSE = \left[\frac{1}{P} \sum_{n=1}^{P} (M(t)_{\exp} - \overline{M}(t)_{pre})^2 \right]^{1/2} \quad (13)$$

where $M(t)_{\exp}$ is the experimental average moisture content of material at time t, $\overline{M}(t)_{pre}$ the predicted average moisture content and P the number of experimental data. The lower the value of RMSE is the better the goodness of fit. In this work, a modified Nelder-Mead simplex method was used to estimate the constant parameters in Eqs. (10), (11) and (12). The RMSE was set as the objective function with a tolerance of 10^{-9}. The initial guesses obtained by least squares fits of the data calculated from the method of slopes [12]. The model with the lowest value of RMSE and highest value of R^2 was considered the best model to correlate the experimental data. The code for numerical solution was written in Microsoft Visual C++ 6.0 programming language. All computations were implemented using Intel C++ Compiler [13] and run on a PC with 3.0 GHz.

RESULTS AND DISCUSSION

Identification of effective moisture diffusivity model

To find the appropriate diffusion equation, two sets of the moisture adsorption data at 40°C and 66% RH as well as at 35°C and 83% RH were demonstrated. The estimated constant parameters for Eqs (10), (11) and (12) along with their values of RMSE and R^2 are presented in Table. 1. The R^2-value for all diffusion models is above 0.99 and the values of RMSE were lower than 0.007. When using these constant parameters for calculating the moisture content, it was found that all diffusion models can predict moisture content in agreement with the experiment as can be seen in Figs. 1a and 1d.

Table 1 Estimated parameters of empirical models for selected conditions

Estimated parameters	Experimental conditions					
	40 °C, 66% RH			35 °C, 83% RH		
	Eq.(10)	Eq.(11)	Eq.(12)	Eq.(10)	Eq.(11)	Eq.(12)
D_0	5.947×10^{-10}	8.908×10^{-11}	3.962×10^{-10}	1.709×10^{-10}	6.326×10^{-11}	1.236×10^{-10}
e_1	11.108	-	-	4.604	-	-
e_2	-27.508	-	-	-7.172	-	-
D_x	-	-0.463	-	-	-0.244	-
a	-	-	-3.914	-	-	-1.210
R^2	0.996	0.999	0.998	0.995	0.999	0.998
RMSE	0.0035	0.00101	0.00114	0.0065	0.00306	0.00336

However, when considering moisture diffusivity obtained from the models, it can be seen from Figs 1c and 1f that the diffusivity values of all diffusion models decrease with increasing moisture content. According to theses results, it implied that difference in the values of effective moisture diffusivity determined from the models was insensitive to the calculation of moisture content; the moisture contents calculated using the diffusion models were almost superimposed. Hence, it is very difficult to identify the suitable model for predicting the moisture content based on the values of RMSE and R^2, and one more criterion was used to quantify the quality of estimated constant parameters.

The local relative error (E) was used to identify the suitable diffusion model and it is defined as

$$E(t) = 100 \frac{\left| M_{\exp}(t) - M_{calc}(t) \right|}{M_{\exp}(t)} \quad (14)$$

where $M_{exp}(t)$ is the experimental moisture content at time t and $M_{calc}(t)$ is the moisture content from prediction. If the estimation of moisture content is perfect, the value of E at time t is zero. The values of E for the three empirical diffusion models are shown in Figs. 1b and 1e, indicating that the value of E was less than 1% throughout the exposure time when the relationship between effective moisture diffusivity and moisture content was described by Eq. (11) whilst the error from prediction by using other equations were higher than 1 %.

The prediction of adsorbed moisture content at the early period with high accuracy is very important to crispy product since the product quickly loses its crispy texture when the product adsorbs the water vapor up to certain moisture content. From this study, the banana foam will lose crispiness at moisture content about 5% d.b. as can be seen in section of texture banana foam. From these results, it can be deduced that Eq. (11) is reasonably used to describe the moisture adsorption of banana foam. This power-law model is also used to describe moisture adsorption in the snack foods such as sponge cake [14], showing the similar tend of moisture diffusivity with moisture content.

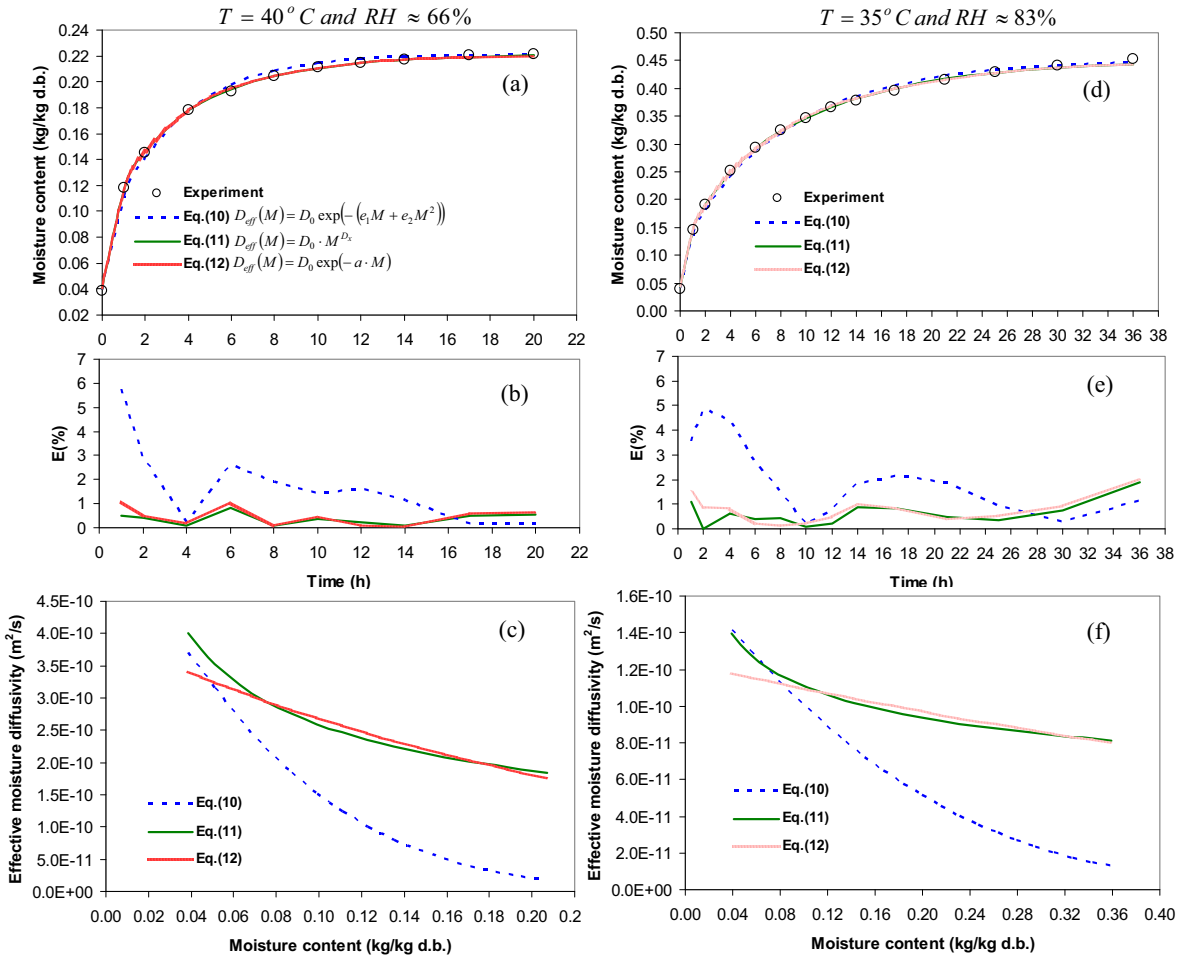

Fig. 1. Validation of the moisture uptake estimated and the variation of effective diffusion coefficient with moisture content of two selected cases

Effect of relative humidity on effective moisture diffusivity

Fig. 2 shows the moisture adsorption at 35°C and relative humidity of 32 to 83% for the banana foam density of 0.21 g/cm^3. As expected, the faster adsorption rate was accomplished with higher relative humidity. The predictions of moisture content using Eqs. (1) and (11) agreed well with experimental data over a wide range of relative humidities.

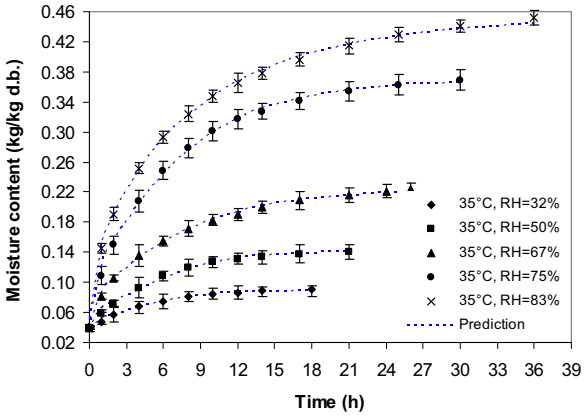

Fig. 2. Effect of relative humidities on moisture adsorption kinetics at 35°C for the foam density of 0.21 g/ cm^3

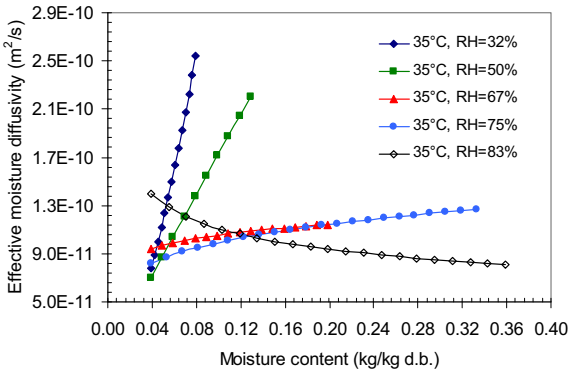

Fig. 3. Variation of effective diffusion coefficient with moisture content at various relative humidities for the dried banana foam density of 0.21 g/cm^3

Fig. 3 shows the changes of D_{eff} with moisture content at 35°C and at different relative humidities. The trend of changing D_{eff} with moisture content was very different amongst relative humidities. The values of D_{eff} remarkably increased with increasing moisture content at relative humidity of 32% and when the relative humidity increased continually, the change of D_{eff} with moisture content became smaller, as indicated by a lower slope,

until at relative humidity of 83% the D_{eff} trend was reversed, showing a decrease in D_{eff} when the sample adsorbed water vapor. The D_{eff} trends at other temperatures such as 40 and 45°C were similar to Fig.3, but the tendency for D_{eff} to decrease with moisture content occurred at lower relative humidity (66% RH at 40-45°C).

Such different trends of D_{eff} can be explained by the fact that at the relative humidity of 32% the water vapour can diffuse rapidly through the voids of the banana foam mats and is then adsorbed onto the pore wall. Since the equilibrium moisture content at this relative humidity is very low (< 0.13 kg/kg d.b.), the moisture content at this level is called bound water. The molecular mobility of bound water increases with the level of moisture content. Hence, the increase of D_{eff} with increasing moisture content could be attributed to contributions from diffusion in the solid matrix of food and vapour diffusion in pores.

When the relative humidity increased, the water vapor molecules frequently collide amongst themselves in the pore space and the condensation of water vapor may occur inside the pore spaces in particular small pores. The occurrence of condensation is due to the increasing van der Waals interactions between vapor molecules inside pore space. When the pores inside the porous food are filled with the condensed water, the water vapour cannot diffuse through these pores and this, in turn, provides the smaller flux of water vapor diffusing through the porous food. Hence, the D_{eff} decreased. As shown in Fig. 3, for example, when compared at the same moisture content, the value of D_{eff} was significantly lower at relative humidity of 50% than at 75%. From the condensation effect, the change of moisture diffusivity with moisture content became smaller at higher relative humidity.

At the relative humidity of 83% at which the banana foam surface of banana foam started getting wet at moisture content of approximately 0.12 kg/kg d.b. This may cause a sharp decrease of D_{eff} for the moisture range of 0.04 kg/kg d.b. to 0.12-0.16 kg/kg d.b. Beyond this range, the D_{eff} changed slightly, implying that the transport of moisture is contributed from the liquid diffusion.

Effect of temperature and initial foam density on effective moisture diffusivity

Fig. 4 shows the changes of D_{eff} at 35 and 40°C. As expected, the D_{eff} increased with increase in temperature.

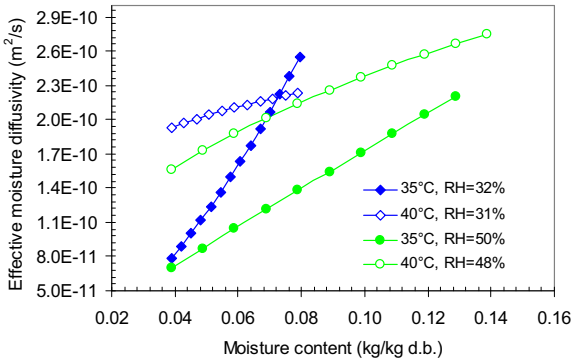

Fig. 4. Effect of temperatures on the D_{eff} at the foam density of 0.21 g/cm^3

Fig. 5 shows the D_{eff} value for both foam densities at an illustrated temperature of 35°C for the relative humidities approximately 32 and 50%. As shown in this figure, at the same relative humidity, the D_{eff} was slightly lower at the foam density of 0.26 g/cm^3 than at the density of 0.21 g/cm^3. The difference in the D_{eff} can be accounted for the morphology difference among both samples as can be seen in the SEM.

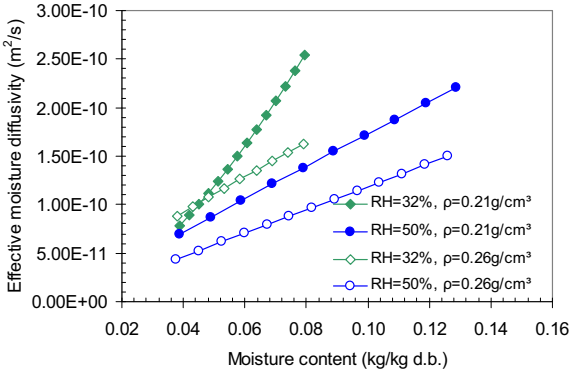

Fig. 5. Effect of initial foam densities on D_{eff} at the temperature of 35°C

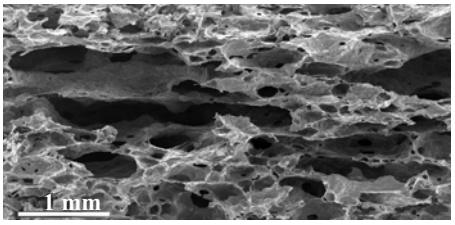

(a) 0.21 g/cm^3

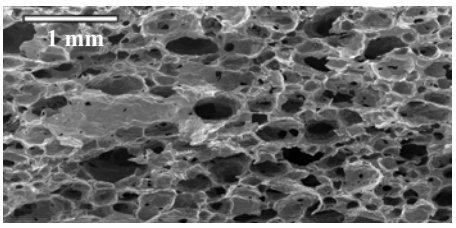

(b) 0.26 g/cm^3

Fig. 6. SEM micrographs of dried banana foam mats at different initial foam densities

The microstructures of dried banana foam mats characterized by SEM are shown in Figs. 6a and 6b for two initial foam densities. It is clear from these figures that the sample with an initial foam density of 0.21 g/cm^3 had larger pore than higher foam density. In the porous banana foam studied, the void area fractions for the banana foam densities of 0.21 and 0.26 g/cm^3 were 31 and 26 %, respectively. High porosity in porous foods provides less diffusional flux resistance and thus greatly facilitates the moisture transport to those porous foods.

Texture of banana foams

Fig. 7 shows the curves of the force measured versus displacement recorded by texture analyzer at different moisture content levels. As observed from this figure, the maximum force decreased with increasing the moisture content levels. The jagged pattern of the force-deformation

curve reflects the higher crispy behavior of the banana foam mats. When the sample was adsorbed more moisture, this fracture pattern was absent, revealing the sample is not expected to have the crisp and hard eating character.

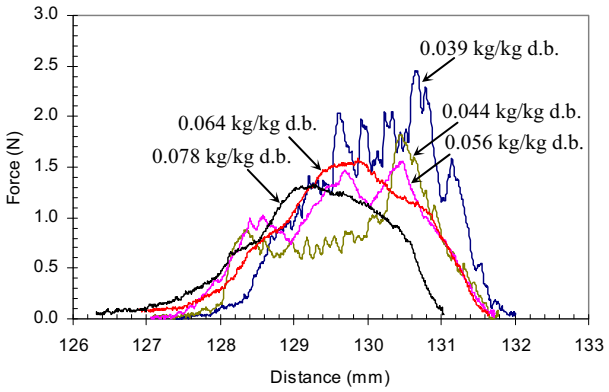

Fig. 7. Variation in force-deformation curve during compression test at various moisture content levels for foam density of 0.21 g/cm^3

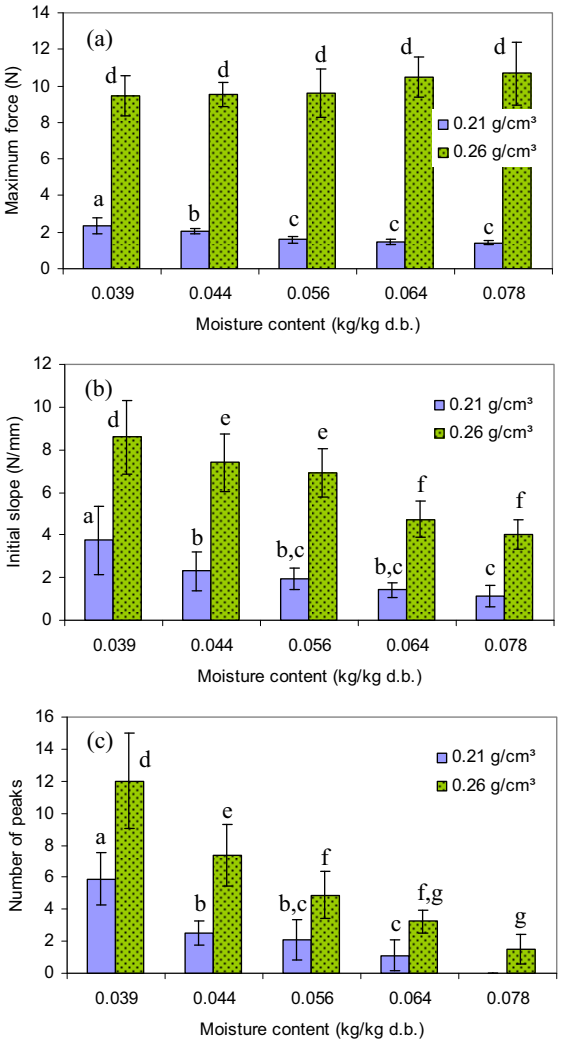

Fig. 8. Effect of moisture content and initial foam densities on (a) maximum force, (b) initial slope and (c) number of peaks of the banana foam mats

The textural parameters such as maximum force, initial slope and number of peaks are determined from force-deformation curve and the results are shown in Fig. 8. The number of peaks was counted when the force amplitude is more than the threshold values, which was set at 30 g. The statistical analysis results were also shown in Figs. 8b and 8c. The number of peaks and initial slope for both foam densities significantly decreased with increasing moisture content, but the maximum forces of each initial foam densities were insignificantly different when the moisture content increased. The number of peaks for both foam densities approaches zero at moisture content of about 0.078 kg/kg d.b., which indicate that the product lost all its characteristic crispness.

In the tropical countries such as Thailand, the relative humidity was around 65-73%. At this range of relative humidity, the equilibrium moisture content of the banana foam was approximately 0.24-0.36 kg/kg d.b. Hence, the banana foam mat can lose its textures. To maintain the crispy texture of product, the banana foam should be kept at low relative humidity or kept with a good packing system.

CONCLUSION

An optimization technique using Nelder-simplex method was applied to estimate the effective moisture diffusivity. Three empirical equations describing the dependence of the effective moisture diffusivity on moisture content were tested. The statistical analysis shows that a power law function suitably described the relationship of the effective moisture diffusivity with moisture content in banana foam mat. The relative humidity strongly affected the moisture diffusion mechanisms as indicated by the subtle changes of effective moisture diffusivity at conditions. In addition to the moisture content and relative humidity, the effective moisture diffusivity depended on the temperature and foam density. As the banana foam adsorbed water vapor, the number of peaks and initial slope decreased, but the maximum force did not change.

ACKNOWLEDGMENTS

The authors would like to express their appreciation to the Commission on Higher Education, Thailand for supporting by grant fund under the program Strategic Scholarships for Frontier Research Network for the Ph.D. Program Thai Doctoral degree for this research. This work was also supported in part by the Thailand Research Fund and King Mongkut's University of Technology Thonburi.

REFERENCES

1. Tong, C.H. and Lund, D.B. Effective moisture diffusivity in porous materials as a function of temperature and moisture content. Biotechnol. Prog. 6: 67-75 (1990)
2. Saravacos, G.D. and Maroulis, Z.B. Transport properties of foods, Marcel Dekker, New York (2001)

3. Zogzas, N.P., Maroulis, Z.B. and Marinos-Kouris, D. Moisture Diffusivity Data Compilation in Foodstuffs. Drying Technology. 14: 2225-2253 (1996)
4. Loulou, T., Adhikari, B. and Lecomte, D. Estimate of concentration-dependent diffusion coefficient in drying process from the space-average concentration versus time with experimental data. Chemical Engineering Science. 61: 7185-7198 (2006)
5. Bourlieu, C., Guillard, V., Powell, H., Vallès-Pàmies, B., Guilbert, S., and Gontard, N. Modelling and control of moisture transfers in high, intermediate and low a_w composite food. Food Chemistry. 106: 1350-1358 (2008)
6. Kaya, S. and Kahyaoglu, T. Thermodynamic properties and sorption equilibrium of pestil (grape leather). Journal of Food Engineering. 71: 200-207 (2005)
7. AOAC. Official Methods of Analysis, 16th ed, Association of Official Agricultural Chemists, Washington, DC (1995)
8. Thuwapanichayanan, R., Prachayawarakorn, S., and Sopornronnarit, S. Modeling of diffusion with shrinkage and quality investigation of banana foam mat drying. Drying Technology. 26: 1326-1333 (2008)
9. Olek, W. and Weres, J. Effects of the method of identification of the diffusion coefficient on accuracy of modeling bound water transfer in wood. Transport Porous Media (2006)
10. Guillard, V., Broyart, B., Bonazzi, C., Guilbert, S. and Gontard, N. Moisture diffusivity in sponge-cake as related to porous structure evaluation and moisture content. Journal of Food Science. 68: 555-562 (2003)
11. Sakin, M., Kaymak-Ertekin, F., and Ilicali, C. Modeling the moisture transfer during baking of white cake. Journal of Food Engineering. 80: 822-831 (2007)
12. Karathanos, V. T., Villalobos, G., and Saravacos, G. D. Comparison of two methods of estimation of the effective moisture diffusivity from drying data. Journal of Food Science. 55: 218-233 (1990).
13. Intel® Software Network. Available (2009) at: http://www.intel.com/cd/software/products/asmo-na/eng/368972.htm
14. Roca, E., Guillard, V., Guilbert, S. and Gontard, N. Moisture migration in a cereal composite food at high water activity: Effects of initial porosity and fat content, Journal of Cereal Science. 43: 144-151 (2006)

10 Superheated-Steam Drying Applied in Food Engineering

Somkiat Prachayawarakorn
and Somchart Soponronnarit

CONTENTS

10.1 INTRODUCTION

The primary aim of food drying is to preserve the product, as a decrease in the product moisture content can prevent the growth of microorganisms and enzymatic reactions. However, drying may have an adverse effect on physical, chemical, and nutritional values of food products. The success or failure of a drying process depends on the product quality obtained after drying and also on the efficiency of the process.

An idea of using superheated steam instead of hot gas (air, combustion, or flue gases) for drying was initially introduced in Germany in 1908 as reported by Douglas (1994), but its application was limited to only a few industries. Later, its use has widely been acknowledged in many applications, i.e., paper (Svensson, 1980; Douglas, 1994), foods (Iyota et al., 2001; Taechapairoj et al., 2003; Tang et al., 2005),

coal (Chen et al., 2000), and wood (Pang and Dakin, 1999). The product quality after drying is usually better in superheated-steam drying (SSD) than in hot-air drying, particularly in terms of less shrinkage and higher product porosity.

A superheated-steam dryer is normally designed as a closed loop in which exhaust steam may be either reused or employed in other processes resulting in net energy savings. The temperature of superheated steam used under atmospheric pressure generally varies between 100°C and 150°C. The high temperature restricts its application to foods that are not sensitive to heat. Mostly, the applications of SSD are related to starch-based products such as parboiled rice, noodles, potato chips, and durian chips (Iyota et al., 2001; Markowski et al., 2003; Taechapairoj et al., 2004; Jamradloedluk et al., 2007).

In this chapter, the basic concepts of SSD, drying characteristics, mathematical modeling of the process operation, and quality consideration of the selected food products are outlined and discussed.

10.2 ADVANTAGES AND LIMITATIONS OF SUPERHEATED STEAM DRYING

When water in a liquid state is contained in a closed vessel and heated under a given pressure, its temperature increases up to the boiling point as shown in Figure 10.1. At this point, water is called saturated liquid (shown by letter a in Figure 10.1). Upon continued heating, the temperature would remain constant at that saturation value and water would continually vaporize. During this heating period, the system contains two phases, liquid and vapor. After the last droplet of water vaporizes, there is only water vapor in the system, which is called saturated steam (shown by letter b in Figure 10.1). From a practical viewpoint, saturated steam cannot be used to dry any materials since the steam is wet. To obtain dry or superheated steam, saturated steam

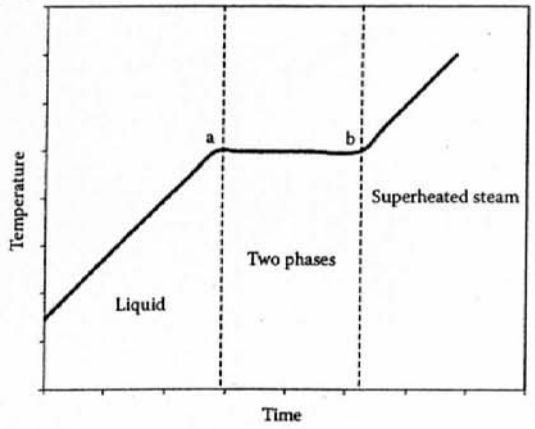

FIGURE 10.1 Illustration of changing states of water during heating.

needs to be further heated by flowing it through a heat exchanger. As a result, the temperature of steam increases beyond its saturation temperature. The temperature difference between superheated and saturated steam is called degree of superheat.

Using superheated steam in an industrial process can lead to substantial energy savings if the vapor evaporating from the product being dried is condensed and if the latent heat of condensation can be recovered and used in other unit operations. This benefit makes superheated steam a more attractive drying medium for industrial use, especially if the energy cost for drying is a major proportion of the total production cost. In addition, the use of superheated steam for drying foods has advantages to both consumers and industry as detailed by many researchers (Lane and Stern, 1956; Shibata and Mujumdar, 1994; Tang and Cenkowski, 2000; Deventer and Heijmans, 2001; Soponronnarit et al., 2006):

1. Use of superheated steam as the drying medium leads to an oxygen-free drying system, which prevents oxidative reactions, resulting in an improvement of the product quality.
2. SSD allows pasteurization, sterilization, and deodorization of food products during drying. In addition, products are partially cooked, with possible favorable changes in their textural properties.
3. SSD may reduce processing time and processing steps. For example, in producing parboiled rice by a conventional process, the process consists of three main stages, namely, soaking, steaming, and drying. However, steaming and drying can be combined into one stage with the use of SSD, thereby allowing a significantly shorter processing time.
4. Higher drying rates are obvious in both constant and falling rate periods if the product can be dried at a temperature above the inversion temperature since the temperature difference between particle and fluid stream is larger in superheated steam than in hot air, resulting in higher heat flux from the gas to the particle surface. More details about the inversion temperature will be given in Section 10.3. The higher drying rates would increase the dryer performance, which leads to a reduction in equipment size or an increase in drying capacity.
5. SSD may have high thermal efficiency if the exhaust steam can be used elsewhere in the process.
6. SSD enhances physical food qualities as it leads to less shrinkage and high product porosity due to evolution of moisture inside the product during drying.

However, SSD also has the following limitations:

1. There is unavoidable condensation at the beginning of drying because raw materials are generally fed into the system at ambient temperature. This results in an increase in the moisture content of materials by approximately 2%–3%, resulting in an increase in the drying time by 10%–15%. In addition to the increase in the moisture content, condensation may interrupt the drying system, particularly in the case of a fluidized-bed dryer. Condensation of steam causes particle surface to be very wet and hence the particles would

agglomerate, resulting in more difficulty in fluidizing them. To alleviate this problem, raw materials need to be warmed up before being fed into the dryer.
2. An SSD system is more complicated and requires higher investment for insulation and auxiliary heating than in the case of a hot-air drying system. Shut down and start up also take longer for a superheated-steam dryer than for a hot-air dryer.
3. Application of SSD for heat-sensitive materials is unfavorable. Products that may suffer degradation at higher temperatures cannot be dried in superheated steam. However, it may be possible to use a two-stage drying technique, i.e., SSD followed by hot-air drying to alleviate this shortcoming. For example, drying of chicken meat using this two-stage technique appears to produce a higher quality dried product, i.e., product with less brown color and higher rehydration ability (Nathakaranakule et al., 2007).

10.3 FUNDAMENTALS OF DRYING IN SUPERHEATED STEAM

During drying, moisture from a drying product vaporizes into the drying medium, which then carries the water vapor away. The drying rate remains constant as long as the evaporated moisture of the material is available at its surface. During this constant drying rate period, heat transfer controls the moisture evaporation rate. In the case of hot-air drying, the moisture evaporation rate can be calculated by:

$$\frac{dM_w}{dt} = \frac{hA\left(T_{\text{drying medium}} - T_{\text{samp sur}}\right)}{\Delta H_w^{\text{vap}}} \tag{10.1}$$

where

dM_w/dt is the drying rate (kg water s^{-1})
h is the heat transfer coefficient (W m^{-1}·K^{-1})
A is the surface area of material in contact with the drying medium (m^2)
ΔH_w^{vap} is the latent heat of evaporation of moisture (J kg^{-1})
T is the temperature (K)

The temperature at sample surface is equal to the wet bulb temperature of hot air. However, when hot air is replaced by superheated steam, $T_{\text{samp sur}}$ in Equation 10.1 is replaced by the saturation (boiling) temperature of steam at the dryer operating pressure. Equation 10.1 is derived based on the assumptions that other modes of heat transfer from the gas medium to the solid sample, such as sensible heat effects and heat losses from solid sample, are neglected.

According to Equation 10.1, the evaporation rate of moisture into superheated steam and hot air may have different values, depending on the temperature difference between the sample surface and the bulk gas/vapor phase, and on the heat transfer coefficient of the drying medium. When the drying temperature is lower than the so-called inversion temperature, the evaporation rate of moisture into hot air is higher than that into superheated steam as illustrated in Figure 10.2. On the other hand, the moisture evaporation rate into a superheated-steam environment becomes

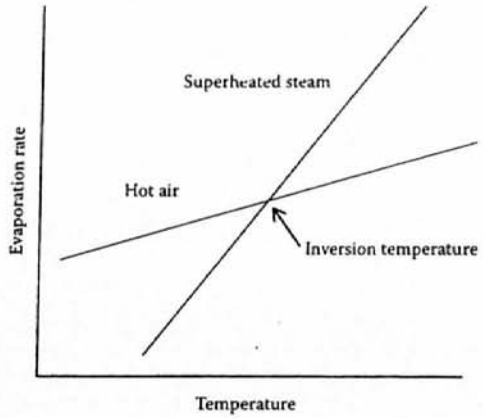

FIGURE 10.2 Variation of the evaporation rates with drying temperatures.

higher than that associated with a hot-air environment at temperatures beyond the inversion temperature.

Below the inversion temperature, the higher moisture evaporation rate in hot-air drying is related to the heat-transfer coefficient and the temperature difference between the sample surface and bulk gas phase. Considered at the same drying condition, i.e., a given gas velocity and a fixed operating pressure, both the heat-transfer coefficient and the temperature difference are higher for hot air than for superheated steam, being the latter variable more important. When the drying temperature reaches the inversion value, the temperature difference in Equation 10.1 is, in turn, smaller in hot-air drying than in SSD. However, this result can be compensated by the higher heat transfer coefficient for hot-air dying, and, hence, the drying rates in SSD and hot-air drying are equal at the inversion temperature. From this point on, the temperature difference is significantly larger for SSD. Moreover, the larger temperature difference in SSD is more dominant than the heat-transfer coefficient in hot-air drying. Thus, it provides higher heat flux and subsequently higher moisture evaporation rate in SSD.

The first experimental investigation to explore the inversion phenomenon was carried out by Yoshida and Hyōdō (1970). They reported an inversion temperature between 160°C and 176°C for the water–air countercurrent flow in a wetted-wall column. Chow and Chung (1983a,b) later presented numerical results of the evaporation of water into superheated steam and dry air for laminar (Chow and Chung, 1983a) and turbulent (Chow and Chung, 1983b) forced convection over a flat plate. Their analysis showed an inversion temperature of 250°C for laminar flow and 190°C for turbulent flow. Schwartze and Bröcker (2002) theoretically studied the evaporation of water into superheated steam, dry air, and humid air. They found the inversion temperature of 199°C for turbulent flow in a wetted-wall column.

The above findings are the results of evaporation rate, which is governed by convective transport phenomena. Several reports have shown that the inversion

temperature was also found in the case of porous food drying, in which internal moisture movement mainly governs overall transport mechanisms. The inversion temperature in this case varies from material to material. Prachayawarakorn et al. (2002), for example, dried shrimp in superheated steam and hot air and found the inversion temperature to be between 140°C and 150°C. For drying of potato slices, however, there existed an inversion temperature between 145°C and 160°C for the first drying stage, in which the moisture content was above 2.6 dry basis (d.b.) and between 125°C and 145°C during the last drying stage, when the moisture content was below 2.6 d.b. (Tang and Cenkowski, 2000).

10.3.1 Drying Characteristic Curves

During air-drying, the moisture content of the material decreases continually with time. An illustrative example of this phenomenon is shown in Figure 10.3. With superheated steam, however, the drying characteristic curve is different from that found with hot air; there is a gain in the moisture content in the early stage of drying. This increase in the moisture content is caused by the condensation of steam. However, for longer drying times, the drying curve becomes similar to the one in hot air.

Condensation occurs when superheated steam contacts the material surface, which is at a lower temperature. As a result, superheated steam releases its energy and changes its phase from vapor to liquid. The amount of steam condensed depends on the degree of superheat, which is defined as the difference between the actual

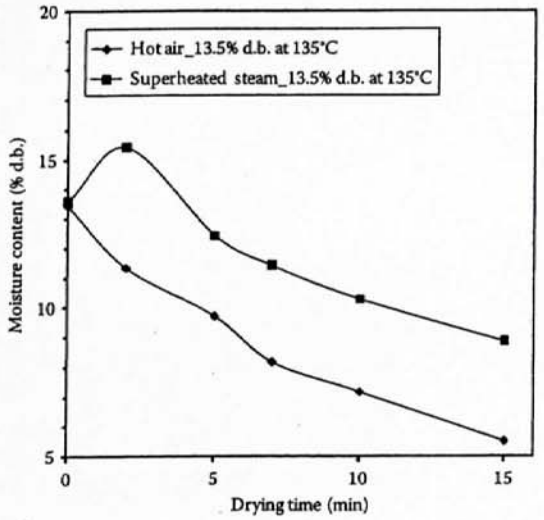

FIGURE 10.3 Drying curves of soybean in superheated-steam and hot-air fluidized bed. (From Prachayawarakorn, S. et al., *LWT-Food Sci. Technol.*, 39, 773, 2006. With permission.)

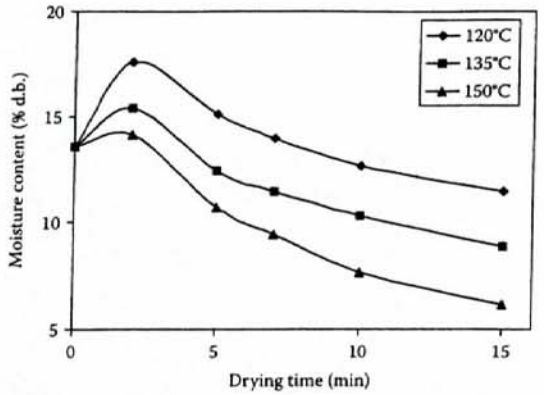

FIGURE 10.4 Change of moisture content of soybean at three different inlet steam temperatures. (From Prachayawarakorn, S. et al., *Drying Technol.*, 22, 2105, 2004. With permission.)

superheated-steam temperature and its saturation value at the dryer operating pressure. A higher degree of superheat obviously leads to a smaller amount of steam condensation, and thus to a smaller increase in the moisture content of the material. The effect of the degree of superheat on the moisture uptake can be seen in Figure 10.4.

Condensation of steam may render the dryer operation unstable, particularly in the case of a fluidized-bed dryer. Condensation and formation of liquid around the feed stream of food material leads to a difficulty in maintaining a desired level of fluidization. In such cases, solid preheating may be a useful option because the amount of steam condensation would then decrease.

Nevertheless, steam condensation does not have only the disadvantages as mentioned earlier. Actually, it sometimes provides several advantages. James et al. (2000) compared three different treatment methods for decontaminating lamb carcasses, namely, steam condensation, hot-water immersion, and chlorinated-hot-water immersion. All three treatments significantly reduced aerobic plate counts on the carcasses. There was no significant difference between steam and hot-water treatments; both treatments reduced the counts by approximately 1 $\log_{10}$ CFU cm^{-2}. In all cases, no significant differences were found in the evaluation of lean appearance, color appearance, odor, and overall acceptability of treated and untreated carcasses after 48 h of chilling and chilled storage. However, the use of steam seemed to have the greatest potential for industrial application since legislation and consumer concern would limit the use of chemical substances such as chlorine in decontamination applications, whereas the use of hot water may present problems in filtering, cleaning, and disposal stages.

In addition, steam condensation helps with gelatinization of starch. It has been reported that gelatinization of many starches is more complete in superheated steam than in hot air, in particular on the material surface, from which the moisture can easily be removed. Figure 10.5, for instance, shows morphologies of durian slices dried with superheated steam and hot air at 150°C (Jamradloedluk et al., 2007).

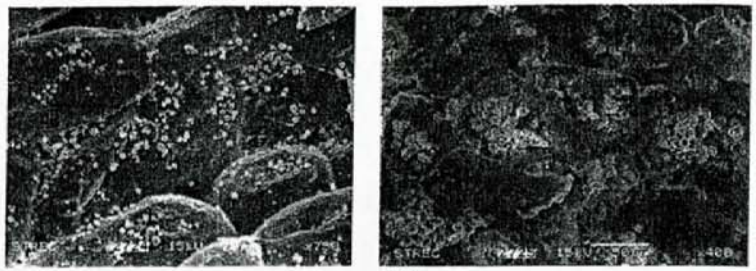

(a) (b)

(c)

FIGURE 10.5 Scanning electron micrographs of durian. (a) Surface of raw sample. (b) Surface of sample dried with hot air. (c) Surface of sample dried with superheated steam. (From Jamradloedluk, J. et al., *J. Food Eng.*, 78, 203, 2007. With permission.)

As shown in Figure 10.5a, durian starch granules are spherical with an average diameter of 1–3 μm. When the samples were dried with superheated steam, the starch granules disappeared as shown in Figure 10.5c, indicating that starch was gelatinized. In contrast, ungelatinized starch granules still appeared when durian was subjected to hot-air drying as shown in Figure 10.5b. The gelatinization of starch granules on the material surface led to a smoother surface, produced a transparent layer, and provided a glossy product.

10.3.2 Moisture Diffusivity

Moisture diffusivity is a fundamental parameter for analyzing, designing, and optimizing a drying system. When a material is being dried with hot air, moisture inside it moves through interfacial void spaces, evaporating and reaching the surface. Moisture is then transported away to the flowing stream on account of the moisture concentration difference between the thin, air boundary layer on the material surface and the bulk air stream. Inside the material, the transport of moisture in the falling rate period may occur by several mass transfer mechanisms, such as Knudsen diffusion, molecular diffusion, and capillary flow. All the drying mechanisms, as well as the effect of the porous structure of the solid material, are lumped together into an effective (apparent) diffusion coefficient. This effective moisture diffusivity can be determined from an experimental drying curve under a constant drying temperature, using classical analytical solutions of the diffusion equation, given by Crank (1975).

In SSD, the transport of moisture is driven by the pressure difference between the material surface and bulk stream and there is no mass transfer resistance on the gas side. During drying, the pressure at the material surface is equal to the saturation pressure at material temperature, and the pressure in the bulk stream is equal to the operating pressure. Moisture that exists inside the material starts to be removed when the material temperature reaches the saturation temperature of steam. The mechanisms of moisture movement inside the material in SSD are possibly similar to those in hot-air drying as mentioned above.

The morphology of the food material undergoing SSD may also be different from that of the material undergoing hot-air drying. Differences in such morphologies, in turn, affect the effective moisture diffusivity. Figure 10.6 shows experimental values and trends of the effective moisture diffusivity for foods dried by superheated steam and hot air, indicating lower values of this parameter when superheated steam is used (Poomsa-ad et al., 2002; Taechapairoj et al., 2004; Uengkimbuan et al., 2006; Jamradloedluk et al., 2007). The lower moisture diffusivity is due to the physically dense structures of food materials created during SSD. This led consequently to a lower drying rate in superheated steam compared to hot air.

10.3.3 Mathematical Modeling

This section describes a mathematical model that can be used to predict the temperature and moisture content of a material, especially cereal grain, in a batch superheated-steam dryer, operating near the atmospheric pressure. The model is first derived based on the fundamental transport equations for a drying particle, together with energy and mass balances for the dryer (fluidized bed), neglecting heat transfer by radiation, particle shape or size deformation (disregarding particle shrinkage or growth), and temperature gradients inside the particle. Superheated steam is injected into the bed of particles at constant inlet conditions (i.e., temperature, pressure, and mass flow rate). It is assumed that the inlet steam mass flow rate insures the bed-fluidization regime, and also that bubble formation and flow do not directly affect drying operation in SSD as they do in hot-air fluidized-bed dryers. Note that the free-bubbling regime assures a well mixing of superheated steam, but bubbles pass through the bed as an inactive phase, without the establishment of any concentration gradient to bring about water vapor transport, contrary to what occurs in hot-air drying. During drying, the wet particle with initially low temperature comes into contact with superheated steam. This naturally leads to steam condensation and an increase in both the particle moisture content and temperature. This initial condensation period is described in the mathematical model as the heating-up period. After the particle temperature reaches the saturation temperature of 100°C at an atmospheric pressure, condensation stops. Once the period of initial condensation is over, moisture evaporation starts. During the evaporation period, drying is presumably divided into two subperiods: constant drying-rate period and falling rate periods.

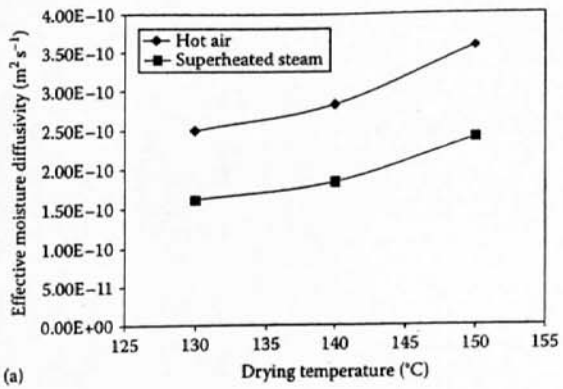

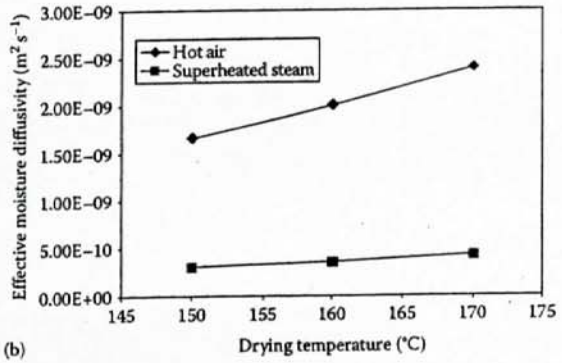

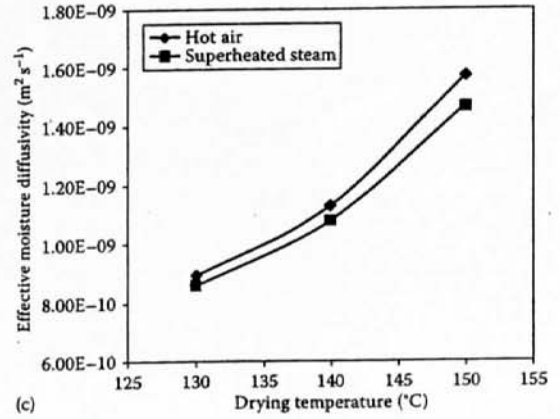

FIGURE 10.6 Comparison of effective moisture diffusivities of food materials dried with superheated steam and hot air. (a) Durian slice. (From Jamradloedluk, J. et al., *J. Food Eng.*, 78, 201, 2007. With permission.) (b) Rice. (From Taechapairoj, C. et al., *Drying Technol.*, 22, 729, 2004; and Poomsa-ad, N. et al., *Drying Technol.* 20, 202, 2002. With permission.) (c) Pork slice. (From Uengkimbuan, A. et al., *Drying Technol.* 24, 1666, 2004. With permission.)

10.3.3.1 Heating-Up Period

During the heating-up period, it is assumed that the condensed water forms a layer of liquid uniformly distributed over the entire external surface of each particle in the bed. This layer acts as a resistance to heat transfer from steam to particle surface. The rate of heat transfer, q, to particles into the bed can be described by:

$$q = h_{fl} A_{pfl\text{-}bed} \left(T_{st}^{sat} - T_p\right) \tag{10.2}$$

with $A_{pfl\text{-}bed}$ representing the total heat transfer area of particles into the bed, including the thickness of the liquid film covering them.

This rate of heat transfer is equal to the rate of heat released by steam plus the cooling of the condensate, which is expressed by (Holman, 1997):

$$q = \dot{M}_{cond} \left\{ c_{p,st} \left(T_{st}|_{in} - T_{st}^{sat}\right) + \Delta H^{vap} + \frac{3}{8} c_{p,w} \left(T_{st}^{sat} - T_p\right) \right\} \tag{10.3}$$

or

$$q = \dot{M}_{cond} \, \Delta H^{vap} \tag{10.4}$$

Equation 10.3 is obtained by assuming a linear temperature distribution in the condensed liquid film and a laminar flow of the liquid film. It is also assumed that, in the bed, the condensed water in contact with particles has their temperature. The condensation of steam onto a spherical particle is schematically shown in Figure 10.7.

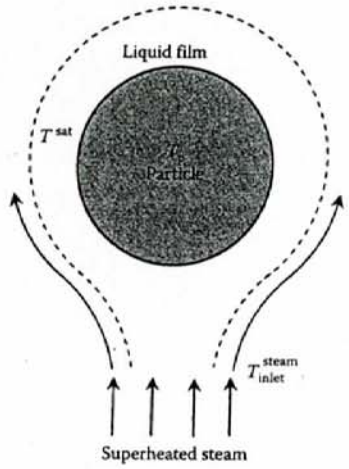

FIGURE 10.7 Liquid film condensation onto the surface of a particle.

Thus, based on these assumptions, the condensation rate of steam, $\dot{M}_{cond}$, can be calculated. The value of $\dot{M}_{cond}$ calculated with Equation 10.3 may not be precisely accurate since the thin liquid film may not be stagnated in reference to the fluidized particles and there are strong interactions amongst the solid particles, resulting in less uniformity of liquid film covering the entire particle surface. When the condensation rate is higher than the mass flow rate of steam entering the bed, one would expect that the steam flowing through the bed be completely condensed. In this case, the warming up of particles can be calculated using Equation 10.3, with $\dot{M}_{cond}$ replaced by the mass flow rate of steam. This situation may occur if the temperature of particles that are fed into the fluidized-bed dryer is rather low. Hence, the particles in the bed cannot fluidize.

For an energy balance of the solid phase, heat released from steam condensation can warm up both the particles and the condensed water, thus:

$$q = \left[M_{ss}\left(c_{p,s} + \bar{m}\, c_{p,w}\right) + M_{flw} c_{p,w}\right]\frac{dT_p}{dt} \tag{10.5}$$

where

c_p is the specific heat capacity
$\bar{m}$ is the average moisture content of particles
M_{flw} is the mass of condensed water covering the particle surface

The initial condition for solving Equation 10.5 is the particle temperature being equal to the ambient air temperature.

The heat transfer coefficient of the film condensation can be calculated from an empirical equation for an isolated sphere (Holman, 1997):

$$h_{fl} = 0.815\left[\frac{\rho_w(\rho_w - \rho_{st})g\Delta H^{vap}\lambda_{st}^3}{\mu_{st} d_p\left(T_{st}^{sat} - T_p\right)}\right]^{\frac{1}{4}} \tag{10.6}$$

The physical properties of steam and of condensed water are evaluated at the film temperature, $T_{fl} = \frac{T_{st}^{sat} + T_p}{2}$. Using Equation 10.6 to calculate the condensation heat transfer coefficient in the fluidized bed may lead to some errors since the fluidized particles change the gas fluid dynamics and subsequently the formation of boundary layers around the particles, which are not similar to the boundary layer around a single sphere.

The resulting steam condensation in the bed increases the moisture content of the particles, and this can be mathematically described by a differential mass balance for moisture in the particle. Assuming the food particle to be spherical with a constant volume, and neglecting convective effects, this mass balance (in spherical coordinates) is then expressed by

$$\frac{\partial m}{\partial t} = D_m^{eff}\left[\frac{\partial^2 m}{\partial r^2} + \frac{2}{r}\frac{\partial m}{\partial r}\right] \tag{10.7}$$

where D_m^{eff} is the effective diffusion coefficient ($m^2 s^{-1}$), assumed to be independent of the particle moisture content and temperature dependent. The value of D_m^{eff} during sorption of condensed water can be determined directly from soaking experiments at a given temperature. Initial and boundary conditions associated with Equation 10.7 are given by

$$m(r,t) = m_0, \quad \text{at } t = 0 \tag{10.8}$$

$$\left.\frac{\partial m}{\partial r}\right|_{r=0} = 0, \quad \text{at } t > 0 \tag{10.9}$$

$$m\left(\frac{d_p}{2}, t\right) = m_{eq,c} \quad \text{at } t > 0 \tag{10.10}$$

Equations 10.9 and 10.10 imply, respectively, that the minimum moisture content is at the center of the particle and that the surface moisture of the particle is in equilibrium with the condensed water. $m_{eq,c}$ is the moisture content at the particle surface, which is supposed to equilibrate with the condensed water covering the surface. The value of $m_{eq,c}$ can be determined by soaking the particles in hot water at the boiling-point temperatures until the particle mass does not change. The average moisture content of the particle, $\bar{m}$, is given by

$$\bar{m}(t) = \frac{4\pi}{V_p}\int_0^{d_p/2} m(r,t) r^2 dr \tag{10.11}$$

where V_p is the particle volume (m^3). The amount of the condensed water sorbed by all particles in the bed at time t, $M_{sor}(t)$, is

$$M_{sor}(t) = M_{ss}\left[\bar{m}(t) - \bar{m}(t - \Delta t)\right] \tag{10.12}$$

where the time interval, Δt, should be infinitesimal (i.e., tends to zero).

The amount of the remaining condensate in the bed at time t, M_{flw}, is thus:

$$M_{flw}(t) = \sum_{i=0}^{t}\left(\dot{M}_{cond}(i)\Delta t - M_{sor}(i)\right) \tag{10.13a}$$

Initial condensation of steam enables faster development of particle temperature. However, subsequent condensation rate decreases, whereas the rate of water, sorbed by particles, increases. These opposite behavior might result in the sorption rate being faster than the condensation rate. If such a case occurs, the gain in moisture by particles would come from the water condensation at the present time plus the remaining condensed water on the particle surface, resulting in a smaller amount of condensed water into the bed. In this case, the remaining water at the present time is calculated by Equation 10.13a, which can be rewritten as

$$M_{flw}(t) = \dot{M}_{cond}(t)\Delta t - M_{sor}(t) + \sum_{i=0}^{t-\Delta t} M_{flw}(i) \tag{10.13b}$$

As there is no available condensed water left at the particle surface before condensation stopped, the increase in moisture content cannot be calculated directly by Equation 10.7. Therefore, at this time t_H (time just before condensation stop), $M_{flw}(t_H) = 0$, $T_p(t_H) = T_{st}^{sat}$, and $M_{sor}(t) = M_{ss}\left[\bar{m}(t_H) - \bar{m}(t_H - \Delta t)\right]$. Then, upon dividing Equation 10.13b by M_{ss} and using these equations at $t = t_H$, one obtains:

$$\bar{m}(t_H) = \bar{m}(t_H - \Delta t) + \frac{\dot{M}_{cond}(t_H)\Delta t}{M_{ss}} + \sum_{i=0}^{t_{cond}-\Delta t} \frac{M_{flw}(i)}{M_{ss}} \tag{10.14}$$

From Equation 10.14, one may expect the occurrence of the constant drying rate period when the average particle moisture content is higher than the critical moisture content. Accordingly, the drying period should be divided into two: constant drying rate and the falling rate.

10.3.3.2 Drying Period

A mathematical description of the temperature changes of steam and particles within the bed is derived from an energy balance in the solid and gas phases. The solid-phase energy balance can generally be written as

$$hA_{p-bed}\left(T_{st}|_{bed} - T_p\right) = \left(-M_{ss}\frac{d\bar{m}}{dt}\right)\left[\Delta H^{vap} + c_{p,st}\left(T_{st}|_{bed} - T_p\right)\right] + M_{ss}\left(c_{p,s} + \bar{m}\,c_{p,w}\right)\frac{dT_p}{dt} \tag{10.15}$$

Equation 10.15 represents the energy used for vaporizing water and heating up this vapor to the steam temperature inside the bed, $T_{st|bed}$, (indicating that the steam within the bed is in a gaseous state), as well as for heating up the bed particles. When the particle temperature reaches the steam saturation value and drying starts in the constant rate regime, the last term on the right hand side of Equation 10.15 is neglected. However, this term is relevant for the falling rate period.

As observed from the experiments carried out in a fluidized bed (Soponronnarit et al., 2006), while the material is being dried, the temperature of steam inside the bed dryer, $T_{st}|_{bed}$, is lower than the one at the inlet, $T_{st}|_{in}$, but $T_{st}|_{bed}$ is insignificantly different from the exhaust steam temperature, $T_{st}|_{out}$. Therefore, at least for shallow fluidized-bed dryers, the gas phase can be considered to flow in perfect mixing inside the dryer chamber (i.e., $T_{st}|_{bed} = T_{st}|_{out}$), with its energy balance written as

$$\dot{M}_{st,in}\,c_{p,st}\left(T_{st}|_{in} - T_{ref}\right) - \dot{M}_{st,out}\,c_{p,st}\left(T_{st}|_{bed} - T_{ref}\right) = hA_{p-bed}\left(T_{st}|_{bed} - T_p\right) + \Gamma_{st-amb}A_{wall}\left(T_{st}|_{bed} - T_{amb}\right) \tag{10.16}$$

The first and second terms on the left-hand side of Equation 10.16 represent the energy carried by steam that, respectively, enters and leaves the drying chamber. This energy change is equivalent to the heat supplied for drying and heating particles plus the heat lost to the environment, whose temperature, T_{amb}, is known. In Equation 10.16, $\Gamma_{st\text{-}amb}$ represents the overall heat transfer coefficient between the steam inside the dryer and the surroundings, and A_{wall} is the contact area between the dryer walls and the surroundings, adopted as reference in the calculation of $\Gamma_{st\text{-}amb}$. It is assumed that the dryer internal wall is only in contact with steam, and particles therefore cannot lose their energy directly to the surroundings.

The gas-phase mass balance is now considered. The mass flow rate of steam leaving the drying chamber at any instant, $\dot{M}_{st,out}$, can be calculated by

$$\dot{M}_{st,out} = \dot{M}_{st,in} + \left(-M_{ss}\frac{d\bar{m}}{dt}\right) \tag{10.17}$$

Equation 10.17 represents an evaporation operation ($d\bar{m}/dt < 0$) leading to the mass flow rate of steam at the outlet being higher than that at the inlet under normal operation. Condensation, on the other hand, decreases the steam mass flow rate within the bed ($d\bar{m}/dt > 0$).

10.3.3.2.1 Constant-Rate Drying Period

As mentioned earlier, when the period of condensation finishes, the particle temperature reaches the steam saturation temperature ($T_p = T_{st}^{sat}$) and drying starts with the evaporation of unbound water from particle. Since only free water is removed in this case, drying occurs at a constant rate dictated by external conditions (steam flow rate, temperature, and pressure). This constant-rate drying period can be divided into two subperiods: the first one concerning the evaporation of the condensed water film covering particles, and the second one regarding the unbound water on the surface of particles.

During the first subperiod, one can consider that the interface at which water evaporates moves with decreasing film thickness until reaching the particle surface. Therefore, the moisture profile inside the particle remains unchanged until all condensed water has been removed from the surface. The temperatures of both the particle and the condensed water remain equal to T_{st}^{sat} and Equation 10.15 is reduced to

$$h_{fl}A_{pfl-bed}\left(T_{st}|_{bed} - T_{st}^{sat}\right) = \left(-\frac{dM_{flw}}{dt}\right)\left[\Delta H^{vap} + c_{p,st}\left(T_{st}|_{bed} - T_{st}^{sat}\right)\right] \tag{10.18a}$$

After the condensed water film has been removed, unbound water starts to be evaporated at particle surface, which marks the beginning of the second drying subperiod. In this case, Equation 10.18a is changed to Equation 10.18b:

$$hA_{p-bed}\left(T_{st}|_{bed} - T_{st}^{sat}\right) = \left(-M_{ss}\frac{d\bar{m}}{dt}\right)\left[\Delta H^{vap} + c_{p,st}\left(T_{st}|_{bed} - T_{st}^{sat}\right)\right] \tag{10.18b}$$

where h, the heat transfer coefficient between particle and steam, is determined from Ranz and Marshall (1952). The changes in internal moisture content of particle, and therefore the vaporization rate, can be calculated using Equation 10.7, with the following initial and boundary conditions:

$$m(r,t) = m(r,t_1), \quad \text{at } t = t_1 \tag{10.19}$$

$$\left.\frac{\partial m}{\partial r}\right|_{r=0} = 0, \quad \text{at } t > t_1 \tag{10.20}$$

$$-\frac{6D_m^{eff}}{d_p}\left.\frac{\partial m}{\partial r}\right|_{r=\frac{d_p}{2}} = N_c, \quad \text{at } t > t_1 \tag{10.21}$$

where

t_1 is the time at the end of condensed water removal period (s)

N_c is the constant drying rate (kg evaporated water/s·kg dry matter), which can be determined experimentally

Equation 10.19 represents the existing moisture gradients at the beginning of the second subperiod of constant-rate drying. As mentioned earlier, this moisture profile inside the particle is the one obtained at the end of the condensed water removal period, since during the first subperiod of constant-rate drying only the condensed water film covering the particle is removed.

For both subperiods, the energy balance for the gas phase (steam) is still similar to Equation 10.16, with T_p replaced by T_{ti}^{sat}.

10.3.3.2.2 Falling-Rate Drying Period

After the moisture content of the particle drops below the critical moisture content, further reduction of moisture occurs in the falling-rate drying period. The critical moisture content of the particle can be determined from the experiment and this value is an input parameter in the model. Equation 10.7 still describes water diffusion inside particle, now with the following initial and boundary conditions:

$$m(r,t) = m(r,t_2), \quad \text{at } t = t_2 \tag{10.22}$$

$$\left.\frac{\partial m}{\partial r}\right|_{r=0} = 0, \quad \text{at } t > t_2 \tag{10.23}$$

$$m\left(\frac{d_p}{2},t\right) = m_{eq}, \quad \text{at } t > t_2 \tag{10.24}$$

where

t_2 is the drying time at the end of the constant-rate drying period (s)

m_{eq} is the equilibrium moisture content, whose value is the moisture content of the particle in equilibrium with superheated steam at a given temperature and pressure

In SSD near the atmospheric pressure, the value of m_{eq} is assumed to be zero since the high drying temperature of 100°C is used The calculations of the steam bed temperature. the particle temperature, and the steam flow still follow Equations 10.15 through 10.17, with the particle temperature increasing with time from the steam saturation temperature to one close to the steam bed temperature ($=T_{si}|_{out}$).

In Figure 10.8, the predicted and experimental data of moisture content vs. time for drying paddy in a superheated-steam fluidized-bed dryer at 150°C are compared. These results show that the prediction of the time evolution of the paddy moisture content from the mathematical model presented is very closed to experimental data. The calculations also indicated that the period of steam condensation in the bed of particles being fluidized depends on the steam velocity, being shorter at higher steam velocities. More specifically, the condensation periods were around 2–2.5 s for the steam velocities of 1.3 and 1.5 u_{mf} (corresponding to the superficial velocities of 2.6–3 m/s). For the thin layer dryer, in which superheated steam flows across material and the material is not fluidized, condensation takes longer than in the fluidized-bed dryer. Pronyk et al. (2004) investigated the drying characteristics of foodstuffs using a superheated-steam thin-layer dryer at velocities between 0.25 and 0.35 ms^{-1} and steam temperatures from 125°C to 165°C. It was found that the condensation time was in the range of 6–7 s for Asian noodle before drying started.

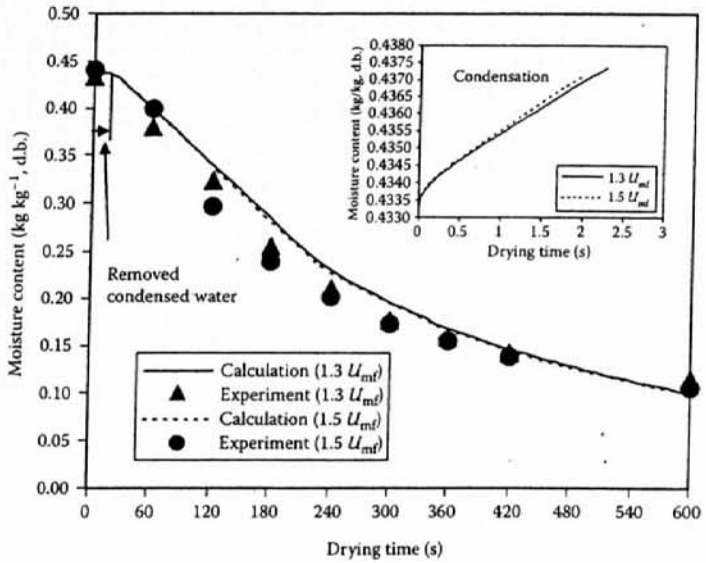

FIGURE 10.8 Comparison between predicted and experimental data of moisture content of paddy at superficial velocities of 1.3 and 1.5 times minimum fluidization velocity and inlet steam temperature of 150°C. (From Soponronnarit, S. et al., *Drying Technol.*, 24, 1462, 2006. With permission.)

10.4 APPLICATIONS OF SUPERHEATED STEAM DRYING TO FOOD MATERIALS

10.4.1 Parboiled Rice

Parboiled rice offers some advantages over unparboiled rice, such as strengthening of kernel integrity, high milling yield, and decrease in solid loss after cooking. Other characteristics of parboiled rice are its firmer and less sticky texture. A process for producing parboiled rice consists essentially of three steps including soaking of paddy, steaming, and drying to the predetermined moisture content. Figure 10.9 shows the conventional production process of parboiled rice that is currently operated in some countries. This process generally takes 3–4 h for the steps of soaking and drying to a moisture content of 22% d.b. A hot-air fluidized-bed dryer is used to dry paddy to moisture content of 39% d.b. (28.5% w.b.). Then, paddy is tempered (see No. 5) and dried again in a fluidized-bed dryer to 21% d.b.

Recently, however, Taechapairoj et al. (2004) found that drying of paddy in a superheated-steam fluidized bed could give a rice texture similar to the parboiled rice; milling yield was also noted to be higher. The moisture content of paddy after drying should not be lower than 18% d.b., otherwise the head rice yield would be very low. The kinetics of rice-starch gelatinization during SSD could suitably be explained by a zeroth-order reaction rate whose rate constant, N_k (s^{-1}), was related to the bed depth and drying temperature in the following form:

$$N_k = -3.0340\times10^{1} + 3.1920H_{bed} - 1.0984\times10^{-1}H_{bed}^2 - \exp\left(-\frac{1.5186\times10^{3}}{T}\right) \quad (10.25)$$

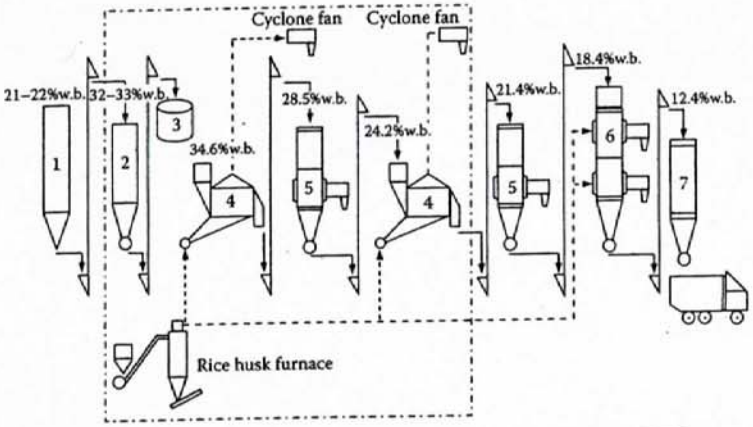

1. Soaking tank 2. Steamer 3. Ambient air ventilation 4. Fluidized bed dryer 5. Tempering and air ventilation 6. LSU dryer 7. Storage bin

FIGURE 10.9 Conventional parboiled rice process. (From Rordprapat, W. et al., *J. R. Inst. Thailand*, 30, 377, 2005. With permission.)

where
H_{bed} is the bed depth (cm)
T is the drying temperature (K)

The values of correlation coefficient and absolute mean error associated with Equation 10.25 were 0.97 and 3.66, respectively. Complete gelatinization of rice starch could be established within 5–6 min at steam temperatures of 150°C–160°C, and within 4 min at a steam temperature of 170°C.

The findings of parboiled rice characteristics in SSD would make a significant progress in the parboiling process because superheated steam itself can act as both steaming and drying media at the same time, thereby reducing steps in the parboiling process. With superheated steam, steaming and drying can be combined into one step. Thus, all the units from No. 2 to No. 5, shown in Figure 10.9 by the dash-dot line (Rordprapat et al., 2005), could be replaced by a single superheated-steam dryer. Additionally, the processing time would be much shorter.

Soponronnarit et al. (2006) successfully fabricated and tested a pilot-scale, continuous superheated-steam fluidized-bed dryer, with a capacity of 100 kg h^{-1}. A cyclonic rice husk furnace was used as a heating source to generate steam for the dryer. A schematic diagram of the referred pilot-scale dryer is shown in Figure 10.10.

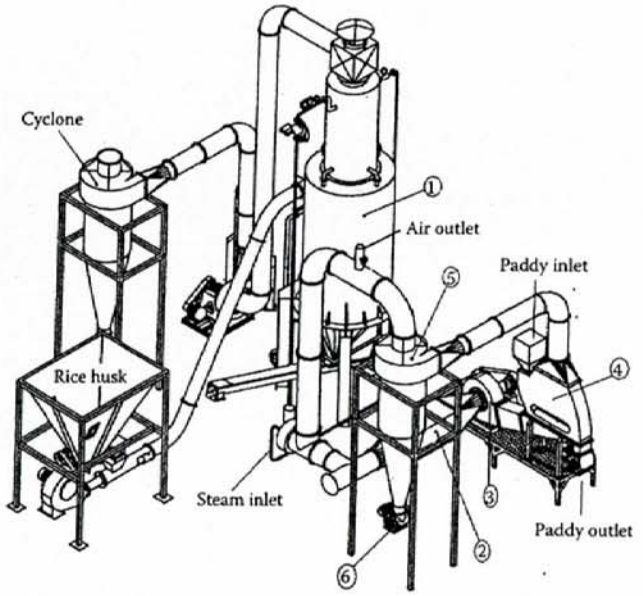

1. Bolier 2. Superheater 3. Blower 4. Drying chamber 5. Cyclone 6. Rotary value

FIGURE 10.10 Schematic diagram of a pilot-scale superheated-steam fluidized bed. (From Soponronnarit, S. et al., *Drying Technol.*, 24, 1462, 2006. With permission.)

TABLE 10.1
Paddy Qualities (Chainat 1 Variety) Soaked at 70°C for 7–8 h and Dried at Different Inlet Steam Temperatures

Drying Condition	Feed Rate ($kg\,h^{-1}$)	Moisture Content (d.b.)	Head Rice Yield (%)	Whiteness	White Belly (%)	Hardness (N)	Water Adsorption (g Water/g Rice)
After soaking	—	0.456 ± 0.008	56.6 ± 1.1[a]	39.0 ± 0.2[a]	5.7 ± 0.6*[a]	37.9 ± 1.3[a]	3.51 ± 0.07[a]
128°C	106	0.290 ± 0.008	63.5 ± 0.6[b]	32.2 ± 0.8[b]	0[b]	48.6 ± 0.9[b]	2.82 ± 0.05[b]
144°C	98	0.23 ± 0.004	66.9 ± 0.6[c]	29.4 ± 0.5[c]	0[b]	51.9 ± 0.6[c]	2.19 ± 0.01[c]
160°C	120	0.218 ± 0.004	67.9 ± 0.6[c]	28.0 ± 0.6[c]	0[b]	55.0 ± 1.3[d]	3.99 ± 0.05[d]

Source: Soponronnarit, S. et al., *Drying Technol.*, 24, 1462, 2006. With permission.
Note: Same letters on the same column indicate that values are insignificantly different at $p < 0.05$.
* Chalky grains.

The equipment was also installed in and demonstrated to some parboiled rice factories. Table 10.1 shows the paddy quality after drying with superheated steam. Before drying, paddy was soaked with hot water at 70°C for 7–8 h. The head rice yield of the reference paddy, which was dried in shade, was 56.6%, and the white belly, representing the incomplete gelatinization, was 5.6%. After drying, the head rice yield was improved, being in the range of 63%–68%, and the white belly was not observed. Moreover, the value of hardness of dried parboiled rice significantly increased while less water was adsorbed.

Figure 10.11 shows the pasting viscosity of rice flour after SSD. It can be seen that the peak viscosity, final viscosity, and setback viscosity of dried rice flour are lower than those of the reference rice flour. The lowering of setback viscosity implies a firmer texture of rice flour. The trend of changing pasting viscosity of rice flour dried in SSD was similar to that of commercial parboiled rice obtained from the conventional process, but the values themselves are lower. Note that the extent to which the viscosity of rice flour obtained from the superheated-steam treatment is lower depends on the drying temperature. The pasting curve of flour made from rice dried at a temperature of 128°C is comparable to that of the commercially produced parboiled rice flour.

10.4.2 Soybean Meal

Full-fat soybean or soybean prior to oil extraction is used as a feedstuff because of its high-oil and high-quality protein contents. However, the presence of biologically active compounds in raw full-fat soybean such as trypsin inhibitors, hemagglutinins,

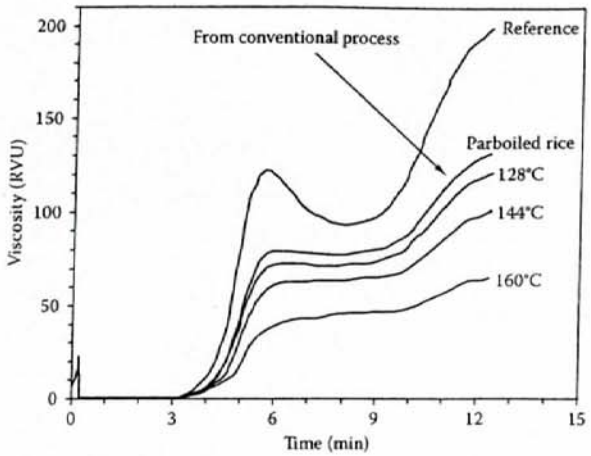

FIGURE 10.11 Pasting viscosities of rice flour samples dried at different steam temperatures. (From Soponronnarit, S. et al., *Drying Technol.*, 24, 1466, 2006. With permission.)

lectins, and saponins limits the utilization of its nutritive values (Hensen et al., 1987; Liener, 1994), resulting in compromised health and performance of nonruminants and immature ruminants. To eliminate these antinutritional factors, heat treatment is needed. Trypsin inhibitors are the main parameter used to control the quality of soybean meal. However, direct measurement of trypsin inhibitors is not frequently practiced. Instead, the urease activity is usually measured to indicate the activity of trypsin inhibitors because their inactivation rate is equal to that of the urease enzyme (Baker and Mustakas, 1973). The residual urease activity for adequately treated soybean is in the range of 10% and 20%; a value below 10% indicates overheating.

Heat-treatment methods frequently used are, for example, cooking, microwave, and roasting (Raghavan and Harper, 1974; Hensen et al., 1987; Stewart et al., 2003). Prachayawarakorn et al. (2006) studied the treatment of full-fat soybean using superheated steam and hot-air fluidized-bed dryers. It was found that both heating media could eliminate the urease enzyme, but at different rates, although the medium temperature used was the same. Insufficient inactivation was obvious with hot air at 120°C for soybean with initial moisture content of 13.5% d.b. As shown in Figure 10.12, the residual urease activity remained steadily at 40% although an extended drying period was applied. As the initial moisture content of soybean increased to 19.5% d.b., however, sufficient inactivation was noted at a heating time of over 25 min. In contrast to hot air, inactivation of the urease enzyme could be achieved at a superheated-steam temperature of 120°C; the levels of residual activity were below 20% for soybean with initial moisture contents of 13.5% and 19.5% d.b. when heated for 7 and 5 min, respectively. The thermal inactivation of urease followed a modified first-order reaction model, which is expressed by

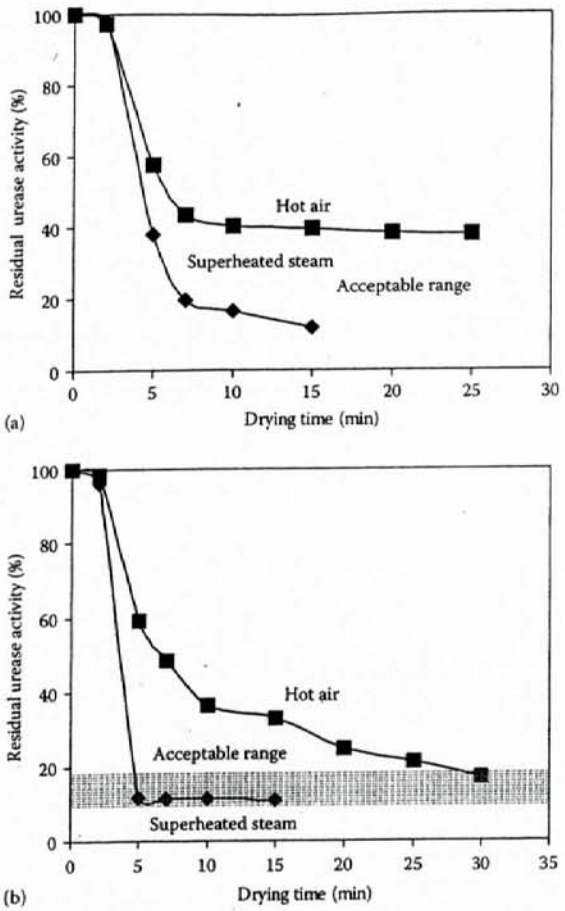

FIGURE 10.12 Apparent inactivation kinetics of urease inactivation present in soybean during thermal treatments with superheated steam and hot air at 120°C: (a) M_{in} = 13.5 % d.b. and (b) M_{in} = 19.5% d.b. (From Prachayawarakorn, S. et al., *LWT-Food Sci. Technol.*, 39, 775, 2006. With permission.)

$$\frac{a_{ur}(t) - a_{ur}|_{eq}}{a_{ur}|_{in} - a_{ur}|_{eq}} = \exp(-N_k t) \tag{10.26}$$

where

$a_{ur}(t)$ is the residual urease activity at time t (%)
$a_{ur}|_{in}$ is the urease activity at the beginning of heat treatment (%)
$a_{ur}|_{eq}$ is the residual urease activity at infinite time (%)
N_k is the apparent constant kinetic rate (min^{-1})
t is the drying time (min)

The apparent constant kinetic rate could be expressed as a function of the operating parameters, i.e., heating temperature and moisture content, as

$$N_k = \left[-1.01\times10^4 + 7.50\times10^{-2}T^2 - 7.66\times10^4 m_{in} + 1.89\times10^4 m_{in}^2 + \frac{2.62\times10^7 m_{in}}{T}\right] \times \exp\left(-\frac{5.35\times10^{-1}}{m_{in}} - \frac{1.51\times10^3}{T}\right) \tag{10.27}$$

In addition, the expression for $a_{ur}|_{eq}$ is given by

$$a_{ur}|_{eq} = \left(-4.7523\times10^{-2} + 7.1742\times10^{-2} m_{in}^2 + 1.2200\times10^{-4} T\right) \times \exp\left(\frac{3.2273\times10^3 - 9.7815\times10^2 m_{in}}{T}\right) \tag{10.28}$$

Equations 10.27 and 10.28 both presented a correlation coefficient equal to 0.95, and root mean square errors of 0.347 and 1.47, respectively.

Prachayawarakorn et al. (2006) recommended that a fluidized-bed dryer should be operated at 135°C–150°C for hot air and below 135°C for superheated steam to eliminate the urease enzyme present in soybean. This could simultaneously preserve the nutritional qualities, protein solubility, and lysine content. Under such temperature ranges, the use of superheated steam as the heating/drying medium resulted in higher protein solubility of treated sample than the use hot-air drying when applied to the dried soybean (13.5% d.b.), as can be seen in Table 10.2. In addition, the protein solubility of soybean was similar to that treated by an industrial micronizer (Wiriyaumpaiwong et al., 2004). For the moist soybean, the heating medium types did not affect the quality since the urease enzyme was inactivated over a short period of time before protein denaturation largely occurred.

10.4.3 Snack Foods

Snack foods, e.g., potato chips, banana chips, durian chips, are generally commercially produced by deep-fat frying. The development of a porous structure provides snacks with better quality, especially in terms of texture, compared with air-dried products. Snack products typically have a high oil content and cannot be kept for a long period of time due to possible lipid oxidation, leading to rancidity. In addition, consumers who are concerned with their health may dislike these products. The product with low fat content is an interesting commodity to the consumer.

High-temperature drying could be an alternative to frying to produce low-fat snack products. During high-temperature drying, the product moisture vaporizes and expands rapidly, thereby allowing the formation of pores. Li et al. (1999) studied superheated-steam-impingement drying of tortilla chips and founded that a higher steam temperature resulted in more pores, coarser appearance, and higher modulus of deformation of tortilla chips. In addition, the superheated steam-dried tortilla chips had fewer but

TABLE 10.2
Protein Solubility and Lysine Content of Soybean Treated with Superheated Steam and Hot Air at Various Temperatures

Temperature (°C)		m_{in} (% d.b.)	Heating Time (min)	$m(t)$ (% d.b.)	Urease Activity (%)	Protein Solubility (%)	Lysine Content (mg g^{-1} Soybean)
Raw soybean					100	94.28	2.9–3.1
Hot air	120	13.5	50	3.9	37	71.1	N/A
		19.5	30	6.9	19	70.98	3.0
	135	13.5	5	9.7	15	78.68	3.1
		19.5	5	14.4	13	84.33	N/A
	150	13.5	5	8.2	16	74.17	N/A
		19.5	2	15.5	10	87.86	N/A
Superheated steam	120	13.5	7	13.9	16	85.66	2.8
		19.5	5	18.3	12	85.2	2.7
	135	13.5	5	12.4	11	71.76	2.7
		19.5	5	16.5	9	82.25	2.7
	150	13.5	5	10.6	12	54.94	2.8
		19.5	2	18.9	11	83.84	N/A

Source: Prachayawarakorn, S. et al., *LWT-Food Sci. Technol.*, 39, 776, 2006. With permission.
N/A, not available.

larger pores than the air-dried product. Similar results were also found for dried durian chips (Jamradloedluk et al., 2007). In spite of the different morphologies of products obtained from the two drying media, textural properties such as hardness and stiffness were not significantly different. In the case of some particular fruits such as banana, however, though pores could be formed during high-temperature drying and the texture of the final product might be acceptable, the color of the product normally becomes brown when its moisture content is reduced below 80% d.b. (Prachayawarakorn et al., 2008). In addition, some pores might collapse during the early drying period, resulting in shrinkage of the product and subsequent less crispiness and hard texture. To avoid shrinkage, the structure should be rigid so that it can resist stresses generated during drying. This can be achieved by drying the product at temperatures below the glass transition temperature, and the freezing drying technique is normally applied.

Another technique that provides less material shrinkage involves puffing, by which the moisture inside the material is rapidly vaporized. Vapor expansion inside the product then creates voids or ruptures the existing structure, leading to a more porous dried product. Boualaphanh et al. (2008) studied the textural properties of banana after puffing with superheated steam at different conditions; their experimental results are shown in Figure 10.13, indicating that puffing temperature and moisture content of banana before puffing strongly affected the textural properties and shrinkage of the product. The sample shrunk least, approximately 10%–15%, when the moisture content of banana before puffing ranged between 20% and 25% d.b.

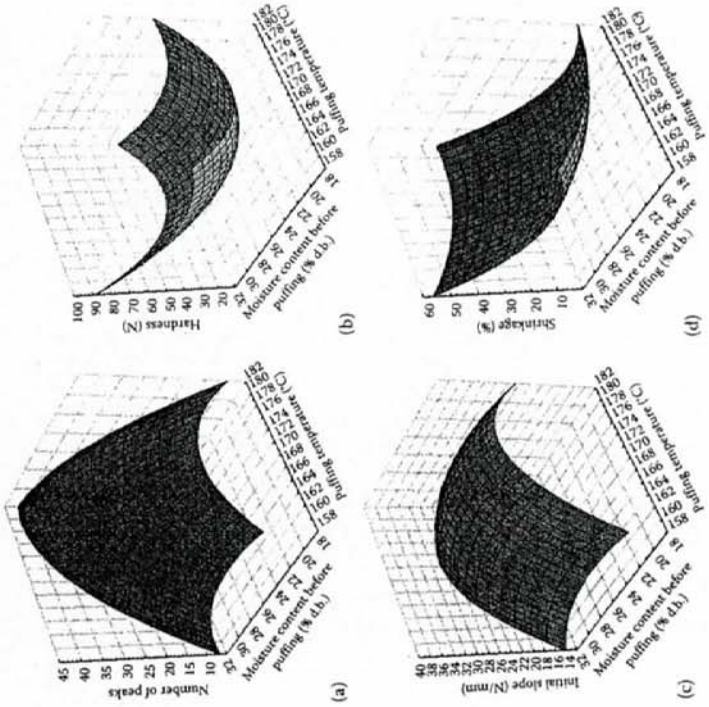

FIGURE 10.13 Quality attributes of banana puffed at different conditions (2 min puffing time). (a) Number of peaks. (b) Hardness. (c) Initial slope. (d) Shrinkage. (From Boualaphanh, K. et al., Optimization of the superheated steam puffing of banana, in *Proceedings of the 9th Thai Society of Agricultural Engineering Conference*, Chiang Mai, Thailand, January 31–February 1, 2008, CR2-16 [in Thai]. With permission.)

and the puffing temperature was in the range of 170°C–180°C. Under these puffing conditions, the color of the sample fell into the color group of grayed-orange 163C, and the textural property values were in ranges of 35 ± 5 N/mm for the initial slope, 37 ± 5 for the number of peaks and 33 ± 11 N for the hardness. These quality attributes were similar to those of the commercially vacuum fried product; the textural property values of the commercial product were 48 ± 8 N for the hardness, 42 ± 5 for the number of peaks and 45 ± 16 for the initial slope.

Figure 10.14 shows the morphology of puffed banana, indicating the very large voids within the banana sample and the small pores at the exterior. The produced large pores imply the vaporization and expansion of moisture during superheated-steam puffing.

However, a drawback of superheated steam became evident when it was applied to pop amaranth seeds (Iyota et al., 2005). Amaranth, a well-known product in the market as a source of food and high nutritional components, can be consumed after popping. The volume expansion after popping is an important parameter; a high volume expansion produces softer and more appealing texture. Figure 10.15 shows the volume expansion ratio of popped amaranth seeds at different temperatures. In hot air, the maximum expansion ratio reached 7.7 at 260°C. A decrease in expansion ratio and browning occurred at higher temperature of 290°C. In the case of superheated steam, the expansion ratio was approximately 10% lower than that obtained in hot air. This occurred because the seed coats were apparently softened by steam condensation.

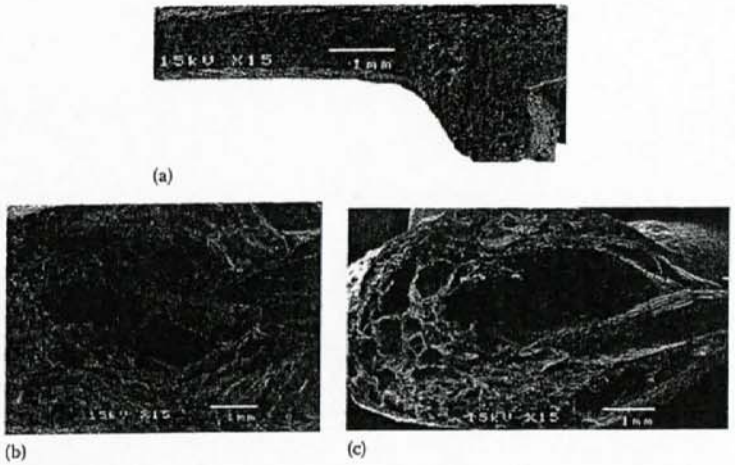

FIGURE 10.14 Morphologies of banana at different puffing temperatures. (a) No puffing. (b) Puffing temperature of 170°C. (c) Puffing temperature of 180°C. (From Boualaphanh, K. et al., Optimization of the superheated steam puffing of banana, in *Proceedings of the 9th Thai Society of Agricultural Engineering Conference*, Chiang Mai, Thailand, January 31–February 1, 2008, CR2-16 [in Thai]. With permission.)

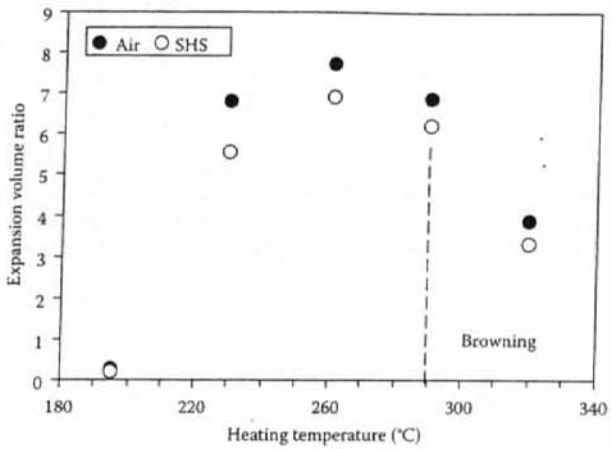

FIGURE 10.15 Effect of heating temperature on volume expansion ratio of amaranth seed in hot air and superheated steam (SHS) (initial moisture content of 13% d.b.). (From Iyota, H. et al., *Drying Technol.*, 23, 1287, 2005. With permission.)

10.5 CONCLUDING REMARKS

SSD is a feasible alternative to hot-air drying for a number of food products. The condensation of steam onto the material surface provides a rapid temperature rise, and this causes the food quality obtained from SSD to be different from that related to hot-air drying. The physical appearance of foods is better in SSD than in the hot-air drying, particularly when SSD is applied to starchy foods. Superheated-steam dried products such as tortilla, potato, and durian chips have a smoother surface and are glossier since the starch present in them can form a gel network to a larger extent in SSD than in the case of hot-air drying. Paddy dried by superheated steam has physicochemical and physical properties similar to those of parboiled rice. A temperature of 150°C is recommended for the dryer operation to produce parboiled rice.

In addition to the drying of starch-based foods, superheated steam can also be applied to eliminate the antinutritional factors present in legumes. However, the treatment of soybean with superheated steam should be done at temperatures below 135°C to preserve the protein solubility at the level that is required for feed meal.

A mathematical model for SSD that includes both steam condensation and drying has been derived based on the transport equations for drying a single particle, together with the energy and mass balances in the dryer. It can predict the change of moisture content of product during SSD relatively well. The mathematical model developed for the fluidized-bed dryer can be extended to other dryer types, with some modifications in the governing equations.

ACKNOWLEDGMENTS

The authors express their sincere appreciation to the Thailand Research Fund and Commission on Higher Education for the financial support of projects for more than 10 years.

REFERENCES

Baker, E.C. and Mustakas, G.C. 1973. Heat inactivation of trypsin inhibitor, lipoxgygenase and urease in soybeans: Effect of acid and base additives. *J. Am. Oil Chem. Soc.* 50:137–141.

Boualaphanh, K., Prachayawarakorn, S., and Soponronnarit, S. 2008. Optimization of the superheated steam puffing of banana. In *Proceedings of the 9th Thai Society of Agricultural Engineering Conference*. Chiang Mai, Thailand, January 31–February 1, 2008, CR2-16 (in Thai).

Chen, Z., Wu, W., and Agarwal, P.K. 2000. Steam-drying of coal. Part 1. Modeling the behavior of a single particle. *Fuel* 79:961–973.

Chow, L.C. and Chung, J.N. 1983a. Evaporation of water into a laminar stream of air and superheated steam. *Int. J. Heat Mass Transfer* 26:373–380.

Chow, L.C. and Chung, J.N. 1983b. Water evaporation into a turbulent stream of air, humid air or superheated steam. In *Proceedings of the ASME National Heat Transfer Conference*, No. 83-HT-2 ASME, New York.

Crank, J. 1975. *The Mathematics of Diffusion*, 2nd ed. Oxford, NY: Clarendon Press.

Deventer, H.C. and Heijmans R.M.H. 2001. Drying with superheated steam. *Drying Technol.* 19:2033–2045.

Douglas, W.J.M. 1994. Drying paper in superheated steam. *Drying Technol.* 12:1341–1355.

Hensen, B.C., Flores, E.S., Tanksley, Jr., T.D., and Knabe, D.A. 1987. Effect of different heat treatments during processing of soybean meal on nursery and growing pig performance. *J. Anim. Sci.* 65:1283–1291.

Holman, J.P. 1997. *Heat Transfer*, 8th ed. New York: McGraw-Hill.

Iyota, H., Konishi, Y., Inoue, T., Yoshida, K., Nishimura, N., and Nomura, T. 2005. Popping of amaranth seeds in hot air and superheated steam. *Drying Technol.* 23:1273–1287.

Iyota, H., Nishimura, N., Onuma, T., and Nomura, T. 2001. Drying of sliced raw potatoes in superheated steam and hot air. *Drying Technol.* 19:1411–1424.

James, C., Thornton, J.A., Ketteringham, L., and James, S.J. 2000. Effect of steam condensation, hot water or chlorinated hot water immersion on bacterial numbers and quality of lamb carcasses. *J. Food Eng.* 43:219–225.

Jamradloedluk, J., Nathakaranakule, A., Soponronnarit, S., and Prachayawarakorn, S. 2007. Influences of drying medium and temperature on drying kinetics and quality attributes of durian chip. *J. Food Eng.* 78:198–205.

Lane, A.M. and Stern, S. 1956. Application of superheated-vapor atmospheres to drying. *Mech. Eng.* 78:423–426.

Li, Y.B., Seyed-Yagoobi, J., Moreira, R.G., and Yamsaengsung, R. 1999. Superheated steam impingement drying of tortilla chips. *Drying Technol.* 17:191–213.

Liener, I.E. 1994. Implications of antinutritional components in soybean foods. *Crit. Rev. Food Sci. Nutr.* 34:31–67.

Markowski, M., Cenkowski, S., Hatcher, D.W., Dexter, J.E., and Edwards, N.M. 2003. The effect of superheated steam dehydration kinetics on textural properties of Asian noodles. *Trans. ASAE* 46:389–395.

Nathakaranakule, A., Kraiwanichkul, W., and Soponronnarit, S. 2007. Comparative study of different combined superheated steam drying techniques for chicken meat. *J. Food Eng.* 80:1023–1030.

Pang, S. and Dakin, M. 1999. Drying rate and temperature profile for superheated steam vacuum drying and moist air drying of softwood lumber. *Drying Technol.* 17:1135–1147.

Poomsa-ad, N., Soponronnarit, S., Prachayawarakorn, S., and Terdyothin, A. 2002. Effect of tempering on subsequent drying of paddy using fluidization. *Drying Technol.* 20:195–210.

Prachayawarakorn, S., Prachayawasin, P., and Soponronnarit, S. 2006. Heating process of soybean using hot-air and superheated-steam fluidized-bed dryer. *LWT-Food Sci. Technol.* 39:770–778.

Prachayawarakorn, S., Soponronnarit, S., Wetchacama, S., and Jaisut, D. 2002. Desorption isotherms and drying characteristics of shrimp in superheated steam and hot air. *Drying Technol.* 20:669–684.

Prachayawarakorn, S., Tia, W., Plyto, N., and Soponronnarit, S. 2008. Drying kinetics and quality attributes of low-fat banana slices dried at high temperature. *J. Food Eng.* 85:509–517.

Pronyk, C., Cenkowski, S., and Muir, W.E. 2004. Drying foodstuffs with superheated steam. *Drying Technol.* 22:899–916.

Raghavan, G.S.V. and Harper, J.M. 1974. Nutritive value of salt-bed roasted soybean for broiler chicks. *Poultry Sci.* 53:547–553.

Ranz, W. and Marshall, W. 1952. Evaporation from drops-Part I. *Chem. Eng. Prog.* 48, 141.

Rordprapat, W., Nathakaranakule, A., Tia, W., and Soponronnarit, S. 2005. Development of a superheated-steam-fluidized-bed dryer for parboiled rice. *J. R. Inst. Thailand.* 30:363–378 (in Thai).

Schwartze, J.P. and Bröcker, S. 2002. A theoretical explanation for the inversion temperature. *Chem. Eng. J.* 86:61–67.

Shibata, H. and Mujumdar, A.S. 1994. Steam drying technologies: Japanese R&D. *Drying Technol.* 12:1485–1524.

Soponronnarit, S., Prachayawarakorn, S., Rordprapat, W., Nathakaranakule, A., and Tia, W. 2006. A superheated-steam fluidized-bed dryer for parboiled rice: Testing of a pilot-scale and mathematical model development. *Drying Technol.* 24:1457–1467.

Stewart, O.J., Raghavan, G.S.V., Orsat, V., and Golden, K.D. 2003. The effect of drying on unsaturated fatty acids and trypsin inhibitor activity in soybean. *Process Biochem.* 39:483–489.

Svensson, C. 1980. Steam drying of pulp. In *Drying '80*, vol. 2, Ed. A.S. Mujumdar, pp. 301–307. New York: Hemisphere.

Taechapairoj, C., Dhuchakallaya, I., Soponronnarit, S., Wetchacama, S., and Prachayawarakorn, S. 2003. Superheated steam fluidised bed paddy drying. *J. Food Eng.* 58:67–73.

Taechapairoj, C., Prachayawarakorn, S., and Soponronnarit, S. 2004. Characteristics of rice dried in superheated steam fluidized-bed. *Drying Technol.* 22:719–743.

Tang, Z. and Cenkowski, S. 2000. Dehydration dynamics of potatoes in superheated steam and hot air. *Can. Agr. Eng.* 42:43–49.

Tang, Z., Cenkowski, S., and Izydorczyk, M. 2005. Thin-layer drying of spent grains in superheated steam. *J. Food Eng.* 67:457–465.

Uengkimbuan, N., Soponronnarit, S., Prachayawarakorn, S., and Nathkarankule, A. 2006. A comparative study of pork drying using superheated steam and hot air. *Drying Technol.* 24:1665–1672.

Wiriyaumpaiwong, S., Soponronnarit, S., and Prachayawarakorn, S. 2004. Comparative study of heating processes for full-fat soybeans. *J. Food Eng.* 65:371–382.

Yoshida, T. and Hyōdō, T. 1970. Evaporation of water in air, humid air, and superheated steam. *Ind. Eng. Chem. Process Des. Dev.* 9:207–214.